Consequences Of Uridine mRNA Modifications On Translation

by

Monika Kristine Franco

A dissertation submitted in partial fulfillment
of the requirements for the degree of
Doctor of Philosophy
(Chemical Biology)
in the University of Michigan
2022

Doctoral Committee:

Assistant Professor Kristin Koutmou, Chair
Associate Professor Amanda Lee Garner
Associate Professor Jayakrishnan Nandakumar
Professor Nils G. Walter

Monika K. Franco

mkfranco@umich.edu

ORCID iD: 0000-0001-8059-8476

Dedication

I dedicate this dissertation to those who love me, who supported me, who struggled with me and to those made me who I am today. Thank you.

Acknowledgements

They say it takes a village to raise a child. Well, it took a village plus some of support to help me obtain this PhD. It is hard to put into words how thankful I am to each and every one of you. I can never repay you all for your support, but letting you know here in my Dissertation how much you mean to me is a start, isn't it? First and foremost, I would like to recognize my advisor, Professor Kristin Koutmou, thank you for everything. Thank you for your continued support, your guidance, and your mentorship. Thank you for all the times you let me cry in your office, comforting me through the tragic incident of diluting my pellets in 10X buffer instead of 1X, and letting me explore my career options. I couldn't have done this without you.

Next, I would like to thank the members of my thesis committee: Professors Amanda Lee Garner, Jayakrishnan Nandakumar, and Nils G. Walter. Thank you for pushing me when I needed it, helping me cultivate a fantastic dissertation, and supporting me in my career transition into science policy. I would also like to show some recognition to my collaborators and hosts during my internship at New England Biolabs (NEB): Dr. Bijoyita Roy and Dr. Monica Wu. You both taught me so much as a young female scientist. I gained more confidence in myself, and my abilities. Dr. Roy, you helped me become a better presenter, and for that I am always grateful. Thank you for helping me find my own voice. Also, shoutout to NEB! I had a wonderful experience there, it was a great company to work for, and I met so many wonderful people.

Last but not least, I would like to thank my science policy mentor and someone I personally look up to, Professor of Public Policy; Director, Science, Technology, and Public Policy (STPP) program, Dr. Shobita Parthasathy. I don't think words can describe what you have

done for me or how integral you have been in my journey into the science policy field. My time in the STPP program was life changing, and having you as a professor for a whole year was one of the best things that ever happened to me. You taught me how to write effective memos, taught me about policy, about society and so much more, and most importantly, you helped me discover my passion. I am now going to be working at a non-profit as a full time science policy analyst, it is like a dream come true.

Next I need to thank the members of my lab. You shared this journey with me and I love you all so much. Thank you for sharing the hard times, dealing with all my mini break downs, and just being my friends. First, off Dr. Dan Eyler. Dan, you were a fantastic support and mentor through this whole experience. Not only did you help cultivate my skills as a researcher, you pushed me to be more confident in myself. Thank you for always looking out for me, like when you made sure that no one sent me that one TLC result so that I could comfortably recover from surgery and not worry about work. I don't know where the lab would be without you. Dr. Josh Jones, it has been a pleasure working with you, I mean, we have worked on almost every paper together. You have been crucial in my work as a scientist, helpful at the bench, and a great friend all together. Our chats were always so much fun, and you became one of my best friends. Thank you for always checking in on me. I can't wait to see the scientist you become, because, if I am being honest, you are already pretty great. Dr. Jeremey Monroe, thank you for your continued friendship and support. I mean it. It has meant the world to me. There were multiple days that would have been my breaking point, and I am just thankful for you to pull me through. Including but not limited to all our radioactive gels. I will always cherish our literature discussions and all the laughs we had. Thank you for all the times you let me cry and break down in front of you. Laura Snyder, thank you for always giving me a person to talk too. Thank you for always being

honest with me. We had so much fun together and I will miss that. Minli, I am so happy you joined our lab. I am just heartbroken that we could not spend more time together. You are an intelligent, creative, caring, hardworking and amazing person. Don't ever loose that. I can't wait to see how successful you will become.

Next, I would like to shoutout my friends who kept me sane through this experience. Dr. Aria Ganzwaple, we have been friends since college, and can honestly say that I love having you in my life. You are an incredible, hilarious, and unique person. You are unapologetically yourself, and god I am so proud of you. Our sleepovers, D&D party, brunch/dinner dates, and phone calls have kept me sane. Thank you for always being available to answer my medical questions, and getting me through hard times. I love you with all my heart and can't wait to be bridesmaid in your wedding. This little blurb may not be much but you mean the world to me. Raji, there are so many things I could say. You are an amazing human being, and being at your house is like a second home. Thank you for all the times you stole me away for dinner or a weekend full of your moms cooking and dramas. Thank you for all the phones calls and the support you gave me. I always knew I had someone in my corner. Thank you for our dinner dates and sleepovers, and for introducing me to so much many shows/books that I feel in love with, that helped me escape the pressures of life. I love you. Kaylyn our phone calls during my drive homes were always a great way to decompress, and going to Spain during my PhD was something I never thought I could do. You showed me some wonderful things, and always supported my dreams. Dr Saffron Little, I am so thankful that grad school brought us together. We are one in the same, but you bring so much more into my life than you can imagine. Our coffee/lunch/dinner dates are always so much fun and we can talk for hours. Especially in the hallway in between our labs. Thank you for everything. Also, I would love to thank my D&D

party, Tyler, Brenny, Hal, Carla, and Emma, for the constant adventures, laughs, and escape from the stresses of life and graduate school. You all make my life more special, and no words can express how much you all mean to me.

Of course, I would not be here if it were not for my family. Dominick, you are such a sweet and caring little brother. Thank you for the late night phone calls that we would have when I was waiting for the bus or walking to my car. Thank you for all the dinners you heated up or made for me, and thank you for always being down to play video games with me or watch a good anime. Sam, little sister, I am so proud of you. Thank you for the constant phone calls or Facetimes when things got hard. You always find a way to make me laugh, even when you drive me crazy. Thank you also for always talking to your friends about your "smart scientist sister", and attempting to read my papers even if biochemistry isn't your favorite subject. Mom, I love you so much and words can't describe how thankful I am for everything you have done for me and given to me. Multiple jobs, working on no sleep, moving us here, the list goes on. You struggled so I could make this life for myself and I won't ever forget that. Thank you for all the support, both financially and emotionally. I knew I always had someone to talk to and always had a place to call home. Quite literately, especially when I moved back home my last year. I love you all so much, and am glad I got to live near you all during my graduate experience.

I would like to finish this off by thanking my friends, and chosen family. Dr. Tyler J Smith and Dr. Meredith K Purchal. Not to get to emotional here but this is the part I dreaded writing the most, not because I have a hard time telling you both how much I love you, but because I knew that if I was writing this that our time together in lab was coming to an end. That is something I don't think I could have prepared myself for. Who would have known that I would not only leave grad school with a PhD but with a bigger family. Well here goes nothing.

Meredith, you are a beautiful person both inside and out. I can remember first time meeting you and thinking, “wow, she’s so cool. I want to be her friend.” Who would have thought that you would become more than a friend, but family. You have this personality that is so big, and bright. You are intelligent, funny, caring, and one of the least judgmental people I know. We have shared so many experiences during this process, and I know I couldn’t have done it with without you. From crying in your studio during candidacy, to living together, thru break up and heartaches, thorough the happy moments and the dark, you were there. Thank you isn't enough, and I don't think a simple paragraph can ever express how much I care for you. I love you. Thank you though, for not only loving me as I am but allowing me the space to grow, to learn, and to find out who I am. With you, I could always be myself, and I can’t verbalize what that means to me. I don’t know where life is going to take me, but I know you will always be in it.

Tyler, I am so grateful that you entered my life. I remember when we both started that summer rotation, and our competitive sides automatically put a guard up, but that quickly changed and we became best friends. Thank you for everything. The laughs, the support, and a truly pure friendship. I know that we will always have each other’s backs, we are family. I never laughed so much in my life, like I have in that office. I will always cherish our talks about everything and anything, and of course anime, D&D, and video games. You let me be myself, sometimes knew me better than I did, and even then still called me your best friend. Thank you for being there when things got bad, making the fun times even brighter, and for putting me in your campaign. That has given me more happiness than I could ever imagine. You are such a talented person. Your creativity is outstanding, vivid and downright entertaining. You are a hell of a scientist, teacher, person, and quite the voice actor too. You are such a wonderful person that

brings joy into so many others lives, well I know you did for mine. I love you best friend, I couldn't have done this without you.

Getting a PhD is not a walk in the park, it's more like an endurance race, and I'll be honest, I hate running. I couldn't have finished the race without the people I love cheering me on. As excited as I am to approach the finish line, I can't help but feel sad. I know these people will always be in my life, but nothing beats coming to lab every day and seeing people who care about you and make you smile. The best thing about grad school, hands down, are the people you meet and the connections you make. I am not only leaving with a Doctorate in Philosophy but an even bigger family.

Table Of Contents

List Of Tables

List Of Figures

List Of Appendices

Abstract

Messenger RNAs play a crucial role as a road map for the ribosome to decode during protein synthesis. In the past decade, it was discovered that a small subset of modifications can be post-transcriptionally incorporated into messenger RNA (mRNA) sequences responsible for directing protein synthesis. In addition, non-coding RNAs have long been known to contain chemical modifications that are recognized as key modulators of their structure and function in cells. The enzymatic incorporation of mRNA modifications has the potential to influence every step of the mRNA lifecycle including, mRNA stability, protein recruitment, and translation. This collection of work focuses on the consequences that incorporation of these modification have on mRNA translation and tRNA function, specifically uridine modifications. First, I investigated how one of the most common mRNA modifications, pseudouridine, impacts mRNA translation.

We first discovered that pseudouridine has the ability to alter amino addition rates, decrease translation fidelity, alter GTP hydrolysis rate and has a distal effect on the CCA 3' end of $tRNA^{phe}$ when present at the first position of a UUU codon. We then explored the newly discovered uridine modification, 5-methyluridine (m^5U) also known as ribothymidine. Using LC-MS/MS techniques we not only discovered multiple methylated mRNA modifications, but were also able to identify the enzymes that incorporated them. In this work, it was revealed that 5-methyluridine is incorporated into yeast mRNAs by the tRNA (uracil-5-)-methyltransferase 2 enzyme (Trm2). I also revealed that the m^5U modification has different effects on mRNA translation and tRNA role in the translation process respectively. Interestingly, both pseudouridine and m^5U show that context is important when displaying a specific phenotype,

each acting in a position dependent manner regarding the 1st, 2nd, or 3rd position in a codon. In this dissertation, I was specifically interested in investigating how mRNA modifications impact translation. I was able to highlight that each modification plays specific and distinct roles in how it affects mRNA translation, and that it is important for the field to characterize them individually.

The scope of this research surpasses merely understanding the mechanist impacts modifications has on translation, but open avenues of exploration into drug resistance, therapeutics, protein evolution, and the overall cellular stress response. In the past decade, a new field of therapeutics directed around mRNA emerged. This process was particularly streamlined to commercial availability by the COIVD-19 pandemic. In fact, both the Moderna and Pfizer mRNA vaccines contain modified mRNA by adding N1-methylpseudouridine; which helps with both mRNA stability and immune response. Therefore, understanding how these modifications function could help incorporate more of them into mRNA therapeutics, and help create better treatments. In addition, it is newly discovered that tRNA modifications may have a function in antibiotic resistance, making the modifying enzymes associated with them great drug targets. This is further supported by my work showing that knocking out Trm2 changes the response to translation inhibiting antibiotics. Furthermore, my work implies that these uridine modifications function may be linked to cellular stress responses. For pseudouridine specifically, it is known it increases during stress, and it is hypothesized that this could be a function of pseudouridine itself. In fact, this coupled with my research, could show that pseudouridine is incorporated into mRNA to allow for small miscoding events create alternative proteins during stress and/or promote protein evolution.

Chapter 1 Chemical Modifications To mRNA Nucleobases Impact Translation Elongation And Termination

Work presented in this chapter was published in

Biophysical Chemistry.

Franco, Monika K., and Kristin S. Koutmou. "Chemical modifications to mRNA nucleobases impact translation elongation and termination." *Biophysical Chemistry* **(2022)**: 106780.

1.1 Introduction

RNA molecules serve a variety of essential roles in the cellular protein synthesis machinery. Ribosomal RNAs (rRNAs) form the core of the ribosome, messenger RNAs (mRNAs) act as templates for the ribosome to ensure that amino acids are added in the correct order, and transfer RNAs (tRNAs) bring amino acids into the ribosome (Figure 1A). These diverse functions are accomplished despite the relatively redundant chemical properties of the four nucleoside building blocks (cytidine, uridine, guanosine and adenosine) used to make all RNAs (Figure 1B).

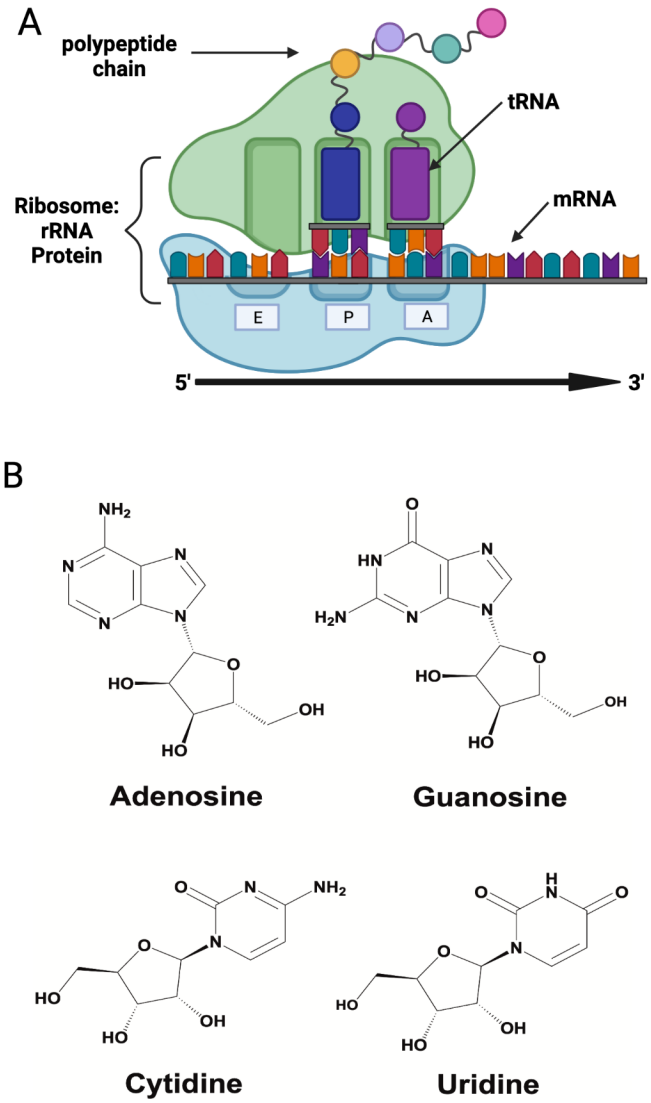

Figure 1.1: ***RNAs form the basis of the protein synthesis machinery(A)*** *Depiction of the basic components of the translational machinery, with the three central RNA species highlighted (rRNA, tRNA and mRNA).* ***(B)*** *The four chemical building blocks of RNA: adenosine (A), guanosine (G), cytidine (C) and uridine (U).*One strategy that cells use to overcome the monotonous nature of the standard nucleosides is to enzymatically modify their structures after they are linked together to form RNAs. In all organisms post-transcriptional modifications increase the topologies, chemistries and functionalities available to RNA molecules [1]–[8]. While the significance of modified nucleosides in tRNA and rRNAs have been well-known for decades, mRNA modifications are only recently gaining recognition as modulators of mRNA maturation, structure, stability and translation [3], [5], [7], [9]–[12].

Consistent with the idea that mRNA modifications have the potential to play important biological roles, the dysregulation of mRNA incorporating enzymes is linked to development a variety of diseases, including intellectual disorders and cancers [13]–[21] [22]–[26] [27]. In this review we present data suggesting that most modifications influence how quickly and accurately the ribosome decodes an mRNA. We also discuss the limitations in our current capacity to predict which sites of mRNA modification are likely to promote biologically significant perturbations to protein synthesis.

To date > 20 chemical modifications have been detected in eukaryotic protein coding mRNAs [3], [4], [28] (Figure 2).

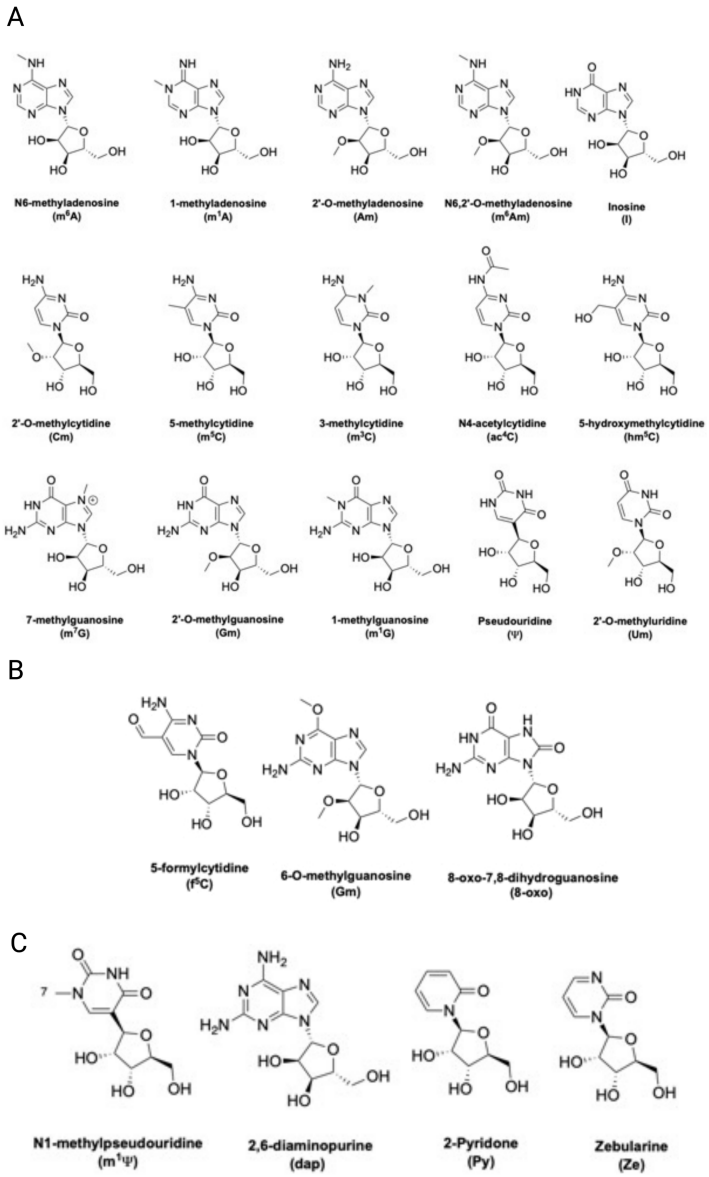

Figure 1.2: ***Modifications in mRNAs (A)*** *Modifications reported to be enzymatically incorporated into mRNAs.* ***(B)*** *Modifications that can be incorporated as a result of RNA damage.* ***(C)*** *Modifications found naturally found in mRNAs that are either incorporated into mRNA vaccines ($m^1\Psi$) or have been used to probe translation termination.*

Modifications can be added by enzymes or through non-enzymatic damage, such as alkylation or oxidation [28]–[30]. RNA-seq based technologies enabled the development of maps reporting where 13 enzymatically incorporated modifications can reside in all RNAs within a cell: N6-methyladenosine (m^6A), pseudouridine (Ψ), dihydrouridine (D), N4-acetylcytidine (ac^4C), N1-methyladenosine (m^1A), N7-methylguanosine (m^7G), 2′O-methyl modifications (Cm, Am, Gm,

Um), 5-methylcytidine (m^5C), and 5-hydroxymethylcytidine (hm^5C), and inosine (I) [1], [31]–[40]. Apart from the m^7G cap incorporated into the 5' end of all eukaryotic mRNAs, quantitative liquid chromatography coupled to tandem mass spectrometry (LC-MS/MS) studies reveal that N6-methyladenosine (m^6A), inosine (I) and pseudouridine (Ψ) are the most common modifications incorporated into mRNA by enzymes (Figure 2A) [3]. m^6A, Ψ and I exist in concentrations 10 to 100-fold above those of other reported modifications [3]. mRNA modifications resulting from oxidation, alkylation, or UV damage are typically present at lower levels than enzymatically incorporated modifications [30]. Damage to RNA bases is usually found at the most chemically reactive groups (N- or O-) in the purine and pyrimidine rings of all four nucleosides [e.g. 8-oxoguanosine, N3-methylcytidine, O4-methyluridine and 1-methyladenosine] (Figure 2B) [30]. Regardless of their origin, all nucleoside chemical modifications have the potential to impact how the ribosome decodes an mRNA (Figure 3A).

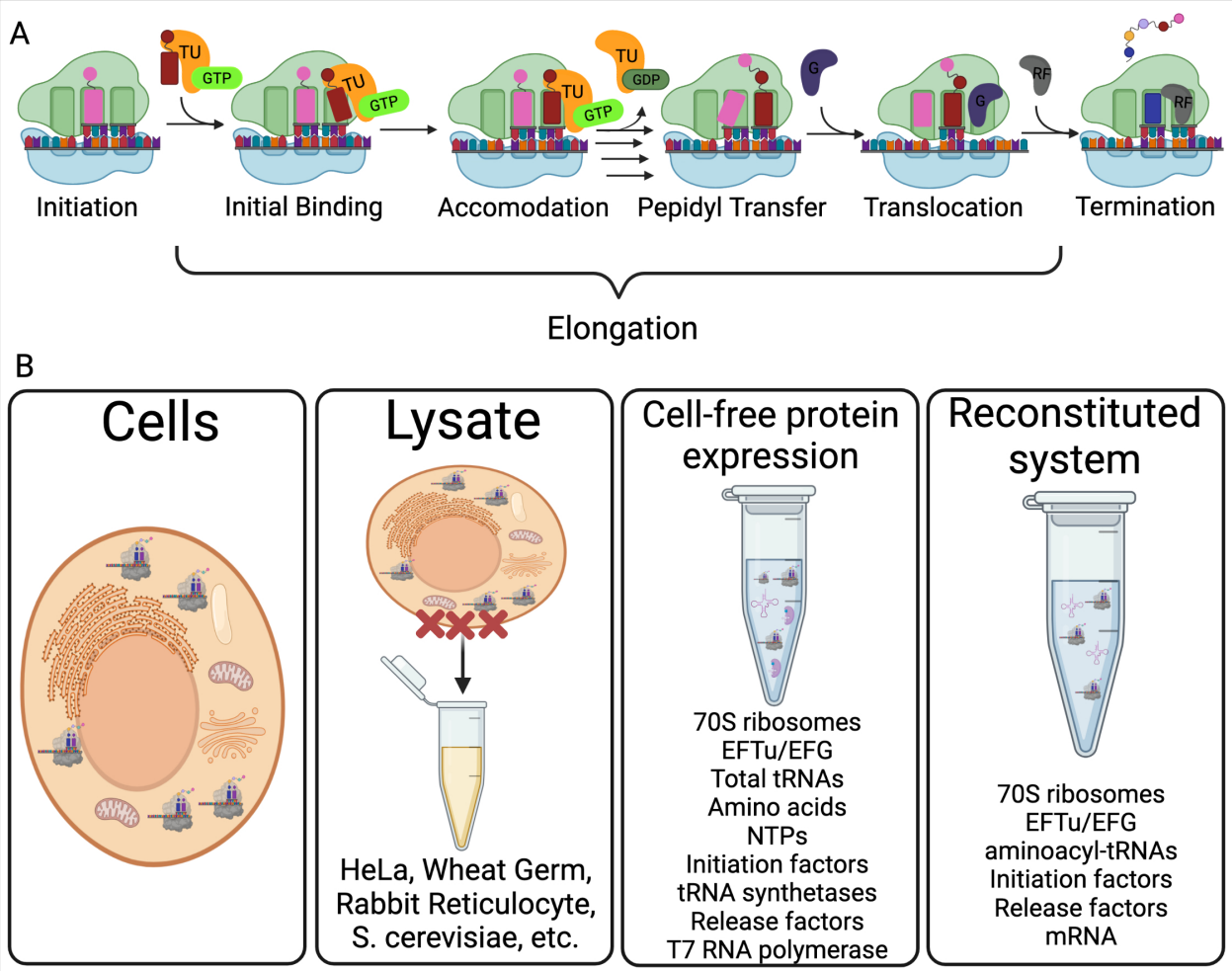

Figure 1.3: ***Assessing protein synthesis.*** ***(A)*** *Schematic of the steps in the protein protein synthesis, using bacterial nomenclature. In the first step (initiation), initiation factors help the 70S ribosome form on a start codon with fMet-tRNA^{fMet} bound in the ribosomal P site. During the elongation phase of translation, aminoacyl-tRNAs (aa-tRNAs) are brought into the ribosome A site by EF-Tu:GTP (initial binding). The tRNA is then positioned properly in the A site during accommodation, and EF-Tu exits following GTP hydrolysis. The amino acid on the P site tRNA is then transferred to the aa-tRNA in the A site during peptidyl-transfer. After a new peptide bond is catalyzed by the ribosome, EF-G moves (translocates) the ribosome and associated tRNAs to the next codon. The cycle of elongation continues until the ribosome reaches a stop codon (UAA, UGA or UAG), and release factors bind to the A site to catalyze the hydrolysis of the complete polypeptide.* ***(B)*** *Common approaches used to study translation. The kinetic resolution and mechanistic detail possible to attain increases as with the purification level of the translation system (from cells to reconstituted translation).*

In addition to the modifications present in cellular mRNAs, there is an emerging need to understand the consequences on translation for including non-naturally occurring modifications into mRNA nucleosides. This information is essential because such modifications are required components of many RNA-based therapeutics [41]–[46]. For mRNA therapeutics, non-naturally occurring modifications, such as N1-methylpseudouridine (m^1Y), enable the mRNA sequences

evade degradation by the innate immune response [41]. Indeed, incorporation of mRNA modifications was crucial to the success of the recent COVID-19 mRNA vaccines [43]. Developing a comprehensive understanding of the consequences of RNA modifications on translation will be essential for the continued rapid development of therapeutic mRNA technologies.

Discerning how individual modifications impact protein synthesis is challenging in cells because most of the enzymes that incorporate mRNA modifications also catalyze the addition of modifications into multiple non-coding RNAs essential to translation (rRNA, tRNA; Figure 1A) [3], [28]. This makes it difficult to discern the discrete causes of changes to protein production when modifying enzymes are depleted. Furthermore, mRNA modifications are generally incorporated at sub-stoichiometric frequencies, and a mixed population of modified and unmodified mRNAs of the same sequence exist in cells [47]–[52]. Therefore, our most direct understanding of how mRNA modifications impact translation comes from studies investigating protein production from *in vitro* modified mRNA transcripts in translationally active lysates or fully purified reconstituted translation systems (Figure 3B). With this in mind, below we examine how 16 individual mRNA modifications can influence the elongation and termination steps in protein synthesis (Figure 4A), emphasizing work conducted in lysate and purified translation systems (Table 1).

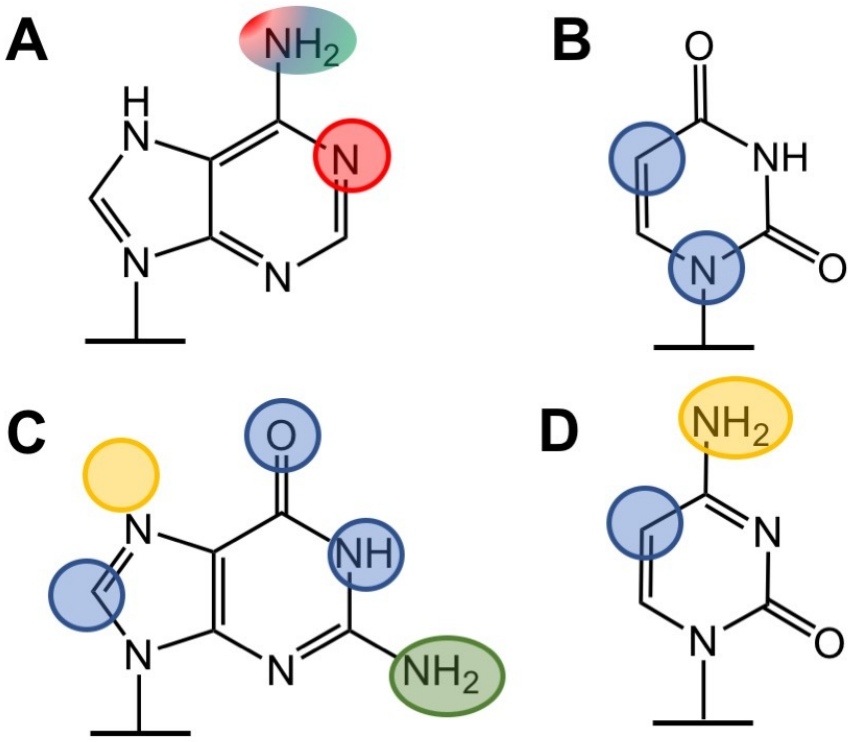

Figure 1.4: ***Modification of a variety of nucleobase positions impacts translation.*** *Positions in adenosine* ***(A)****, uridine* ***(B)****, guanosine* ***(C)*** *and cytidine* ***(D)*** *that impede only elongation rates (red), elongation rates and amino acid mis-incorporation (blue), translation termination (green) are circled. The data are too preliminary to confidently assign impacts to positions highlighted in orange. (For interpretation of the references to color in this figure legend, the reader is referred to Table 1.)*

Table 1.1: Summary of modifications and their impact on translation.

Modification	**Reported Consequence on Translation**	**References**
Adenosine		
N6-methyladenosine (m^6A)	In cells: Increases protein expression, may increase cap-independent translation. *In vitro*: Modestly slows translation elongation. Impedes tRNA binding and accommodation.	Heilman et al., 1996; A. Li et al., 2017; Shi et al., 2017; Wang et al., 2015; Coots et al., 2017; Lin et al., 2016; Meyer et al., 2015; Choi et al., 2016; Hoernes, Clementi, et al., 2016; Hoernes et al., 2019; Hudson & Zaher, 2015; Karikó et al., 2008; You et al., 2017
1-methyladenosine (m^1A)	Generally represses translation, marks mRNA for degradation.	Safra et al., 2017; Hoernes et al., 2019; You et al., 2017; Thomas et al., 2020

Inosine (I)	Alters translation accuracy of elongation and termination in some contexts, slows elongation.	Licht et al., 2019; Hoernes, Faserl, et al., 2018; Svitkin et al., 2021b
Uridine		
Pseudouridine (Ψ)	Enhances protein production, modestly decreases elongation rates, promotes initiation, can promote low level amino acid mis-incorporation in some contexts	B. R. Anderson et al., 2010; Karikó et al., 2008; Hoernes, et al. 2016; Eyler et al., 2019; Svitkin et al., 2021b
Guanosine		
7-methylguanosine (m^7G)	5' m^7G cap: Enhances mRNA maturation, nuclear export, prevents degradation, promotes translation initiation	Malbec et al., 2019
1-methylguanosine (m^1G)	Abolishes translation when present at 1st or 2nd position of a codon, reduces ribosome accuracy and protein production	You et al., 2017
6-O-methylguanosine (m^6G)	Reduces the rate constant for amino acid addition and ribosome accuracy in a position dependent manner.	Kersten et al., 1981; You et al., 2017 Hudson & Zaher, 2015
8-oxo-7,8-dihydroguanosine (8-oxo)	Stalls elongation, decreases yield of protein product	Shan et al., 2007; Simms et al., 2014
Cytidine		
5-methylcytidine (m^5C)	In cells: Repress and enhance translation In vitro: Decrease protein production, enhance miscoding	Hoernes, Clementi, et al., 2016; Huang et al., 2019
N4-acetylcytidine (ac^4C)	Increases translation efficiency	Arango et al., 2018
Ribose		
2'-O-methylations (Am, Gm, Um, Cm)	Decreases translational efficiency in position and sequence dependent manner	Hoernes, Clementi, et al., 2016
Non-naturally occurring		
N1-methylpseudouridine ($m^1\Psi$)	Increases protein yield, slows elongation, increases initiation	Svitkin et al., 2017; Mauger et al., 2019; Ding et al., 2014; Re et al., 2014;

		Schoenberg, 2011; Svitkin et al., 2021b
2-Pyridone (Py)	Abolishes stop codon recognition by release factors.	Hoernes, Clementi, et al., 2018
Zebularine (Ze)	Abolishes stop codon recognition, promotes read through.	Hoernes, Clementi, et al., 2018
Purine (P)	Decreases stop codon recognition by RF2, but not RF1, in a position dependent manner.	Hoernes, Clementi, et al., 2018
2,6-diaminopurine (DAP)	Decreases stop codon recognition by RF2, but not RF1, in a position dependent manner.	Hoernes, Clementi, et al., 2018

1.2 Adenosine modifications

Post-transcriptional chemical additions to adenosine represent the most well-studied class of mRNA modifications. Three enzymatically incorporated adenosine modifications that change Watson-Crick face of nucleobases have been reported: N6-methyladenosine (m^6A), N1-methyladenosine (m^1A) and inosine (I). Notably, N1-methyladenosine can also be added non-enzymatically, as the result of alkylative damage. Each of these modifications has the potential to change hydrogen bonding interactions between an A site mRNA codon and an incoming tRNA or release factor. Given that the ribosome relies heavily on precise hydrogen bonding patterns to ensure rapid and accurate translation, it is unsurprising that all three of these modifications perturb mRNA decoding by the ribosome. However, the severity of these effects varies widely between m^6A, m^1A and I, suggesting that additional factors beyond the simple disruption of mRNA:tRNA basepairs contribute to their consequences on translation.

1.2.1 N6-methyladenosine (m6A)

m^6A can be incorporated at thousands of locations in the transcriptome [53]–[56]. It was the first mRNA modification discovered and is a clear modulator of mRNA stability [6], [57]–

[59]. While m^6A has been observed throughout mRNA transcripts, it is enriched in mRNA 3' untranslated regions (3' UTR) and coding sequences (CDS) around stop codons [7], [56]. Initial studies speculated that these sites increased translation [60]. Consistent with this, recent ribosome profiling, RIP-seq and reporter assays suggest that m^6A binding proteins (YTHDF1, 3 and METTL3) increase the translation efficiency of m^6A-containing mRNAs in cells and may promote cap independent translation [61]–[63] [27], [64], [65]. While these correlative studies suggest the possibility that m^6A increases protein expression, investigations with modified mRNAs in lysates and reconstituted translation systems reach different conclusions.

Studies with *in vitro* transcribed mRNAs in translationally active lysates and purified translation systems reveal that the elongation of growing polypeptides by the ribosome slows on m^6A containing codons [66]–[72]. The impact of m^6A on translation elongation is dependent upon the position of the modification within a given codon. The largest reductions in peptide formation are observed when m^6A is incorporated into the first position of a codon, while the smallest effects are seen when m^6A is in the 3^{rd} position [66], [67], [72]. The reduced impact on elongation at the 3^{rd} position could possibly be attributed to the permissive base-pairing between the tRNA and mRNA tolerated by the ribosome at the wobble-position [73]. The detrimental influence of m^6A on translation elongation has been observed in both bacterial and eukaryotic cells, though the reported effects are most significant in the fully purified *E. coli* translation system [67], [72] [68]. Mechanistic studies of purified *E. coli* ribosomes reveal m^6A disrupts a crucial step in ribosome decoding, the hydrolysis of GTP by EF-Tu (Figure 3A) [66]. These findings are consistent with NMR studies reporting that m^6A destabilizes duplex A–U base pairs [74]. Despite the potential of m^6A to change mRNA:tRNA base-pairing, and its ability to perturb tRNA binding and accommodation, it does not increase the propensity of the ribosome to select the wrong tRNAs

during elongation [69], [75]. These data suggest the possibility that the inclusion of m^6A into codons may present cells with a way to transiently slow the ribosome. Programmed transitory pauses have the potential to help facilitate co-translational processes, such as nascent protein folding and modification, without detrimentally impacting the accuracy of protein production.

1.2.2 N1-methyladenosine (m^1A)

The prevalence of m^1A in mRNA transcripts has been controversial, with some groups reporting that it exists at low frequency within thousands of eukaryotic transcripts and others suggesting that m^1A is rarely incorporated into a handful cytoplasmic mRNAs and a single mitochondrial mRNA [76]–[78], [78], [79]. Establishing the location and abundance of m^1A is complicated both by the ability of m^1A to be added non-enzymatically under alkylative stress, and the influence of tissue type and cellular conditions on m^1A incorporation [29], [30], [78]. Regardless of when m^1A is present or how it is incorporated, when the ribosome encounters the modification it has the potential to impact translation.

m^1A contains a methyl group attached the N1 position of the ring, causing the nucleobase to be positively charged (Figure 2). Relative to adenosine, m^1A has significantly disrupted hydrogen bonding accepting potential, and as such, can be reasonably expected to disrupt tRNA:mRNA interactions [80]. Consistent with this, polysome fractionation experiments and luciferase-based reporter assays in human cells demonstrate that m^1A containing mRNAs are translationally repressed [78]. These findings are supported by reports that the insertion of m^1A robustly inhibits mRNA translation in bacterial, yeast and wheat germ lysate based translation systems [68], [72]. Pre-steady state kinetic analyses of cognate and near-cognate amino acid addition on m^1A modified codons reveal that the modification generally inhibits the ability of adenosine to form base pairs [81]. In light of this observation, it makes sense that when the

ribosome decodes m^1A modified mRNA in *E. coli* it activates the mRNA quality control pathway (tmRNA) that targets damaged mRNAs for degradation [81]. We expect similar quality control mechanisms, such as No-Go Decay (NGD), to be activated in eukaryotes when the ribosome encounters a m^1A containing codon [82].

1.2.3 Inosine (I)

The deamination of adenosine to form inosine within mRNAs is catalyzed by a family of enzymes called adenosine deaminases acting on RNA (ADARs) [83]. Inosine was among the first modifications to be discovered in mRNA, and the consequences of inosine incorporation change depending on where it is localized within a transcript [84]. The majority of inosine sites are located in untranslated regions of mRNA where they modulate mRNA stability, structure, and localization [85], [86]. Nonetheless, over 1000 sites have been reported in mRNA coding regions, indicating that this modification is regularly encountered by the ribosome in cells [87].

While inosine is created from adenosine, and therefore lacks an amine group at the C2 position, its chemical structure also closely resembles that of guanosine – with a carbonyl at C6 (Figure 2A). Because its structure is intermediate between adenosine and guanosine, inosine has the ability to base pair with adenosine, cytidine, and uridine - though it preferentially binds to cytidine [86]. The significance of this property is highlighted by the observation that inosine modifications in tRNA anti-codons can be recognized as guanosine by the ribosome during translation [88]. As such, it is unsurprising the incorporation of inosine into mRNA codons can lead to the incorporation of a variety of amino acids at the modified position [89]. It is hypothesized that ability to incorporate non-cognate amino acids could be a way to alter protein activities. Indeed, this has been shown to happen in the glutamate receptor GluR-B, where the presence of an inosine in an mRNA leads to the incorporation of arginine instead of glutamine [90]. This is a

functionally significant change, influencing the receptor efficiency and selectivity. However, inosine does not always cause the re-coding of an mRNA. The ability to promote alternative amino acid incorporation appears to depend strongly on the position of the modification within a codon and context of the surrounding sequence. Some codons containing inosine modifications promote amino acid substitution < 1% of the time, and others result in substitutions nearly every time 25% [89]. While the ribosome appears to mis-incorporate amino acids most often when inosine as at the 1st position in a codon, the parameters dictating context dependent still need to be established.

Not only does inosine have the ability to change the identity of protein products, iterated inosines also cause ribosomes to stall and the generate truncated peptide products [89], [91]. Multiple factors likely contribute to these stalling events, including inosine impacting EF-Tu binding and anti-codon/codon interactions [91]. Furthermore, the substitution of A for I in UAG, UGA and UAA stop codons can change the specificity of bacterial release factors, with UIG and UGI substitutions increasing stop-codon read-through (by up to 90%) [92], [93][89]. Together these findings suggest that the promiscuity in inosine base pairing is likely to impact all steps of translation that depend on hydrogen bonding to ensure accuracy.

1.3 Uridine modifications

In contrast to modifications of other nucleosides, uridine modifications have been more generally more difficult to discover and quantify in mRNAs due to the lower limits of detection possible for these nucleosides on mass-spectrometry in LC-MS/MS. Nonetheless, the two most common uridine modifications in non-coding RNAs, pseudouridine (Ψ) and dihydrouridine (D), have also been reported in mRNAs [31], [94]–[97]. D was discovered only recently, and the loss of the enzymes that incorporate it into mRNAs (which also target tRNAs) appears to slow translation [31]. Ψ is the second most abundant modification in mRNAs, and is also notable

because it is related to the 1-methylpseudouridine ($m^1\Psi$) modification included in many mRNA vaccines and therapeutics [41], [43] (Figure 4B, and 'non-natural mRNA modifications' section below). While decades of studies demonstrate that Ψs present in tRNA make important contributions to translation, it has only recently come to light that Ψ in mRNA may also have significant consequences on protein synthesis.

1.3.1 Pseudouridine (Ψ)

Pseudouridine is unique among mRNA modifications because it is the only isomer of a nucleoside base that occurs (Figure 2). Studies mapping the position of Ψ in the transcriptome indicate that this modification is present in hundreds of mRNA transcripts, with the majority of Ψ sites being localized in mRNA introns and CDS regions [94]–[97] [98], [99]. Initial reporter studies in cells suggested that the inclusion of Ψ in mRNA codons enhances translation and promotes protein production [70], [100]. However, i*n vitro* studies reached contradictory conclusions, indicating that Ψ slows translation [67][68], [75], [101]. These findings have since been reconciled by a recent study demonstrating that Ψ containing mRNAs slow elongation to induce stalling events, but still generate high levels of protein because they exhibit increased levels of ribosome loading onto transcripts [102]. The impact of Ψ on translation termination has also been investigated. The insertion of Ψ has been reported to suppress translation termination at stop codons, though the degree to which this occurs in cells remains controversial [75], [92], [101], [103], [104]. Taken together these studies demonstrate that Ψ can influence multiple steps along the translation pathway.

Ψ has long been studied for its ability to form non-canonical base pairs. Similar to inosine - though to a lesser degree - Ψ also promotes the addition of near-cognate amino acids in a highly

context dependent manner [75]. *In vitro* translation studies reveal that the inclusion of Ψ increases the rate constant for valine mis-incorporation on phenylalanine UUU codons when Ψ is at the first and third codon positions. Investigations of amino acid mis-incorporation into reporters produced from Ψ substituted mRNAs in HEK293 cells support these findings. Luciferase peptides generated from fully Ψ substituted mRNAs have much higher (> 20-fold) levels of mis-incorporated amino acids than peptides made from mRNAs only containing canonical uridine nucleosides [75]. However, consistent with the context dependence observed in *in vitro* translation studies, amino acid addition was not observed on every Ψ substituted codon. The position dependent modulations in ribosome accuracy by Ψ is akin to what has been reported for inosine. Understanding the rules that govern these context dependent effects will be important for researchers seeking to identify which Ψ-modified mRNA sites have the greatest potential to translationally control gene expression.

1.4 Guanosine modifications

Methylations account for all of the mRNA modifications reported in guanosine nucleosides to date. These modifications result from either enzymatic reactions (N7-methylguanosine) and non-specific RNA damage (6-O-methylguanosine, 1-methylguanosine, 8-oxoguanosine) (Figure 2). Similar to analogous purine methylations in adenosine, guanosine modifications impact the speed and fidelity of translation (Figure 4C). As might be expected, the promiscuously incorporated RNA damage products all strongly reduce the ability of the ribosome to catalyze protein synthesis.

1.4.1 N7-methylguanosine (m^7G)

The N7-methylguanasine cap present at the 5' of all eukaryotic mRNAs is perhaps the most well studied mRNA modification. In contrast to the other modifications discussed thus far, the m^7G cap is attached to the 5' end of an mRNA UTR by a tri-phosphate linkage [105]. The m^7G is a key feature of eukaryotic mRNAs, making crucial contributions to mRNA maturation, nuclear export, preventing degradation and translation initiation [106]. Recently the m^7G modification was also discovered in mRNAs outside of the 5' cap in the 3' UTR and CDS regions of mRNAs [106]–[108]. As the many functions of the m^7G cap have been widely reviewed elsewhere [109], [110], we will limit our brief discussion to the new class of internal mRNA m^7G modifications.

Like other methylations, the location of m^7G sites within mRNA transcripts is dynamic, redistributing under varying stress conditions [106]. Analysis of human ribosome profiling data suggest that the inclusion of m^7G increases the translation efficiency of modified mRNAs [106]. However, whether the observed impact is mediated by a cellular protein, occurs at initiation, or is a direct consequence of modifications at discrete sites on translation elongation or termination remains to be seen. Given the known ability of m^7G in rRNAs and tRNAs to alter duplex structure and dynamics [111]–[113] we anticipate that direct studies with purified components (Figure 3B) will reveal that m^7G impedes tRNA binding and accommodation, similar to other methylations that change RNA structure and dynamics. Knowing this information would allow future studies to direct their investigations towards identifying RNA-protein interactions that may help to improve translation efficiency, akin to the proposed role YTHDF reader proteins in enhancing the translation of m6A-modified transcripts [61].

1.4.2 1-methylguanosine (m^1G)

1-methylguanosine (m^1G) is among the least abundant modifications reported in mammalian mRNAs [3]. Translation studies in wheat germ lysates and the reconstituted *E. coli*

PURE translation system suggest that, much like m^1A, m^1G can have dramatic effects on protein synthesis [72]. The incorporation of m^1G into the 1st and 2nd codon positions abolishes the translation of a reporter mRNAs (Figure 3B), though protein production is unaffected when m^1G was instead present in the 3rd position (wobble). The introduction of m^1G into the first position of an mRNA codon also reduces protein production and ribosome accuracy (being decoded as either uridine or cytidine) in translationally active wheat germ lysates. However, the extent of ribosome miscoding on m^1G codons is more dramatic in *E. coli* PURE translation system than in wheat germ lysates. m^1G changes translation in a similar way as m^1A, suggesting that methylations to the N1 position of purine rings generally disrupts ribosome function [81].

1.4.3 6-O-Methylguanosine (m^6G)

While the alkylation of adenosine at the N6 position is accomplished enzymatically, the analogous modification in guanosine (6-O-Methylguanosine (m^6G)) occurs through RNA damage [29], [30]. Despite its discovery over 30 years ago the impact of m^6G on translation has only been recently assessed [69], [72], [114]. m^6G changes in the guanosine Watson-Crick basepairing face so that it permits the nucleoside to be decoded as an adenosine. This results in the increased mis-incorporation of amino acids by both bacterial and eukaryotic ribosomes [69], [72]. In cells, this change in basepairing has the potential to alter protein composition, or an overall impact of the rate of protein synthesis.

Investigations across multiple translation systems (lysate, *E. coli PURE*, and fully-reconstituted; Figure 3B) demonstrate that m^6G perturbs protein synthesis in a position dependent manner. When poised in the first position of a codon, m^6G reduces the rate constants for amino acid addition by the ribosome and impedes the cognate tRNA selection [69]. Substitution of m^6G for G at the second position in a codon also reduces peptide bond formation with cognate aa-tRNA

by 1000-fold, but unlike the first position, it does not alter tRNA selection to permit non-cognate aa-tRNA to react [69], [72]. In contrast, the presence of m^6G at the 3rd position in a codon does not appear to affect cognate aa-tRNA interactions with the ribosome, but does enhance the incorporation of near cognate amino acids [69], [72]. Interestingly, the ability of m^6G to promote miscoding when in the 1st and 3rd positions of a codon, but not in the second, is reminiscent of effects of *Ψ*. This differs markedly from the behavior of m^6A, suggesting that adding an electron donating methyl-group to the hydrogen bond acceptor of a nucleobase is more detrimental than adding a methyl group to an hydrogen bond donor in N6 position of a purine ring.

1.4.4 8-Oxoguanine (8-oxoG)

It is estimated that 8-oxoG is generated once per every 10^5 unmodified guanosine nucleosides. It results from oxidative damage, and mRNAs are particularly susceptible to such damage due to their single stranded structures [115], [116]. 8-oxoG is among the most abundant RNA damage products and significantly disrupts RNA structure [117], [118]. As might be reasonably expected, when present in mRNAs 8-oxoG has been shown to stall translation elongation, decreasing the yield of protein product in both eukaryotic lysates and fully purified bacterial translation systems [119], [120]. Consistent with this, kinetic studies in a reconstituted translation system demonstrate the inclusion of 8-oxoG in an mRNA codon reduces the rate constants for amino acid addition by four orders of magnitude [120]. In contrast to many other modifications, the extent to which 8-oxoG changes amino acid addition is independent of where the modification is localized within a codon. 8-oxoG is recognized by near-cognate tRNAs, though the peptide bond formation efficiency for these reactions is low, and the rate constants for near-cognate incorporation for codons containing 8-oxoG are only slightly faster (< 10%) than unmodified [120]. As such, it is unlikely that 8-oxoG causes miscoding in the cell. The steric clash

between the oxygen at the 8th position of the base and the phosphate group at the 5th, which changes the base pairing potential of 8-oxoG, likely contributes to the observed uniformity of 8-oxoG mediated disruptions to translation. Given the large magnitude of disruptions to translation caused by 8-oxoG, we expect ribosomes to stall significantly, resulting in collisions that ultimately lead to the degradation of 8-oxoG containing transcripts by co-translational mRNA surveillance mechanisms [121]–[123].

1.5 Cytidine modification

While a variety cytidine modifications have been reported in mRNAs (ac^4C, m^3C, hm^5C, m^5C, Cm), the consequences of only two nucleobase modifications, 5-methylcytidine and N4-actylcytidine, have been investigated. These initial studies reveal that the activities of enzymes incorporating m^5C and ac^4C into non-coding RNAs and mRNAs are important for translation. They also raise the possibility that cytidine mRNA modifications may have the unique ability to both slow and speed-up translation elongation.

1.5.1 5-methylcytidine (m^5C)

The most common cytidine modification in both non-coding and protein coding mRNAs is m^5C. The presence of m^5C in tRNA influences aminoacylation, structure, stability and codon recognition [124]–[126]. The ability of m^5C in tRNA to effect codon:anti-codon interactions suggests that it may have a similar impact when present in mRNA codons. Much like other common modifications, m^5C was first identified within mRNAs several decades ago, though its location within transcripts has only recently been mapped [127]–[130]. The abundance and frequency of m^5C in mRNAs is not yet clear, though transcriptome wide maps of m^5C sites indicate that the modification is more common in mRNA UTRs than coding regions [131].

Ribosome profiling studies have reached opposing conclusions about the effect of m^5C in mRNA transcripts on translation, with some studies suggesting that these modifications enhance translation, and others indicating that they either repress, or do not change protein synthesis [131]–[133]. For example, comparison of ribosome profiling datasets collected from wild-type mice and *Nsun2*$^{-/-}$ mice lacking a key m^5C modifying enzyme, Nsun2 [131] reveals that mRNAs with m^5C present in coding sites have increased levels of translation when Nsun2 is absent. Conversely, another studies showed that when Nsun2 is positive regulator of CDK1 [133]. However, contradictory results are not surprising given that these studies are looking at m^5C sites at different regions of the mRNA transcript. Subsequently, cellular assays and *in vitro* studies reach contradictory conclusions about the consequence of m^5C in mRNA CDS regions. While the inclusion of m^5C in mRNAs translated in human cell lines and rabbit reticulate lysate does not reduce the levels of protein production [68], the insertion of a single m^5C into an mRNA reporter decreases the production of peptide in a reconstituted *E. coli* translation system by ~40% [67]. Furthermore, *in vitro* m^5C increases amino acid mis-incorporation levels [67]. Such significant effects on both the extent and accuracy of protein production may help to explain why m^5C is more likely to be added into mRNA UTRs than in coding regions. Additional studies will be needed to deconvolute the impacts of m5C in UTRs and CDS, as it is possible that m^5C in UTR regions enhance translation, while that in CDS regions may repress elongation.

1.5.2 N4-actylcytidine (ac^4C)

The only acetylation reported in mRNA nucleosides is found on the N4 position of cytidine. Ac^4C is common in non-coding RNAs and has recently also been observed in yeast, human and hyperthermophilic archaea mRNAs [130], [134], [135]. The N-acetyltransferase 10 (Nat10 in humans) enzyme is responsible for incorporating ac^4C in yeast and humans [130], [134]. One

recent study conducted an in-depth investigation into the role of ac^4C in mRNA [134]. This work used transcriptome-wide approaches to compare the stability and translation of mRNAs in wild-type *nat10*Δ cells. Their findings suggest that the presence of ac^4C in mRNA increases translation efficiency, which the authors attribute to stabilizations in mRNA structure. However, the fact that Nat10 catalyzes ac^4C addition not only into mRNAs, but also into tRNAs and rRNAs, and the prediction that most ac^4C sites have relatively low frequencies of incorporation, present challenges in the interpretation of these data. Additional biochemical studies will be required to verify these initial studies and fully detangle the contributions of ac^4C in mRNA and non-coding RNAs during translation.

1.6 Ribose modifications (2' OMe)

2'-O-methylations have been reported on all four standard nucleosides (Am, Gm, Um, Cm) and some modified bases (m^6Am) in mRNAs [136]. When present in mRNA CDS regions, 2'OMe decreases translational efficiency in a position and sequence dependent manner [67], [137]. Kinetic analyses, together with x-ray crystallography studies, demonstrate that 2'OMe disrupts the ribosome decoding center, resulting in defects in tRNA accommodation during translation elongation [137]. NMR studies reveal that 2'OMe modifications have large impacts on RNA dynamics, suggesting the possibility that these modifications modulate the secondary structure ensembles of mRNAs in the ribosome active site – perhaps subtly favoring conformations that are not optimal for translation [138].

1.7 Non-naturally occurring mRNA modifications

There is growing interest in understanding the impact of mRNA modifications not present in nature on translation. The inclusion of modifications, such as N1-methylpseudouridine ($m^1\Psi$),

in mRNAs vaccines and therapeutics, underscores the need to be able to predict how changing individual positions in a nucleobase will impact translation[43]. Below we present what is known about the influence of $m^1\Psi$ on translation and discuss investigations of a series of non-naturally occurring modifications that revealed the chemical basis for stop-codon recognition by release factors during translation termination.

1.7.1 N1-methylpseudouridine ($m^1\Psi$)

$m^1\Psi$ is present in both tRNA and rRNA, but has not yet been detected in mRNA [28], [139], [140]. However, it is decoded by the ribosome when it is included in therapeutic mRNA, such as the SARS-CoV-2 mRNA vaccines [43]. Protein yield from $m^1\Psi$-modified mRNAs is increased because the modification helps transcripts to evade the cellular immune response [41], [141]. Studies of fully $m^1\Psi$ modified mRNA reporters in cell-free rabbit reticulocyte lysate translation systems indicate that $m^1\Psi$ also impacts protein synthesis. Like Y, m^1 Y induces ribosome stalling to slowpolypeptide elongation, while still creating large amounts of protein product [102], [142]. Similar to *Ψ*, these two observations can be reconciled by increased translation initiation rates and the ability of cellular membranes to prevent ribosome collisions [143]. Moreover, the ability of $m^1\Psi$ to stabilize RNA structure may also account for some of the observed effects of $m^1\Psi$ on mRNA half-life and translation [141]. Structure generally increases RNA half-life, and stabilization of some structures in mRNA coding regions can enhance protein expression [142], [144].

Though it seems counterintuitive, there are multiple ways that modest decreases in ribosome elongation speed could lead to increase levels of protein product [142]. Slowed progression of the ribosome along an mRNA can enhance co-translational protein folding (and therefore stability) [142], [145], provide time for important RNA binding proteins to interact with

a transcript [142], [146], or the ribosome itself can protect an mRNA from endonucleases [142], [147]. Furthermore, because m^1Y reduces eIF2a-phosphorylation levels, slowed elongation might be beneficial in preventing ribosome collisions that might otherwise occur with rapidly loaded ribosomes. These possibilities can help to rationalize the observed impact of incorporating $m^1\Psi$ into mRNAs on the ultimate levels of their resulting protein products.

1.7.2 Pyridone (Py), zebularine (Ze), 2,6-diaminopurine (DAP), purine (P)

Pyridone (Py), zebularine (Ze), 2,6-diaminopurine (DAP) and purine (P) have all been introduced into stop codons (UAA, UAG, UGA) to assess the chemical requirements of nucleobases essential for translation termination. At the stringently monitored U1 position, removal of the ability of stop-codon nucleobases to donate and accept hydrogen bonds by the inclusion of Py and Ze abolishes the recognition of stop-codons release factors [92]. However, these modifications had differential effects – with Ze promoting translational readthrough, and Py leading to stalled ribosomes. In contrast to the U1 pyrimidine modifications, the bacterial release factor 1 (RF1) still robustly catalyzes release on codons containing DAP and Purine at the 2^{nd} and 3^{rd} position [92]. However, release factor 2 (RF2) is only able to perform peptide hydrolysis when Purine is in the 3^{rd} codon position, and DAP is in the 2^{nd} position of a stop codon. These studies reveal that RF1 more flexibly recognizes stop-codons than RF2. Additionally, the accuracy of RF2 stop codon recognition is enhanced in the presence of an amino or carbonyl group at the second stop-codon nucleotide, and N6 in the last nucleoside of a stop codon. Analogous studies with non-natural nucleosides in other codons could be informative for gaining insight into how modified nucleosides in tRNA anticodons interact with mRNA in the ribosome A site.

1.8 Conclusions

Post-transcriptional modifications to mRNA nucleosides have been observed at thousands of sites in the eukaryotic transcriptome [54], [94]–[97], [108]. Although all of the modifications investigated so far can alter translation (Figure 4), they do so to different degrees. The largest impacts on amino acid addition rate constants are observed for methylations to the N1 positions on purine nucleobases that abolish the ability of the base to form hydrogen bonds at this crucial position (m^1G, m^1A). This is in contrast to modifications made to the adjacent O6 and N6 functional groups (m^6A, O^6G, inosine), which generally alter tRNA binding and accommodation by the ribosome, but still permit amino acid addition. In general, non-methyl modifications to the 6-membered ring in purines and pyrimidines appear to have the biggest effect on ribosome accuracy (inosine, Ψ), likely because such modifications most significantly change strength and pattern of possible hydrogen bonding interactions between codons and tRNA anti-codons. Notably, the mere disruption of Watson-Crick hydrogen bonding does not necessarily promote the misreading of codons. Illustrative of this, both inosine and m^6A disrupt base pairing to slow translation elongation, but only inosine promotes amino acid mis-incorporation. This suggests that *changing*, not abrogating, the hydrogen bonding potential of nucleobases has a larger influence on tRNA selection. These observations are consistent with what is already known about the fundamental principles that shape mRNA:tRNA interactions, and alterations in Watson-Crick pairing have consequences on translation regardless of whether modifications are incorporated onto tRNA anticodons or mRNA codons.

The parameters that dictate how modifications not on the Watson-Crick face of nucleobases impact translation are less clear. It is possible that such modifications, like Ψ, m^5C or 8-oxoG, change nucleobase ring electronics to perturb the strength of the hydrogen bond donors

and acceptors involved in base pairing. Additionally, modifications have the capacity to change intra-molecular interactions with an mRNA, or interactions between rRNA and mRNA within the A site. There is growing evidence that such factors, and not only anticodon:codon interactions, have a bigger contribution to translation elongation than previously recognized. This idea is supported by the common conclusion reached in studies of multiple modifications that the effect of a given modification on amino acid addition and translation accuracy largely depends on the sequence context in which the modification is placed.

The *in vitro* work discussed in this review assesses translation on mRNAs that have every site of interest 100% modified. In cells this is rarely the case. While there are not yet measurements available of the occupancy of most modified sites, we do know that the two most common mRNA modifications, m^6A and Ψ, are generally incorporated at sub-stoichiometric levels (ranging from ~5-80%) [52], [97], [148], [149]. The biological impact of any given modified site on translation will therefore depend largely on its occupancy. This is analogous to what has been observed for protein post-translational modifications, which are also incorporated at similarly sub-stoichiometric levels [150]. We anticipate that sites with higher levels of modification incorporation are likely to have more significant impacts on protein production. Future systematic biochemical and computational studies will be needed to uncover both the stoichiometry of modified mRNA sites as well as the context dependence of translational effects. This information will be broadly useful as researchers seek to identify which of the many chemically-modified positions reported mRNA codons are the most likely to have consequences for translation in cells.

1.9 References

[1] W. V. Gilbert, T. A. Bell, and C. Schaening, "Messenger RNA modifications: Form, distribution, and function," *Science*, vol. 352, no. 6292, pp. 1408–1412, Jun. 2016, doi: 10.1126/science.aad8711.

[2] J. E. Jackman and J. D. Alfonzo, “Transfer RNA modifications: nature’s combinatorial chemistry playground: Transfer RNA modifications,” *Wiley Interdiscip. Rev. RNA*, vol. 4, no. 1, pp. 35–48, Jan. 2013, doi: 10.1002/wrna.1144.
[3] J. D. Jones, J. Monroe, and K. S. Koutmou, “A molecular-level perspective on the frequency, distribution, and consequences of messenger RNA modifications,” *Wiley Interdiscip. Rev. RNA*, vol. 11, no. 4, p. e1586, 2020.
[4] P. J. McCown *et al.*, “Naturally occurring modified ribonucleosides,” *WIREs RNA*, vol. 11, no. 5, p. e1595, 2020, doi: 10.1002/wrna.1595.
[5] S. Nachtergaele and C. He, “The emerging biology of RNA post-transcriptional modifications,” *RNA Biol.*, vol. 14, no. 2, pp. 156–163, 2017.
[6] S. Nachtergaele and C. He, “Chemical Modifications in the Life of an mRNA Transcript,” *Annu. Rev. Genet.*, vol. 52, pp. 349–372, Nov. 2018, doi: 10.1146/annurev-genet-120417-031522.
[7] I. A. Roundtree, M. E. Evans, T. Pan, and C. He, “Dynamic RNA modifications in gene expression regulation,” *Cell*, vol. 169, no. 7, pp. 1187–1200, 2017.
[8] X. Wang and C. He, “Dynamic RNA modifications in posttranscriptional regulation,” *Mol. Cell*, vol. 56, no. 1, pp. 5–12, Oct. 2014, doi: 10.1016/j.molcel.2014.09.001.
[9] E. M. Harcourt, A. M. Kietrys, and E. T. Kool, “Chemical and structural effects of base modifications in messenger RNA,” *Nature*, vol. 541, no. 7637, pp. 339–346, 2017.
[10] T. P. Hoernes, A. Hüttenhofer, and M. D. Erlacher, “mRNA modifications: Dynamic regulators of gene expression?,” *RNA Biol.*, vol. 13, no. 9, pp. 760–765, 2016.
[11] K. D. Meyer and S. R. Jaffrey, “Rethinking m6A Readers, Writers, and Erasers,” *Annu. Rev. Cell Dev. Biol.*, vol. 33, pp. 319–342, Oct. 2017, doi: 10.1146/annurev-cellbio-100616-060758.
[12] E. Peer, G. Rechavi, and D. Dominissini, “Epitranscriptomics: regulation of mRNA metabolism through modifications,” *Curr. Opin. Chem. Biol.*, vol. 41, pp. 93–98, 2017.
[13] M. T. Angelova *et al.*, “The emerging field of epitranscriptomics in neurodevelopmental and neuronal disorders,” *Front. Bioeng. Biotechnol.*, vol. 6, p. 46, 2018.
[14] M. S. Ben-Haim, S. Moshitch-Moshkovitz, and G. Rechavi, “FTO: linking m 6 A demethylation to adipogenesis,” *Cell Res.*, vol. 25, no. 1, pp. 3–4, 2015.
[15] X.-Y. Chen, J. Zhang, and J.-S. Zhu, “The role of m 6 A RNA methylation in human cancer,” *Mol. Cancer*, vol. 18, no. 1, pp. 1–9, 2019.
[16] Q. I. Cui *et al.*, “m6A RNA methylation regulates the self-renewal and tumorigenesis of glioblastoma stem cells,” *Cell Rep.*, vol. 18, no. 11, pp. 2622–2634, 2017.
[17] T. Du *et al.*, “An association study of the m6A genes with major depressive disorder in Chinese Han population,” *J. Affect. Disord.*, vol. 183, pp. 279–286, 2015.
[18] P. J. Hsu, H. Shi, and C. He, “Epitranscriptomic influences on development and disease,” *Genome Biol.*, vol. 18, no. 1, pp. 1–9, 2017.
[19] N. Jonkhout, J. Tran, M. A. Smith, N. Schonrock, J. S. Mattick, and E. M. Novoa, “The RNA modification landscape in human disease,” *Rna*, vol. 23, no. 12, pp. 1754–1769, 2017.
[20] X. Wang *et al.*, “Reduced m6A mRNA methylation is correlated with the progression of human cervical cancer,” *Oncotarget*, vol. 8, no. 58, p. 98918, 2017.
[21] X. Zhao *et al.*, “FTO-dependent demethylation of N6-methyladenosine regulates mRNA splicing and is required for adipogenesis,” *Cell Res.*, vol. 24, no. 12, pp. 1403–1419, 2014.

[22] Y. Bykhovskaya, K. Casas, E. Mengesha, A. Inbal, and N. Fischel-Ghodsian, "Missense mutation in pseudouridine synthase 1 (PUS1) causes mitochondrial myopathy and sideroblastic anemia (MLASA)," *Am. J. Hum. Genet.*, vol. 74, no. 6, pp. 1303–1308, Jun. 2004, doi: 10.1086/421530.

[23] S. W. Knight *et al.*, "1.4 Mb candidate gene region for X linked dyskeratosis congenita defined by combined haplotype and X chromosome inactivation analysis," *J. Med. Genet.*, vol. 35, no. 12, pp. 993–996, Dec. 1998, doi: 10.1136/jmg.35.12.993.

[24] J. E. Mangum *et al.*, "Pseudouridine synthase 1 deficient mice, a model for Mitochondrial Myopathy with Sideroblastic Anemia, exhibit muscle morphology and physiology alterations," *Sci. Rep.*, vol. 6, p. 26202, May 2016, doi: 10.1038/srep26202.

[25] J. R. Patton, Y. Bykhovskaya, E. Mengesha, C. Bertolotto, and N. Fischel-Ghodsian, "Mitochondrial myopathy and sideroblastic anemia (MLASA): missense mutation in the pseudouridine synthase 1 (PUS1) gene is associated with the loss of tRNA pseudouridylation," *J. Biol. Chem.*, vol. 280, no. 20, pp. 19823–19828, May 2005, doi: 10.1074/jbc.M500216200.

[26] D. Ruggero *et al.*, "Dyskeratosis congenita and cancer in mice deficient in ribosomal RNA modification," *Science*, vol. 299, no. 5604, pp. 259–262, Jan. 2003, doi: 10.1126/science.1079447.

[27] S. Lin, J. Choe, P. Du, R. Triboulet, and R. I. Gregory, "The m6A methyltransferase METTL3 promotes translation in human cancer cells," *Mol. Cell*, vol. 62, no. 3, pp. 335–345, 2016.

[28] P. Boccaletto *et al.*, "MODOMICS: a database of RNA modification pathways. 2017 update," *Nucleic Acids Res.*, vol. 46, no. D1, pp. D303–D307, Jan. 2018, doi: 10.1093/nar/gkx1030.

[29] E. J. Wurtmann and S. L. Wolin, "RNA under attack: cellular handling of RNA damage," *Crit. Rev. Biochem. Mol. Biol.*, vol. 44, no. 1, pp. 34–49, Feb. 2009, doi: 10.1080/10409230802594043.

[30] L. L. Yan and H. S. Zaher, "How do cells cope with RNA damage and its consequences?," *J. Biol. Chem.*, vol. 294, no. 41, pp. 15158–15171, Oct. 2019, doi: 10.1074/jbc.REV119.006513.

[31] W. Dai *et al.*, "Activity-based RNA-modifying enzyme probing reveals DUS3L-mediated dihydrouridylation," *Nat Chem Biol*, vol. 17, no. 1178–1187, 2021, doi: https://doi.org/10.1038/s41589-021-00874-8.

[32] O. Finet *et al.*, "Transcription-Wide Mapping of Dihydrouridine (D) Reveals that mRNA Dihydrouridylation is Essential for Meiotic Chromosome Segregation," *Available SSRN 3569550*.

[33] A. V. Grozhik and S. R. Jaffrey, "Distinguishing RNA modifications from noise in epitranscriptome maps," *Nat. Chem. Biol.*, vol. 14, no. 3, pp. 215–225, Feb. 2018, doi: 10.1038/nchembio.2546.

[34] M. Helm and Y. Motorin, "Detecting RNA modifications in the epitranscriptome: predict and validate," *Nat. Rev. Genet.*, vol. 18, no. 5, pp. 275–291, May 2017, doi: 10.1038/nrg.2016.169.

[35] X. Li, X. Xiong, and C. Yi, "Epitranscriptome sequencing technologies: decoding RNA modifications," *Nat. Methods*, vol. 14, no. 1, pp. 23–31, Dec. 2016, doi: 10.1038/nmeth.4110.

[36] P. A. Limbach and M. J. Paulines, “Going global: the new era of mapping modifications in RNA,” *Wiley Interdiscip. Rev. RNA*, vol. 8, no. 1, Jan. 2017, doi: 10.1002/wrna.1367.
[37] Y. Motorin and M. Helm, “Methods for RNA Modification Mapping Using Deep Sequencing: Established and New Emerging Technologies,” *Genes*, vol. 10, no. 1, p. E35, Jan. 2019, doi: 10.3390/genes10010035.
[38] A. Sarkar *et al.*, “Detecting the epitranscriptome,” *WIREs RNA*, vol. 12, no. 6, p. e1663, 2021, doi: 10.1002/wrna.1663.
[39] S. Schwartz, “Cracking the epitranscriptome,” *RNA N. Y. N*, vol. 22, no. 2, pp. 169–174, Feb. 2016, doi: 10.1261/rna.054502.115.
[40] S. Schwartz and Y. Motorin, “Next-generation sequencing technologies for detection of modified nucleotides in RNAs,” *RNA Biol.*, vol. 14, no. 9, pp. 1124–1137, Sep. 2017, doi: 10.1080/15476286.2016.1251543.
[41] O. Andries, S. Mc Cafferty, S. C. De Smedt, R. Weiss, N. N. Sanders, and T. Kitada, “N(1)-methylpseudouridine-incorporated mRNA outperforms pseudouridine-incorporated mRNA by providing enhanced protein expression and reduced immunogenicity in mammalian cell lines and mice,” *J. Control. Release Off. J. Control. Release Soc.*, vol. 217, pp. 337–344, Nov. 2015, doi: 10.1016/j.jconrel.2015.08.051.
[42] D. Bumcrot, M. Manoharan, V. Koteliansky, and D. W. Y. Sah, “RNAi therapeutics: a potential new class of pharmaceutical drugs,” *Nat. Chem. Biol.*, vol. 2, no. 12, pp. 711–719, Dec. 2006, doi: 10.1038/nchembio839.
[43] K. D. Nance and J. L. Meier, “Modifications in an Emergency: The Role of N1-Methylpseudouridine in COVID-19 Vaccines,” *ACS Cent. Sci.*, vol. 7, no. 5, pp. 748–756, May 2021, doi: 10.1021/acscentsci.1c00197.
[44] N. Pardi and D. Weissman, “Nucleoside Modified mRNA Vaccines for Infectious Diseases,” *Methods Mol. Biol. Clifton NJ*, vol. 1499, pp. 109–121, 2017, doi: 10.1007/978-1-4939-6481-9_6.
[45] U. Sahin, K. Karikó, and Ö. Türeci, “mRNA-based therapeutics--developing a new class of drugs,” *Nat. Rev. Drug Discov.*, vol. 13, no. 10, pp. 759–780, Oct. 2014, doi: 10.1038/nrd4278.
[46] A. A. Seyhan, “RNAi: a potential new class of therapeutic for human genetic disease,” *Hum. Genet.*, vol. 130, no. 5, pp. 583–605, Nov. 2011, doi: 10.1007/s00439-011-0995-8.
[47] M. A. Garcia-Campos *et al.*, “Deciphering the ‘m6A code’ via antibody-independent quantitative profiling,” *Cell*, vol. 178, no. 3, pp. 731–747, 2019.
[48] N. Liu, M. Parisien, Q. Dai, G. Zheng, C. He, and T. Pan, “Probing N6-methyladenosine RNA modification status at single nucleotide resolution in mRNA and long noncoding RNA,” *Rna*, vol. 19, no. 12, pp. 1848–1856, 2013.
[49] K. D. Meyer, “DART-seq: an antibody-free method for global m 6 A detection,” *Nat. Methods*, vol. 16, no. 12, pp. 1275–1280, 2019.
[50] B. Molinie, J. Wang, K. S. Lim, R. Hillebrand, Z. X. Lu, and N. Van Wittenberghe, “620 Howard BD, Daneshvar K, Mullen AC, Dedon P, Xing Y, Giallourakis CC. 621 2016. m (6) A-LAIC-seq reveals the census and complexity of the m (6) A 622 epitranscriptome,” *Nat Methods*, vol. 13, pp. 692–698.
[51] M. Tegowski, M. N. Flamand, and K. D. Meyer, “scDART-seq reveals distinct m6A signatures and mRNA methylation heterogeneity in single cells,” *Mol. Cell*, 2022.

[52] W. Zhang, M. J. Eckwahl, K. I. Zhou, and T. Pan, “Sensitive and quantitative probing of pseudouridine modification in mRNA and long noncoding RNA,” *Rna*, vol. 25, no. 9, pp. 1218–1225, 2019.
[53] K. Chen *et al.*, “High-resolution N6-methyladenosine (m6A) map using photo-crosslinking-assisted m6A sequencing,” *Angew. Chem.*, vol. 127, no. 5, pp. 1607–1610, 2015.
[54] D. Dominissini *et al.*, “Topology of the human and mouse m 6 A RNA methylomes revealed by m 6 A-seq,” *Nature*, vol. 485, no. 7397, pp. 201–206, 2012.
[55] B. Linder, A. V. Grozhik, A. O. Olarerin-George, C. Meydan, C. E. Mason, and S. R. Jaffrey, “Single-nucleotide resolution mapping of m6A and m6Am throughout the transcriptome,” *Nat. Methods*, vol. 12, no. 8, pp. 767–772, Aug. 2015, doi: 10.1038/nmeth.3453.
[56] K. D. Meyer, Y. Saletore, P. Zumbo, O. Elemento, C. E. Mason, and S. R. Jaffrey, “Comprehensive analysis of mRNA methylation reveals enrichment in 3′ UTRs and near stop codons,” *Cell*, vol. 149, no. 7, pp. 1635–1646, 2012.
[57] S. Ke *et al.*, “m ^{6} A mRNA modifications are deposited in nascent pre-mRNA and are not required for splicing but do specify cytoplasmic turnover,” *Genes Dev.*, vol. 31, no. 10, pp. 990–1006, May 2017, doi: 10.1101/gad.301036.117.
[58] U. Lavi, R. Fernandez-Mufioz, and J. E. Darnell, “Content of N-6 methyl adenylic acid in heterogeneous nuclear and messenger RNA of HeLa cells,” *Nucleic Acids Res.*, vol. 4, no. 1, pp. 63–69, 1977, doi: 10.1093/nar/4.1.63.
[59] S. Sommer *et al.*, “The methylation of adenovirus-specific nuclear and cytoplasmic RNA,” *Nucleic Acids Res.*, vol. 3, no. 3, pp. 749–766, Mar. 1976, doi: 10.1093/nar/3.3.749.
[60] K. L. Heilman, R. A. Leach, and M. T. Tuck, “Internal 6-methyladenine residues increase the in vitro translation efficiency of dihydrofolate reductase messenger RNA,” *Int. J. Biochem. Cell Biol.*, vol. 28, no. 7, pp. 823–829, Jul. 1996, doi: 10.1016/1357-2725(96)00014-3.
[61] A. Li *et al.*, “Cytoplasmic m 6 A reader YTHDF3 promotes mRNA translation,” *Cell Res.*, vol. 27, no. 3, pp. 444–447, 2017.
[62] H. Shi *et al.*, “YTHDF3 facilitates translation and decay of N 6-methyladenosine-modified RNA,” *Cell Res.*, vol. 27, no. 3, pp. 315–328, 2017.
[63] X. Wang *et al.*, “N6-methyladenosine modulates messenger RNA translation efficiency,” *Cell*, vol. 161, no. 6, pp. 1388–1399, 2015.
[64] R. A. Coots *et al.*, “m6A facilitates eIF4F-independent mRNA translation,” *Mol. Cell*, vol. 68, no. 3, pp. 504–514, 2017.
[65] K. D. Meyer *et al.*, “5′ UTR m6A promotes cap-independent translation,” *Cell*, vol. 163, no. 4, pp. 999–1010, 2015.
[66] J. Choi *et al.*, “N(6)-methyladenosine in mRNA disrupts tRNA selection and translation-elongation dynamics,” *Nat. Struct. Mol. Biol.*, vol. 23, no. 2, pp. 110–115, Feb. 2016, doi: 10.1038/nsmb.3148.
[67] T. P. Hoernes *et al.*, “Nucleotide modifications within bacterial messenger RNAs regulate their translation and are able to rewire the genetic code,” *Nucleic Acids Res.*, vol. 44, no. 2, pp. 852–862, Jan. 2016, doi: 10.1093/nar/gkv1182.
[68] T. P. Hoernes *et al.*, “Eukaryotic Translation Elongation is Modulated by Single Natural Nucleotide Derivatives in the Coding Sequences of mRNAs,” *Genes*, vol. 10, no. 2, p. E84, Jan. 2019, doi: 10.3390/genes10020084.

[69] B. H. Hudson and H. S. Zaher, “O6-Methylguanosine leads to position-dependent effects on ribosome speed and fidelity,” *RNA N. Y. N*, vol. 21, no. 9, pp. 1648–1659, Sep. 2015, doi: 10.1261/rna.052464.115.
[70] K. Karikó *et al.*, “Incorporation of pseudouridine into mRNA yields superior nonimmunogenic vector with increased translational capacity and biological stability,” *Mol. Ther. J. Am. Soc. Gene Ther.*, vol. 16, no. 11, pp. 1833–1840, Nov. 2008, doi: 10.1038/mt.2008.200.
[71] T. Smith, M. Tardu, H. R. Khatri, and K. S. Koutmou, “mRNA and tRNA modification states influence ribosome frame maintenance during poly(lysine) peptide synthesis,” *Submitted*, Submitted.
[72] C. You, X. Dai, and Y. Wang, “Position-dependent effects of regioisomeric methylated adenine and guanine ribonucleosides on translation,” *Nucleic Acids Res.*, vol. 45, no. 15, pp. 9059–9067, Sep. 2017, doi: 10.1093/nar/gkx515.
[73] P. F. Agris, “Decoding the genome: a modified view,” *Nucleic Acids Res.*, vol. 32, no. 1, pp. 223–238, 2004, doi: 10.1093/nar/gkh185.
[74] B. Liu *et al.*, “A potentially abundant junctional RNA motif stabilized by m6A and Mg2,” *Nat. Commun.*, vol. 9, no. 1, p. 2761, Jul. 2018, doi: 10.1038/s41467-018-05243-z.
[75] D. E. Eyler *et al.*, “Pseudouridinylation of mRNA coding sequences alters translation,” *Proc. Natl. Acad. Sci. U. S. A.*, vol. 116, no. 46, pp. 23068–23074, Nov. 2019, doi: 10.1073/pnas.1821754116.
[76] D. Dominissini *et al.*, “The dynamic N(1)-methyladenosine methylome in eukaryotic messenger RNA,” *Nature*, vol. 530, no. 7591, pp. 441–446, Feb. 2016, doi: 10.1038/nature16998.
[77] A. V. Grozhik, A. O. Olarerin-George, M. Sindelar, X. Li, S. S. Gross, and S. R. Jaffrey, “Antibody cross-reactivity accounts for widespread appearance of m1A in 5’UTRs,” *Nat. Commun.*, vol. 10, no. 1, p. 5126, Nov. 2019, doi: 10.1038/s41467-019-13146-w.
[78] M. Safra *et al.*, “The m1A landscape on cytosolic and mitochondrial mRNA at single-base resolution,” *Nature*, vol. 551, no. 7679, pp. 251–255, Nov. 2017, doi: 10.1038/nature24456.
[79] S. Schwartz, “m1A within cytoplasmic mRNAs at single nucleotide resolution: a reconciled transcriptome-wide map,” *RNA N. Y. N*, vol. 24, no. 11, pp. 1427–1436, Nov. 2018, doi: 10.1261/rna.067348.118.
[80] H. Zhou *et al.*, “m(1)A and m(1)G disrupt A-RNA structure through the intrinsic instability of Hoogsteen base pairs,” *Nat. Struct. Mol. Biol.*, vol. 23, no. 9, pp. 803–810, Sep. 2016, doi: 10.1038/nsmb.3270.
[81] E. N. Thomas, K. Q. Kim, E. P. McHugh, T. Marcinkiewicz, and H. S. Zaher, “Alkylative damage of mRNA leads to ribosome stalling and rescue by trans translation in bacteria,” *eLife*, vol. 9, p. e61984, Sep. 2020, doi: 10.7554/eLife.61984.
[82] S. Meydan and N. R. Guydosh, “A cellular handbook for collided ribosomes: surveillance pathways and collision types,” *Curr. Genet.*, vol. 67, no. 1, pp. 19–26, Feb. 2021, doi: 10.1007/s00294-020-01111-w.
[83] B. L. Bass *et al.*, “A standardized nomenclature for adenosine deaminases that act on RNA,” *RNA N. Y. N*, vol. 3, no. 9, pp. 947–949, Sep. 1997.
[84] B. L. Bass and H. Weintraub, “An unwinding activity that covalently modifies its double-stranded RNA substrate,” *Cell*, vol. 55, no. 6, pp. 1089–1098, Dec. 1988, doi: 10.1016/0092-8674(88)90253-x.

[85] H. A. Hundley and B. L. Bass, “ADAR editing in double-stranded UTRs and other noncoding RNA sequences,” *Trends Biochem. Sci.*, vol. 35, no. 7, pp. 377–383, Jul. 2010, doi: 10.1016/j.tibs.2010.02.008.
[86] S. Srinivasan, A. G. Torres, and L. Ribas de Pouplana, “Inosine in Biology and Disease,” *Genes*, vol. 12, no. 4, p. 600, Apr. 2021, doi: 10.3390/genes12040600.
[87] E. Picardi, C. Manzari, F. Mastropasqua, I. Aiello, A. M. D’Erchia, and G. Pesole, “Profiling RNA editing in human tissues: towards the inosinome Atlas,” *Sci. Rep.*, vol. 5, p. 14941, Oct. 2015, doi: 10.1038/srep14941.
[88] C. Basilio, A. J. Wahba, P. Lengyel, J. F. Speyer, and S. Ochoa, “Synthetic polynucleotides and the amino acid code. V,” *Proc. Natl. Acad. Sci. U. S. A.*, vol. 48, pp. 613–616, Apr. 1962, doi: 10.1073/pnas.48.4.613.
[89] K. Licht, M. Hartl, F. Amman, D. Anrather, M. P. Janisiw, and M. F. Jantsch, “Inosine induces context-dependent recoding and translational stalling,” *Nucleic Acids Res.*, vol. 47, no. 1, pp. 3–14, Jan. 2019, doi: 10.1093/nar/gky1163.
[90] B. Sommer, M. Köhler, R. Sprengel, and P. H. Seeburg, “RNA editing in brain controls a determinant of ion flow in glutamate-gated channels,” *Cell*, vol. 67, no. 1, Art. no. 1, Oct. 1991, doi: 10.1016/0092-8674(91)90568-j.
[91] T. P. Hoernes *et al.*, “Translation of non-standard codon nucleotides reveals minimal requirements for codon-anticodon interactions,” *Nat. Commun.*, vol. 9, no. 1, p. 4865, Nov. 2018, doi: 10.1038/s41467-018-07321-8.
[92] T. P. Hoernes *et al.*, “Atomic mutagenesis of stop codon nucleotides reveals the chemical prerequisites for release factor-mediated peptide release,” *Proc. Natl. Acad. Sci. U. S. A.*, vol. 115, no. 3, pp. E382–E389, Jan. 2018, doi: 10.1073/pnas.1714554115.
[93] K. Ito, M. Uno, and Y. Nakamura, “A tripeptide ‘anticodon’ deciphers stop codons in messenger RNA,” *Nature*, vol. 403, no. 6770, pp. 680–684, Feb. 2000, doi: 10.1038/35001115.
[94] T. M. Carlile, M. F. Rojas-Duran, B. Zinshteyn, H. Shin, K. M. Bartoli, and W. V. Gilbert, “Pseudouridine profiling reveals regulated mRNA pseudouridylation in yeast and human cells,” *Nature*, vol. 515, no. 7525, pp. 143–146, Nov. 2014, doi: 10.1038/nature13802.
[95] X. Li *et al.*, “Chemical pulldown reveals dynamic pseudouridylation of the mammalian transcriptome,” *Nat. Chem. Biol.*, vol. 11, no. 8, pp. 592–597, Aug. 2015, doi: 10.1038/nchembio.1836.
[96] A. F. Lovejoy, D. P. Riordan, and P. O. Brown, “Transcriptome-wide mapping of pseudouridines: pseudouridine synthases modify specific mRNAs in S. cerevisiae,” *PloS One*, vol. 9, no. 10, p. e110799, 2014, doi: 10.1371/journal.pone.0110799.
[97] S. Schwartz *et al.*, “Transcriptome-wide mapping reveals widespread dynamic-regulated pseudouridylation of ncRNA and mRNA,” *Cell*, vol. 159, no. 1, pp. 148–162, Sep. 2014, doi: 10.1016/j.cell.2014.08.028.
[98] N. M. Martinez *et al.*, “Pseudouridine synthases modify human pre-mRNA co-transcriptionally and affect pre-mRNA processing,” *Mol. Cell*, 2022.
[99] M. A. Nakamoto, A. F. Lovejoy, A. M. Cygan, and J. C. Boothroyd, “mRNA pseudouridylation affects RNA metabolism in the parasite Toxoplasma gondii,” *RNA N. Y. N*, vol. 23, no. 12, pp. 1834–1849, Dec. 2017, doi: 10.1261/rna.062794.117.
[100] B. R. Anderson *et al.*, “Incorporation of pseudouridine into mRNA enhances translation by diminishing PKR activation,” *Nucleic Acids Res.*, vol. 38, no. 17, pp. 5884–5892, Sep. 2010, doi: 10.1093/nar/gkq347.

[101] E. Svidritskiy, R. Madireddy, and A. A. Korostelev, “Structural Basis for Translation Termination on a Pseudouridylated Stop Codon,” *J. Mol. Biol.*, vol. 428, no. 10 Pt B, pp. 2228–2236, May 2016, doi: 10.1016/j.jmb.2016.04.018.
[102] Y. V. Svitkin, A.-C. Gingras, and N. Sonenberg, “Membrane-dependent relief of translation elongation arrest on pseudouridine- and N1-methyl-pseudouridine-modified mRNAs,” *Nucleic Acids Res.*, p. gkab1241, Dec. 2021, doi: 10.1093/nar/gkab1241.
[103] I. S. Fernández, C. L. Ng, A. C. Kelley, G. Wu, Y.-T. Yu, and V. Ramakrishnan, “Unusual base pairing during the decoding of a stop codon by the ribosome,” *Nature*, vol. 500, no. 7460, pp. 107–110, Aug. 2013, doi: 10.1038/nature12302.
[104] J. Karijolich and Y.-T. Yu, “Converting nonsense codons into sense codons by targeted pseudouridylation,” *Nature*, vol. 474, no. 7351, pp. 395–398, Jun. 2011, doi: 10.1038/nature10165.
[105] A. J. Shatkin, “Capping of eucaryotic mRNAs,” *Cell*, vol. 9, no. 4, Part 2, pp. 645–653, Dec. 1976, doi: 10.1016/0092-8674(76)90128-8.
[106] L. Malbec *et al.*, “Dynamic methylome of internal mRNA N7-methylguanosine and its regulatory role in translation,” *Cell Res.*, vol. 29, no. 11, pp. 927–941, Nov. 2019, doi: 10.1038/s41422-019-0230-z.
[107] J.-M. Chu *et al.*, “Existence of Internal N7-Methylguanosine Modification in mRNA Determined by Differential Enzyme Treatment Coupled with Mass Spectrometry Analysis,” *ACS Chem. Biol.*, vol. 13, no. 12, pp. 3243–3250, Dec. 2018, doi: 10.1021/acschembio.7b00906.
[108] L.-S. Zhang *et al.*, “Transcriptome-wide Mapping of Internal N7-Methylguanosine Methylome in Mammalian mRNA,” *Mol. Cell*, vol. 74, no. 6, pp. 1304-1316.e8, Jun. 2019, doi: 10.1016/j.molcel.2019.03.036.
[109] W. Filipowicz, “Functions of the 5′-terminal m7G cap in eukaryotic mRNA,” *FEBS Lett.*, vol. 96, no. 1, pp. 1–11, 1978, doi: 10.1016/0014-5793(78)81049-7.
[110] A. Ramanathan, G. B. Robb, and S.-H. Chan, “mRNA capping: biological functions and applications,” *Nucleic Acids Res.*, vol. 44, no. 16, pp. 7511–7526, 2016.
[111] C. Enroth, L. D. Poulsen, S. Iversen, F. Kirpekar, A. Albrechtsen, and J. Vinther, “Detection of internal N7-methylguanosine (m7G) RNA modifications by mutational profiling sequencing,” *Nucleic Acids Res.*, vol. 47, no. 20, p. e126, Nov. 2019, doi: 10.1093/nar/gkz736.
[112] R. V. Kastrup and P. G. Schmidt, “1H NMR of valine tRNA modified bases. Evidence for multiple conformations,” *Nucleic Acids Res.*, vol. 5, no. 1, pp. 257–269, Jan. 1978, doi: 10.1093/nar/5.1.257.
[113] H. Sierzputowska-Gracz, H. D. Gopal, and P. F. Agris, “Comparative structural analysis of 1-methyladenosine, 7-methylguanosine, ethenoadenosine and their protonated salts IV: 1H, 13C, and 15N NMR studies at natural isotope abundance,” *Nucleic Acids Res.*, vol. 14, no. 19, pp. 7783–7801, Oct. 1986, doi: 10.1093/nar/14.19.7783.
[114] H. Kersten, M. Albani, E. Männlein, R. Praisler, P. Wurmbach, and K. H. Nierhaus, “On the role of ribosylthymine in prokaryotic tRNA function,” *Eur. J. Biochem.*, vol. 114, no. 2, pp. 451–456, Feb. 1981, doi: 10.1111/j.1432-1033.1981.tb05166.x.
[115] T. Hofer, C. Badouard, E. Bajak, J.-L. Ravanat, A. Mattsson, and I. A. Cotgreave, “Hydrogen peroxide causes greater oxidation in cellular RNA than in DNA,” *Biol. Chem.*, vol. 386, no. 4, pp. 333–337, Apr. 2005, doi: 10.1515/BC.2005.040.

[116] I. Parsa, S. Friedman, and C. M. Cleary, “Visualization of O6-methylguanine in target cell nuclei of dimethylnitrosamine-treated human pancreas by a murine monoclonal antibody,” *Carcinogenesis*, vol. 8, no. 6, pp. 839–846, Jun. 1987, doi: 10.1093/carcin/8.6.839.
[117] G. W. Hsu, M. Ober, T. Carell, and L. S. Beese, “Error-prone replication of oxidatively damaged DNA by a high-fidelity DNA polymerase,” *Nature*, vol. 431, no. 7005, pp. 217–221, Sep. 2004, doi: 10.1038/nature02908.
[118] B. Sampoli Benítez, Z. R. Barbati, K. Arora, J. Bogdanovic, and T. Schlick, “How DNA polymerase X preferentially accommodates incoming dATP opposite 8-oxoguanine on the template,” *Biophys. J.*, vol. 105, no. 11, pp. 2559–2568, Dec. 2013, doi: 10.1016/j.bpj.2013.10.014.
[119] X. Shan, Y. Chang, and C. G. Lin, “Messenger RNA oxidation is an early event preceding cell death and causes reduced protein expression,” *FASEB J. Off. Publ. Fed. Am. Soc. Exp. Biol.*, vol. 21, no. 11, pp. 2753–2764, Sep. 2007, doi: 10.1096/fj.07-8200com.
[120] C. L. Simms, B. H. Hudson, J. W. Mosior, A. S. Rangwala, and H. S. Zaher, “An active role for the ribosome in determining the fate of oxidized mRNA,” *Cell Rep.*, vol. 9, no. 4, pp. 1256–1264, Nov. 2014, doi: 10.1016/j.celrep.2014.10.042.
[121] A. A. Bicknell and E. P. Ricci, “When mRNA translation meets decay,” *Biochem. Soc. Trans.*, vol. 45, no. 2, pp. 339–351, Apr. 2017, doi: 10.1042/BST20160243.
[122] E. D. Karousis and O. Mühlemann, “Nonsense-Mediated mRNA Decay Begins Where Translation Ends,” *Cold Spring Harb. Perspect. Biol.*, vol. 11, no. 2, p. a032862, Feb. 2019, doi: 10.1101/cshperspect.a032862.
[123] A. van Hoof and E. J. Wagner, “A brief survey of mRNA surveillance,” *Trends Biochem. Sci.*, vol. 36, no. 11, Art. no. 11, Nov. 2011, doi: 10.1016/j.tibs.2011.07.005.
[124] P. F. Agris, “Bringing order to translation: the contributions of transfer RNA anticodon-domain modifications,” *EMBO Rep.*, vol. 9, no. 7, pp. 629–635, Jul. 2008, doi: 10.1038/embor.2008.104.
[125] J. T. Anderson and X. Wang, “Nuclear RNA surveillance: no sign of substrates tailing off,” *Crit. Rev. Biochem. Mol. Biol.*, vol. 44, no. 1, pp. 16–24, Feb. 2009, doi: 10.1080/10409230802640218.
[126] M. Helm, “Post-transcriptional nucleotide modification and alternative folding of RNA,” *Nucleic Acids Res.*, vol. 34, no. 2, pp. 721–733, 2006, doi: 10.1093/nar/gkj471.
[127] D. T. Dubin and R. H. Taylor, “The methylation state of poly A-containing messenger RNA from cultured hamster cells,” *Nucleic Acids Res.*, vol. 2, no. 10, pp. 1653–1668, Oct. 1975, doi: 10.1093/nar/2.10.1653.
[128] J. E. Squires *et al.*, “Widespread occurrence of 5-methylcytosine in human coding and non-coding RNA,” *Nucleic Acids Res.*, vol. 40, no. 11, pp. 5023–5033, 2012.
[129] J. E. Squires and T. Preiss, “Function and detection of 5-methylcytosine in eukaryotic RNA,” *Epigenomics*, vol. 2, no. 5, pp. 709–715, Oct. 2010, doi: 10.2217/epi.10.47.
[130] M. Tardu, J. D. Jones, R. T. Kennedy, Q. Lin, and K. S. Koutmou, “Identification and quantification of modified nucleosides in Saccharomyces cerevisiae mRNAs,” *ACS Chem. Biol.*, vol. 14, no. 7, pp. 1403–1409, 2019.
[131] T. Huang, W. Chen, J. Liu, N. Gu, and R. Zhang, “Genome-wide identification of mRNA 5-methylcytosine in mammals,” *Nat. Struct. Mol. Biol.*, vol. 26, no. 5, pp. 380–388, May 2019, doi: 10.1038/s41594-019-0218-x.

[132] H. Tang *et al.*, "NSun2 delays replicative senescence by repressing p27 (KIP1) translation and elevating CDK1 translation," *Aging*, vol. 7, no. 12, pp. 1143–1158, Dec. 2015, doi: 10.18632/aging.100860.
[133] J. Xing *et al.*, "NSun2 Promotes Cell Growth via Elevating Cyclin-Dependent Kinase 1 Translation," *Mol. Cell. Biol.*, vol. 35, no. 23, pp. 4043–4052, Dec. 2015, doi: 10.1128/MCB.00742-15.
[134] D. Arango *et al.*, "Acetylation of cytidine in mRNA promotes translation efficiency," *Cell*, vol. 175, no. 7, pp. 1872–1886, 2018.
[135] A. Sas-Chen *et al.*, "Dynamic RNA acetylation revealed by quantitative cross-evolutionary mapping," *Nature*, vol. 583, no. 7817, pp. 638–643, Jul. 2020, doi: 10.1038/s41586-020-2418-2.
[136] L. Ayadi, A. Galvanin, F. Pichot, V. Marchand, and Y. Motorin, "RNA ribose methylation (2'-O-methylation): Occurrence, biosynthesis and biological functions," *Biochim. Biophys. Acta Gene Regul. Mech.*, vol. 1862, no. 3, pp. 253–269, Mar. 2019, doi: 10.1016/j.bbagrm.2018.11.009.
[137] J. Choi *et al.*, "2'-O-methylation in mRNA disrupts tRNA decoding during translation elongation," *Nat. Struct. Mol. Biol.*, vol. 25, no. 3, pp. 208–216, Mar. 2018, doi: 10.1038/s41594-018-0030-z.
[138] H. Abou Assi *et al.*, "2′-O-Methylation can increase the abundance and lifetime of alternative RNA conformational states," *Nucleic Acids Res.*, vol. 48, no. 21, pp. 12365–12379, Oct. 2020, doi: 10.1093/nar/gkaa928.
[139] R. C. Brand, J. Klootwijk, R. J. Planta, and B. E. Maden, "Biosynthesis of a hypermodified nucleotide in Saccharomyces carlsbergensis 17S and HeLa-cell 18S ribosomal ribonucleic acid," *Biochem. J.*, vol. 169, no. 1, pp. 71–77, Jan. 1978, doi: 10.1042/bj1690071.
[140] C. G. Edmonds *et al.*, "Posttranscriptional modification of tRNA in thermophilic archaea (Archaebacteria)," *J. Bacteriol.*, vol. 173, no. 10, pp. 3138–3148, May 1991, doi: 10.1128/jb.173.10.3138-3148.1991.
[141] Y. V. Svitkin, Y. M. Cheng, T. Chakraborty, V. Presnyak, M. John, and N. Sonenberg, "N1-methyl-pseudouridine in mRNA enhances translation through eIF2α-dependent and independent mechanisms by increasing ribosome density," *Nucleic Acids Res.*, vol. 45, no. 10, pp. 6023–6036, Jun. 2017, doi: 10.1093/nar/gkx135.
[142] D. M. Mauger *et al.*, "mRNA structure regulates protein expression through changes in functional half-life," *Proc. Natl. Acad. Sci. U. S. A.*, vol. 116, no. 48, pp. 24075–24083, Nov. 2019, doi: 10.1073/pnas.1908052116.
[143] Y. V. Svitkin, A.-C. Gingras, and N. Sonenberg, "Membrane-dependent relief of translation elongation arrest on pseudouridine- and N1-methyl-pseudouridine-modified mRNAs," *Nucleic Acids Res.*, p. gkab1241, Dec. 2021, doi: 10.1093/nar/gkab1241.
[144] Y. Ding, Y. Tang, C. K. Kwok, Y. Zhang, P. C. Bevilacqua, and S. M. Assmann, "In vivo genome-wide profiling of RNA secondary structure reveals novel regulatory features," *Nature*, vol. 505, no. 7485, pp. 696–700, Jan. 2014, doi: 10.1038/nature12756.
[145] R. Rauscher and Z. Ignatova, "Timing during translation matters: synonymous mutations in human pathologies influence protein folding and function," *Biochem. Soc. Trans.*, vol. 46, no. 4, pp. 937–944, Aug. 2018, doi: 10.1042/BST20170422.

[146] A. Re, T. Joshi, E. Kulberkyte, Q. Morris, and C. T. Workman, “RNA-protein interactions: an overview,” *Methods Mol. Biol. Clifton NJ*, vol. 1097, pp. 491–521, 2014, doi: 10.1007/978-1-62703-709-9_23.
[147] D. R. Schoenberg, “Mechanisms of endonuclease-mediated mRNA decay,” *Wiley Interdiscip. Rev. RNA*, vol. 2, no. 4, pp. 582–600, Aug. 2011, doi: 10.1002/wrna.78.
[148] M. A. Garcia-Campos *et al.*, “Deciphering the ‘m6A code’ via antibody-independent quantitative profiling,” *Cell*, vol. 178, no. 3, Art. no. 3, 2019.
[149] M. K. Purchal *et al.*, “Pseudouridine synthase 7 is an opportunistic enzyme that binds and modifies substrates with diverse sequences and structures,” *Proc. Natl. Acad. Sci.*, vol. 119, no. 4, p. e2109708119, Jan. 2022, doi: 10.1073/pnas.2109708119.
[150] G. Prus, A. Hoegl, B. T. Weinert, and C. Choudhary, “Analysis and Interpretation of Protein Post-Translational Modification Site Stoichiometry,” *Trends Biochem. Sci.*, vol. 44, no. 11, pp. 943–960, Nov. 2019, doi: 10.1016/j.tibs.2019.06.003.

Chapter 2 Pseudouridinylation Of mRNA Coding Sequences Alters Translation[1]

Work presented in this chapter was published in the

Proceedings of the National Academy of Sciences.

Monika K. Franco†, Eyler, Daniel E. †, Zahra Batool, Monica Z. Wu, Michelle L. Dubuke, Malgorzata Dobosz-Bartoszek, Joshua D. Jones, Yury S. Polikanov, Bijoyita Roy, and Kristin S. Koutmou. "Pseudouridinylation of mRNA coding sequences alters translation." 116, no. 46 *Proc. Natl. Acad. Sci. USA* **(2019)**: 23068-23074.

† Authors contributed equally

2.1 Introduction

Nucleosides in messenger RNAs (mRNAs) can be enzymatically modified post-transcriptionally (1, 2) to expand the chemical and topological properties of these essential biomolecules. Transcriptome-wide mapping of individual modifications revealed the presence of modifications in both the untranslated and protein-coding regions of mRNAs (2, 3). The localization of modifications throughout mRNAs suggests that modifications could potentially alter protein production by multiple mechanisms, including affecting interactions of the translating ribosomal complex with the mRNA, mRNA structure, and mRNA stability. Amongst

[1] In this paper, I performed work on miscoding, and most of the RF work (P site data, release factors rates). Dr. Dan Eyler did the GTP hydrolysis assays, some work with the miscoding assays, and amino acid addition. Dr. Monica Z. Wu, Dr. Michelle L. Dubuke, Dr. Malgorzata Dobosz-Bartoszek, and Dr. Bijoyit Roy all did work contributing to the in-cellular work in HEK cells, contributing to investigating pseudouridine and miscoding in-cellular. Dr. Zahra Batool and Dr. Yury S. Polikanov did the crystal structure work.

the mRNA modifications identified to date, N6-methyladenonsine (m^6A) and pseudouridine (Ψ) are the most prevalent (2, 4). m^6A modifications are estimated to occur in half of the human mRNAs and cells contain a complement of proteins reported to write, read, and erase the modification (5, 6).

Ψ has been mapped to hundreds of mRNA sequences (7-9) and mass spectrometry studies report the Ψ/U ratio in human cell lines to be comparable to that of m^6A/A (~0.3% for Ψ/U vs. ~0.5% m^6A/A) (10, 11). While the frequency of Ψ at most mapped sites not been established, estimates of Ψ-frequency based on Ψ-seq experiments, and the direct measurement of Ψ occupancy at a discrete site (in EEF1A1) indicate that Ψ can be incorporated at frequencies (> 50%) comparable to well-occupied m^6A sites (8, 10). The preponderance of Ψ moieties in mRNA are in coding regions (> 60%), and while a host of pseudouridinylating enzymes have been identified that incorporate Ψ into both mRNAs and non-coding RNAs in a reproducible, specific, and inducible manner (7-10, 12-14), no proteins that read or erase Ψ have been discovered. Consequently, the ribosome surely encounters Ψ in cells and it has been hypothesized that it could serve as a key cellular component to read Ψ in mRNAs (2). How, or even if, mRNA pseudouridinylation contributes to gene expression is not yet apparent. Reporter-based studies in human cells and bacterial lysates come to conflicting conclusions regarding the role of Ψ, with some studies suggesting that the presence of Ψ in mRNA codons increases protein production (15) and others reporting a reduction in protein synthesis (16, 17). The clearest evidence of a biological role for Ψ in mRNAs comes from studies in the parasite *Toxoplasma gondii* where Ψ increases mRNA stability and facilitates parasite differentiation (12, 13). Regardless of whether or not further studies reveal a significant role for Ψ in gene

regulation, the ribosome surely translates Ψ-containing codons in cells and it is important to establish the possible outcomes of these events.

Since Ψ can alter the fundamental properties of RNAs, including their secondary structures and base-pairing abilities (18-20), it has been proposed that one consequence of Ψ could be to promote the incorporation of multiple amino acids on a single codon (2, 8). Indeed, Ψ-containing stop codons have been observed to direct the nonsense suppression of translation termination (14, 21), though the effect of Ψ in stop codons remains an unresolved question (22). Thus far, differential decoding of Ψ-containing sense codons has not yet been reported (16, 17). Establishing if Ψ can alter tRNA selection on the ribosome is a timely question given that a wide range of modified nucleosides (Ψ, N1-methyl-Ψ, 2-thiouridine, 5-methyl-cytosine) are being routinely inserted into synthetic mRNAs at high stoichiometric ratios for therapeutic applications (15).

Identifying the consequences of Ψ mRNA modification is complicated in cells because the enzymes that incorporate Ψ into mRNA also catalyze Ψ addition to non-coding RNA species. Furthermore, the impact of mRNA and protein stability on protein output can be difficult to deconvolute from effects on translation in cells. Here, we directly investigate the mechanistic effects of mRNA pseudouridinylation on translation using *in vitro* enzymology as well as X-ray crystallography and support our *in vitro* conclusions with cell-based approaches. Our results demonstrate that the insertion of a single Ψ perturbs ribosome function and promotes the low-level synthesis of multiple peptide products from a single mRNA sequence in a context dependent manner. These studies provide a foundation for understanding the effects of Ψ modification on mRNA translation in cells.

2.2 Results

2.2.1 Ψ reduces rate constants for translation elongation and EF-Tu GTPase activation

We assessed if Ψ impacts translation by performing kinetic assays with a well-established reconstituted E. coli translation system (23, 24). In our assays, 70 nM of E. coli 70S ribosome complexes containing ^{f}Met-^{35}S-labeled methionine in the P site and a UUU codon in the A site were reacted with 0.5-5 μM Phe-tRNA^{Phe}•EF-Tu•GTP (ternary complex) at 37^{o} C and the products were visualized by electrophoretic TLC (Fig. S1). We measured the rate of phenylalanine (Phe) addition on UUU, ΨUU, UΨU, and UUΨ codons because the rate constant for dipeptide formation on UUU codon is well established (23) and Ψ is found regularly in UUU codons in cells (7, 10) (Fig. 1B and C; details of oligonucleotide quality assessment by UHPLC-MS/MS in SI Appendix). Phe was incorporated robustly on unmodified mRNAs with reaction end-point and rate constants similar to those previously reported (23, 25) (Fig. 1, Table S1). ^{f}Met-Phe di-peptide formation catalyzed by ribosomes on Ψ-containing mRNAs also went to completion (Table S1) and the k_{max} for Phe incorporation under 5 μM concentrations of Phe-tRNA^{Phe} (15.7 ± 0.9 s^{-1}) was unaffected (Fig. 1B, Table S1). However, the rate constant for ^{f}Met-Phe di-peptide formation was modestly reduced by 2-fold under reaction conditions with sub-saturating concentrations of Phe-tRNA^{Phe} (Fig. 1C, Table S1). We approximated the $K_{1/2}$ for Phe incorporation on UUU and ΨUU and found that the value is increased by 2-fold on ΨUU. Consistent with this we find that the production of a full-length luciferase peptide in the reconstituted in vitro translation system (NEB PURExpress) is 3-fold slower on luciferase reporter mRNA with every U substituted for Ψ (Fig. S2).

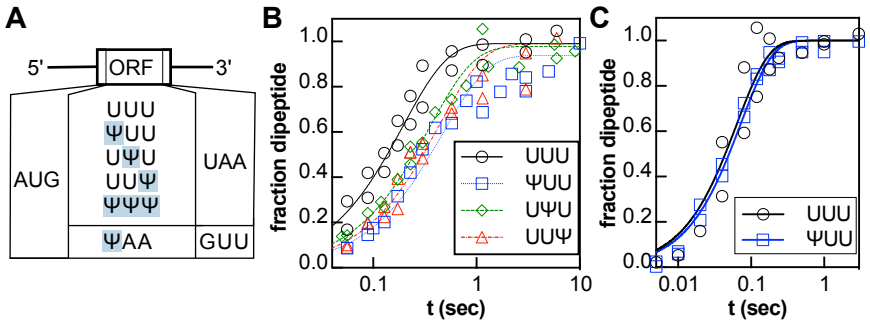

Figure 2.1: ***Ψ changes amino acid incorporation by the ribosome. (A)*** *Coding sequences for the Ψ-containing mRNA constructs.* ***(B-C)*** *Time courses displaying the formation of ^{f}Met-Phe peptide on an unmodified and modified UUU codon [UUU (black circles), ΨUU (blue squares), UΨU (green diamonds), UUΨ (red triangles)]. Time courses were collected under single-turnover conditions (70-100 nM 70S ribosome initiation complexes, with either* ***(B)*** *near-saturating (1 μM) or* ***(C)*** *high (5 μM) levels of Phe-tRNA^{Phe}.*

The decreased observed rate constants for amino acid incorporation on pseudouridinylated codons under sub- and near-saturating concentrations of Phe-tRNA^{Phe} could reflect changes in the rate constants for one or more of the four upstream kinetic steps (23) (Fig. S3). To gain further insight into which steps are affected by Ψ, we measured the rate constants for GTP hydrolysis by EF-Tu after binding of the aa-tRNA●EF-Tu●GTP ternary complex to the A site. In these assays, 1.8 μM ^{3}H-^{f}Met-labeled complexes were mixed with 100 nM of α-^{32}P-GTP labeled ternary complex. The observed rate constant for GTP hydrolysis on the unmodified UUU codon ($k_{GTP} = 78 \pm 10$ s^{-1}) was consistent with previously reported values (23), while the rate constant was slower on the ΨUU codon ($k_{GTP} = 42 \pm 6$ s^{-1}) (Fig. 2A and B, Table S1).

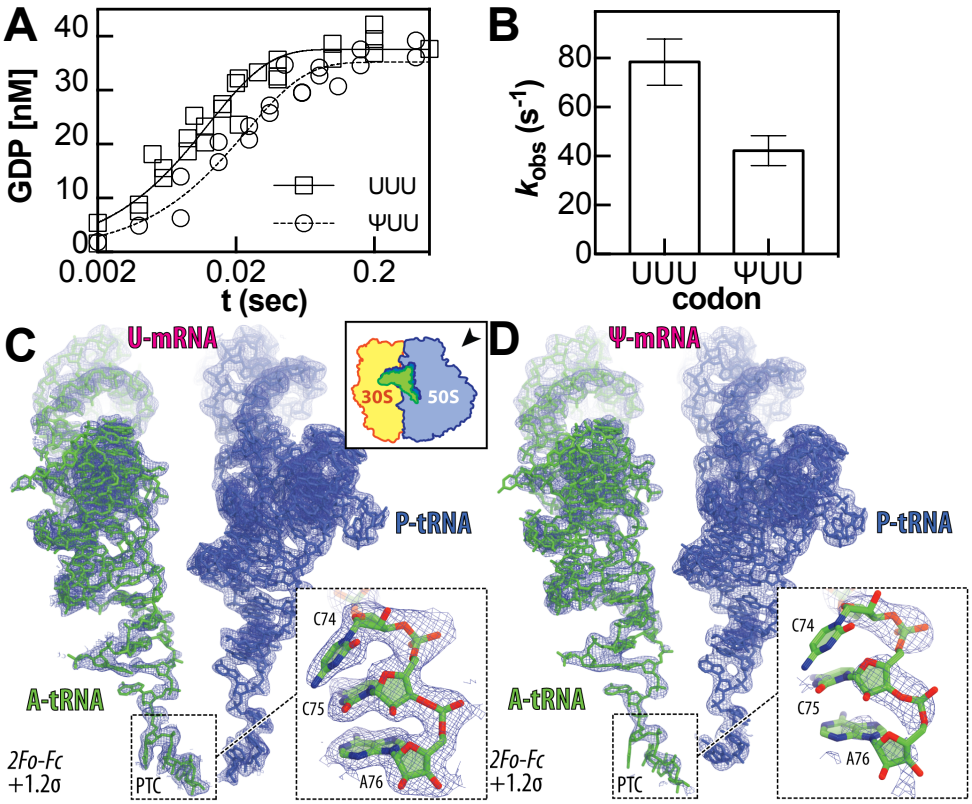

Figure 2.2: ***Ψ alters GTP hydrolysis during ternary complex binding to the ribosome (A)*** *Time courses displaying the formation of GDP when 1.6 μM ^{3}H-fMet-labeled complexes were mixed with 100 nM of γ-^{32}P-GTP labeled ternary complex formed with Phe-tRNA^{Phe} and nucleotide-free EF-Tu. Single-exponential curves were fitted to data collected in three independent experiments.* ***(B)*** *Observed rate constants for data fit in* ***(A).*** *Error bars are the standard error of the fitted value of k_{obs}.* ***(C, D)*** *2Fo-Fc electron difference Fourier maps (blue mesh) for the ribosome-bound A site (green) and the P site (dark blue) tRNAs interacting with unmodified* ***(C)*** *or Ψ-containing mRNA* ***(D)****. In* ***(C)****, both the map and the model are from PDB entry 4Y4P. The direction of the view for both panels in indicated on the upper right inset in panel* ***(C)****. The refined models of mRNA (magenta) and tRNA (green) are displayed in their respective electron densities contoured at 1.2σ. Close-up views of the CCA-ends of the A-site tRNAs are shown by lower right insets in each of the panels. The electron density corresponding to the CCA-end of the tRNA interacting with the Ψ-containing mRNA is much weaker compared to the CCA-end of the tRNA interacting with the unmodified mRNA, while the electron density corresponding to the bodies of the A-site tRNAs are comparable between the two complexes.*

2.2.2 tRNA^{Phe} 3'CCA is not ordered in the crystal structure of 70S bacterial ribosome complex with ΨUU

To investigate whether the presence of Ψ in the mRNA codon alters tRNA interactions with the ribosome during translation elongation, we solved a crystal structure of Thermus thermophilus 70S ribosome in complex with ΨUU-containing mRNA, P-site tRNA$_i^{Met}$ and A-site tRNA^{Phe} (on a ΨUU A site codon) at 2.9 Å resolution (Figs. 2C and 2D, Table S2, PDB 6OU1). We compared this structure to our previously published structure of the same 70S ribosome complex containing tRNA^{Phe} from the same preparation in the ribosomal A site recognizing

unmodified Phe codon. In our ΨUU-containing structure we observed a strong electron density corresponding to the body and the anticodon stem-loop of the A-site $tRNA^{Phe}$ interacting with the mRNA codon (Fig. S4), similar to the previous structures containing unmodified mRNAs (26). The RMSD value of 0.612 calculated for the entire body of the A-site tRNA (residues 1-73) indicates that it remains in its normal position.

The observed electron density corresponding to the CCA-end of tRNAs in the ribosomal A site is strong and well-defined in most of the previously published structures (26). As expected, this is the case for the fully accommodated CCA-end of the $tRNA^{Phe}$ interacting with the unmodified mRNA (Fig. 2C). However, when the Ψ-containing mRNA is present we observed no electron density for the bases of the CCA-end of the same A-site $tRNA^{Phe}$ even though the rest of the tRNA body was visible (Fig. 2D). Even after the refinement of our X-ray data against a 70S ribosome model containing full-length $tRNA^{Phe}$ in the A site, no density for the bases of the CCA-end could be observed in the (2Fo-Fc) electron density map (Fig. 2D, inset). These data point to the flexibility of the CCA-end of the A-site tRNA interacting with the ΨUU codon. As a consequence, the CCA end of this tRNA is unable to form canonical interactions in the A site of the peptidyl transferase center (PTC) on the large ribosomal subunit – formation of the Watson-Crick base-pair between the C75 nucleotide of the A-site tRNA and the G2553 of the 23S rRNA. Since the primary difference of the 70S complex crystallized in this study is the substitution of the uridine with Ψ in a canonical Phe codon, the absence of the CCA-end in the electron density is likely attributed to changes in codon decoding, which occur at the opposite end of the tRNA molecule in the decoding center and apparently propagates all the way to the PTC (Figs. 2C, D). The displacement of the A-site tRNA CCA-end has been observed in multiple structures of the ribosome bound to antibiotics (e.g. Madumycin II (27) or Hygromycin

A (28)). In these antibiotic-bound ribosome structures, the observed conformational changes in the CCA end resulted from steric interference between the CCA-end and the drug, which prevented proper positioning of the tRNA acceptor stem in the 70S ribosome PTC.

2.2.3 Ψ promotes amino acid substitution in a reconstituted E. coli translation system

Ψ has the potential to change base-pairing interactions between tRNA anticodons and mRNA. This has raised the possibility that Ψ might, at some frequency, cause the ribosome to accept an aminoacyl-tRNA (aa-tRNA) that would not be cognate on a U-containing codon. To test this possibility, we prepared pools of total aa-tRNA by charging total *E. coli* tRNA using an S100 extract. We then presented 70S ribosome complexes with a dilute mixture of aa-tRNAs bound to EF-Tu instead of pure Phe-tRNA^{Phe}. If aa-tRNA selection is not altered then we should see ^{f}Met-Phe dipeptide formation almost exclusively. As expected, 97% of the dipeptides formed on UUU codons were the ^{f}Met-Phe product (Fig. 3, Fig. S5). In contrast, mRNAs containing ΨUU or UUΨ directed the synthesis of multiple products (Fig. 3) with reasonable efficiency; nearly half of total peptides produced on ΨUU mRNAs were alternative non-^{f}Met-Phe products (Figs. 3B and S5A). The extent to which Ψ promotes amino acid substitution appears to be context dependent - we found different levels of amino acid substitution on ribosome complexes programmed with modified stop codon (ΨAA) in the A site (Fig. 3C). Significantly, these experiments were performed under conditions that mimic starvation and result in reduced translational fidelity. We do not expect near-cognate tRNAs to compete as effectively against appreciable concentrations of cognate aa-tRNAs.

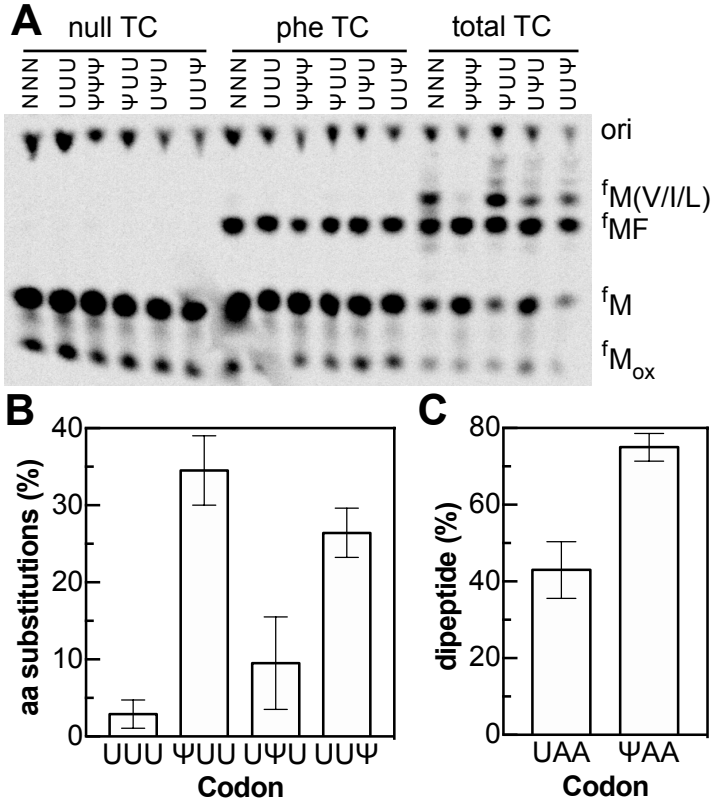

Figure 2.3:Ψ promotes incorporation of alternative amino acids by the ribosome at limiting concentrations of aa-tRNA. ***(A)*** *Electrophoretic TLC displaying the translation products a mixture of mRNAs containing a single randomized codon (NNN), and unmodified and Ψ-containing UUU messages in the presence of no tRNA (null), Phe-tRNA^{Phe} tRNA (phe TC), and total aa-tRNA (total TC). Translation of the NNN pool of mRNAs with random codons in the A site demonstrates the presence of multiple aa-tRNA^{aa} species in the total tRNA preparation.* ***(B)*** *Percent of amino acid substituted dipeptides, relative to the correct fMet-Phe product, on unmodified and modified UUU codons (e.g. % not forming expected MF peptide).* ***(C)*** *Percent of ribosomes that react with 2 μM Lys-tRNA^{Lys} ternary complex on UAA and ΨAA stop codons to form a MK peptide after 10 minutes. The near-cognate Lys-tRNA^{Lys} reacts to produce twice as much peptide produced is produced on ΨAA than on UAA. All of the data displayed in plots reflects the averages and standard errors of at least three experiments.*

To determine which amino acids are incorporated on the Ψ-containing UUU codons we performed translation reactions with total tRNA charged one at a time with either valine (Val), isoleucine (Ile), leucine (Leu), or serine (Ser) (Figs. 4 and S5). These amino acids were selected for investigation based on the migration of amino acid substituted peptides in electrophoretic TLC experiments (Fig. 3A) and their tRNA anticodons. Val and Leu were incorporated on ΨUU and UUΨ codons, Ile was incorporated only on ΨUU, and Ser was not incorporated above background (Figs. 4B and S5B). Our data are consistent with the known possible base-pairing interactions of Ψ (29-31), and additionally suggest that a Ψ:U basepair can satisfy the

requirements for decoding at the first position (Table S3). This is a surprising degree of flexibility for the decoding site, which as a general rule strictly monitors the codon-anticodon interaction.

To quantitatively determine if Ψ reduces the ability of *E. coli* ribosomes to discriminate between cognate and near-/non-cognate aa-tRNAs, we performed kinetic assays with the near-cognate Val-tRNA^{Val}. We reacted 10 μM Val-tRNA^{Val} ternary complexes with 100 nM 70S ribosomes containing ^{35}S-^{f}Met-tRNA^{Met} in the P site and UUU or ΨUU in the A site in the presence of EF-Ts and an energy regeneration mix (32). We observed a burst followed by a long linear phase (Fig. S7). Both the burst and the rate constant were 2-fold greater on ΨUU (Figs. 5A and S7). These differences could reflect changes in any step before and including peptidyl-transfer, but – given our experimental conditions ($[Mg(II)]_{free}$ = 10 mM) – likely report on the relative rates of accommodation and rejection of Val-tRNA^{Val} on UUU and ΨUU, similar to what was previously observed for the incorporation of a Leu-tRNA^{Leu} on a UUU codon (33). These findings are consistent with the 2-fold increase we observe in Val incorporation on ΨUU reacted with Val-tRNA^{Val} charged from a mixture of total tRNA (Fig. 4B).

2.2.4 Ψ increases the levels of amino acid substitution in human embryonic kidney cells

We next investigated the effect of Ψ on amino acid substitution during translation in eukaryotic cells. Luciferase mRNA was transcribed *in vitro* with either uridine or Ψ and transfected into 293H cells (Fig. S8). Full-length luciferase protein was purified (Fig. S9) and analyzed by mass spectrometry with a focus on a specific luciferase peptide with favorable ionization characteristics (42, 43). Amino acid substitutions in this peptide, which totaled ~1%, were only observed in peptides generated from Ψ-containing mRNAs (Figs. 4C and S10, Tables S4 and S5). We also extended our analyses to the entire luciferase dataset. Luciferase protein

translated from Ψ-containing mRNAs possessed a significantly higher rate of amino acid substitution (totaling ~1.5%, integrated over all Ψ-containing codons) relative to protein synthesized from uridine-containing mRNAs (substitutions only on two < 0.05% Val codons were observed) (Table S6). The miscoding events that we observed in our unmodified uridine-containing samples (Val substitutions) are likely relatively common substitutions as they have also been seen by more sophisticated mass-spectrometry approaches investigating unmodified EF-Tu sequences (34). These observations are consistent with the expected levels of amino acid substitution that we would estimate from our *in vitro* kinetic studies with cognate Phe-tRNA^{Phe} and near-cognate Val-tRNA^{Val}, which suggest that under conditions where all tRNAs are equally well charged and available, the expected total level of amino acid substitution on ΨUU codons should be ~1 % (Fig. S7).

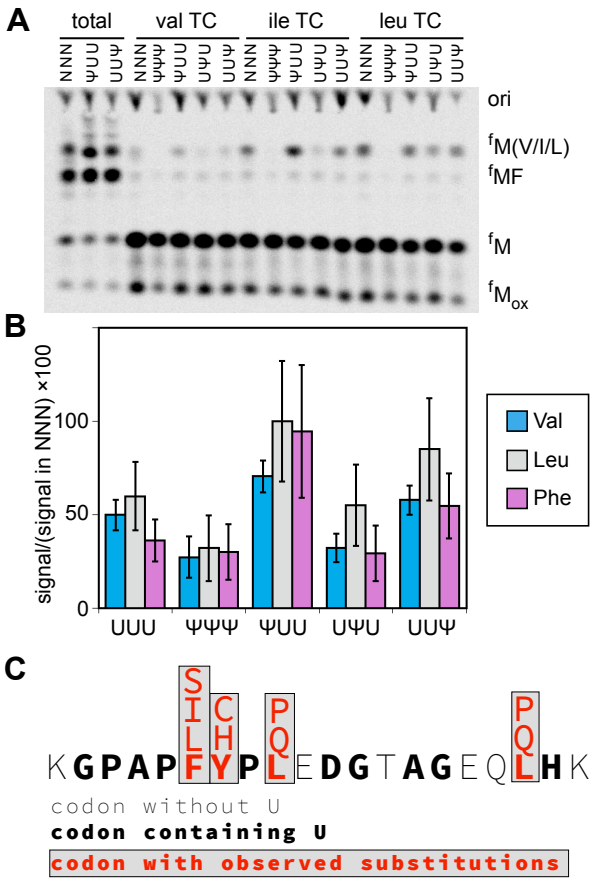

Figure 2.4: ***Amino acids from near-cognate and non-cognate tRNAs are incorporated on Ψ-containing codons*** ***(A)*** *Electrophoretic TLC displaying the translation products of NNN and Ψ-containing messages in the presence of total aa-tRNA (total), total tRNA aminoacylated with valine (val TC), total tRNA aminoacylated with isoleucine (ile TC), and total aa-tRNA aminoacylated with leucine (leu TC).* ***(B)*** *Percent of MV/ML/MI products generated on UUU and Ψ-containing codons relative to NNN. The values plotted are the mean of four experiments and the error bars reflect the standard error.* ***(C)*** *Summary of amino acid substitutions observed by mass-spectrometry in a luciferase peptide incorporated on Ψ-containing mRNAs translated in 293H cells*.**.**

2.2.5 mRNA:tRNA mismatches on ΨUU in the P site not surveilled by E. coli ribosome

Our data indicate that the ribosome can interact differently with near-/non-cognate aa-tRNAs when Ψ is present within the A-site codons. To assess if Ψ also alters how the ribosome perceives mRNA:tRNA interactions in the P site, we investigated if the ribosome detects mRNA:tRNA mismatches on Ψ-containing P site codons. On unmodified codons *E. coli* ribosomes sense P site mismatches, and release factors 2 and 3 (RF2/3) catalyze the hydrolysis of truncated peptides containing substituted amino acids from sense (non-stop) codon to ensure translational fidelity (Fig. 5B) (35). We tested if mismatches involving a pseudouridinylated codon are similarly surveilled by reacting ribosome initiation complexes containing UAA or ΨAA in the A site with ternary complexes containing Lys-tRNA^{Lys} in the presence of elongation factor G (EF-G). This generated a mixture of mismatched ribosome complexes containing either Met-Lys-tRNA^{Lys} or Met-Lys-Lys-tRNA^{Lys} in the P site (Figs. 5, S11A and B). We then added RF2 or RF2/RF3 and measured the rate constants for ^{f}Met-Lys (MK) and ^{f}Met-Lys-Lys (MKK) peptide release from these mRNAs. If a mismatch is detected, we expect that RF2/RF3 will catalyze premature peptide release much faster than RF2 alone (35). On the unmodified mRNA we observed that MK and MKK peptides are released by RF/RF3 at rates comparable to those previously reported for other mismatched complexes (Figs. 5, S11C and D) (35). In contrast, when ΨAA is in the P site, the MK peptide was not released (Fig. 5C, S11E). However, when ΨAA is translocated into the E site, MKK peptide release is catalyzed by RF2/RF3; this means that the mismatch between the tRNA^{Lys} and the GUU codon in the P site is surveilled on the Ψ-

containing transcript (Fig. S11F). Our data demonstrate that mRNA:tRNA mismatches on ΨAA P-site codons are not sensed, suggesting that Ψ can alter how the ribosome interacts with near-/non-cognate aa-tRNAs in the P site.

2.2.6 Class I release factor 1 (RF1) is modestly impeded by the presence of Ψ

The presence of Ψ in stop codons has been reported to promote nonsense suppression, incorporating Ser or Thr instead of terminating translation on UAA codons, in both bacteria and yeast cells (14, 21). Computational studies have predicted that this is due to alterations in release factor activity on pseudouridinylated stop codons (36). To assess if Ψ alters the ability of class I release factors to catalyze the hydrolysis of the peptide from peptidyl-tRNA, we measured the rate constants for peptide release on mRNAs encoding methionine followed by the universal stop codon (UAA/ΨAA) (Fig. 5D, E). At saturating concentrations of RF1 or RF2, peptide release on the UAA codon occurred with rate constants ($k_{max,release}$) between 0.06-0.24 s^{-1} at 22° C, consistent with previously published values (35, 37) (Fig. 5D, E and Table S7).

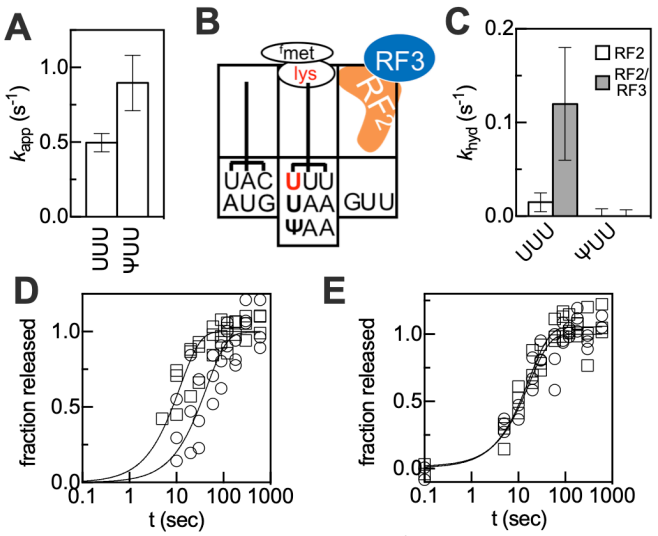

Figure 2.5: ***Ψ changes how codons are read. (A)*** *k_{app} values for ^{f}Met-Val and formation on UUU (blue) and ΨUU (red) codons in the presence of 10 nM EFTu and 10 μM Val-tRNA^{Val}.* ***(B)*** *Position of the codons and peptidyl-tRNA in the purified ribosome elongation complexes prior to addition of RF2 and RF2/RF3P-site mismatch surveillance assay.* ***(C)*** *Rate constants for premature hydrolysis of ^{f}Met-Lys from ^{f}Met-Lys-tRNA^{lys} bound to UAA or ΨAA in the P-site catalyzed by RF2 (white) and RF2/RF3 (gray).* ***(D-E)*** *^{f}Met release on UAA (squares), ΨAA (circles) stop codons catalyzed by 500 nM RF1* ***(D)*** *or RF2* ***(E).***

Peptide release on the ΨAA codon was only modestly perturbed: $k_{max,release}$ for RF1 was decreased ~3-fold, but $k_{max,release}$ for RF2, and the $K_{1/2}$ for both RF1 and RF2 were unchanged (Fig. 5DE, S12 and Table S7). Our results are mostly consistent with a previous study utilizing RF1 and the A246T variant of RF2 (38) which found no difference in rate constants for peptide release on wild-type and Ψ-containing stop codons (22). The modest impact on RF1 activity appears to be specific to Ψ, as we find that m^6A impedes RF2–, but not RF1–, mediated peptide release (Figs. S13 and S14). Together, the low magnitude decrease in the rate constant for RF1 catalyzed release, our failure to incorporate Ser on ΨAA in the absence of release factors (Fig. S15), and our inability to detect extended products from a fully-Ψ substituted luciferase reporter in the NEB PURE *in vitro* translation system, suggest that Ψ is unlikely to significantly suppress translation termination under normal cellular conditions.

2.3 Discussion

The inability to knock out the enzymes that incorporate Ψ into mRNAs without also impacting non-coding RNA modification, coupled with the lack of known Ψ reader or eraser proteins, has made it difficult to investigate the biological consequences of Ψ mRNA modifications. We approached this challenge by using a fully-reconstituted *in vitro* translation assay and asked how the function of one possible Ψ reader, the ribosome, is impacted by the pseudouridinylation of mRNAs. Our studies show that the presence of Ψ in codons subtly changes how the ribosome interacts with both cognate and non-/near-cognate aa-tRNAs. We observed that Ψ-containing codons perturb the translation of cognate codons, and promote the synthesis of a variety of peptide products from a single mRNA more often than from unmodified mRNAs both in a reconstituted bacterial translation system and human cells.

Consideration of our kinetic and structural data with respect to the established mechanistic paradigm for aa-tRNA binding to the A site (Fig. S3) (23) provides some insight into the mechanistic effects of Ψ. We observed reductions in the rate constants for amino acid addition (k_{obs}) and EF-Tu catalyzed GTP-hydrolysis (k_{GTP}) on Ψ-containing codons, consistent with our finding that Ψ-substituted codons decrease the overall rate of full-length protein production. The changes to k_{obs}, k_{GTP}, and Mg(II) dependence of our observations (Fig. S16) are reminiscent of those seen for near-cognate tRNAs (33), although more subtle, suggesting that pseudouridinylated codon recognition exists somewhere on a spectrum between cognate and near-cognate complexes. While the decrease in k_{GTP} indicates that at least one step in elongation prior to GTP hydrolysis is affected, it is insufficient to explain the decrease in k_{obs} for amino acid addition. Therefore, we can infer that one or more steps after GTP hydrolysis are also affected. Our structural data provide further evidence that the ribosome interacts differently with tRNAs bound to Ψ-containing codons. We find that the 3' CCA of the A-site tRNA becomes disordered, suggesting that the unconventional decoding of the ΨUU A-site codon at the decoding center in the small ribosomal subunit leads to long-range changes in the acceptor stem of the A-site tRNA located in the PTC on the large ribosomal subunit. Taken as a whole, our kinetic and structural results indicate that Ψ modestly impacts multiple steps in the translation kinetic pathway to exert an overall observed effect on amino acid addition.

Our kinetic and mass-spectrometry data demonstrate that while amino acid substitution is increased in the presence of Ψ, these events are relatively rare in unstressed cells (<1.5%). Furthermore, many amino acid substitutions would likely be neutral, so the incorporation of Ψ in mRNAs would not be expected to generate significant quantities of non-functional protein under normal cellular conditions. Nonetheless, there could be some conditions or sequence contexts in

which Ψ-mediated amino acid substitution happens more robustly. Our observation that Ψ alters decoding by the ribosome in cells differs from previous reporter-based studies that did not observe amino acid substitutions at a single, defined position in a full-length ErmCL reporter peptide or in a fully Ψ-substituted GFP reporter (16, 17). There are several potential explanations for this discrepancy. First, our mass-spectrometry assays were able to detect multiple in vivo amino acid substitution events that occurred at frequencies (0.1-0.4%; Tables S5 and S6) lower than the reported limit of detection for the GFP study (~1%). Second, the effect of Ψ on decoding could depend strongly on local mRNA sequence and structure (39). This would be unsurprising, given that our studies indicate the degree of alternative amino acid incorporation depends both on codon identity, and nucleotide position within a codon (Figs. 3). Such context dependence has been previously observed for inosine; both how inosine is decoded and the frequency of amino acid substitution (0.5 - 25%) range widely depending on sequence context (40). Third, cellular stresses change the available pool of aa-tRNAs and distribution of mRNA modifications (7, 41). The extent of amino acid substitution should be highly sensitive to the relative levels of aa-tRNAs, so different cellular conditions will likely modulate the degree of amino acid substitution. Lastly, it is possible that the observability of alternative decoding in different mRNAs could be quite distinct based on the identity of the mRNA and the post-translational fate of the amino acid substituted peptide.

We observed that Ψ-containing codons modestly affect the ability of the ribosome to incorporate Phe, in line with studies by ourselves (Fig. S2) and others demonstrating that overall protein production is reduced by on mRNA reporters containing either a single- (< 2-fold) (16, 17) or fully- Ψ substituted codons (3- fold) in a fully reconstituted *E. coli* translation system and human cells (17). We anticipate that the effect of Ψ on the rate of codon translation may depend

on the sequence context of the codon; we have seen that incorporating Ψ into different mRNAs sequences coding for identical luciferase peptides can have very different protein expression outcomes in 293H cells (Fig. S17). Overall, our findings are similar to what has been reported for the decoding of m^6A and 2' O-methyl containing codons (32, 42) suggesting that mRNA modifications might generally alter aa-tRNA binding and accommodation. Given the propensity of the ribosome to react with near- and non-cognate aa-tRNAs during the translation of Ψ-containing mRNAs (Figs. 3 and 4), these small rate defects could become important for cognate aa-tRNA selection under conditions of cellular stress or starvation. We speculate that it could be advantageous for cells to maintain a small reservoir of protein diversity for evolution and adaptation to environmental stresses (43, 44). Indeed, increased levels of amino acid substitution have been shown to increase cellular fitness under oxidative and temperature stress, and during transition from stationary to cell growth conditions (41, 45, 46). The idea that amino acid substitution levels might vary in response to cellular conditions is supported by a recent study demonstrating that the frequency of amino acid substitutions in the *E. coli* EF-Tu varies by as much as two orders of magnitude depending on protein expression level (34). Ultimately, the full suite of modern scientific tools – including ensemble and single-molecule biochemistry, deep sequencing, and cell biology – will be required to understand how a single modification is coupled to mRNA stability and protein synthesis in the cell.

2.4 Methods

2.4.1 E. coli ribosomes

Ribosomes were purified from *E. coli* MRE600. Cultures were inoculated with a 1:200 dilution of a saturated overnight culture and incubated with shaking at 37°C until an OD_{600} of 0.6. Cultures were transferred to an ice-water bath for 30 minutes before harvesting by centrifugation. Cell pellets were resuspended in Buffer A (20 mM Tris-Cl, 100 mM NH_4Cl, 10

mM $MgCl_2$, 0.5 mM disodium EDTA, 6 mM β-ME, pH 7.5) and lysed on a microfluidizer. The lysate was clarified by two subsequent centrifugations at 30,000×*g* for 15 minutes. Clarified lysate was layered onto 35 mL of Buffer D (20 mM Tris-Cl, 1.1 M sucrose, 500 mM NH_4Cl, 10 mM $MgCl_2$, 0.5 mM disodium EDTA, pH 7.5) and centrifuged for 18 hours at 4°C in a Beckman Type 45 Ti rotor. The centrifuge was set for minimal acceleration and deceleration rates. The supernatant was carefully removed, and the surface of the clear glassy pellets was rinsed with Buffer A. Pellets were resuspended in <5 mL of Buffer A by orbital shaking at 4°C. Tight-couple 70S particles were then isolated by rate-zonal ultracentrifugation in a Beckman Ti-15 zonal rotor through a 10-40% (w/v) sucrose gradient in Zonal Buffer (20 mM Tris-Cl, 60 mM NH_4Cl, 5.25 mM $MgCl_2$, 0.25 mM disodium EDTA, 3 mM β-ME, pH 7.5). A 50% (w/v) sucrose cushion in Zonal Buffer was used at the bottom of the rotor. After loading, the sample was centrifuged at 28,000 rpm for 19 hours at 4°C with no braking at the end of the run. A UA-6 absorbance detector with a high flow rate flow cell (Teledyne ISCO) was used to identify 70S-containing fractions. These fractions were pooled and ribosomes were concentrated by pelleting in the Type 45 Ti rotor. Pelleted 70S tight couples were resuspended in Buffer A, aliquoted, flash-frozen in liquid nitrogen, and stored at -80°C until use.

2.4.2 mRNAs and tRNAs for in vitro assays

Unmodified mRNAs were prepared by run-off T7 transcription of DNA oligonucleotides (1). mRNAs containing modified nucleotides were synthesized and HPLC purified by Dharmacon. mRNA sequences were generally of the form GGUGUCUUGCGAGGAUAAGUGCAUU AUG UUU UAA GCCCUUCUGUAGCCA; the coding sequence is underlined. Purified *E. coli* transfer RNAs were purchased from MP Biomedical, Chemical Block, tRNA Probes (College Station, TX), or purified in our lab from

bulk tRNA, and aminoacylated using S100 enzymes or partially purified synthetases (2). Bulk *E. coli* tRNA was purchased from Sigma.

2.4.3 Measurement of Ψ levels in purchased mRNA oligos by UHPLC-MS/MS

In the UHPLC-MS/MS assays RNA (200 ng) were first hydrolyzed to the composite mononucleosides via a two-step enzymatic hydrolysis using Nuclease P1 (500 U/μg RNA, overnight, pH 5.5, Thermo Fisher Scientific, Pittsburgh, PA) and recombinant shrimp alkaline phosphatase (2 U/μg RNA, four hours, pH 7.9, New England BioLabs, Ipswich, MA). The samples were lyophilized and reconstituted in 20 μL of water. LC-MS/MS analysis was performed using a Waters Acquity UPLC HSS T3 (100 x 2.1 mm, 1.8 μm, 100 Å) on a Vanquish ultrahigh-pressure liquid chromatograph (Thermo Fisher Scientific, Gemering, Germany) interfaced to a TSQ Quantum Ultra triple quadrupole mass spectrometer (Thermo Fisher Scientific, San Jose, CA). Mobile phase A was 0.01% (v/v) formic acid in water, and mobile phase B was 0.01% (v/v) formic acid in acetonitrile. The flowrate was 0.4 mL/min, and the gradient used was designed as previously published (3). The sample injection volume was 5 μL. The autosamples was kept at 4°C, and the column was held at 25°C in still air mode. Electrospray ionization was used in positive mode at 4.0 kV. The capillary temperature was 200°C, the vaporizer temperature was 350°C, the sheath gas was 10, and the auxiliary gas was 5. Ions were detected in tandem mass spectrometry (MS/MS) mode.

To quantify RNA nucleosides, calibration curves were created for the four main bases and four uridine modifications (pseudouridine, 5-methyluridine, 5-hydroxyuridine, and 2'-O-methyluridine). [^{13}C][^{15}N]-G (10 nM) was used as an internal standard. Automated peak integration was performed using XCalibur 3.0 MS software. All peaks were visually inspected to ensure proper integration (Figure S18). We observed peaks for only the four major bases and

pseudouridine. Other modified bases were not present above background (<1% of total nucleosides). Comparison of the U:Ψ ratio in the oligos containing a UΨU codon suggests that there is a minority population (~20%) of "modified" oligos that contain U instead of Ψ. Since the effects of Ψ are relatively subtle (~2-fold), we are not able to distinguish the two populations in our ensemble experiments. Instead, the effect of the unmodified subpopulation is to shift the average behavior of the entire population towards the behavior of the unmodified mRNAs used as a control. As a consequence, our estimates of the effects of Ψ are under-estimates.

2.4.4 E. coli translation factors

Constructs for translation factors were from the laboratory of Dr. Rachel Green unless otherwise noted. IF-1 was expressed in BL21(DE3) at 17°C in Terrific broth overnight. Lysis, wash, and elution buffers contained 50 mM sodium phosphate, pH 7.8, 300 mM NaCl, 5 mM β-ME, and 10, 25, or 300 mM imidazole, respectively. IF-1 was purified by a single nickel-IMAC step and dialyzed overnight against storage buffer (100 mM Tris-Cl, 140 mM NH_4Cl, 60 mM KCl, 14 mM $MgCl_2$, 2 mM DTT), then diluted 2-fold with 50% glycerol and stored at −80°C. IF-2 was purified similarly, except that expression was at 37°C for 3 hours. IF-3 was expressed in LB media with 0.5 mM IPTG at 37°C for 3 hours. Lysis, wash, and elution buffers for nickel-IMAC were 20 mM Tris-Cl pH 7.5, 300 mM NaCl, 1 mM β-ME, with 5, 20, and 250 mM imidazole, respectively. Fractions containing IF-3 were pooled, concentrated, and dialyzed against storage buffer (50 mM Tris-Cl pH 7.5, 70 mM NH_4Cl, 7 mM $MgCl_2$, 1 mM DTT, 30 mM KCl, 20% glycerol (v/v)). EF-Tu was expressed in Terrific broth with 0.5 mM IPTG at 30°C overnight and purified by nickel-IMAC. Lysis buffer contained 20 mM Tris-Cl, 300 mM NaCl, 1 mM β-ME and 5 mM imidazole at pH 7.5. Wash buffer was 20 mM Tris-Cl, 500 mM NaCl, 1 mM β-ME, and 20 mM imidazole at pH 7.5. Elution buffer contained 20 mM Tris-Cl, 300 mM

NaCl, 1 mM β-ME, and 250 mM imidazole at pH 8.5. Fractions containing EF-Tu were dialyzed against cleavage buffer (20 mM Tris-Cl, 200 mM NaCl, 2 mM β-ME) at 4°C overnight. TEV protease was added at a 1:100 mass ratio and incubated at 4°C overnight. TEV was removed by passage over a nickel-IMAC column. The unbound fraction was dialyzed against storage buffer (25 mM Tris-Cl, 75 mM NH_4Cl, 2.5 mM $MgCl_2$, 3 mM β-ME, 20 uM GDP, and 10% (v/v) glycerol) at 4°C overnight. EF-G was expressed and purified according to the same protocol as EF-Tu. Purified RF1 was a gift from Dr. Rachel Green. RF2 was purified from an RF2 overexpression strain (4) via three chromatographic steps: nickel-IMAC, Resource Q anion exchange, and Superdex 75 16/60 gel filtration. Lysis buffer was 30 mM Tris-Cl, 60 mM KCl, 5 mM β-ME at pH 7.5. IMAC-bound RF2 was washed with IMAC wash buffer A (30 mM Tris-Cl, 0.5 M KCl, 5 mM β-ME, pH 7.5), IMAC wash buffer B (30 mM Tris-Cl, 60 mM KCl, 10 mM imidazole, 5 mM β-ME, pH 7.5), and eluted with a gradient to 0.5 M imidazole in Wash Buffer B. Fractions containing RF2 were pooled, diluted with buffer IEX-A (30 mM Tris-Cl, 30 mM KCl, 5 mM β-ME, pH 7.5), and applied to a 6 mL Resource Q anion exchange column (GE Healthcare). Bound proteins were eluted with a linear gradient to buffer IEX-B (30 mM Tris-Cl, 1 M KCl, 5 mM β-ME, pH 7.5). Fractions containing RF2 were pooled, concentrated in centrifugal concentrators, and applied to a Superdex 75 16/60 gel filtration column equilibrated with storage buffer (30 mM Tris-Cl, 100 mM NH_4Cl, 30 mM KCl, 5 mM β-ME). RF2-containing fractions were pooled and glycerol was added to 25% (v/v). Purified RF2 was concentrated and stored at −80°C.

2.4.5 Formation of E. coli ribosome initiation complexes

Initiation complexes (ICs) were prepared in 1X 219-Tris buffer (50 mM Tris pH 7.5, 70 mM NH_4Cl, 30 mM KCl, 7 mM $MgCl_2$, 5 mM β-ME) with 1 mM GTP. This buffer has been

used extensively in the literature (5-7). Tight-couple 70S ribosomes (1 μM) were incubated with 1 μM mRNA, 2 μM each of IF-1, IF-2, and IF-3, and 1 μM f-[^{35}S]-Met-tRNA^{fMet} at 37°C for 30 minutes. Magnesium chloride was added to a final concentration of 12 mM. Complexes were layered onto 1 mL of Buffer D (see "Ribosomes") in thick-wall polycarbonate tubes and centrifuged at 69,000 rpm in a Beckman TLA 100.3 rotor for 2 hours at 4°C. Pelleted complexes were resuspended in 1X 219-Tris buffer, flash-frozen in small aliquots and stored at −80°C.

2.4.6 In vitro amino acid addition assays

Ternary complex was prepared by incubating EF-Tu with 10 mM GTP in 1X 219-Tris for 10 minutes at 37°C, then adding aminoacylated tRNA and incubating for another 15 minutes. Peptidyl transfer reactions contained 70 nM ICs and 1-2 μM ternary complex (1-2 μM aminoacylated tRNA, 20 μM EF-Tu, 5 mM GTP) in 1X 219-Tris buffer. Reaction aliquots were quenched with 500 mM KOH (final concentration) at discrete time points (0-600 seconds) either by hand or on a KinTek quench-flow apparatus. The reactants, intermediates and products at each time point were separated by electrophoretic TLC in pyridine-acetate buffer (20% acetic acid adjusted to pH 2.8 with pyridine) as previously described (6). Electrophoretic TLCs were visualized by phosophorimaging and quantified with ImageQuant. The data were fit using Equation 1:

Fraction product =A·(1-ekobst)

2.4.7 In vitro translation termination assays

Pre-termination complexes were prepared on mRNAs containing the coding sequence AUG-UAA-GUU and AUG- ΨAA-GUU. Peptide release assays were performed in 1X219-Tris buffer at room temperature (100 nM pre-TCs, RF1/RF2 ranging from 50 nM to 10 μM).

Reaction aliquots were quenched with 4% formic acid (final) at varying time points. Free f-[^{35}S]-Met was separated from f-[^{35}S]-Met-tRNA^{fMet} by electrophoretic TLC and quantified by phosphorimaging. For each timecourse the fraction of released ^{f}Met was fitted using Equation 1 to obtain an observed rate constant. $K_{1/2}$ values were obtained by fitting the k_{obs} vs. [RF] data points using

Equation 2:

kobs=kmax·[RF]/(K12+[RF])

2.4.8 In vitro assays with total aa-tRNA^{aa}

Initiation complexes and mRNA were generated as described above. Translation assays were performed by reacting IC complexes (70 nM final) with ternary complex (1 μM total tRNA aminoacylated with S100 enzymes or specific synthetases, 40 μM EF-Tu, 10 mM GTP) at room temperature for 10 minutes. All assays were performed in 219-Tris buffer and quenched with 500 mM KOH (final concentration). Products were visualized by electrophoretic TLC, as described above.

2.4.9 EF-Tu single turnover GTP hydrolysis assays

Partially purified *E. coli* initiator tRNA$_{fMet}$ (~3 nmol) was charged with [^{3}H]-methionine (specific activity 770 mCi/mmol) using purified synthetase and transformylase. After 30 minutes, the following components were added to the indicated final concentrations: 219-Tris buffer (1X), ribosomes (1.5 μM), mRNA (1.5 μM), IFs (3 μM), and GTP (1 mM). Incubation was continued for 30 minutes at 37°C, and initiation complexes were pelleted as described above. EF-Tu●phe-tRNA$_{phe}$●[^{32}P]-GTP ternary complex was prepared by incubating EF-Tu (~2 nmol, 40 μM) with [^{32}P]-GTP (50 μM, specific activity 47×10^{3} mCi/mmol) and EFTs (4.1 μM)

for 15 minutes at 37 C. Purified phe-$tRNA_{phe}$ (~1 nmol) was added and incubation was continued for 10 minutes. Ternary complex was separated from free [^{32}P]-GTP on a ~3 mL G25 column in 1X219 buffer. Fractions containing the void volume peak were pooled, aliquoted, and snap frozen in liquid nitrogen. Aliquots of initiation complexes (~3 μM) and ternary complex (~600 nM) were thawed immediately before use and TC concentration was adjusted to ~200 nM with 1X219 buffer. Reactions were performed on a Kintek RQF-3 rapid quench using 10% formic acid as the quench solution. Timepoints were clarified by centrifugation and aliquots of each timepoint were separated on PEI-cellulose TLC plates in 0.5 M KPO_4, pH 3.5.

2.4.10 P site mis-match surveillance assays

Procedure was adapted from Zaher and Green (6). Initiation complexes (ICs) were prepared on unmodified T7 transcripts (5'-GGUGUCUUGCGAGGAUAAGUGCAUUAUGUAAGUUGCCCUUCUGUAGCCA-3', see above) or synthetic mRNAs (Dharmacon; 5'-GGUGUCUUGCGAGGAUAAGUGCAUUAUGΨAAGUUGCCCUUCUGUAGCCA-3') in 1X 219-Tris buffer with 2 mM GTP. Initiation complexes were formed with 1 μM 70S *E. coli* ribosomes, 1 μM mRNA, 2 μM IF-1, IF-2, and IF-3, and 0.5 μM f-[^{35}S]-Met-$tRNA^{fMet}$ at 37°C for 30 minutes as described above. Ribosome Nascent Chain complexes (RNCs) were then formed by mixing equivalent volumes of initiation complexes and ternary complex containing EF-Tu (20 μM), Lys-$tRNA^{Lys}$ (4 μM), EF-G (10 μM), and GTP (5 mM) in 1X 219-Tris buffer and incubating at 37 °C for 15 minutes. Magnesium chloride was added to a final concentration of 12 mM and RNCs were then layered onto 1mL of Buffer D and then pelleted (please refer to **Formation of *E. coli* ribosome initiation complexes** above). P site mis-match surveillance assays were performed by mixing RNCs (70-100 nM final concentration) with RF2 (30mM) or a

mixture containing both RF2 (30mM) and RF3 (30mM) in 2 mM GTP. The final magnesium concentration in these assays was 7mM. The reaction was quenched in 4% formic acid at discrete time points over a period of 10 minutes. Products were visualized by electrophoretic TLC, as described above.

2.4.11 In vitro assays for Val incorporation on UUU and YUU codons

Initiation complexes were prepared on mRNAs containing AUG-UUU-UAA or AUG-ΨUU-UAA mRNAs, pelleted, and resuspended at a concentration of 1 μM (see **Formation of E. coli ribosome initiation complexes**). Ternary complex was prepared in energy regeneration mix (1X Tris-219 buffer, 7 mM additional $MgCl_2$ for a total $MgCl_2$ concentration of 14 mM, 1 mM GTP, 3 mM phosphoenolpyruvate, 0.1 μg/mL pyruvate kinase) using 40 μM EFTu, 10 μM EFTs, and 10 μM Val-$tRNA_{Val}$. Reactions were performed in energy regeneration mix with 0.1 uM initiation complex and 10 μM Val-$tRNA_{Val}$•EFTu•GTP ternary complex. Aliquots were withdrawn at timepoints and quenched with an equal volume of 1 M KOH. After quenching samples were neutralized with acetic acid, and peptide products were separated by electrophoretic TLC (pyridine-acetate buffer, pH 2.8, 1200V, 35 minutes) and quantified by phosphorimaging.

2.4.12 Crystallographic structure determination

Ribosome complex containing mRNA and tRNAs was pre-formed by mixing 5 μM 70S Tth ribosomes with 10 μM Ψ-mRNA and incubation at 55°C for 10 minutes, followed by addition of 20 μM P site ($tRNA_i^{Met}$) and 20 μM A site ($tRNA^{Phe}$) substrates (with minor changes from (8)). At each of these two steps ribosome complexes were incubated for 10 minutes at 37°C in the buffer containing 5 mM HEPES-KOH (pH 7.6), 50 mM KCl, 10 mM NH_4Cl, and 10 mM

$Mg(CH_3COO)_2$. Crystals were grown by vapor diffusion in sitting drop crystallization trays at 19°C. Initial crystalline needles were obtained by screening around previously published ribosome crystallization conditions (9-11). The best-diffracting crystals were obtained by mixing 2-3 µL of the ribosome-mRNA-tRNA complex with 3-4 µL of a reservoir solution containing 100 mM Tris-HCl (pH 7.6), 2.9% (w/v) PEG-20K, 7-12% (v/v) MPD, 100-200 mM arginine, 0.5 mM β-mercaptoethanol (8). Crystals appeared within 3-4 days and grew up to 200 × 200 × 1000 µm in size within 10-12 days. Crystals were cryo-protected stepwise using a series of buffers with increasing concentrations of MPD until reaching the final concentration of 40% (v/v) MPD, in which they were incubated overnight at 19°C. In addition to MPD, all stabilization buffers contained 100 mM Tris-HCl (pH 7.6), 2.9% (w/v) PEG-20K, 50 mM KCl, 10 mM NH_4Cl, 10 mM $Mg(CH_3COO)_2$ and 6 mM β-mercaptoethanol. After stabilization, crystals were harvested and flash frozen in a nitrogen cryo-stream at 80K.

Diffraction data were collected on the beamlines 24ID-C and 24ID-E at the Advanced Photon Source (Argonne National Laboratory, Argonne, IL). A complete dataset for each ribosome complex was collected using 0.979Å wavelength at 100K from multiple regions of the same crystal using 0.3° oscillations. The raw data were integrated and scaled using the XDS software package (12). All crystals belonged to the primitive orthorhombic space group $P2_12_12_1$ with approximate unit cell dimensions of 210Å x 450Å x 620Å and contained two copies of the 70S ribosome per asymmetric unit. Each structure was solved by molecular replacement using PHASER from the CCP4 program suite (13). The search model was generated from the previously published structure of the *T. thermophilus* 70S ribosome with bound mRNA and tRNAs (PDB entry 4Y4P from (8)). The initial molecular replacement solutions were refined by rigid body refinement with the ribosome split into multiple domains, followed by ten cycles of

positional and individual B-factor refinement using PHENIX (14). Non-crystallographic symmetry restraints were applied to 4 domains of the 30S ribosomal subunit (head, body, spur, helix 44), and 4 domains of the 50S subunit (body, L1-stalk, L10-stalk, C-terminus of the L9 protein).

The final model of the 70S ribosome in complex with mRNA/tRNAs was generated by multiple rounds of model building/fitting in COOT (15), followed by refinement in PHENIX (14). The statistics of data collection and refinement are compiled in Table S2. All figures showing atomic models were generated using PyMol software (*www.pymol.org*).

After we first observed no density for the CCA-end of the A-site tRNA, we repeated this experiment multiple times and collected about a dozen of datasets. The dataset reported here was collected from a single crystal. This dataset has the best resolution and overall best quality out of all collected datasets. Basically, there is a complete absence of any presence of the CCA end. In all our control datasets, in which we've used the same batch of $tRNA^{Phe}$ and regular unmodified mRNA, the CCA tail was clearly visible in the electron density and formed canonical WC interactions with the A loop of the 23S rRNA:Phe tRNA. The quality of the electron density and the resolution of the ΨUU containing structure in the vicinity of the PTC is not any worse than any of the datasets that we used as controls, which all have the same overall resolution. Specifically, the electron density is clearly visible for all of the key nucleotides in the PTC, such as 2451, as well as the nucleotides forming the A and P loops. Moreover, the P-loop interactions of the P-site tRNA are clearly visible in the P site.

2.4.13 Plasmid construction for in vitro transcription of luciferase mRNA for in vivo expression

The template for *in vitro* synthesis of luciferase mRNA comprise, from 5′ to 3′: the T7 promoter, followed by an N-terminal 3× Hemagglutinin (HA) tag fused in-frame with the firefly luciferase gene, in-frame C-terminal StrepII and FLAG tags. The open reading frame spans from the 3xHA tag to the FLAG tag enabling the purification of full-length luciferase protein and not translation truncated products. The beta-globin 5' and 3' untranslated region (UTR) sequences were used for the expression of luciferase mRNA. Plasmids were generated by PCR and standard molecular cloning techniques.

***In vitro* transcription of luciferase mRNA.**

mRNA was transcribed using T7 RNA polymerase (New England Biolabs) from a linearized plasmid or PCR-amplified linear template. All four nucleoside triphosphates in the reaction, natural or modified, were used at a final concentration of 4 mM. For generation of nucleoside-modified mRNAs, UTP was replaced with triphosphate-derivative of pseudouridine (Trilink). The *in vitro* transcribed RNAs were treated with Turbo DNaseI (Invitrogen) and followed by spin column clean-up (New England Biolabs). The mRNAs were post-transcriptionally capped with Vaccinia capping enzyme and treated with Cap 2'-O Methyl Transferase (New England Biolabs) to increase the stability and the translation efficiency of the luciferase mRNA.

2.4.14 mRNA transfection and expression analyses

Synthesized, purified mRNAs were transfected into 293H cells using TransIT-mRNA transfection kit as recommended by the manufacturer (Mirus). The expression of the luciferase mRNA was analyzed by western blot analyses at various time points (15, 30, 60, 90, 120, 180, 240, 300, 360 minutes post-transfection) and cells were harvested 6-hours post transfection. Tandem purification of the luciferase translation products was performed using the FLAG tag

followed by selection for the N-terminal HA tag as described previously (16, 17). The purified products were analyzed on 8% SDS-PAGE, gels were then silver stained (ProteoSilver, Sigma) and processed for mass spectrometry. Three independent transfections were performed for uridine/Ψ -containing mRNAs. For western blot analyses of the luciferase protein, proteins were separated by SDS-PAGE and blotted to 0.45 μm PVDF membranes (GE Healthcare). The blots were probed with an anti-HA antibody (Sigma). IR Dye™ -680 and -800 conjugated secondary conjugated antibodies were from Cell Signaling Technologies.

2.4.15 In-gel Digestion and LC-MS/MS Analysis

Silver-stained gel bands containing the luciferase protein were de-stained in 1 mL of 15 mM potassium ferricyanide and 50 mM sodium thiosulfate, with gentle shaking, for 30 minutes. The gel band was then subjected to in-gel trypsin digestion after reduction with dithiothreitol and alkylation with iodoacetamide. Peptides eluted from the gel were lyophilized and re-suspended in 25μL of 5% acetonitrile (0.1% (v/v) TFA). A 3 μL injection was loaded by a Waters NanoAcquity UPLC in 5% acetonitrile (0.1% formic acid) at 4.0 μL/min for 4.0 min onto a 100 μm I.D. fused-silica pre-column packed with 2 cm of 5 μm (200Å) Magic C18AQ (Bruker-Michrom). Peptides were eluted at 300 nL/min from a 75 μm I.D. gravity-pulled analytical column packed with 25 cm of 3 μm (100Å) Magic C18AQ particles using a linear gradient from 5-35% of mobile phase B (acetonitrile + 0.1% formic acid) in mobile phase A (water + 0.1% formic acid) over 45 minutes. Ions were introduced by positive electrospray ionization via liquid junction at 1.4kV into a Thermo Scientific Q Exactive hybrid mass spectrometer. Mass spectra were acquired over *m/z* 300-1750 at 70,000 resolution (*m/z* 200) with an AGC target of 1e6, and data-dependent acquisition selected the top 10 most abundant precursor ions for tandem mass spectrometry by HCD fragmentation using an isolation width of 1.6 Da, max fill time of

110 ms, and AGC target of 1e5. Peptides were fragmented by a normalized collisional energy of 27, and fragment spectra acquired at a resolution of 17,500 (*m/z* 200).

2.4.16 Data Analysis – Identification of amino acid substitutions

Raw data files were peak-picked by Proteome Discoverer (version 2.1), and preliminary searches were performed using the MASCOT search engine (version 2.4) against the *SwissProt Human* FASTA file (downloaded 05/2018) modified to include the luciferase protein sequence. Search parameters included Trypsin/P specificity, up to 2 missed cleavages, a fixed modification of carbamidomethyl cysteine, and variable modifications of oxidized methionine, pyroglutamic acid for Q, and N-terminal acetylation. The processed peak list was then re-searched in MASCOT against luciferase only, using an error-tolerant search allowing for all amino acid substitutions. High probability substitutions, as determined by greater than 90% peptide probability in Scaffold (version 4.8.8), were then added back to the original search parameters in Proteome Discoverer for interrogation by MASCOT as variable modifications for confirmation.

2.4.17 Data Analysis – Quantitation of amino acid substitutions

The final search, with confirmed variable modifications, was loaded into Skyline-daily (University of Washington, version 4.1) as a spectral library. Each raw file was loaded, generating an extracted ion chromatogram for each peptide of interest, and each peak was manually inspected for proper peak picking, isotope dot product ≥ 0.8, good fragment ion coverage, and elution times in line with the time of MS/MS identification of the peptide. The sum of the top 3 isotopes were then exported for each modification for further analysis.

2.4.18 In vitro translation of luciferase mRNA

Luciferase mRNAs transcribed either with 100% uridine or 100% pseudouridine (see In vitro transcription of luciferase mRNAs) were translated *in vitro* using PURExpress® (New England Biolabs). Each reaction contained 60-100 pmol luciferase mRNA and 50-76 μCi of L-[35S]-Methionine (Perkin Elmer), and PURExpress® (NEB) kit components according to manufacturer instructions. Reactions were incubated at 37 °C and aliquots removed at various time points (0, 2, 10, 30, 60, 120, 180, 240 mins). Samples were quenched with 1X SDS loading buffer (final concentrations 0.25mM Tris-HCl pH 6.8,12.5% Glycerol, 0.5% Bromophenol blue, 5% SDS, 50 mM β-mercatoethanol), and placed on ice. Samples were heated at 95 °C for five minutes and then loaded on a 4–12% Criterion™ XT Bis-Tris Protein Gel (BioRad) and electrophoresed at 90 V for 3 hours in 1X XT MOPS buffer (BioRad). The gel was then fixed in a solution of methanol/acetic acid/water (45%/10%/45% v/v/v) for 5 minutes at room temperature. The gels were then dried on filter paper at 80 °C for one hour. Gels were visualized by phosophorimaging and quantified with ImageQuant.

2.5 References

[1] B. S. Zhao, I. A. Roundtree, and C. He, "Post-transcriptional gene regulation by mRNA modifications," *Nature reviews Molecular cell biology*, vol. 18, no. 1, pp. 31–42, 2017.

[2] W. V. Gilbert, T. A. Bell, and C. Schaening, "Messenger RNA modifications: Form, distribution, and function," *Science*, vol. 352, no. 6292, pp. 1408–1412, Jun. 2016, doi: 10.1126/science.aad8711.

[3] D. Arango *et al.*, "Acetylation of cytidine in mRNA promotes translation efficiency," *Cell*, vol. 175, no. 7, Art. no. 7, 2018.

[4] B. S. Zhao *et al.*, "m6A-dependent maternal mRNA clearance facilitates zebrafish maternal-to-zygotic transition," *Nature*, vol. 542, no. 7642, pp. 475–478, 2017.

[5] K. D. Meyer and S. R. Jaffrey, "Rethinking m6A Readers, Writers, and Erasers," *Annu Rev Cell Dev Biol*, vol. 33, pp. 319–342, Oct. 2017, doi: 10.1146/annurev-cellbio-100616-060758.

[6] Y. Fu, D. Dominissini, G. Rechavi, and C. He, "Gene expression regulation mediated through reversible m6A RNA methylation," *Nature Reviews Genetics*, vol. 15, no. 5, pp. 293–306, 2014.

[7] T. M. Carlile, M. F. Rojas-Duran, B. Zinshteyn, H. Shin, K. M. Bartoli, and W. V. Gilbert, "Pseudouridine profiling reveals regulated mRNA pseudouridylation in yeast and human cells," *Nature*, vol. 515, no. 7525, pp. 143–146, Nov. 2014, doi: 10.1038/nature13802.

[8] S. Schwartz *et al.*, “Transcriptome-wide mapping reveals widespread dynamic-regulated pseudouridylation of ncRNA and mRNA,” *Cell*, vol. 159, no. 1, pp. 148–162, Sep. 2014, doi: 10.1016/j.cell.2014.08.028.
[9] A. F. Lovejoy, D. P. Riordan, and P. O. Brown, “Transcriptome-wide mapping of pseudouridines: pseudouridine synthases modify specific mRNAs in S. cerevisiae,” *PLoS One*, vol. 9, no. 10, p. e110799, 2014, doi: 10.1371/journal.pone.0110799.
[10] X. Li *et al.*, “Chemical pulldown reveals dynamic pseudouridylation of the mammalian transcriptome,” *Nat Chem Biol*, vol. 11, no. 8, pp. 592–597, Aug. 2015, doi: 10.1038/nchembio.1836.
[11] G. Zheng *et al.*, “ALKBH5 Is a Mammalian RNA Demethylase that Impacts RNA Metabolism and Mouse Fertility,” *Molecular Cell*, vol. 49, no. 1, Art. no. 1, Jan. 2013, doi: 10.1016/j.molcel.2012.10.015.
[12] M. A. Nakamoto, A. F. Lovejoy, A. M. Cygan, and J. C. Boothroyd, “mRNA pseudouridylation affects RNA metabolism in the parasite Toxoplasma gondii,” *RNA*, vol. 23, no. 12, pp. 1834–1849, Dec. 2017, doi: 10.1261/rna.062794.117.
[13] M. Z. Anderson, J. Brewer, U. Singh, and J. C. Boothroyd, “A pseudouridine synthase homologue is critical to cellular differentiation in Toxoplasma gondii,” *Eukaryotic cell*, vol. 8, no. 3, pp. 398–409, 2009.
[14] J. Karijolich and Y.-T. Yu, “Converting nonsense codons into sense codons by targeted pseudouridylation,” *Nature*, vol. 474, no. 7351, Art. no. 7351, Jun. 2011, doi: 10.1038/nature10165.
[15] K. Karikó *et al.*, “Incorporation of pseudouridine into mRNA yields superior nonimmunogenic vector with increased translational capacity and biological stability,” *Mol Ther*, vol. 16, no. 11, pp. 1833–1840, Nov. 2008, doi: 10.1038/mt.2008.200.
[16] T. P. Hoernes *et al.*, “Nucleotide modifications within bacterial messenger RNAs regulate their translation and are able to rewire the genetic code,” *Nucleic Acids Res*, vol. 44, no. 2, pp. 852–862, Jan. 2016, doi: 10.1093/nar/gkv1182.
[17] T. P. Hoernes *et al.*, “Eukaryotic Translation Elongation is Modulated by Single Natural Nucleotide Derivatives in the Coding Sequences of mRNAs,” *Genes (Basel)*, vol. 10, no. 2, p. E84, Jan. 2019, doi: 10.3390/genes10020084.
[18] D. R. Davis, “Stabilization of RNA stacking by pseudouridine,” *Nucleic Acids Res*, vol. 23, no. 24, pp. 5020–5026, Dec. 1995, doi: 10.1093/nar/23.24.5020.
[19] M. I. Newby and N. L. Greenbaum, “Investigation of Overhauser effects between pseudouridine and water protons in RNA helices,” *Proceedings of the National Academy of Sciences*, vol. 99, no. 20, pp. 12697–12702, 2002.
[20] E. Kierzek, M. Malgowska, J. Lisowiec, D. H. Turner, Z. Gdaniec, and R. Kierzek, “The contribution of pseudouridine to stabilities and structure of RNAs,” *Nucleic acids research*, vol. 42, no. 5, pp. 3492–3501, 2014.
[21] I. S. Fernández, C. L. Ng, A. C. Kelley, G. Wu, Y.-T. Yu, and V. Ramakrishnan, “Unusual base pairing during the decoding of a stop codon by the ribosome,” *Nature*, vol. 500, no. 7460, pp. 107–110, Aug. 2013, doi: 10.1038/nature12302.
[22] E. Svidritskiy, R. Madireddy, and A. A. Korostelev, “Structural Basis for Translation Termination on a Pseudouridylated Stop Codon,” *J Mol Biol*, vol. 428, no. 10 Pt B, pp. 2228–2236, May 2016, doi: 10.1016/j.jmb.2016.04.018.

[23] T. Pape, W. Wintermeyer, and M. V. Rodnina, “Complete kinetic mechanism of elongation factor Tu-dependent binding of aminoacyl-tRNA to the A site of the E. coli ribosome,” *The EMBO journal*, vol. 17, no. 24, pp. 7490–7497, 1998.
[24] M. Y. Pavlov and M. Ehrenberg, “Rate of Translation of Natural mRNAs in an Optimizedin VitroSystem,” *Archives of biochemistry and biophysics*, vol. 328, no. 1, pp. 9–16, 1996.
[25] K. S. Koutmou, A. P. Schuller, J. L. Brunelle, A. Radhakrishnan, S. Djuranovic, and R. Green, “Ribosomes slide on lysine-encoding homopolymeric A stretches,” *Elife*, vol. 4, 2015.
[26] Y. S. Polikanov, S. V. Melnikov, D. Söll, and T. A. Steitz, “Structural insights into the role of rRNA modifications in protein synthesis and ribosome assembly,” *Nature structural & molecular biology*, vol. 22, no. 4, pp. 342–344, 2015.
[27] I. A. Osterman *et al.*, “Madumycin II inhibits peptide bond formation by forcing the peptidyl transferase center into an inactive state,” *Nucleic acids research*, vol. 45, no. 12, pp. 7507–7514, 2017.
[28] Y. S. Polikanov *et al.*, “Distinct tRNA accommodation intermediates observed on the ribosome with the antibiotics hygromycin A and A201A,” *Molecular cell*, vol. 58, no. 5, pp. 832–844, 2015.
[29] M. Charette and M. W. Gray, “Pseudouridine in RNA: what, where, how, and why,” *IUBMB life*, vol. 49, no. 5, pp. 341–351, 2000.
[30] J. Ofengand and A. Bakin, “Mapping to nucleotide resolution of pseudouridine residues in large subunit ribosomal RNAs from representative eukaryotes, prokaryotes, archaebacteria, mitochondria and chloroplasts,” *Journal of molecular biology*, vol. 266, no. 2, pp. 246–268, 1997.
[31] P. P. Seelam, P. Sharma, and A. Mitra, “Structural landscape of base pairs containing post-transcriptional modifications in RNA,” *RNA*, vol. 23, no. 6, pp. 847–859, 2017.
[32] J. Choi *et al.*, “N(6)-methyladenosine in mRNA disrupts tRNA selection and translation-elongation dynamics,” *Nat Struct Mol Biol*, vol. 23, no. 2, pp. 110–115, Feb. 2016, doi: 10.1038/nsmb.3148.
[33] T. Pape, W. Wintermeyer, and M. Rodnina, “Induced fit in initial selection and proofreading of aminoacyl-tRNA on the ribosome,” *The EMBO journal*, vol. 18, no. 13, pp. 3800–3807, 1999.
[34] R. Garofalo, I. Wohlgemuth, M. Pearson, C. Lenz, H. Urlaub, and M. V. Rodnina, “Broad range of missense error frequencies in cellular proteins,” *Nucleic acids research*, vol. 47, no. 6, pp. 2932–2945, 2019.
[35] H. S. Zaher and R. Green, “Quality control by the ribosome following peptide bond formation,” *Nature*, vol. 457, no. 7226, pp. 161–166, 2009.
[36] M. Parisien, C. Yi, and T. Pan, “Rationalization and prediction of selective decoding of pseudouridine-modified nonsense and sense codons,” *Rna*, vol. 18, no. 3, pp. 355–367, 2012.
[37] B. Hetrick, K. Lee, and S. Joseph, “Kinetics of stop codon recognition by release factor 1,” *Biochemistry*, vol. 48, no. 47, pp. 11178–11184, 2009.
[38] V. Dinçbas-Renqvist, Å. Engström, L. Mora, V. Heurgué-Hamard, R. Buckingham, and M. Ehrenberg, “A post-translational modification in the GGQ motif of RF2 from Escherichia coli stimulates termination of translation,” *The EMBO journal*, vol. 19, no. 24, pp. 6900–6907, 2000.

[39] D. M. Mauger *et al.*, “mRNA structure regulates protein expression through changes in functional half-life,” *Proc Natl Acad Sci U S A*, vol. 116, no. 48, pp. 24075–24083, Nov. 2019, doi: 10.1073/pnas.1908052116.
[40] K. Licht, M. Hartl, F. Amman, D. Anrather, M. P. Janisiw, and M. F. Jantsch, “Inosine induces context-dependent recoding and translational stalling,” *Nucleic Acids Res*, vol. 47, no. 1, pp. 3–14, Jan. 2019, doi: 10.1093/nar/gky1163.
[41] Y. Fan, J. Wu, M. H. Ung, N. De Lay, C. Cheng, and J. Ling, “Protein mistranslation protects bacteria against oxidative stress,” *Nucleic acids research*, vol. 43, no. 3, pp. 1740–1748, 2015.
[42] J. Choi *et al.*, “2’-O-methylation in mRNA disrupts tRNA decoding during translation elongation,” *Nat Struct Mol Biol*, vol. 25, no. 3, Art. no. 3, Mar. 2018, doi: 10.1038/s41594-018-0030-z.
[43] P. J. O’Brien and D. Herschlag, “Catalytic promiscuity and the evolution of new enzymatic activities,” *Chemistry & biology*, vol. 6, no. 4, pp. R91–R105, 1999.
[44] D. Allan Drummond and C. O. Wilke, “The evolutionary consequences of erroneous protein synthesis,” *Nature Reviews Genetics*, vol. 10, no. 10, pp. 715–724, 2009.
[45] M. H. Schwartz and T. Pan, “Temperature dependent mistranslation in a hyperthermophile adapts proteins to lower temperatures,” *Nucleic acids research*, vol. 44, no. 1, pp. 294–303, 2015.
[46] Y. Fan *et al.*, “Heterogeneity of Stop Codon Readthrough in Single Bacterial Cells and Implications for Population Fitness,” *Molecular Cell*, vol. 67, no. 5, Art. no. 5, Sep. 2017, doi: 10.1016/j.molcel.2017.07.010.

Chapter 3 Methylated Guanosine And Uridine Modifications In *S. Cerevisiae* Mrnas Modulate Translation Elongation[2]

Work presented in this chapter was submitted for publication in
RSC Chemical Biology.

Joshua D. Jones[1], Monika K. Franco[2], Tyler J. Smith[1], Laura R. Snyder[1], Anna G. Anders[1], Brandon T. Ruotolo[1], Robert T. Kennedy[1,2], Kristin S. Koutmou[1,2]*

[1]University of Michigan, Department of Chemistry. [2]University of Michigan, Program in Chemical Biology. 930 N University, Ann Arbor, MI 48109, * corresponding author

3.1 Introduction

Post-transcriptional modifications to RNA molecules can change their structure, localization, stability, and function[1], [2]. To date, over 150 different nucleoside chemical modifications have been identified within non-coding RNAs (ncRNA), and many are important, or even essential, for a myriad of cellular processes[1], [3]. The significance of RNA modifications to cellular health is underscored by decades of observations implicating the mis-regulation of ncRNA modifying enzymes in cancer and other diseases[4]–[9]. Recent advances in next generation RNA sequencing (RNA-seq)[10]–[19] and liquid chromatography coupled to tandem mass spectrometry (LC-MS/MS) technologies[20]–[24] enabled the detection of chemical modifications in protein encoding messenger RNAs (mRNA). Over 15 mRNA modifications have

[2] In this paper, I used the in-vitro reconstituted system to collect translation kinetics of m^5U. Josh Jones did all LC-MS/MS set up, experimental design, and analysis. Tyler Smith performed work using the in-vitro reconstitutions system with m^1G and m^2G.

been reported, including N6-methyladensoine (m^6A), inosine (I), N7-methylguanosine (m^7G), and pseudouridine (Ψ)[1], [12], [13], [22], [25]–[28]. There are >10-fold more types of modifications reported in ncRNA than in mRNA, raising the possibility that the diversity of mRNA modifications has not yet been revealed.

While the biological significance of ncRNA modifications has been extensively studied, the consequences of mRNA modifications on gene expression are just beginning to be explored. Modified nucleosides resulting from RNA damage (e.g. oxidation, alkylation, or UV) commonly perturb protein synthesis and can trigger RNA degradation pathways[29], [30]. Despite typically being present at lower levels than their enzymatically incorporated counterparts[31], there is evidence that oxidized mRNAs can accumulate in neurodegenerative diseases[31]–[33]. The most abundant and well-studied modification added by enzymes into mRNA coding regions, m^6A, has been implicated as a key modulator of multiple facets of the mRNA lifecycle including nuclear export[34]–[36], mRNA stability[37]–[39], and translational efficiency[19], [38], [40]–[43]. Given these potential contributions to mRNA function, it is unsurprising that the mis-regulation of m^6A is linked to a host of diseases such as endometrial cancer[44] and type 2 diabetes[45]. While initial studies of m^6A provide an example of the biological impact mRNA modifications can have, most other mRNA modifications have been minimally investigated. The development of additional sensitive and quantitative techniques to comprehensively evaluate the mRNA modification landscape will be essential to direct future investigations that characterize the molecular level consequence of emerging mRNA modifications.

LC-MS/MS has been a powerful approach to characterize chemical modifications of all three major classes of biomolecules central to protein synthesis (DNA, RNA, and protein). In particular, the sensitivity and specificity of LC-MS/MS methodologies have enabled the

identification and extensive characterization of post-translational protein modifications[46]. While post-transcriptional modifications of ncRNA have been studied for decades using 2D thin layer chromatography[47] and LC coupled to ultraviolet detection[48], [49], recent developments in LC-MS/MS analyses provided some of the first insight into RNA modification abundance and dynamics under cellular stress[50]–[56]. Such methods can broadly detect and provide absolute quantification of modifications in any purified RNA sample[25]. These features have made LC-MS/MS an attractive technology to adopt for mRNA modification discovery. Currently, published methods can assay up to 40 ribonucleosides in a single analysis and use calibration curves from standards to enable quantification with high accuracy and selectivity[20]. However, despite these advantages and the proven utility of LC-MS/MS methodologies for investigating ncRNA modifications, LC-MS/MS has yet to be widely used to study mRNA modifications unlike the comprehensive characterization of post-translational protein modifications by LC-MS/MS technologies over the past few decades.

Here, we identify two factors that have impeded application of LC-MS/MS to mRNA modification analysis: the quantity of mRNA required for current LC-MS/MS sensitivities, and the difficulty to obtain highly pure mRNA. We integrated an improved chromatographic approach with an enhanced mRNA purification and validation process to overcome these limitations and develop a robust workflow for mRNA modification characterization. Our method is capable of quantifying 50 ribonucleoside variants in a single analysis. Analysis of purified *S. cerevisiae* mRNA samples reveals that 1-methylguanosine (m^1G), N2-methylguanosine (m^2G), N2, N2-dimethylguanosine ($m^2{}_2G$), and 5-methyluridine (m^5U) are likely incorporated into mRNAs both enzymatically (Trm10, Trm11, Trm1, and Trm2) and non-enzymatically. We also use a fully purified *in vitro* translation system to demonstrate that the inclusion of these methylated

nucleosides into mRNA codons can slow amino acid addition by the ribosome. Together, our findings advance available chromatography and mRNA purification and validation methods to enhance the high-confidence and high-throughput detection of modified nucleosides by LC-MS/MS and support a growing body of evidence that the inclusion of mRNA modifications commonly alters the peptide elongation during protein synthesis.

3.2 Results

3.2.1 Development of highly sensitive LC-MS/MS method for simultaneously quantifying 50 ribonucleosides

RNA-seq based technologies capable of identifying the location of RNA modifications have revealed that modified nucleosides can be found in thousands of mRNAs[57]. These powerful methodologies have enabled the widespread study of mRNA modifications, but are computationally laborious, not generally quantitative, and typically detect a single modification at a time. In contrast, LC-MS/MS analyses rapidly and quantitatively identify the presence of RNA modifications but cannot report on where they exist throughout the transcriptome[25]. Therefore, the integration of orthogonal LC-MS/MS and RNA-seq based methodologies is required to develop robust platforms for detecting mRNA modifications[57]–[66]. However, the application of LC-MS/MS for nucleoside discovery has been limited by lingering questions regarding mRNA purity, as many reports do not present the comprehensive quality controls necessary for confident mRNA modification analysis. Indeed, a few reported mRNA modifications have not yet been mapped to discrete mRNAs in the transcriptome by RNA-seq based methodologies (e.g., m^1G), likely due to their low abundance and/or possible non-specific incorporation. While there is evidence that the insertion of some mRNA modifications are programmed, suggesting a biological function, other modifications are likely added in a less specific manner (e.g., RNA damage, off

target modification by ncRNA enzymes). Modifications incorporated at lower levels are unlikely to be detected by sequencing-based methods, but can have consequences for cellular health, as illustrated by links between RNA-damage and disease. Therefore, regardless of why a modification is present, it is still essential for us to fully elucidate the mRNA modification landscape and interrogate how these modifications affect cellular function.

Ribonucleosides are most commonly separated using reversed phase chromatography and quantified using multiple reaction monitoring (MRM) on a triple quadrupole mass spectrometer[20], [50], [52], [67], [68]. These methods have reported limits of detection (LODs) down to ~60 attomole for select ribonucleosides using standard mixtures with canonical and modified nucleosides at equal concentrations[50]. However, the abundance of unmodified and modified nucleosides in RNAs are not equivalent in cells, with canonical bases existing in 20- to 10,000-fold higher concentrations than RNA modifications **(Figure 1A)**. In currently available chromatography methods, modified nucleosides (e.g., m^5U, m^1G, $m^1\Psi$, and s^2U) commonly coelute with canonical nucleosides, reducing the detectability of some modified bases[50], [52], [53]. Coelution limits the utility of available LC-MS/MS methods because it results in ion suppression of modified nucleoside signals, with abundant canonical nucleosides outcompeting modified nucleosides for electrospray droplet surface charge. Additionally, this phenomenon makes calibration curves non-linear and worsens the quantifiability of modifications at concentrations necessary for mRNA modification analyses. Recent efforts have been made to derivatize ribonucleosides prior to LC-MS/MS analysis to increase sensitivity and retention on reversed-phase chromatography[21], [69]–[71]. The analogous benzoyl chloride derivatization of neurochemicals has previously been an important separation strategy for many neurochemical monitoring applications[72], [73]. However, labeling strategies are unlikely to prove as useful for

investigating mRNA modifications because derivatizing agents are typically nucleobase specific, limiting the ability of LC/MS-MS assays to be multiplexed[21], [69], [70]. Furthermore, labeling increases the amount of mRNA sample required due to additional sample preparation steps following derivatization. This is an important consideration given that mRNAs represent only ~1-2% of the total RNAs in a cell, and it is already challenging to purify sufficient quantities of mRNA for LC-MS/MS analysis.

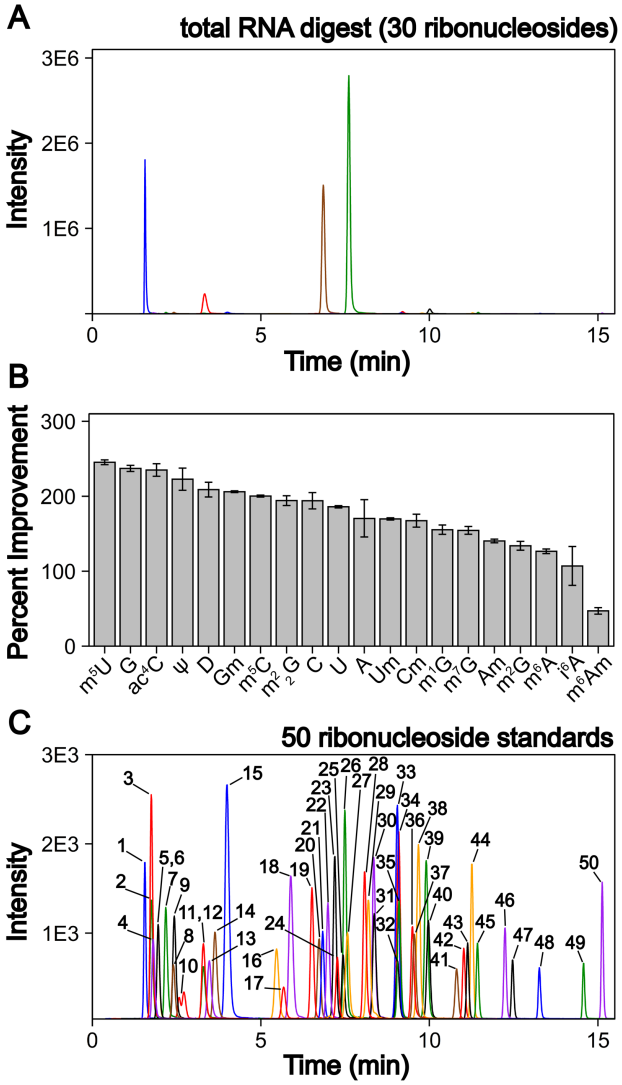

Figure 3.1: ***LC-MS/MS method development to quantify 50 ribonucleosides in a single analysis. A)*** *Extracted ion chromatogram for the 30 ribonucleosides (4 canonical bases and 26 naturally occurring modifications) detected in a S. cerevisiae total RNA digestion displaying that the canonical bases exist at much larger levels than the ribonucleoside modifications.* ***B)*** *LC-MS/MS signal percent improvement using 1 mm chromatography at 100 µL/min compared to 2 mm chromatography at 400 µL/min.* ***C)*** *Extracted ion chromatogram for 50 ribonucleoside*

standards (4 canonical bases, 45 naturally occurring modifications, and 1 non-natural modifications). The concentrations of each ribonucleoside standards within the standard mix and their corresponding peak numbers are displayed in ***Supplemental Table S2****. For the chromatograms, each color peak represents a separate ribonucleoside in the method, and the colors are coordinated between panel A and C.*

We addressed these limitations by first improving upon existing chromatography techniques. Current methods typically utilize 2 mm internal diameter (I.D.) columns that require higher flow rates (300 to 400 μL/min), which worsens ionization efficiencies than smaller I.D. chromatography with lower flow rates. We utilized a 1 mm I.D. column with flow rates at 100 μL/min to lessen these effects. In principle, even smaller bore columns (i.e., "nano-LC"), which are commonly used in in proteomics[74], could be used. Indeed, some studies have shown their effectiveness for nucleosides[75], [76]; however, smaller bore columns can suffer from robustness issues in some conditions. Also, low binding capacity of more polar nucleosides results in poor peak shapes in nano-LC because of relatively large injection volumes. Another limitation has been the stationary phases used, where porous graphitic carbon columns yield poor chromatographic performance for some ribonucleosides (e.g., methylated guanosine modifications) and many C18 phases have low binding capacity for some ribonucleosides (e.g., cytidine and pseudouridine) making them difficult to retain. We used a polar endcapped C18 column to provide more retention and good performance for all nucleosides. We also used mobile phase buffers which have previously been shown to provide high ESI-MS sensitivity for modified ribonucleosides[50]. These alterations combined increased the sensitivity of the assay by 50 to 250% for all nucleosides tested compared to standard 2 mm I.D. chromatography at 400 μL/min **(Figure 1B)** while maintaining adequate ribonucleoside binding capacity for early eluting ribonucleosides. We also altered the chromatographic conditions including increased temperature (35℃ vs 25℃) and modified mobile phase gradients to prevent coelution of the highly abundant canonical nucleosides with the modified nucleosides. Notably, in contrast to most available methods, m^5U, m^1G, $m^1\Psi$

do not coelute with unmodified nucleosides in our method **(Figure 1C)**. This improved separation greatly reduced ionization suppression of these nucleosides. Together, these advancements led to a wider linear dynamic range than previous reports with over four orders of magnitude for most modifications and LODs down to 3 amol (0.6 pM) using a single internal standard and no derivatization steps. Our method represents at least a 10-fold improvement over previous ultrahigh-performance LC (UHPLC) and nano-LC analyses for most modifications analyzed **(Supplemental Table S1 and Supplemental Figures S1 through S4)**. Therefore, the method described here provides a linear dynamic range and LODs capable of analyzing both highly modified ncRNA in addition to the less modified mRNA without large sample requirements. To perform an in-depth RNA modification analysis, approximately 50 to 200 ng of total RNA or mRNA is required per replicate which is achievable using standard eukaryotic and bacterial cell culture techniques. Overall, this assay can quantify the 4 canonical nucleosides, 45 naturally occurring modified nucleosides, and 1 non-natural modified nucleoside (internal control) **(Figure 1C, Supplemental Table S2)**. This work ameliorates current quantitative ribonucleoside LC-MS/MS methodologies by improving chromatographic conditions and characterizing quantifiability at nucleoside concentrations representative of typical RNA digest samples to enable higher confidence total RNA and mRNA modification analyses.

3.2.2 Three-stage mRNA purification and validation pipeline provides highly pure S. cerevisiae mRNA

Total RNA is mainly comprised of the highly modified transfer RNA (tRNA) and ribosomal RNA (rRNA) with a small percentage of mRNA. Unlike RNA-seq, LC-MS/MS assays are unable to distinguish between modifications arising from ncRNA or mRNA. In total RNA digestions, mRNA modifications typically exist at least 100X lower concentrations than in the

corresponding total RNA samples[20]. Thus, even low-level contamination of tRNA and rRNA in purified mRNA samples can lead to inaccurate quantifications as well as false mRNA modifications discoveries. Most of the published mRNA purification pipelines use a combination of poly(A) enrichment and rRNA depletion steps to obtain mRNA[10], [12], [20], [22], [24], [77], [78]. However, previously this was found to be insufficient for removing all signal from contaminating ncRNA modifications during LC-MS/MS analyses, especially from contaminating tRNA[20], [79]. The inability to obtain convincingly pure mRNA samples has long limited the utility of LC-MS/MS for studying these molecules. Recently, small RNA depletion steps have begun to be incorporated into mRNA purification pipelines to remove residual tRNA contamination[80]; however, the highest efficiency purifications typically require expensive instrumentation and materials (liquid chromatograph and size exclusion column)[23] or expertise in RNA gel purification[21]. Despite these improvements, most reports do not provide adequate mRNA purity quality control to confirm removal of ncRNA for confident mRNA modification analyses. In order to apply our LC-MS/MS assay to studying mRNAs, we developed and implemented a three-stage purification pipeline comprised of a small RNA depletion step, two consecutive poly(A) enrichment steps, and ribosomal RNA depletion to selectively deplete the small ncRNA (e.g., tRNA and 5S rRNA) in addition to the 18S rRNA and 28S rRNA using fully commercial kits **(Figure 2)**.

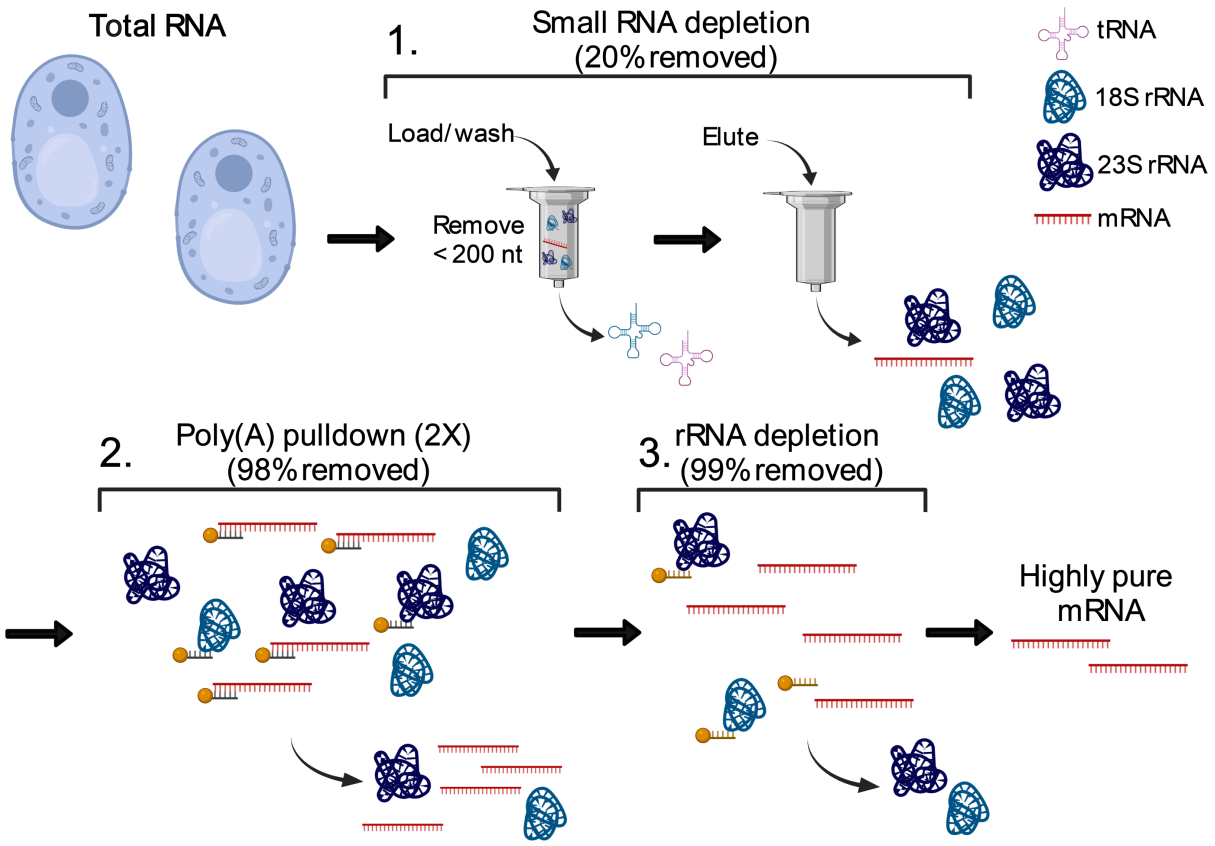

Figure 3.2: ***Three-stage mRNA purification pipeline.*** *Total RNA from S. cerevisiae is purified to mRNA using a three-stage purification pipeline: 1. Small RNA (e.g., tRNA and 5S rRNA) is depleted; 2. mRNA is enriched from the small RNA depleted fraction through two consecutive poly(A) enrichment steps; 3. Remaining rRNA is depleted to result in highly purified mRNA. The displayed percent removed is the additive percent of total RNA removed throughout the three-stage purification pipeline.*

Additionally, we performed extensive quality control on our mRNA samples prior to LC-MS/MS analysis – assessing the purity of our mRNA following the three-stage purification pipeline using chip electrophoresis (Bioanalyzer), RNA-seq, and qRT-PCR. The highly purified mRNA contained no detectable tRNA and rRNA peaks based on our Bioanalyzer electropherograms **(Figure 3A)**.

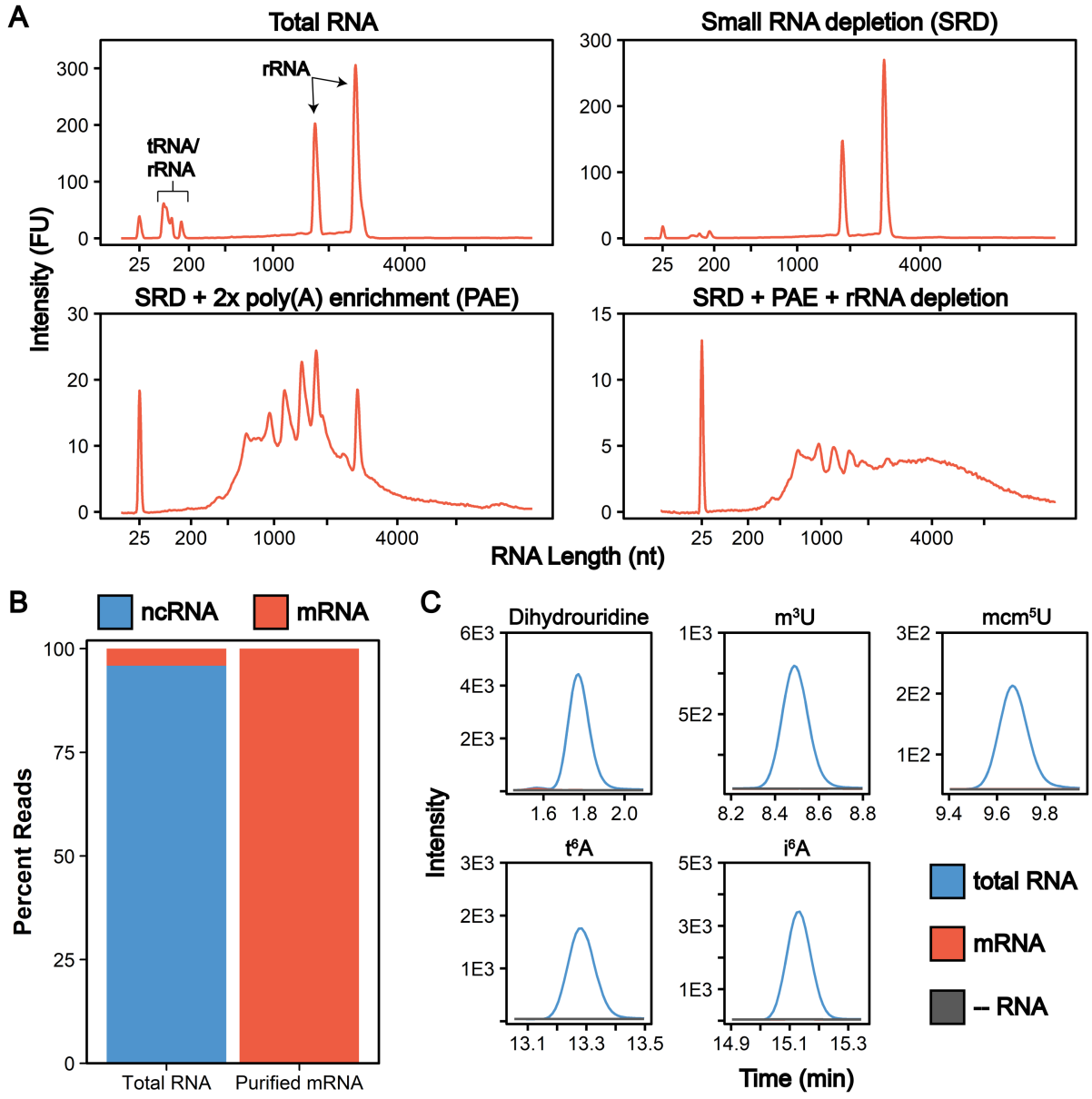

Figure 3.3: ***mRNA purity following three-stage purification pipeline. A)*** *Bioanalyzer electropherograms displaying the RNA distribution following each stage of our purification pipeline.* ***B)*** *Average percentage of reads mapping to ncRNA (rRNA, tRNA, snRNA, etc.) and mRNA determined by RNA-seq of two biological replicate total RNA and purified mRNA samples.* ***C)*** *Representative overlaid extraction ion chromatograms for five RNA modifications that exist solely in ncRNA. These five modifications, in addition to eight additional ncRNA modifications, were detected in our total RNA samples (blue) while not detected in our mRNA samples (red) above our control digestions without RNA added (grey).*

The Bioanalyzer RNA 6000 pico assay provides an LOD of 25 pg/uL for a single RNA[81]; thus, the maximum theoretical tRNA or rRNA contamination would be 0.8% if it was just below our detection limit (3000 pg/uL sample analyzed). Similarly, RNA-seq indicated the mRNA is

enriched from 4.1% in our total RNA to 99.8% purified mRNA samples **(Figure 3B, Supplemental Table S3)**. Additionally, we observed a >3000-fold depletion of 25S and 18S rRNAs and an >9-fold enrichment of actin mRNA based on qRT-PCR **(Supplemental Figure S5)**. Despite recent improvements in RNA-seq technologies and reverse transcriptases, the ability to accurately measure tRNA abundance by RNA-seq remains a struggle due to RNA modifications in these highly structured RNAs. While similar purities by RNA-seq have been achieved without a small RNA depletion step[20], [78], we previously found that this protocol was insufficient at removing all contaminating ncRNA signals by LC-MS/MS[20] since RNA-seq does not accurately report on tRNA contamination[82]. Thus, quality control analyses in addition to RNA-seq are necessary to judge tRNA contamination in purified mRNA.

Since our highly multiplexed LC-MS/MS methodology is capable of quantifying known ncRNA and mRNA modifications in a single analysis, we can use this assay to further confirm the purity of our mRNA from the three-stage purification pipeline **(Figure 2)**. In these assays, total RNA and purified mRNA are degraded to ribonucleosides using a two-stage enzymatic digestion with Nuclease P1 and bacterial alkaline phosphatase **(Figure 4A)**.

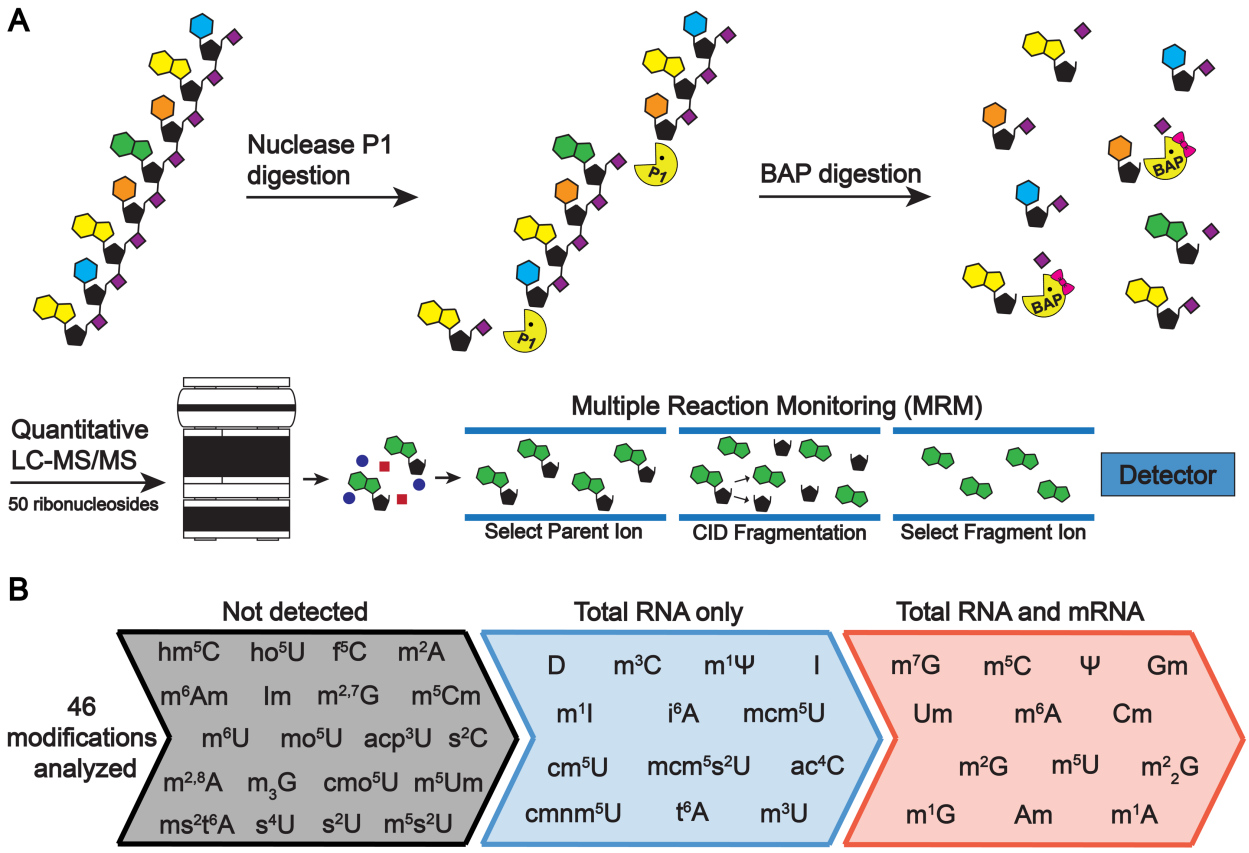

Figure 3.4: ***Enzymatic digestion and LC-MS/MS analysis of S. cerevisiae total RNA and mRNA. A)*** *RNA is enzymatic digested to ribonucleosides through a two-stage process. RNA is first digested to nucleotide monophosphates by nuclease P1 and then dephosphorylated to ribonucleosides by bacterial alkaline phosphatase. The resulting ribonucleosides are separated using reverse phase chromatography and then quantified using MRM on a triple quadrupole mass spectrometer.* ***B)*** *S. cerevisiae total RNA and mRNA were analyzed using the LC-MS/MS method developed to quantify 46 modifications in a single analysis. In total RNA, 26 modifications were detected while 13 ribonucleosides were detected in the highly purified mRNA.*

The resulting modified ribonucleosides are quantified and their concentrations are normalized to their corresponding canonical nucleosides (e.g., m^6A/A) to account for variations in RNA quantities digested. In our total RNA samples, we detected 26 out of 30 known *S. cerevisiae* ribonucleoside modifications that we assayed for, where f^5C, s^2U, $m^{2,7}G$, and m_3G were not detected **(Figure 4B, Supplemental Table S4)**. This was expected because these modifications likely exist at levels below our LOD in our total RNA samples as they either arise from oxidative damage of m^5C (f^5C)[83], [84], are present at very low levels on *S. cerevisiae* tRNA (s^2U)[85]–[87], or are only found in low abundance snRNA and snoRNA ($m^{2,7}G$ and m_3G)[88]–[90].

Additionally, we do not detect the 16 ribonucleoside modifications in our assay that have never been reported in *S. cerevisiae* (1 non-natural and 15 natural) **(Figure 4B, Supplemental Table S4)**. Our purified mRNA samples contained markedly fewer modifications than total RNA, as expected. In addition to the 16 non-*S. cerevisiae* modifications, we do not detect 13 *S. cerevisiae* non-coding RNA modifications that were present in our total RNA samples **(Figure 3C and Supplemental Table S4)**. All modifications not detected in the purified mRNA are reported to be exclusively located in *S. cerevisiae* tRNAs or rRNAs (e.g., i^6A, m^3C)[3], result from oxidative damage (f^5C)[64], or were only previously detected in *S. cerevisiae* mRNAs purified from cells in grown under H_2O_2 stress (ac^4C)[20]. The highly abundant dihydrouridine (DHU) modification provides a key example of such a common ncRNA modification that is not detected in our purified samples. DHU is located at multiple sites on every *S. cerevisiae* tRNA and is present at high levels (1.9 DHU/U%) in our total RNA samples **(Supplemental Table S5 and S6)**. However, we do not detect DHU above our LOD in our purified mRNA **(Figure 3C)**. The inability of our assay to detect highly abundant ncRNA modifications such as DHU provides further evidence that our three-stage purification pipeline produces highly pure mRNA. Commonly, mRNA modification LC-MS/MS analyses characterize only a select few target modifications, which prevents the utilization of LC-MS/MS to judge purity of mRNA. The LC-MS/MS assay described here quantifies up to 46 ribonucleoside modifications in a single analysis, enabling us to use our method to thoroughly characterize mRNA purity. Our analyses ensure that rRNA and tRNA specific modifications are not present at a detectable level in our highly purified mRNA. This highly sensitive corroboration of our Bioanalyzer findings is essential because RNA-seq is not able to sufficiently report on tRNA contamination.

Since all RNA present in our samples will be enzymatically degraded to ribonucleosides during sample preparation **(Figure 4A)**, contaminating highly modified ncRNA will lead to inaccurate modifications quantification in mRNA samples. Thus, extensive quality control for mRNA purity is necessary to give us confidence in downstream LC-MS/MS analyses; however, such data are rarely provided in previous mRNA modification LC-MS/MS studies. Together, we provide four types of evidence (Bioanalyzer, RT-qPCR, RNA-seq, and LC-MS/MS) that our protocol yields highly pure mRNA appropriate for LC-MS/MS analysis. While previous mRNA purification pipelines may inaccurately portray the modification landscape, this pipeline will enable the accurate characterization and quantification of mRNA modifications by providing highly purified mRNA for the analysis using solely commercial kits. We believe that our purification and rigorous purity assessment pipeline could provide a standard method to purify polyadenylated mRNA from total RNA for LC-MS/MS analysis.

3.2.3 m^1G, m^2G, $m^2{}_2G$, and m^5U detected in S. cerevisiae mRNA

In our purified mRNA samples, we detected 13 ribonucleoside modifications that ranged in abundance from pseudouridine (0.023 Ψ/U%) to 1-methyladenosine (0.00014 m^1A/A%) **(Figure 4B, Supplemental Figure S6 and Supplemental Tables S5 and S6)**. These abundances are lower than other previous mRNA modification LC-MS/MS analyses, including a previous *S. cerevisiae* study[20]. We attribute this to the fact that our mRNA is more pure than the mRNA used in previous studies, which leads to lower modification abundances in our samples since there is less contaminating highly modified ncRNA. Most of these modifications we observed in our samples are known to be present in *S. cerevisiae* mRNA; however, we detected four modifications for the first time in *S. cerevisiae* (m^1G, m^2G, $m^2{}_2G$, and m^5U) **(Figure 5A)**. This finding

corroborates previous studies that detected m^1G[24] and m^5U[15], [21], [91] in *Arabidopsis thaliana* and multiple mammalian cell lines at similar levels, respectively.

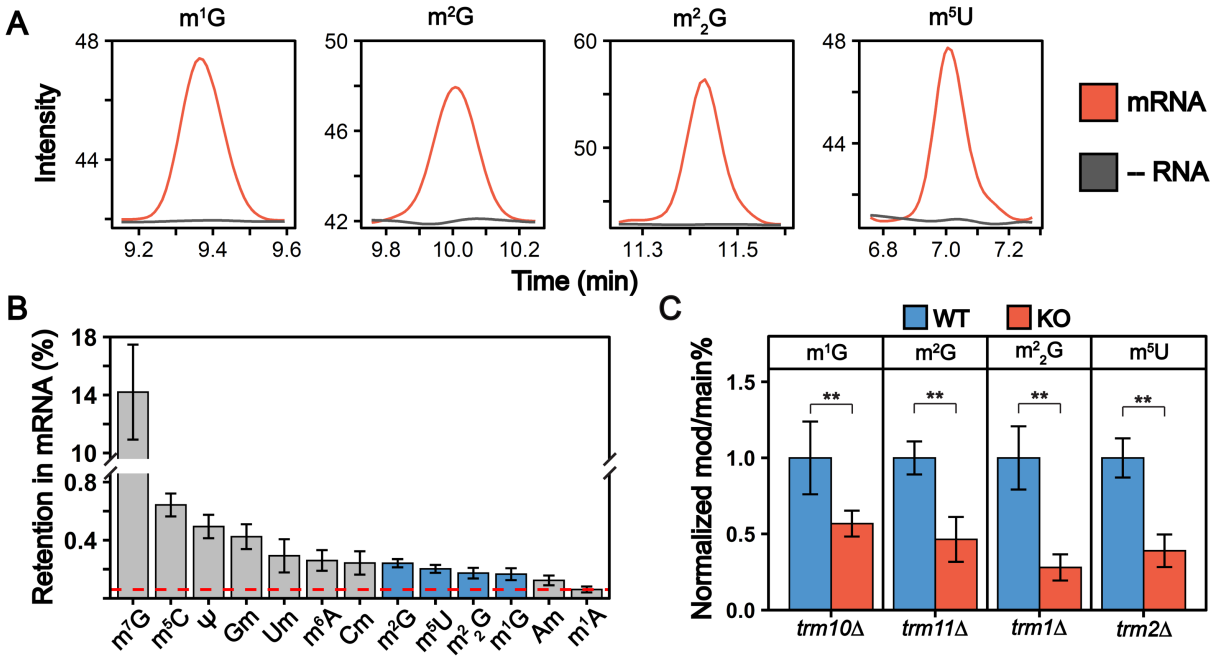

Figure 3.5: ***m1G, m2G, m22G, and m5U are present in S. cerevisiae mRNA.*** ***A)*** *Overlaid extracted ion chromatograms displaying m^1G, m^2G, $m^2{}_2G$, and m^5U are detected in our mRNA samples (red) above our digestion control samples without RNA added (grey).* ***B)*** *m^1G, m^2G, $m^2{}_2G$, and m^5U are only present in S. cerevisiae tRNA; thus, we reasoned that they would be retained at a higher percentage than other highly abundant tRNA modifications if they are present in mRNA. Dihydrouridine, which is the most abundant non-mRNA modification in tRNA, was not detected in our purified mRNA samples. If dihydrouridine existed at levels just below our limit of detection (530 amol), the maximum retention of solely tRNA modifications would be 0.06% (red dashed line). The four new mRNA modifications we detect, along with all other known mRNA modifications, are retained at greater extents which proves these modifications exist in S. cerevisiae mRNA. The error bars are the standard deviation of the percent retention.* ***C)*** *m^1G, m^2G, $m^2{}_2G$, and m^5U are incorporated into S. cerevisiae mRNA by their corresponding tRNA modifying enzymes (Trm10, trm11, Trm1, and Trm2 respectively). The modification/main base% (e.g., m^1G/G%) were normalized to their levels in the average WT mRNA levels. A significant decrease (**p < 0.01) was detected for all cases. The error bars are the standard deviation of the normalized mod/main base%.*

We next critically considered our findings and contemplated the possibility that the signals we detect originated from minor contaminations of tRNA. Prior to this study, in *S. cerevisiae* m^1G, m^2G, $m^2{}_2G$, and m^5U have only been reported in tRNA[3], [92]. Therefore, we reasoned that if these methylated nucleosides are present in *S. cerevisiae* mRNA, they must be retained at higher levels than other tRNA modifications that are not found in mRNA. DHU is the second most abundant RNA modification in *S. cerevisiae* tRNA and thus provides a measure of maximum tRNA contamination **(Supplemental Table S6)**. We did not detect any DHU in our purified

mRNA samples. Recent sequencing based studies have reported the presence of DHU in mammalian and *S. pombe* mRNA[15], [16], but our findings indicate DHU either does not exist within *S. cerevisiae* mRNA or is incorporated at levels below our limit of detection. If dihydrouridine existed at levels just below our limit of detection (530 amol), **(Supplemental Table S1)** the maximum extent of DHU/U% retention in our purified mRNA would be 0.06% when calculated using the average digest uridine concentration in a sample of digested mRNA. We find that m^1G, m^2G, $m^2{}_2G$ and m^5U (in addition to all other modifications) were retained to a greater extent than the maximum theoretical retention of level of DHU (>2.5-fold more) in our purified mRNA **(Figure 5B and Supplemental Table S7)**.

Since all contaminating ncRNA species will be digested to ribonucleosides along with mRNA, it is essential to carefully assess our mRNA purity quality controls and the retention of known exclusive ncRNA modifications in our mRNA modification LC-MS/MS data. In this work, our extensive mRNA purity quality control by Bioanalyzer, RNA-seq, RT-qPCR, and LC-MS/MS in conjunction with there being no other exclusive highly abundant tRNA and rRNA modifications detected in our purified mRNA samples confirms that these modifications are present in *S. cerevisiae* mRNA.

3.2.4 Trm1, Trm2, Trm10 and Trm11 incorporate methylated guanosine and uridine modifications into S. cerevisiae mRNA

Many of the reported mRNA modifications are incorporated by the same enzymes that catalyze their addition into tRNAs and rRNAs[3]. We investigated if the enzymes responsible for inserting m^1G, m^2G, $m^2{}_2G$, and m^5U into *S. cerevisiae* tRNAs (Trm10, Trm11, Trm1, and Trm2 respectively) also incorporate them into *S. cerevisiae* mRNA. We compared the levels of m^1G, m^2G, $m^2{}_2G$, and m^5U in mRNA purified from wild-type and mutant (*trm10*Δ, *trm11*Δ, *trm1*Δ, and

*trm2*Δ) *S. cerevisiae.* The abundance of all four modifications decreased significantly in mRNAs purified from the knockout cell lines **(Figure 5C and Supplemental Tables S6)**. While this demonstrates that the tRNA modifying enzymes incorporate these modifications into *S. cerevisiae* mRNA, low levels of m^1G, m^2G, $m^2{}_2G$, and m^5U modifications are still detected in the mRNAs from knockout cell lines **(Figure 5C)**. Several explanations could account for this. A second enzyme, Trm5, also catalyzes m^1G addition into tRNAs and could possibly explain the remaining mRNA m^1G signals. However, given that m^1G and m^2G were previously found as minor products of methylation damage in DNA and RNA[31], [93]–[99], it is perhaps more likely that the remaining low-level signals that we detect arise from methylation associated RNA damage or minor off target methylation by other enzymes. Regardless of how they are incorporated, when present, these modifications have the potential to impact mRNA function.

3.2.5 m^1G, m^2G and m^5U containing mRNA codons slow amino acid addition by the ribosome in a position dependent manner

While our LC-MS/MS assays indicate that m^1G, m^2G, $m^2{}_2G$ and m^5U modifications exist within *S. cerevisiae* mRNA, no previous work has revealed the location or biological consequence of these modifications in mRNA. Despite their low abundance compared to ncRNA modifications (typically significantly lower than 1% modified), evidence that mRNA modifications can alter the chemical and topological properties of modified transcripts which resultingly affect their stability and function continues to increase. Analogously, N-linked and O-linked glycosylations of proteins occur at rates less than approximately 1% and 0.04% per target amino acid, respectively[100]; however, these post-translational modifications play important biological roles, such protein localization and receptor interaction[101], [102], and their misregulation is linked to multiple diseases[103] despite their low abundance. mRNAs are all substrates for the ribosome, and post-

transcriptional modifications can change how the ribosome decodes a message by altering the hydrogen bonding patterns between the mRNA codons and aminoacylated-tRNAs[104]–[109]. Indeed, several mRNA modifications have been shown to alter the overall rate and fidelity of protein synthesis in a modification and codon-position dependent manner[40], [41], [110]–[115]. Such perturbations to protein synthesis can have significant consequences even when modifications are incorporated into mRNAs transcripts at very low levels, as exemplified by the biological consequences of oxidatively damaged mRNAs, which exist at levels similar to m^1G, m^2G, $m^2{}_2G$ and m^5U[31], [116]. We investigated how the insertion of m^5U, m^1G, and m^2G into mRNA codons impacts translation using a well-established reconstituted *in vitro* translation system[40] **(Figure 6A)**. This system has long been used to investigate how the ribosome decodes mRNAs because it can be purified in sufficient quantities to conduct high-resolution kinetic studies. Translation elongation is well conserved between bacteria and eukaryotes[117], and prior studies demonstrate that mRNA modifications (e.g. pseudouridine, N6-methyladenosine and 8-oxo-G) that slow elongation and/or change mRNA decoding elongation in the reconstituted *E. coli* system[40], [41], [110], [118] also do so in eukaryotes[40], [119]–[121]. $m^2{}_2G$ was not selected for study because the phosphoramidite required for mRNA oligonucleotide synthesis is not commercially available.

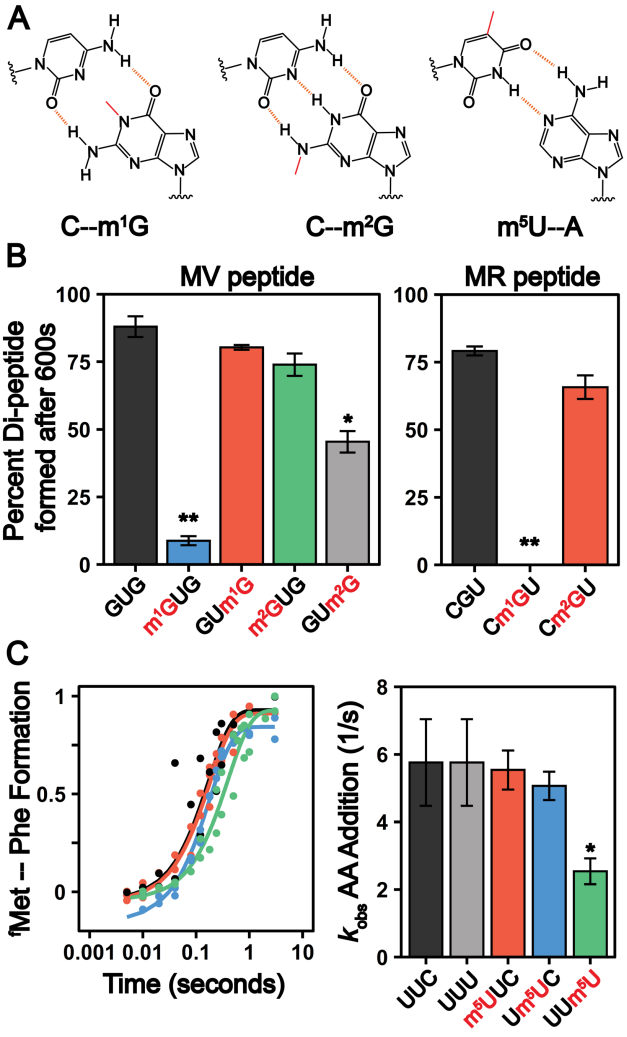

Figure 3.6: **Methylated guanosine and uridine modifications alter amino acid addition. A)** Watson-Crick base pairing of m^1G, m^2G and m^5U. The added methylation is displayed in red and the hydrogen bond interactions displayed as a dashed orange line. **B)** Total peptide formation of translation reactions after 600 seconds using transcribed or single-nucleotide modified mRNAs encoding for either (Left Panel) Met-Val (GUG) or (Right Panel) Met-Arg (CGU) dipeptide. Error bars are the standard deviation. **B)** Time courses displaying the formation of ^{f}Met-Phe dipeptide on an unmodified and singly modified UUC or UUU codons (left panel). Observed rate constants (right panel) were determined from the fit data. The error bars are the standard deviation of the fitted value of k_{obs}.

In our assays, 70S ribosome initiation complexes (ICs) containing ^{35}S-^{f}Met-tRNA^{fmet} programmed in the A site are formed on transcripts encoding Met-Phe, Met-Arg, or Met-Val dipeptides. Ternary complexes comprised of aminoacyl-tRNA:EF-Tu:GTP are added to the ICs to begin translation. Reactions are quenched as desired timepoints by KOH, and the unreacted ^{35}S-^{f}Met-tRNA^{fmet} and dipeptide translation products are visualized by electrophoretic TLC (eTLC) **(Supplementary Figures S7 through S10)**. We evaluated the extent of total dipeptide synthesis

and/or the rate constants (k_{obs}) for amino acid incorporation on unmodified (CGU, GUG, UUC, UUU) and modified (Cm^{1}GU, Cm^{2}GU, m^{1}GUG, m^{2}GUG, GUm^{1}G, GUm^{2}G, m^{5}UUC, Um^{5}UC, Uum^{5}U) codons. The presence of modifications in the codons were verified by direct infusion ESI-MS or nanoelectrospray ionization (nESI)-MS **(Supplemental Figures S11 to S13)**. We observed that the extent of amino acid addition is drastically reduced when m^{1}G is present at the first or second position in a codon but is restored to normal levels when m^{1}G is at the third nucleotide **(Figure 6B and Supplemental Figures S7 through S9)**. Codons containing m^{2}G show a more modest defect in dipeptide production, only significantly impeding dipeptide synthesis (1.9 ± 0.2-fold) when m^{2}G is in the third position of a codon **(Figure 6B and Supplemental Figures S7 through S9)**. These findings are consistent with a previous report indicating that insertion of a single m^{1}G and m^{2}G modification into an mRNA codon reduces the overall protein production and translation fidelity in a position and codon dependent manner[115]. m^{1}G and m^{2}G should both disrupt Watson-Crick base pairing between mRNAs and tRNAs **(Figure 6A)** and might be expected to alter amino acid addition in similar ways. However, our results reveal that the insertion of m^{1}G has a much larger consequence than m^{2}G on peptide production. This can be partially rationalized by the fact that m^{1}G would impede canonical Watson-Crick base-pairing by eliminating a central H-bond interaction, while m^{2}G disrupts only peripheral interactions **(Figure 6A)**. Additionally, the methylation of the analogous position of adenosine (m^{1}A) similarly abolishes the ability of the ribosome to add amino acids[30], suggesting that the conserved N1 position on purine nucleobases is particularly crucial to tRNA decoding. The hydrogen bonding patterns possible between m^{2}G and other nucleosides would be expected to closely resemble those of another well studied modification, inosine. Inosine also has a moderate (if any) impact on the rates of protein synthesis, though it can promote amino acid mis-incorporation[122], [123]. The

limited consequence of both inosine and m^2G on overall peptide production indicates that purine peripheral amines on the Watson-Crick face are less important than the N1 position for ensuring the rapid addition of amino acids by the ribosome.

In contrast to the guanosine modifications that we investigated, transcripts containing m^5U Phe-encoding codons did not reduce the total amount of dipeptide produced **(Figure 6C)**. However, the insertion of m^5U into codons can reduce the rate constants for amino acid addition (k_{obs}) in a position dependent manner, similar to Ψ modified transcripts[40]. The rate constant for Phe incorporation on an unmodified and modified codons at the 1st and 2nd position were comparable to an unmodified codon, with a k_{obs} of ~ $5s^{-1}$ **(Figure 6C and Supplemental Figure S10)**. However, when m^5U is in the 3rd position we see a 2-fold decrease in the k_{obs} at ~ $2.5s^{-1}$ **(Figure 6C and Supplemental Figure S10)**. This is the first evidence that m^5U can influence amino acid addition when encountered by the ribosome. It is less clear how m^5U and other modifications that do not change the Watson-Crick face of nucleobases (e.g., Ψ and 8-oxoG) impact translation[124]. It is possible that such modifications alter nucleobase ring electronics to perturb the strength of the hydrogen bond donors and acceptors involved in base pairing.

While the levels of the mRNA modifications we identified are lower than that of more well-established modifications (m^6A and Ψ), our findings suggest that they still have potential to impact biology. Although our data do not report on the ability of the modifications that we uncover to control gene expression or identify the number of mRNAs that they are in, they do suggest that there will be consequences for translation when these modifications are encountered by the ribosome. It is also important to note that the levels and distributions of mRNA modifications (enzymatic and RNA damage) can change significantly in response to different environmental conditions, so the low levels of modification that we measure in healthy, rapidly growing yeast

have the potential to significantly increase under stress[20], [28], [116], [125]. The three modifications we investigated alter translation differently depending on their location within a codon. Such a context dependence has been observed for every mRNA modification investigated to date[124]. Modifications have the capacity to change intra-molecular interactions with an mRNA, or interactions between rRNA and mRNA within the A site. There is growing evidence that such factors, and not only anticodon:codon interactions, have a larger contribution to translation elongation than previously recognized. For example, ribosome stalling induced by the rare 8-oxo-guanosine damage modification has the potential to perturb ribosome homeostasis or even the small pauses in elongation induced by mRNA pseudouridine modifications can impact levels of protein expression in a gene specific manner[31], [121]. Additionally, transient ribosome pauses have the potential modulate co-translational protein folding or provide time for RNA binding proteins to interact with a transcript[126], [127]. Future systematic biochemical and computational studies are needed to uncover the causes of the context dependence. Additionally, the continued development of RNA-seq technologies is needed to locate these modifications throughout the transcriptome. This information will be broadly useful as researchers seek to identify which of the modified mRNA codons are the most likely to have molecular level consequences when encountered by a translating ribosome.

3.3 Conclusions

Mass spectrometry-based approaches are widely used to study protein post-translational modifications, but the application of similar techniques to investigate mRNA post-transcriptional modifications has not been widely adopted. The current LC-MS/MS workflows for discovering and studying mRNA modifications are hindered by either low-throughput method development, inadequate mRNA purification, or insufficient sensitivities to detect low level mRNA

modifications. This study presents mRNA purification, validation, and LC-MS/MS pipelines that enable the sensitive and highly multiplexed analysis of mRNA and ncRNA modifications. These developments enable us to confidently identify four previously unreported mRNA modifications in *S. cerevisiae* (m^1G, m^2G, $m^2{}_2G$ and m^5U), demonstrating the utility of applying LC-MS/MS to discover and quantify mRNA modifications. In addition to revealing the enzymes that incorporate these modifications, we also demonstrate that the presence of m^1G, m^2G, and m^5U in mRNA can impede translation. However, the impacts of the modifications on amino acid addition are not uniform, with the position and identity of each modification resulting in a different outcome on dipeptide production. This work suggests that the ribosome will regularly encounter a variety of modified codons in the cell and that depending on the identity and position of the modification, these interactions can alter the elongation step in protein synthesis.

3.4 Methods

3.4.1 S. cerevisiae Cell Growth and mRNA Purification

Wild-type, *Δtrm1*, *Δtrm2*, *Δtrm10* and *Δtrm11* BY4741 *S. cerevisiae* (Horizon Discovery) were grown in YPD medium as previously described[20]. Knockout cells lines were grown with 200 μg/mL Geneticin. Briefly, 100 mL of YPD medium was inoculated with a single colony selected from a plate and allowed to grow overnight at 30℃ and 250 RPM. The cells were diluted to an OD_{600} of 0.1 with 300 mL of YPD medium and were grown to an OD_{600} of 0.6-0.8 at 30℃ and 250 RPM. The cell suspension was pelleted at 3,220 x g at 4℃ and used for the RNA extraction.

S. cerevisiae cells were lysed as previously described with minor alterations[20], [128]. The 300 mL cell pellet was resuspended in 12 mL of lysis buffer (60 mM sodium acetate pH 5.5, 8.4 mM EDTA) and 1.2 mL of 10% SDS. One volume (13.2 mL) of acid

phenol:chloroform:isoamyl alcohol (125:24:1; Sigma-Aldrich, USA; P1944) was added and vigorously vortexed. The mixture was incubated in a water bath at 65℃ for five min and was again vigorously vortexed. The incubation at 65℃ and vortexing was repeated once. Then, the mixture was rapidly chilled in an ethanol/dry ice bath until lysate was partially frozen. The lysate was allowed to thaw and then centrifuged for 15 min at 15,000 x g. The upper layer containing the total RNA was washed three additional times with 13.2 mL phenol and the phenol was removed using two chloroform extractions of the same volume. The resulting RNA was ethanol precipitated in the presence of 1/10th volume of 3 M sodium acetate and then a second time in the presence of 1/2 volume of 7.5 M ammonium acetate. The extracted total RNA was treated with 140 U RNase-free DNase I (Roche, 10 U/μL) in the supplied digestion buffer at 37℃ for 30 min. The DNase I was removed through an acid phenol-chloroform extraction. The resulting RNA was ethanol precipitated in the presence of 1/10th volume of 3 M sodium acetate pH 5.2 and then a second time in the presence of 1/2 volume of 7.5 M ammonium acetate. The precipitated RNA was pelleted and resuspended in water. The resulting total RNA was used for our LC-MS/MS, bioanalyzer, and RNA-seq analyses.

mRNA was purified through a three-stage purification pipeline. First, small RNA (tRNA and 5S rRNA) was diminished from 240 μg of total RNA using a Zymo RNA Clean and Concentrator-100 kit to purify RNA > 200nt. Two consecutive poly(A) enrichment steps were applied to 125 μg of the resultant small RNA diminished samples using Dynabeads oligo-dT magnetic beads (Invitrogen, USA). The resulting poly(A) RNA was ethanol precipitated using 1/10th volume of 3 M sodium acetate pH 5.2 and resuspended in 14 μL of water. Then, we removed the residual 5S, 5.8S, 18S, and 28S rRNA using the commercial riboPOOL rRNA depletion kit

(siTOOLs Biotech). The Bioanalyzer RNA 6000 Pico Kit (Agilent) was used to evaluate the purity of the mRNA prior to LC-MS/MS analysis.

3.4.2 qRT-PCR

DNase I treated total RNA and three-stage purified mRNA (200 ng) were reverse transcribed using the RevertAid First Strand cDNA Synthesis Kit (Thermo Scientific) using the random hexamer primer. The resulting cDNA was diluted 5000-fold and 1 μL of the resulting mixture was analyzed using the Luminaris Color HiGreen qPCR Master Mix (Thermo Scientific) with gene-specific primers (**Supplemental Table S8**).

3.4.3 RNA-seq

The WT *S. cerevisiae* mRNA was analyzed by RNA-seq as previously described with minimal alterations[20]. Briefly, 50 ng of DNase I treated total RNA and three-stage purified mRNA from the two biological replicates were fragmented using the TruSeq RNA Library Prep Kit v2 fragmentation buffer (Illumina). First-strand cDNA synthesis was performed using the random hexamer primer, and the second strand was synthesized using the Second Strand Master Mix. The resulting cDNA was purified with AMPure XP beads (Beckman Coulter), the ends were repaired, and the 3' end was adenylated. Lastly, indexed adapters were ligated to the DNA fragments and amplified using 15 PCR cycles. Paired-end sequencing was performed for the cDNA libraries using 2.5% of an Illumina NovaSeq (S4) 300 cycle sequencing platform flow cell (0.625% of flow cell for each sample). All sequence data are paired-end 150 bp reads.

FastQC (v0.11.9)[129] was used to evaluate the quality of the raw and trimmed reads. Then, cutadapt (v1.18)[130] was used to trim to paired-end 50 bp reads and obtain high quality clean reads with the arguments -u 10 -U 10 -l 50 -m 15 -q 10. Following, Bowtie2 (v2.2.5)[131]

was used to align the forward strand reads to *S. cerevisiae* reference genome (R64-1-1) with the default parameters. Following alignment, Rmmquant tool R package (v1.6.0)[132] and the gene_biotype feature in the *S. cerevisiae* GTF file was used to count the number of mapped reads for each transcript and classify the RNA species, respectively.

3.4.4 RNA digestions and LC-MS/MS analysis

RNA (200 ng) was hydrolyzed to composite mononucleosides using a two-step enzymatic digestion. The RNA was first hydrolyzed overnight to nucleotide monophosphates using 300 U/μg Nuclease P1 (NEB, 100,000 U/mL) at 37°C in 100 mM ammonium acetate (pH 5.5) and 100 μM $ZnSO_4$. Following, the nucleotides were dephosphorylated using 50 U/μg bacterial alkaline phosphatase (BAP, Invitrogen, 150U/μL) for 5 hrs at 37°C in 100 mM ammonium bicarbonate (pH 8.1) and 100 μM $ZnSO_4$. Prior to each reaction, the enzymes were buffer exchanged into their respective reaction buffers above using a Micro Bio-Spin 6 size exclusion spin column (Biorad) to remove glycerol and other ion suppressing constituents. After the reactions, the samples were lyophilized and resuspended in 9 μL of water and 1 μL of 400 nM $^{15}N_4$-inosine internal standard.

The resulting ribonucleosides were separated using a Waters Acquity HSS T3 column (1 x 100 mm, 1.8 μm, 100 Å) with a guard column at 100 μL/min on a Agilent 1290 Infinity II liquid chromatograph interfaced to a Agilent 6410 triple quadrupole mass spectrometer. Mobile phase A was 0.01% (v/v) formic acid in water and mobile phase B was 0.01% (v/v) formic acid in acetonitrile. The gradient is displayed in **Supplemental Table S9**. The autosampler was held at 4°C, and 5 μL was injected for each sample. The eluting ribonucleosides were quantified using MRM and ionized using electrospray ionization in positive mode at 4 kV **(Supplemental Table S10)**. The electrospray ionization conditions were optimized by infusing 500 nM uridine at 100 μL/min at 5% mobile phase B. The gas temperature was 350°C, the gas flow rate was 10 L/min,

and the nebulizer gas pressure was 25 psi. After each RNA digestion sample, a wash gradient injection was performed to eliminate any column carryover of late eluting nucleosides (e.g., i^6A) **(Supplemental Table S9)**.

To compare the sensitivity between the 1 mm and 2 mm I.D. column chromatographies, a 2.1 mM Waters Acquity HSS T3 column (2.1 x 100 mm, 1.8 µm, 100A) with a guard column was used at 400 uL/min using the same gradient and mobile phases described above. The source conditions for the 2.1 mm I.D. column were optimized by infusing 500 nM uridine at 400 µL/min at 5% mobile phase B. The gas temperature was 350°C, the gas flow rate was 10 L/min, and the nebulizer gas pressure was 55 psi. For both analyses, 5 uL of ribonucleoside standard mixes containing 1.4 µM canonical nucleosides and 72 nM modifications was injected.

To quantify RNA nucleosides calibration curves were created for the four main bases, 45 natural modified nucleosides, and 1 non-natural modified nucleoside using seven calibration points ranging over four orders of magnitude. $^{15}N_4$-inosine (40 nM) was used as the internal standard for all ribonucleosides. The concentrations of ribonculeoside in the calibration curves standards can be found in **Supplemental Table 11.** Suppliers for ribonucleoside standards can be found in **Supplemental Table 12**. Automated peak integration was performed using the Agilent MassHunter Workstation Quantitative Analysis Software. All peaks were visually inspected to ensure proper integration. The calibration curves were plotted as the $\log_{10}$(response ratio) versus the $\log_{10}$(concentration (pM)) and the RNA sample nucleoside levels were quantified using the resulting linear regression. The limits of detection were calculated using:

$$LOD\ (pM) = 10^{\frac{(3 \times standard\ error\ of\ regression) + (\log_{10} average\ response\ ratio\ of\ blank) - (y\ intercept)}{Slope\ of\ linear\ regression}}$$

The calculated LOD was then converted to amol. For each RNA enzymatic digestion samples, the respective calibration curve was used to calculate nucleoside concentrations in the samples. The retention of modifications in mRNA was calculated using the following equation:

$$Retention\% = \frac{mod/main\%\ in\ mRNA}{mod/main\%\ in\ total\ RNA} x100\%$$

3.4.5 E. coli ribosomes and translation factor purification

Ribosomes were purified from *E. coli* MRE600 as previously described[40]. All constructs for translation factors were provided by the Green lab unless specifically stated otherwise. The expression and purification of translation factors were carried out as previously described[40].

3.4.6 tRNA and mRNA for in vitro translation assay

Unmodified transcripts were prepared using run-off T7 transcription of Ultramer DNA templates that were purchased from Integrated DNA Technologies **(Supplemental Table S13)**. HPLC purified modified mRNA transcripts containing 5-methyluridine, 1-methylguanosine, and N2-methylguanosine were purchased from Dharmacon **(Supplemental Table S14)**. The homogeneity and accurate mass for most of the purchased modified oligonucleotides were confirmed by direct infusion ESI-MS prior to use by Dharmacon **(Supplementary Figure S11 through S13)**. For the remaining purchased oligonucleotides lacking Dharmacon spectra, they were analyzed on a ThermoFisher Q-Exactive UHMR Hybrid Quadrupole-Orbitrap Mass Spectrometer in a negative ionization polarity. Samples were buffer exchanged into 100 mM ammonium acetate (AmOAc) using Micro Bio-Spin P-6 gel columns and directly infused via nanoelectrospray ionization (nESI). nESI was performed using borosilicate needles pulled and coated in-house with a Sutter p-97 Needle Puller and a Quorum SCX7620 mini sputter coater,

respectively. The acquired native mass spectra were deconvoluted using UniDec[133] in negative polarity **(Supplementary Figure S11)**.

Native tRNA was purified as previously described with minor alterations[134]. Bulk *E. coli* tRNA was either bought in bulk from Sigma-Aldrich or purified from a HB101 *E. coli* strain containing pUC57-tRNA that we obtained from Prof. Yury Polikanov (University of Illinois, Chicago). Two liters of media containing Terrific Broth (TB) media (TB, 4 mL glycerol/L, 50 mM NH_4Cl, 2 mM $MgSO_4$, 0.1 mM $FeCl_3$, 0.05% glucose and 0.2% lactose (if autoinduction media was used)) were inoculated with 1:400 dilution of a saturated overnight culture and incubated with shaking at 37℃ overnight with 400 mg/ml of ampicillin. Cells were harvested the next morning by 30 min centrifugation at 5000 RPM and then stored at -80℃. Extraction of tRNA was done by first resuspending the cell pellet in 200 mL of resuspension buffer (20 mM Tris-Cl, 20 mM $Mg(OAc)_2$ pH 7.) The resuspended cells were then placed in Teflon centrifuge tubes with ETFE o-rings containing 100 mL acid phenol/chloroform/isoamyl alcohol mixture. The tubes were placed in a 4℃ incubator and left to shake for 1 hr. After incubation, the lysate was centrifuged for 60 min at 3,220 x g at 4℃. The supernatant was transferred to another container and the first organic phase was then back-extracted with 100mL resuspension buffer and centrifuged down for 60 min at 3,220 x g at 4℃. Aqueous solutions were then combined and a 1/10 volume of 3 M sodium acetate pH 5.2 was added and mixed well. Isopropanol was added to 20% and after proper mixing was centrifuged to remove DNA at 13,700 x g for 60 min at 4℃. The supernatant was collected, and isopropanol was added to 60% and was left to precipitate at -20℃ overnight. The precipitated RNA was pelleted at 13,700 x g for 60 min at 4℃ and resuspended with approximately 10 mL 200 mM Tris-Acetate, pH 8.0. The RNA was incubated at 37℃ for at least 30 min to deacylate the tRNA. After incubation $1/10^{th}$ volume of 3 M sodium acetate pH 5.2 and 2.5 volumes

of ethanol was added to precipitate the RNA. Then, the mixture was centrifuged at 16,000 x g for 60 min at 4°C. The pellet was washed with 70% ethanol, resuspended in water, and desalted using an Amicon 10 kDa MWCO centrifugal filter prior to purification (Millipore-Sigma, USA).

Next, the tRNA was isolated using a Cytiva Resource Q column (6 mL) on a AKTA Pure 25M FPLC. Mobile phase A was 50 mM NH_4OAc, 300 mM NaCl, and 10 mM $MgCl_2$. Mobile phase B was 50 mM NH_4OAc, 800 mM NaCl, 10 mM $MgCl_2$. The resuspended RNA was filtered, loaded on the Resource Q column, and eluted with a linear gradient from 0-100% mobile phase B over 18 column volumes. Fractions were pulled and ethanol precipitated overnight at -20°C.

The precipitated RNA was resuspended in water and filtered prior to purification on a Waters XBridge BEH C18 OBD Prep wide pore column (10 x 250 mm, 5 μm). Mobile phase A was 20 mM NH_4OAc, 10 mM $MgCl_2$, and 400 mM NaCl at pH 5 in 100% water. Mobile phase B was 20 mM NH_4OAc, 10 mM $MgCl_2$, and 400 mM NaCl at pH 5 in 60% methanol. The injection volume was 400 μl. A linear gradient of mobile phase B from 0-35% was done over 35 min. After 35 min, the gradient was increased to 100% mobile phase B over 5 min and held at 100% for 10 min, column was then equilibrated for 10 column volumes before next injection with mobile phase A. TCA precipitations were performed on the fractions to identify fractions containing the phenylalanine tRNA as well as measuring the A_{260} and amino acid acceptor activity.

3.4.7 Formation of E. coli ribosome initiation complexes

Initiation complexes (ICs) were formed in 1X 219-Tris buffer (50 mM Tris pH 7.5, 70 mM NH_4Cl, 30 mM KCl, 7 mM $MgCl_2$, 5 mM β-ME) with 1 mM GTP as previously described[134]. 70S ribosomes were incubated with 1 μM mRNA (with or without modification), initiation factors (1, 2, and 3) all at 2 μM final, and 2 μM of radiolabeled ^{35}S-^{f}Met-$tRNA^{fMet}$ for 30 min at 37°C. After incubation, $MgCl_2$ was added to a final concentration of 12

mM. The ribosome mixture was then layered onto 1 mL cold buffer D (20 mM Tris-Cl, 1.1 M sucrose, 500 mM NH_4Cl, 10 mM $MgCl_2$, 0.5 mM disodium EDTA, pH 7.5) and centrifuged at 69,000 rpm for 2 hrs at 4°C. After pelleting, the supernatant was discarded into radioactive waste, and the pellet was resuspended in 1X 219-tris buffer and stored at -80°C.

3.4.8 In vitro amino acid addition assays

IC complexes were diluted to 140 nM with 1X 219-Tris buffer. Ternary complexes (TCs) were formed by first incubating the EF-Tu pre-loaded with GTP (1X 219-Tris buffer, 10 mM GTP, 60 μM EFTu, 1 μM EFTs) at 37°C for 10 min. The EF-Tu mixture was incubated with the tRNA mixture (1X 219-Tris buffer, Phe-$tRNA^{Phe}$ (1-10 μM), 1 mM GTP) for another 15 min at 37°C. After TC formation was complete, equal volumes of IC complexes (70 nM) and ternary complex (1 μM) were mixed either by hand or using a KinTek quench-flow apparatus. Discrete time-points (0-600 seconds) were taken as to obtain observed rate constants on m^5U-containing mRNAs. Each time point was quenched with 500 mM KOH (final concentration). Time points were then separated by electrophoretic TLC and visualized using phosphorescence as previously described[40], [134]. Images were quantified with ImageQuant. The data were fit using Equation 1:

$$Fraction\ product\ = A \cdot (\ 1 - e^{k_{obs}t})$$

3.5 References

[1] P. J. McCown *et al.*, "Naturally occurring modified ribonucleosides," *WIREs RNA*, vol. 11, no. 5, p. e1595, 2020, doi: https://doi.org/10.1002/wrna.1595.

[2] R. J. Ontiveros, J. Stoute, and K. F. Liu, "The chemical diversity of RNA modifications," *Biochemical Journal*, vol. 476, no. 8, pp. 1227–1245, Apr. 2019, doi: 10.1042/BCJ20180445.

[3] P. Boccaletto *et al.*, "MODOMICS: a database of RNA modification pathways. 2017 update," *Nucleic Acids Res*, vol. 46, no. Database issue, pp. D303–D307, Jan. 2018, doi: 10.1093/nar/gkx1030.

[4] N. Jonkhout, J. Tran, M. A. Smith, N. Schonrock, J. S. Mattick, and E. M. Novoa, “The RNA modification landscape in human disease,” *RNA*, vol. 23, no. 12, pp. 1754–1769, Dec. 2017, doi: 10.1261/rna.063503.117.
[5] X. Zhang *et al.*, “Small RNA modifications in Alzheimer’s disease,” *Neurobiology of Disease*, vol. 145, p. 105058, Nov. 2020, doi: 10.1016/j.nbd.2020.105058.
[6] M. Pereira, S. Francisco, A. S. Varanda, M. Santos, M. A. S. Santos, and A. R. Soares, “Impact of tRNA Modifications and tRNA-Modifying Enzymes on Proteostasis and Human Disease,” *International Journal of Molecular Sciences*, vol. 19, no. 12, Art. no. 12, Dec. 2018, doi: 10.3390/ijms19123738.
[7] J. Ramos *et al.*, “Identification and rescue of a tRNA wobble inosine deficiency causing intellectual disability disorder,” *RNA*, vol. 26, no. 11, pp. 1654–1666, Nov. 2020, doi: 10.1261/rna.076380.120.
[8] J. T. Lant, M. D. Berg, I. U. Heinemann, C. J. Brandl, and P. O’Donoghue, “Pathways to disease from natural variations in human cytoplasmic tRNAs,” *J. Biol. Chem.*, vol. 294, no. 14, pp. 5294–5308, Apr. 2019, doi: 10.1074/jbc.REV118.002982.
[9] H. Lin *et al.*, “CO2-sensitive tRNA modification associated with human mitochondrial disease,” *Nature Communications*, vol. 9, no. 1, Art. no. 1, May 2018, doi: 10.1038/s41467-018-04250-4.
[10] D. Dominissini *et al.*, “Topology of the human and mouse m6A RNA methylomes revealed by m6A-seq,” *Nature*, vol. 485, no. 7397, pp. 201–206, May 2012, doi: 10.1038/nature11112.
[11] C. Enroth, L. D. Poulsen, S. Iversen, F. Kirpekar, A. Albrechtsen, and J. Vinther, “Detection of internal N7-methylguanosine (m7G) RNA modifications by mutational profiling sequencing,” *Nucleic Acids Research*, p. gkz736, Aug. 2019, doi: 10.1093/nar/gkz736.
[12] L. S. Zhang *et al.*, “Transcriptome-wide Mapping of Internal N7-Methylguanosine Methylome in Mammalian mRNA,” *Mol Cell*, vol. 74, no. 6, Art. no. 6, Jun. 2019, doi: 10.1016/j.molcel.2019.03.036.
[13] T. M. Carlile, M. F. Rojas-Duran, B. Zinshteyn, H. Shin, K. M. Bartoli, and W. V. Gilbert, “Pseudouridine profiling reveals regulated mRNA pseudouridylation in yeast and human cells,” *Nature*, vol. 515, no. 7525, pp. 143–146, Nov. 2014, doi: 10.1038/nature13802.
[14] A. F. Lovejoy, D. P. Riordan, and P. O. Brown, “Transcriptome-Wide Mapping of Pseudouridines: Pseudouridine Synthases Modify Specific mRNAs in S. cerevisiae,” *PLOS ONE*, vol. 9, no. 10, p. e110799, Oct. 2014, doi: 10.1371/journal.pone.0110799.
[15] W. Dai *et al.*, “Activity-based RNA-modifying enzyme probing reveals DUS3L-mediated dihydrouridylation,” *Nat Chem Biol*, vol. 17, no. 11, pp. 1178–1187, Nov. 2021, doi: 10.1038/s41589-021-00874-8.
[16] O. Finet *et al.*, “Transcription-wide mapping of dihydrouridine reveals that mRNA dihydrouridylation is required for meiotic chromosome segregation,” *Molecular Cell*, vol. 82, pp. 1–16, Nov. 2021, doi: 10.1016/j.molcel.2021.11.003.
[17] Q. Dai *et al.*, “Nm-seq maps 2′O-methylation sites in human mRNA with base precision,” *Nature Methods*, vol. 14, no. 7, pp. 695–698, Jul. 2017, doi: 10.1038/nmeth.4294.
[18] S. Okada, H. Ueda, Y. Noda, and T. Suzuki, “Transcriptome-wide identification of A-to-I RNA editing sites using ICE-seq,” *Methods*, vol. 156, pp. 66–78, Mar. 2019, doi: 10.1016/j.ymeth.2018.12.007.

[19] D. Arango *et al.*, "Acetylation of Cytidine in mRNA Promotes Translation Efficiency," *Cell*, vol. 175, no. 7, pp. 1872-1886.e24, Dec. 2018, doi: 10.1016/j.cell.2018.10.030.
[20] M. Tardu, J. D. Jones, R. T. Kennedy, Q. Lin, and K. S. Koutmou, "Identification and quantification of modified nucleosides in Saccharomyces cerevisiae mRNAs," *ACS Chem Biol*, vol. 14, no. 7, Art. no. 7, Jul. 2019, doi: 10.1021/acschembio.9b00369.
[21] Q.-Y. Cheng *et al.*, "Chemical tagging for sensitive determination of uridine modifications in RNA," *Chem. Sci.*, vol. 11, no. 7, pp. 1878–1891, 2020, doi: 10.1039/C9SC05094A.
[22] J.-M. Chu *et al.*, "Existence of Internal N7-Methylguanosine Modification in mRNA Determined by Differential Enzyme Treatment Coupled with Mass Spectrometry Analysis," *ACS Chem. Biol.*, vol. 13, no. 12, pp. 3243–3250, Dec. 2018, doi: 10.1021/acschembio.7b00906.
[23] L. Xu *et al.*, "Three distinct 3-methylcytidine (m3C) methyltransferases modify tRNA and mRNA in mice and humans," *J. Biol. Chem.*, vol. 292, no. 35, pp. 14695–14703, Sep. 2017, doi: 10.1074/jbc.M117.798298.
[24] H.-C. Duan *et al.*, "ALKBH10B Is an RNA N6-Methyladenosine Demethylase Affecting Arabidopsis Floral Transition," *Plant Cell*, vol. 29, no. 12, pp. 2995–3011, Dec. 2017, doi: 10.1105/tpc.16.00912.
[25] J. D. Jones, J. Monroe, and K. S. Koutmou, "A molecular-level perspective on the frequency, distribution, and consequences of messenger RNA modifications," *WIREs RNA*, p. e1586, Jan. 2020, doi: 10.1002/wrna.1586.
[26] D. P. Morse and B. L. Bass, "Detection of Inosine in Messenger RNA by Inosine-Specific Cleavage," *Biochemistry*, vol. 36, no. 28, pp. 8429–8434, Jul. 1997, doi: 10.1021/bi9709607.
[27] R. Desrosiers, K. Friderici, and F. Rottman, "Identification of Methylated Nucleosides in Messenger RNA from Novikoff Hepatoma Cells," *Proceedings of the National Academy of Sciences*, vol. 71, no. 10, pp. 3971–3975, Oct. 1974, doi: 10.1073/pnas.71.10.3971.
[28] S. Schwartz *et al.*, "Transcriptome-wide Mapping Reveals Widespread Dynamic-Regulated Pseudouridylation of ncRNA and mRNA," *Cell*, vol. 159, no. 1, pp. 148–162, Sep. 2014, doi: 10.1016/j.cell.2014.08.028.
[29] C. L. Simms, B. H. Hudson, J. W. Mosior, A. S. Rangwala, and H. S. Zaher, "An Active Role for the Ribosome in Determining the Fate of Oxidized mRNA," *Cell Reports*, vol. 9, no. 4, pp. 1256–1264, Nov. 2014, doi: 10.1016/j.celrep.2014.10.042.
[30] E. N. Thomas, K. Q. Kim, E. P. McHugh, T. Marcinkiewicz, and H. S. Zaher, "Alkylative damage of mRNA leads to ribosome stalling and rescue by trans translation in bacteria," *eLife*, vol. 9, p. e61984, Sep. 2020, doi: 10.7554/eLife.61984.
[31] L. L. Yan and H. S. Zaher, "How do cells cope with RNA damage and its consequences?," *J. Biol. Chem.*, vol. 294, no. 41, pp. 15158–15171, Oct. 2019, doi: 10.1074/jbc.REV119.006513.
[32] X. Shan and C. G. Lin, "Quantification of oxidized RNAs in Alzheimer's disease," *Neurobiology of Aging*, vol. 27, no. 5, pp. 657–662, May 2006, doi: 10.1016/j.neurobiolaging.2005.03.022.
[33] Y. Chang *et al.*, "Messenger RNA Oxidation Occurs Early in Disease Pathogenesis and Promotes Motor Neuron Degeneration in ALS," *PLOS ONE*, vol. 3, no. 8, p. e2849, Aug. 2008, doi: 10.1371/journal.pone.0002849.
[34] I. A. Roundtree *et al.*, "YTHDC1 mediates nuclear export of N6-methyladenosine methylated mRNAs," *eLife*, vol. 6, p. e31311, Oct. 2017, doi: 10.7554/eLife.31311.

[35] X. Yang *et al.*, "5-methylcytosine promotes mRNA export - NSUN2 as the methyltransferase and ALYREF as an m5C reader," *Cell Res.*, vol. 27, no. 5, pp. 606–625, May 2017, doi: 10.1038/cr.2017.55.
[36] G. Zheng *et al.*, "ALKBH5 Is a Mammalian RNA Demethylase that Impacts RNA Metabolism and Mouse Fertility," *Molecular Cell*, vol. 49, no. 1, pp. 18–29, Jan. 2013, doi: 10.1016/j.molcel.2012.10.015.
[37] D. Dominissini and G. Rechavi, "N4-acetylation of Cytidine in mRNA by NAT10 Regulates Stability and Translation," *Cell*, vol. 175, no. 7, pp. 1725–1727, Dec. 2018, doi: 10.1016/j.cell.2018.11.037.
[38] X. Wang *et al.*, "N6-methyladenosine-dependent regulation of messenger RNA stability," *Nature*, vol. 505, no. 7481, pp. 117–120, Jan. 2014, doi: 10.1038/nature12730.
[39] Y. Wang, Y. Li, J. I. Toth, M. D. Petroski, Z. Zhang, and J. C. Zhao, "N6-methyladenosine modification destabilizes developmental regulators in embryonic stem cells," *Nat Cell Biol*, vol. 16, no. 2, Art. no. 2, Feb. 2014, doi: 10.1038/ncb2902.
[40] D. E. Eyler *et al.*, "Pseudouridinylation of mRNA coding sequences alters translation," *PNAS*, vol. 116, no. 46, pp. 23068–23074, Nov. 2019, doi: 10.1073/pnas.1821754116.
[41] T. P. Hoernes *et al.*, "Nucleotide modifications within bacterial messenger RNAs regulate their translation and are able to rewire the genetic code," *Nucleic Acids Research*, vol. 44, no. 2, pp. 852–862, Jan. 2016, doi: 10.1093/nar/gkv1182.
[42] K. D. Meyer *et al.*, "5′ UTR m6A Promotes Cap-Independent Translation," *Cell*, vol. 163, no. 4, pp. 999–1010, Nov. 2015, doi: 10.1016/j.cell.2015.10.012.
[43] J. Zhou, J. Wan, X. Gao, X. Zhang, S. R. Jaffrey, and S.-B. Qian, "Dynamic m6A mRNA methylation directs translational control of heat shock response," *Nature*, vol. 526, no. 7574, pp. 591–594, Oct. 2015, doi: 10.1038/nature15377.
[44] X. Lin *et al.*, "RNA m6A methylation regulates the epithelial mesenchymal transition of cancer cells and translation of Snail," *Nat Commun*, vol. 10, p. 2065, May 2019, doi: 10.1038/s41467-019-09865-9.
[45] D. F. De Jesus *et al.*, "m 6 A mRNA methylation regulates human β-cell biology in physiological states and in type 2 diabetes," *Nature Metabolism*, vol. 1, no. 8, pp. 765–774, Aug. 2019, doi: 10.1038/s42255-019-0089-9.
[46] Y. Zhang, B. R. Fonslow, B. Shan, M.-C. Baek, and J. R. Yates, "Protein Analysis by Shotgun/Bottom-up Proteomics," *Chem. Rev.*, vol. 113, no. 4, pp. 2343–2394, Apr. 2013, doi: 10.1021/cr3003533.
[47] H. Grosjean, L. Droogmans, M. Roovers, and G. Keith, "Detection of Enzymatic Activity of Transfer RNA Modification Enzymes Using Radiolabeled tRNA Substrates," in *Methods in Enzymology*, vol. 425, Academic Press, 2007, pp. 55–101. doi: 10.1016/S0076-6879(07)25003-7.
[48] C. W. Gehrke and K. C. Kuo, "Ribonucleoside analysis by reversed-phase high-performance liquid chromatography," *Journal of Chromatography A*, vol. 471, pp. 3–36, Jun. 1989, doi: 10.1016/S0021-9673(00)94152-9.
[49] M. Buck, M. Connick, and B. N. Ames, "Complete analysis of tRNA-modified nucleosides by high-performance liquid chromatography: The 29 modified nucleosides of Salmonella typhimurium and Escherichia coli tRNA," *Analytical Biochemistry*, vol. 129, no. 1, pp. 1–13, Feb. 1983, doi: 10.1016/0003-2697(83)90044-1.

[50] M. Basanta-Sanchez, S. Temple, S. A. Ansari, A. D'Amico, and P. F. Agris, "Attomole quantification and global profile of RNA modifications: Epitranscriptome of human neural stem cells," *Nucleic Acids Res*, vol. 44, no. 3, p. e26, Feb. 2016, doi: 10.1093/nar/gkv971.
[51] C. T. Y. Chan, M. Dyavaiah, M. S. DeMott, K. Taghizadeh, P. C. Dedon, and T. J. Begley, "A Quantitative Systems Approach Reveals Dynamic Control of tRNA Modifications during Cellular Stress," *PLoS Genet*, vol. 6, no. 12, p. e1001247, Dec. 2010, doi: 10.1371/journal.pgen.1001247.
[52] D. Su *et al.*, "Quantitative analysis of tRNA modifications by HPLC-coupled mass spectrometry," *Nat Protoc*, vol. 9, no. 4, pp. 828–841, Apr. 2014, doi: 10.1038/nprot.2014.047.
[53] M. Heiss, F. Hagelskamp, V. Marchand, Y. Motorin, and S. Kellner, "Cell culture NAIL-MS allows insight into human tRNA and rRNA modification dynamics in vivo," *Nature Communications*, vol. 12, no. 1, Art. no. 1, Jan. 2021, doi: 10.1038/s41467-020-20576-4.
[54] V. F. Reichle, S. Kaiser, M. Heiss, F. Hagelskamp, K. Borland, and S. Kellner, "Surpassing limits of static RNA modification analysis with dynamic NAIL-MS," *Methods*, vol. 156, pp. 91–101, Mar. 2019, doi: 10.1016/j.ymeth.2018.10.025.
[55] K. D. Clark, C. Lee, R. Gillette, and J. V. Sweedler, "Characterization of Neuronal RNA Modifications during Non-associative Learning in Aplysia Reveals Key Roles for tRNAs in Behavioral Sensitization," *ACS Cent. Sci.*, vol. 7, no. 7, pp. 1183–1190, Jul. 2021, doi: 10.1021/acscentsci.1c00351.
[56] K. D. Clark, S. S. Rubakhin, and J. V. Sweedler, "Single-Neuron RNA Modification Analysis by Mass Spectrometry: Characterizing RNA Modification Patterns and Dynamics with Single-Cell Resolution," *Anal. Chem.*, vol. 93, no. 43, pp. 14537–14544, Nov. 2021, doi: 10.1021/acs.analchem.1c03507.
[57] Y. Motorin and M. Helm, "Methods for RNA Modification Mapping Using Deep Sequencing: Established and New Emerging Technologies," *Genes*, vol. 10, no. 1, p. 35, Jan. 2019.
[58] W. V. Gilbert, T. A. Bell, and C. Schaening, "Messenger RNA modifications: Form, distribution, and function," *Science*, vol. 352, no. 6292, pp. 1408–1412, Jun. 2016, doi: 10.1126/science.aad8711.
[59] M. Helm and Y. Motorin, "Detecting RNA modifications in the epitranscriptome: predict and validate," *Nat Rev Genet*, vol. 18, no. 5, Art. no. 5, May 2017, doi: 10.1038/nrg.2016.169.
[60] S. Zaccara, R. J. Ries, and S. R. Jaffrey, "Reading, writing and erasing mRNA methylation," *Nat Rev Mol Cell Biol*, vol. 20, pp. 608–624, Sep. 2019, doi: 10.1038/s41580-019-0168-5.
[61] S. Schwartz and Y. Motorin, "Next-generation sequencing technologies for detection of modified nucleotides in RNAs," *RNA Biol*, vol. 14, no. 9, pp. 1124–1137, Oct. 2016, doi: 10.1080/15476286.2016.1251543.
[62] S. Thalalla Gamage, A. Sas-Chen, S. Schwartz, and J. L. Meier, "Quantitative nucleotide resolution profiling of RNA cytidine acetylation by ac4C-seq," *Nature Protocols*, vol. 16, no. 4, Art. no. 4, Apr. 2021, doi: 10.1038/s41596-021-00501-9.
[63] A. V. Grozhik and S. R. Jaffrey, "Distinguishing RNA modifications from noise in epitranscriptome maps," *Nature Chemical Biology*, vol. 14, no. 3, pp. 215–225, Feb. 2018, doi: 10.1038/nchembio.2546.

[64] Y. Wang *et al.*, “Single-Base Resolution Mapping Reveals Distinct 5-Formylcytidine in Saccharomyces cerevisiae mRNAs,” *ACS Chem. Biol.*, vol. 17, no. 1, pp. 77–84, Nov. 2021, doi: 10.1021/acschembio.1c00633.
[65] J. Cui, Q. Liu, E. Sendinc, Y. Shi, and R. I. Gregory, “Nucleotide resolution profiling of m3C RNA modification by HAC-seq,” *Nucleic Acids Research*, vol. 49, no. 5, p. e27, Mar. 2021, doi: 10.1093/nar/gkaa1186.
[66] V. Khoddami, A. Yerra, T. L. Mosbruger, A. M. Fleming, C. J. Burrows, and B. R. Cairns, “Transcriptome-wide profiling of multiple RNA modifications simultaneously at single-base resolution,” *PNAS*, vol. 116, no. 14, pp. 6784–6789, Apr. 2019, doi: 10.1073/pnas.1817334116.
[67] S. Kellner *et al.*, “Profiling of RNA modifications by multiplexed stable isotope labelling,” *Chem. Commun.*, vol. 50, no. 26, pp. 3516–3518, Mar. 2014, doi: c.
[68] S. P. Russell and P. A. Limbach, “Evaluating the reproducibility of quantifying modified nucleosides from ribonucleic acids by LC–UV–MS,” *Journal of Chromatography B*, vol. 923–924, pp. 74–82, Apr. 2013, doi: 10.1016/j.jchromb.2013.02.010.
[69] Y. Feng *et al.*, “Chemical labeling – Assisted mass spectrometry analysis for sensitive detection of cytidine dual modifications in RNA of mammals,” *Analytica Chimica Acta*, vol. 1098, pp. 56–65, Feb. 2020, doi: 10.1016/j.aca.2019.11.016.
[70] Y. Dai *et al.*, “Sensitive and Simultaneous Determination of Uridine Thiolation and Hydroxylation Modifications in Eukaryotic RNA by Derivatization Coupled with Mass Spectrometry Analysis,” *Anal. Chem.*, vol. 93, no. 18, pp. 6938–6946, May 2021, doi: 10.1021/acs.analchem.0c04630.
[71] Y. Xie, K. A. Janssen, A. Scacchetti, R. Bonasio, and B. A. Garcia, “Permethylation of ribonucleosides provides enhanced mass spectrometry quantification of post-transcriptional modifications,” *bioRxiv*, 2022, doi: 10.1101/2022.01.26.477959.
[72] P. Song, O. S. Mabrouk, N. D. Hershey, and R. T. Kennedy, “In Vivo Neurochemical Monitoring Using Benzoyl Chloride Derivatization and Liquid Chromatography–Mass Spectrometry,” *Anal. Chem.*, vol. 84, no. 1, pp. 412–419, Jan. 2012, doi: 10.1021/ac202794q.
[73] J.-M. T. Wong, P. A. Malec, O. S. Mabrouk, J. Ro, M. Dus, and R. T. Kennedy, “Benzoyl chloride derivatization with liquid chromatography–mass spectrometry for targeted metabolomics of neurochemicals in biological samples,” *Journal of Chromatography A*, vol. 1446, pp. 78–90, May 2016, doi: 10.1016/j.chroma.2016.04.006.
[74] S. R. Wilson, T. Vehus, H. S. Berg, and E. Lundanes, “Nano-LC in proteomics: recent advances and approaches,” *Bioanalysis*, vol. 7, no. 14, pp. 1799–1815, 2015, doi: 10.4155/bio.15.92.
[75] L. P. Sarin *et al.*, “Nano LC-MS using capillary columns enables accurate quantification of modified ribonucleosides at low femtomol levels,” *RNA*, vol. 24, no. 10, pp. 1403–1417, Jul. 2018, doi: 10.1261/rna.065482.117.
[76] L. Fu, N. J. Amato, P. Wang, S. J. McGowan, L. J. Niedernhofer, and Y. Wang, “Simultaneous Quantification of Methylated Cytidine and Adenosine in Cellular and Tissue RNA by Nano-Flow Liquid Chromatography–Tandem Mass Spectrometry Coupled with the Stable Isotope-Dilution Method,” *Anal. Chem.*, vol. 87, no. 15, pp. 7653–7659, Aug. 2015, doi: 10.1021/acs.analchem.5b00951.

[77] D. Dominissini *et al.*, “The dynamic N1-methyladenosine methylome in eukaryotic messenger RNA,” *Nature*, vol. 530, no. 7591, pp. 441–446, Feb. 2016, doi: 10.1038/nature16998.
[78] X. Li *et al.*, “Chemical pulldown reveals dynamic pseudouridylation of the mammalian transcriptome,” *Nature Chemical Biology*, vol. 11, no. 8, pp. 592–597, Aug. 2015, doi: 10.1038/nchembio.1836.
[79] C. Legrand *et al.*, “Statistically robust methylation calling for whole-transcriptome bisulfite sequencing reveals distinct methylation patterns for mouse RNAs,” *Genome Res.*, vol. 27, no. 9, pp. 1589–1596, Sep. 2017, doi: 10.1101/gr.210666.116.
[80] M.-Y. Cheng, W.-B. Tao, B.-F. Yuan, and Y.-Q. Feng, “Methods for isolation of messenger RNA from biological samples,” *Anal. Methods*, vol. 13, pp. 289–298, 2021, doi: 10.1039/D0AY01912G.
[81] Agilent Technologies, Inc, “Agilent RNA Kits for the Agilent 2100 Bioanalyzer System,” *Agilent Technologies, Inc*, Feb. 01, 2019. https://www.agilent.com/cs/library/datasheets/public/datasheet-rna-kits-bioanalyzer-5991-7891en-agilent.pdf
[82] A. Behrens, G. Rodschinka, and D. D. Nedialkova, “High-resolution quantitative profiling of tRNA abundance and modification status in eukaryotes by mim-tRNAseq,” *Molecular Cell*, vol. 81, no. 8, pp. 1802-1815.e7, Apr. 2021, doi: 10.1016/j.molcel.2021.01.028.
[83] B. Chen, B.-F. Yuan, and Y.-Q. Feng, “Analytical Methods for Deciphering RNA Modifications,” *Anal. Chem.*, vol. 91, no. 1, pp. 743–756, Jan. 2019, doi: 10.1021/acs.analchem.8b04078.
[84] S. M. Huber *et al.*, “Formation and Abundance of 5-Hydroxymethylcytosine in RNA,” *ChemBioChem*, vol. 16, no. 5, pp. 752–755, 2015, doi: 10.1002/cbic.201500013.
[85] S. Laxman *et al.*, “Sulfur Amino Acids Regulate Translational Capacity and Metabolic Homeostasis through Modulation of tRNA Thiolation,” *Cell*, vol. 154, no. 2, pp. 416–429, Jul. 2013, doi: 10.1016/j.cell.2013.06.043.
[86] C. Chen, B. Huang, M. Eliasson, P. Rydén, and A. S. Byström, “Elongator Complex Influences Telomeric Gene Silencing and DNA Damage Response by Its Role in Wobble Uridine tRNA Modification,” *PLOS Genetics*, vol. 7, no. 9, p. e1002258, Sep. 2011, doi: 10.1371/journal.pgen.1002258.
[87] N. Shigi, “Biosynthesis and functions of sulfur modifications in tRNA,” *Front Genet*, vol. 5, p. 67, Apr. 2014, doi: 10.3389/fgene.2014.00067.
[88] J. Mouaikel, C. Verheggen, E. Bertrand, J. Tazi, and R. Bordonné, “Hypermethylation of the Cap Structure of Both Yeast snRNAs and snoRNAs Requires a Conserved Methyltransferase that Is Localized to the Nucleolus,” *Molecular Cell*, vol. 9, no. 4, pp. 891–901, Apr. 2002, doi: 10.1016/S1097-2765(02)00484-7.
[89] J. Mouaikel, J. M. Bujnicki, J. Tazi, and R. Bordonné, “Sequence–structure–function relationships of Tgs1, the yeast snRNA/snoRNA cap hypermethylase,” *Nucleic Acids Res*, vol. 31, no. 16, pp. 4899–4909, Aug. 2003.
[90] S. Hausmann and S. Shuman, “Specificity and Mechanism of RNA Cap Guanine-N2 Methyltransferase (Tgs1),” *Journal of Biological Chemistry*, vol. 280, no. 6, pp. 4021–4024, Feb. 2005, doi: 10.1074/jbc.C400554200.
[91] J.-M. Carter *et al.*, “FICC-Seq: a method for enzyme-specified profiling of methyl-5-uridine in cellular RNA,” *Nucleic Acids Res*, vol. 47, no. 19, p. e113, Nov. 2019, doi: 10.1093/nar/gkz658.

[92] J. Yang, S. Sharma, P. Watzinger, J. D. Hartmann, P. Kötter, and K.-D. Entian, "Mapping of Complete Set of Ribose and Base Modifications of Yeast rRNA by RP-HPLC and Mung Bean Nuclease Assay," *PLOS ONE*, vol. 11, no. 12, p. e0168873, Dec. 2016, doi: 10.1371/journal.pone.0168873.
[93] D. J. Ashworth, W. M. Baird, C.-J. Chang, J. D. Ciupek, K. L. Busch, and R. G. Cooks, "Chemical modification of nucleic acids. Methylation of calf thymus DNA investigated by mass spectrometry and liquid chromatography," *Biomedical Mass Spectrometry*, vol. 12, no. 7, pp. 309–318, 1985, doi: https://doi.org/10.1002/bms.1200120703.
[94] C.-J. Chang and C.-G. Lee, "Chemical modification of ribonucleic acid. A direct study by carbon-13 nuclear magnetic resonance spectroscopy," *Biochemistry*, vol. 20, no. 9, pp. 2657–2661, Apr. 1981, doi: 10.1021/bi00512a046.
[95] C. J. Chang, J. D. Gomes, and S. R. Byrn, "Chemical modification of deoxyribonucleic acids: a direct study by carbon-13 nuclear magnetic resonance spectroscopy," *J. Org. Chem.*, vol. 48, no. 26, pp. 5151–5160, Dec. 1983, doi: 10.1021/jo00174a002.
[96] J. C. Delaney and J. M. Essigmann, "Mutagenesis, genotoxicity, and repair of 1-methyladenine, 3-alkylcytosines, 1-methylguanine, and 3-methylthymine in alkB Escherichia coli," *PNAS*, vol. 101, no. 39, pp. 14051–14056, Sep. 2004, doi: 10.1073/pnas.0403489101.
[97] P. Ø. Falnes, "Repair of 3-methylthymine and 1-methylguanine lesions by bacterial and human AlkB proteins," *Nucleic Acids Research*, vol. 32, no. 21, pp. 6260–6267, Nov. 2004, doi: 10.1093/nar/gkh964.
[98] P. J. Holland and T. Hollis, "Structural and Mutational Analysis of Escherichia coli AlkB Provides Insight into Substrate Specificity and DNA Damage Searching," *PLOS ONE*, vol. 5, no. 1, p. e8680, Jan. 2010, doi: 10.1371/journal.pone.0008680.
[99] J. O. Kang, "Methylated Purine Bases in Hepatic and Colonic RNA of Rats Treated with 1,2-Dimethylhydrazine," *Biochemical Medicine and Metabolic Biology*, vol. 53, no. 1, pp. 52–57, Oct. 1994, doi: 10.1006/bmmb.1994.1057.
[100] G. A. Khoury, R. C. Baliban, and C. A. Floudas, "Proteome-wide post-translational modification statistics: frequency analysis and curation of the swiss-prot database," *Sci Rep*, vol. 1, no. 1, Art. no. 1, Sep. 2011, doi: 10.1038/srep00090.
[101] E. Bieberich, "Synthesis, Processing, and Function of N-glycans in N-glycoproteins," in *Glycobiology of the Nervous System*, R. K. Yu and C.-L. Schengrund, Eds. New York, NY: Springer, 2014, pp. 47–70. doi: 10.1007/978-1-4939-1154-7_3.
[102] H. H. Wandall, M. A. I. Nielsen, S. King-Smith, N. de Haan, and I. Bagdonaite, "Global functions of O-glycosylation: promises and challenges in O-glycobiology," *The FEBS Journal*, vol. 288, no. 24, pp. 7183–7212, 2021, doi: 10.1111/febs.16148.
[103] C. Reily, T. J. Stewart, M. B. Renfrow, and J. Novak, "Glycosylation in health and disease," *Nat Rev Nephrol*, vol. 15, no. 6, Art. no. 6, Jun. 2019, doi: 10.1038/s41581-019-0129-4.
[104] Y. Fan *et al.*, "Heterogeneity of Stop Codon Readthrough in Single Bacterial Cells and Implications for Population Fitness," *Molecular Cell*, vol. 67, no. 5, pp. 826-836.e5, Sep. 2017, doi: 10.1016/j.molcel.2017.07.010.
[105] Y. Fan, J. Wu, M. H. Ung, N. De Lay, C. Cheng, and J. Ling, "Protein mistranslation protects bacteria against oxidative stress," *Nucleic Acids Research*, vol. 43, no. 3, pp. 1740–1748, Feb. 2015, doi: 10.1093/nar/gku1404.

[106] T. Pan, “Modifications and functional genomics of human transfer RNA,” *Cell Research*, vol. 28, no. 4, Art. no. 4, Apr. 2018, doi: 10.1038/s41422-018-0013-y.
[107] E. M. Phizicky and A. K. Hopper, “tRNA processing, modification, and subcellular dynamics: past, present, and future,” *RNA*, vol. 21, no. 4, pp. 483–485, Apr. 2015, doi: 10.1261/rna.049932.115.
[108] N. Ranjan and M. V. Rodnina, “Thio-Modification of tRNA at the Wobble Position as Regulator of the Kinetics of Decoding and Translocation on the Ribosome,” *J. Am. Chem. Soc.*, vol. 139, no. 16, pp. 5857–5864, Apr. 2017, doi: 10.1021/jacs.7b00727.
[109] M. H. Schwartz and T. Pan, “Temperature dependent mistranslation in a hyperthermophile adapts proteins to lower temperatures,” *Nucleic Acids Research*, vol. 44, no. 1, pp. 294–303, Jan. 2016, doi: 10.1093/nar/gkv1379.
[110] J. Choi *et al.*, “N(6)-methyladenosine in mRNA disrupts tRNA selection and translation-elongation dynamics,” *Nat. Struct. Mol. Biol.*, vol. 23, no. 2, pp. 110–115, Feb. 2016, doi: 10.1038/nsmb.3148.
[111] J. Choi *et al.*, “2′- O -methylation in mRNA disrupts tRNA decoding during translation elongation,” *Nature Structural & Molecular Biology*, vol. 25, no. 3, Art. no. 3, Mar. 2018, doi: 10.1038/s41594-018-0030-z.
[112] T. P. Hoernes *et al.*, “Atomic mutagenesis of stop codon nucleotides reveals the chemical prerequisites for release factor-mediated peptide release,” *PNAS*, vol. 115, no. 3, pp. E382–E389, Jan. 2018, doi: 10.1073/pnas.1714554115.
[113] T. P. Hoernes *et al.*, “Eukaryotic Translation Elongation is Modulated by Single Natural Nucleotide Derivatives in the Coding Sequences of mRNAs,” *Genes*, vol. 10, no. 2, Art. no. 2, Feb. 2019, doi: 10.3390/genes10020084.
[114] B. H. Hudson and H. S. Zaher, “O6-Methylguanosine leads to position-dependent effects on ribosome speed and fidelity,” *RNA*, vol. 21, no. 9, pp. 1648–1659, Sep. 2015, doi: 10.1261/rna.052464.115.
[115] C. You, X. Dai, and Y. Wang, “Position-dependent effects of regioisomeric methylated adenine and guanine ribonucleosides on translation,” *Nucleic Acids Research*, vol. 45, no. 15, pp. 9059–9067, Sep. 2017, doi: 10.1093/nar/gkx515.
[116] Z. Shen, W. Wu, and S. L. Hazen, “Activated Leukocytes Oxidatively Damage DNA, RNA, and the Nucleotide Pool through Halide-Dependent Formation of Hydroxyl Radical,” *Biochemistry*, vol. 39, no. 18, pp. 5474–5482, May 2000, doi: 10.1021/bi992809y.
[117] T. E. Dever, J. D. Dinman, and R. Green, “Translation Elongation and Recoding in Eukaryotes,” *Cold Spring Harb Perspect Biol*, vol. 10, no. 8, p. a032649, Aug. 2018, doi: 10.1101/cshperspect.a032649.
[118] E. N. Thomas, C. L. Simms, H. E. Keedy, and H. S. Zaher, “Insights into the base-pairing preferences of 8-oxoguanosine on the ribosome,” *Nucleic Acids Research*, vol. 47, no. 18, pp. 9857–9870, Oct. 2019, doi: 10.1093/nar/gkz701.
[119] B. Slobodin *et al.*, “Transcription Impacts the Efficiency of mRNA Translation via Co-transcriptional N6-adenosine Methylation,” *Cell*, vol. 169, no. 2, pp. 326-337.e12, 06 2017, doi: 10.1016/j.cell.2017.03.031.
[120] L. L. Yan, C. L. Simms, F. McLoughlin, R. D. Vierstra, and H. S. Zaher, “Oxidation and alkylation stresses activate ribosome-quality control,” *Nat Commun*, vol. 10, no. 1, Art. no. 1, Dec. 2019, doi: 10.1038/s41467-019-13579-3.

[121] O. Levi and Y. S. Arava, “Pseudouridine-mediated translation control of mRNA by methionine aminoacyl tRNA synthetase,” *Nucleic Acids Research*, vol. 49, no. 1, pp. 432–443, Jan. 2021, doi: 10.1093/nar/gkaa1178.
[122] T. P. Hoernes *et al.*, “Translation of non-standard codon nucleotides reveals minimal requirements for codon-anticodon interactions,” *Nat Commun*, vol. 9, p. 4865, Nov. 2018, doi: 10.1038/s41467-018-07321-8.
[123] K. Licht, M. Hartl, F. Amman, D. Anrather, M. P. Janisiw, and M. F. Jantsch, “Inosine induces context-dependent recoding and translational stalling,” *Nucleic Acids Res*, vol. 47, no. 1, pp. 3–14, Jan. 2019, doi: 10.1093/nar/gky1163.
[124] M. K. Franco and K. S. Koutmou, “Chemical modifications to mRNA nucleobases impact translation elongation and termination,” *Biophysical Chemistry*, vol. 285, p. 106780, Jun. 2022, doi: 10.1016/j.bpc.2022.106780.
[125] M. K. Purchal *et al.*, “Pseudouridine synthase 7 is an opportunistic enzyme that binds and modifies substrates with diverse sequences and structures,” *Proceedings of the National Academy of Sciences*, vol. 119, no. 4, p. e2109708119, Jan. 2022, doi: 10.1073/pnas.2109708119.
[126] R. Rauscher and Z. Ignatova, “Timing during translation matters: synonymous mutations in human pathologies influence protein folding and function,” *Biochemical Society Transactions*, vol. 46, no. 4, pp. 937–944, Jul. 2018, doi: 10.1042/BST20170422.
[127] A. Re, T. Joshi, E. Kulberkyte, Q. Morris, and C. T. Workman, “RNA–Protein Interactions: An Overview,” in *RNA Sequence, Structure, and Function: Computational and Bioinformatic Methods*, J. Gorodkin and W. L. Ruzzo, Eds. Totowa, NJ: Humana Press, 2014, pp. 491–521. doi: 10.1007/978-1-62703-709-9_23.
[128] M. E. Schmitt, T. A. Brown, and B. L. Trumpower, “A rapid and simple method for preparation of RNA from Saccharomyces cerevisiae.,” *Nucleic Acids Res*, vol. 18, no. 10, pp. 3091–3092, May 1990.
[129] S. Andrews, “FastQC: a quality control tool for high throughput sequence data,” 2010. https://www.bioinformatics.babraham.ac.uk/projects/fastqc/ (accessed May 27, 2021).
[130] M. Martin, “Cutadapt removes adapter sequences from high-throughput sequencing reads,” *EMBnet.journal*, vol. 17, no. 1, Art. no. 1, May 2011, doi: 10.14806/ej.17.1.200.
[131] B. Langmead and S. L. Salzberg, “Fast gapped-read alignment with Bowtie 2,” *Nature Methods*, vol. 9, no. 4, Art. no. 4, Apr. 2012, doi: 10.1038/nmeth.1923.
[132] M. Zytnicki, “mmquant: how to count multi-mapping reads?,” *BMC Bioinformatics*, vol. 18, no. 1, p. 411, Sep. 2017, doi: 10.1186/s12859-017-1816-4.
[133] M. T. Marty, A. J. Baldwin, E. G. Marklund, G. K. A. Hochberg, J. L. P. Benesch, and C. V. Robinson, “Bayesian Deconvolution of Mass and Ion Mobility Spectra: From Binary Interactions to Polydisperse Ensembles,” *Anal. Chem.*, vol. 87, no. 8, pp. 4370–4376, Apr. 2015, doi: 10.1021/acs.analchem.5b00140.
[134] J. G. Monroe, T. J. Smith, and K. S. Koutmou, “Chapter Sixteen - Investigating the consequences of mRNA modifications on protein synthesis using in vitro translation assays,” in *Methods in Enzymology*, vol. 658, J. E. Jackman, Ed. Academic Press, 2021, pp. 379–406. doi: 10.1016/bs.mie.2021.06.011.

Chapter 4 Modulation Of tRNA Modification Landscape Alters The Efficacy Of Hygromycin B Translation Inhibition[3]

Monika K Franco[1], Joshua D Jones[2], Tyler J. Smith[2], Mehmet Tardu[2], Laura R Snyder[2], Robert T Kennedy[2]*, Kristin S Koutmou[1,2]*

[1]University of Michigan Program in Chemical Biology. [2]University of Michigan, Department of Chemistry.

* Corresponding authors.

4.1 Introduction

Post-transcriptional modifications to RNA impact the structure, function, stability and dynamics of cellular RNAs. Thus, it is unsurprising that the dysregulation of RNA modifications is linked to a myriad of pathologies including diabetes, neurological disorders, and many cancers[1]–[6]. To date, over 150 different ribonucleoside modifications have been reported over the last 50 years within all three kingdoms of life and all RNA species[7]. However, the precise contribution of only a modest subset of these modifications to discrete biological processes has been established. Here, we identify the affect that a prevalent non-coding RNA (ncRNA) modification, 5-methyluridine (m^5U), has under translational inhibition.

[3] In this paper, I performed all in-vitro translation work. Josh jones did all the mass spectrometry analysis, including looking at the modification levels in our cells and tRNAs. Josh Jones, Laura Snyder, and Dr. Mehmet Tardu all did work analyzing how Trm2 impact cellular stress response. Dr. Tardu did the protein reporter assays. Both Dr. Koutmou and Tyler Smith contributed intellectually.

m^5U was originally discovered in 1963 and has since been detected in ncRNAs from all phylogenies and eukaryotic mRNAs[8]. Initial studies of m^5U in tRNAs revealed that it is incorporated into the T-loop of tRNAs by the conserved bacterial and eukaryotic enzyme tRNA (uracil-5-)-methyltransferase (Trm2), and more recent work has detected m^5U in eukaryotic rRNA and most recently the large subunit of bacterial and archaeon rRNAs[9]–[11], [12], [13]. In tRNAs, the tertiary interaction between the T-loop structural motif in tRNAs and the D-loop is known to play an important role in tRNA structure and stability, and the addition of m^5U54 into the T-loop is increases the stability of tRNAs [14]. However, m^5U does not significantly alter the hydrogen bonding pattern in the T-loop. Thus, it is not known whether this stabilizing effect comes from the presence of m^5U54 in the T-loop, however Trm2 and the *E. coli* homologue (TrmA) were found to act as a tRNA folding chaperones which could cause the stabilizing effect [15]. Despite this, the role of m^5U in tRNA and the enzymes that incorporate it have been difficult to define. When a TrmA enzyme is mutated to expunge methyltransferase activity, there were no observed changes in translation in vivo [16]. Nonetheless, cells containing uracil-5-methyltransferase outcompete those without [16], [17]. Additionally, m^5U54 is a highly conserved modification, which suggests that there is an evolutionary significance to the addition of this modifications. Despite its conservation and apparent contributions to tRNA structure, the overall biological significance of the tRNA m^5U modification and its contributions (if any) to protein translation remains unclear.

Recently, modulation of tRNA modification landscapes has been implicated in the bacterial resistance to antibiotics [18]–[21]. For example, it has been reported that the 1-methylguanosine at the 37 position (m^1G37) methylation of tRNA helps produce strong gram-negative OM membrane proteins in *E. coli* and *salmonella* that promote multi drug resistance [21]. Thus, TrmD, the enzyme that catalyzes m^1G37 incorporation, has now become a target for

drug development [19]. There are three targeted mechanisms of action that antibiotics typically take: (1) attacking the cell wall or membrane, (2) attacking the machinery that makes nucleic acids, (3) attacking the ribosome [22]. One example of an antibiotic that works by inhibiting translation is hygromycin B. Hygromycin B is part of the aminoglycoside family of translation inhibitors that works in both prokaryotic and eukaryotic systems. Although Hygromycin B is a widely used translation inhibitor for studying hygromycin resistant genes, as well as a tool for understanding the translation machinery, its mechanism of action is still not fully understood [23], [24]. It is known that hygromycin B strengthens tRNA binding to the A site, but the most important aspect is the ability for it to prevent translocation from occurring [16], [19]. What is particularly interesting about hygromycin B is that it does not need to be in the presence of elongation factors to function compared to other antibiotics in the same family. This highly suggests that its inhibitory actions are due to interactions with mRNA, tRNA and the ribosome itself [26]. There are no current studies that show aminoglycoside interaction with RNA modifications, or that RNA modifications impact translation inhibition by aminoglycosides.

In this work, we identified the first phenotype for tRNA (uracil-5-)-methyltransferase where yeast lacking the methyltransferase has altered cellular growth under translational inhibition by aminoglycosides – hygromycin B, cycloheximide, and paromomycin. In particular, we see that *trm2*Δ yeast grow more efficiently and produce more protein than wildtype yeast under hygromycin B stress. Additionally, we find that the wildtype cells have increased m^5U levels under hygromycin B stress. Since hygromycin B inhibits protein synthesis by preventing the translocation of the tRNA, we sought to investigate how $tRNA^{Phe}$ purified from wildtype and *trmA*Δ cells affects amino acid addition and tripeptide synthesis using a well-established fully reconstituted *in vitro* translation system. In $tRNA^{Phe}$ purified from *trmA*Δ *E. coli*, we find that m^5U

abundance is significantly decreases as expected; however, we see a significant increase in i^6A and decrease in acp^3U abundances in the *trmA*Δ $tRNA^{Phe}$. We found that the *trmA*Δ purified $tRNA^{Phe}$ does not alter amino acid addition or tripeptide synthesis compared to wildtype $tRNA^{Phe}$ using native conditions. However, in the presence of hygromycin B, *trmA*Δ purified $tRNA^{Phe}$ produces more tripeptide than wildtype $tRNA^{Phe}$. We find that hygromycin B interacts with the ms^2i^6A37 in the $tRNA^{Phe}$ based off a crystal structure. These findings reveal that the removal of the hypermodification ms^2i^6A37 provides some antibiotic resistance by promoting translocation within the ribosome

4.2 Results

4.2.1 Trm2 impacts cell growth under translational stress conditions

Despite being studied for over 50 years, the biological role of m^5U remains unclear. While bacterial and eukaryotic cells lacking uracil-5-methyltransferase do not exhibit a growth defect under normal laboratory conditions[15], [17],cells possessing uracil-5-methyltransferase out compete those lacking the enzyme which suggests that m^5U is advantageous for cellular fitness[16], [17]. This is consequential from the dual function of Trm2 which catalyzes m^5U installation and acts as a tRNA folding chaperone[15]. Nonetheless, conditions under which these individual activities are important are still not known.

To better understand the biological function of Trm2 and m^5U incorporation, we sought to identify situations in which the enzyme impacts cell growth. We conducted spot plating assays with wildtype and *trm2*Δ cells to survey the impact of varying temperature (22°C, 30°C, 37°C), carbon source (glucose, sucrose, galactose), pH (4.5, 6.8, 8.5), salt concentration (NaCl, $MgSO_4$), and proteasome (MG132) and translation inhibitors (hygromycin B, cycloheximide, puromycin, paromomycin) on cell growth (Supplemental Figure 1). Wildtype and *trm2*Δ grew similarly

regardless of temperature, carbon source, pH, $MgSO_4$ concentration, or the presence of a proteasome inhibitor. Although the growth of *trm2*Δ cells was unchanged by $MgSO_4$, we observed that deletion of Trm2 resulted in a modest growth enhancement over wildtype under 1 M NaCl salt stress condition. However, the largest effect was observed under the presence of three translation inhibitors: hygromycin B, cycloheximide and paromomycin. Relative to wildtype cells, *trm2*Δ cells were more sensitive cycloheximide, while they were less sensitive to hygromycin B and paromomycin treatment (Figure 1A). These findings were further supported in cellular growth curve assays under the same conditions, where *trm2*Δ grew more robustly in the presence of 1 M NaCl, 50 µg/mL hygromycin B, or 3 mg/mL paromomycin and worse in the presence of 0.1 µg/mL cycloheximide (Supplemental Figure 1). This is the first evidence that uracil-5-methyltransferase and m^5U play a significant biological role.

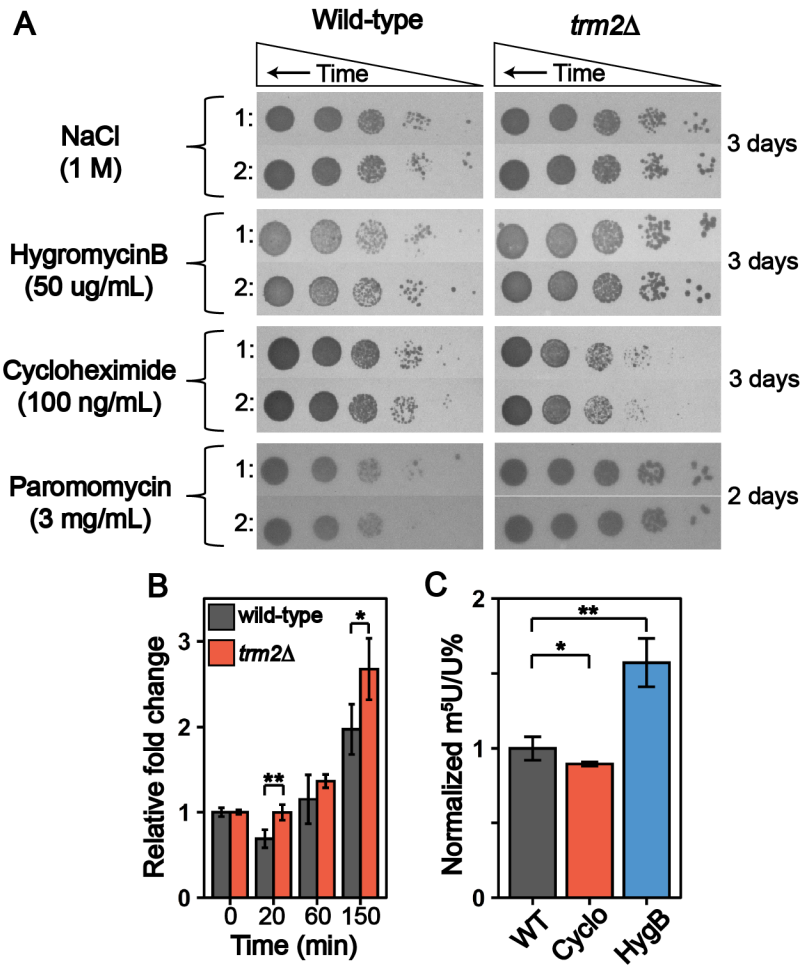

Figure 4.1: ***Translational stress response modulated in trm2 KO cell lines.****(A) Spot platting assays displaying The growth of trm2Δ was affected in the presence of three translation inhibitors: hygromycin B, cycloheximide, and paromomycin.* ***(B)*** *Luciferase reporter assasys shows that protein level significantly decreased in wild-type than trm2Δ after hygromycin B treatment.* ***(C)*** *m5U levels are higher under hygromycin b stress compared to WT conditions and Cycloheximide stress.*

4.2.2 Trm2 influences reporter protein production in cells under translational stress conditions

The influence of the uracil-5-methyltransferase under translational stress cellular fitness could be resultant from altered protein production following the knockout. To investigate this, we tested how hygromycin B and cycloheximide affects protein production in wild-type and *trm2*Δ cells transfected with luciferase mRNA transcript. Both transfected cell lines were grown to an OD_{600} of 0.5 prior to the hygromycin B and cycloheximide stress, and the fluorescent intensity

was recorded at multiple time points after the stress (0 min, 20 min, 60 min, 120 min). We found that luciferase protein level significantly increased in the *trm2*Δ cells compared to the wildtype after hygromycin B treatment (Figure 1B). Interestingly, we see a decrease in luciferase abundance 20 min following hygromycin B stress in the wild-type cells that is not present in the *trm2*Δ cells. This data corroborates that the presence of uracil-5-methyltransferase influences the impact of hygromycin B and cycloheximide treatment, and the alteration in *trm2*Δ cells cellular fitness could be resultant of altered protein product rates under stress. This further leads us to believe that uracil-5-methltransferase and/or m^5U modification impacts translation under translational inhibition.

4.2.3 m^5U levels in tRNAs fluctuate in response to translational stress

It is well documented that cells modulate RNA modification abundance in response to cellular stress or nutrition to alter their biological function. Accordantly, yeast tRNA m^5U abundance was previously shown to be altered under oxidative and alkylative stress [27]. Since m^5U addition by Trm2 displayed an impact under translational translocation stress, we tested how m^5U abundance is affected following hygromycin B and cycloheximide exposure using a previously reported UHPLC-MS/MS methodology[28]. The m^5U/U% levels of yeast total RNA were altered under both stress conditions where hygromycin B- and cycloheximide-stress resulted in an upregulation and downregulation of m^5U, respectively (Figure 1C and Supplemental Figure 2).

This alteration in m^5U/U% can come from multiple different factors – a change in total RNA distribution, altered stoichiometry of m^5U modified sites, or newly modified locations. While the tRNA:rRNA distribution does not drastically change following cycloheximide-stress when compared to the WT, the 18S rRNA expression is downregulated from approximately 20% of the total RNA electropherogram signal to approximately 16% (Supplemental Figures 3). This is

consistent with a previous study that detected a decrease in mature 16S rRNA in *E. coli* following hygromycin B treatment [29]. Since m^5U is not present in *S. cerevisiae* rRNA and the bioanalyzer electropherogram signal > 200nt remains approximately 70% of the overall signal for all three conditions, this would not result in the large increase in m^5U signal we detect under this condition [7]. Additionally, since m^5U is present in almost all *S. cerevisiae* tRNA, it is unlikely that the altered m^5U signals detected under each antibiotic stress is coming from a change in individual tRNA abundance. Instead, we posit the altered abundance is arising from an altered stoichiometry of m^5U at position 54 or additional modification sites within the *S. cerevisiae* tRNA or rRNA. This suggests that m^5U enzymatic incorporation in tRNA plays an important role during translational inhibition by hygromycin B and cycloheximide.

Since the UHPLC-MS/MS assay we utilized can be multiplexed to detect up to 50 ribonucleosides in a single analysis, we also identified that translational inhibition affects the abundance of other total and mRNA modifications. Similar to m^5U, most total RNA modifications are upregulated following hygromycin treatment and downregulated following cycloheximide treatment (Supplemental figure 4). Contrarily, mRNA modifications are preferentially upregulated following treatment by both translational inhibitors (Supplemental figure 2). Messenger RNA was purified using a previously described three-stage purification pipeline, and the mRNA purity was confirmed using Bioanalyzer, RNA-seq, RT-qPCR, and LC-MS/MS (Supplemental figures 2-5). While the total RNA modifications distribution remains similar following translational inhibition, small mRNA (~500 nt) is enriched following both hygromycin and cycloheximide treatment (Supplemental figure 3). Thus, the alteration in mRNA modification abundance could be resulting from a modulation in prevalence or even enrichment in highly modified mRNA transcripts. Nonetheless, this suggests that a multitude of these modifications are important for translation and

adds an additional layer of evidence of the translational inhibitor mechanism of action. While we know how these translational inhibitors interact with the ribosome, this suggests that there are further downstream effects on the cellular biology which ultimately affects the translational machinery in more than one way.

4.2.4 trmAΔ changes the modification landscape of E. coli phenylalanine tRNA

Thus far, we identified that m^5U levels increase and *trm2*Δ cell lines grow more efficiently and produce more protein than wildtype cells under hygromycin B stress, while the opposite is true for cycloheximide stress. We postulate these alterations could be resultant from the following factors: (1) altered amino acid addition rates under native conditions, (2) altered amino acid addition rates during translational stress, (3) altered ability for translocation to occur during the translational stress. Thus, we sought to use a well-established fully reconstituted *in vitro* translation system to interrogate these two phenomena. Within these assays, we can assess translation using *E. coli* $tRNA^{Phe}$ purified from either WT or *trmA*Δ cell lines. For tRNAs purified from *trmA*Δ cells we confirmed that m^5U was not included by a targeted ribonucleoside LC-MS/MS assay (Figure 2A). In these assays were screened over 51 nucleosides. During the same analysis, we surprisingly found a significant alteration in the overall modifications landscape of *E. coli* $tRNA^{Phe}$ when purified from *trmA*Δ cell lines. In the *trmA*Δ tRNA, we detected a significant upregulation of i^6A (~12-fold, Supplemental figure 2), which could be resultant from the depletion of the hypermodification ms^2i^6A within the anticodon. The i6A abundance could be estimated to be approximately 0.8 modifications per the *trmA*Δ $tRNA^{Phe}$. The low abundance selenocysteine tRNA is the only *E. coli* tRNA that contains i6A within the tRNA and our $tRNA^{Phe}$ charging efficiency was approximately the same (700pmol/A260), so we posit that this change is coming from an

altered $tRNA^{Phe}$ modification landscape. We also detected a moderate decrease in acp^3U in the *trmA*Δ $tRNA^{Phe}$ (~1.7-fold, Supplemental figure 2), a modification within the variable loop.

Our studies both confirmed that *trmA*Δ $tRNA^{Phe}$ lacks m^5U, and revealed that the lack of TrmA further alters the modifications landscape of $tRNA^{Phe}$, suggesting that cooperativity may exist between the modifying enzymes and the tRNA structure or current modification landscape. These findings highlight why it is so difficult to study the biological significance of RNA modifications because the removal of RNA modifying enzymes could have further downstream biological consequences. Nonetheless, these results provide a more comprehensive picture of the tRNA landscape, and we utilize this data along with *in vitro* translation assays to piece together why *E. coli trmA*Δ cell line displays a phenotype under translational inhibition.

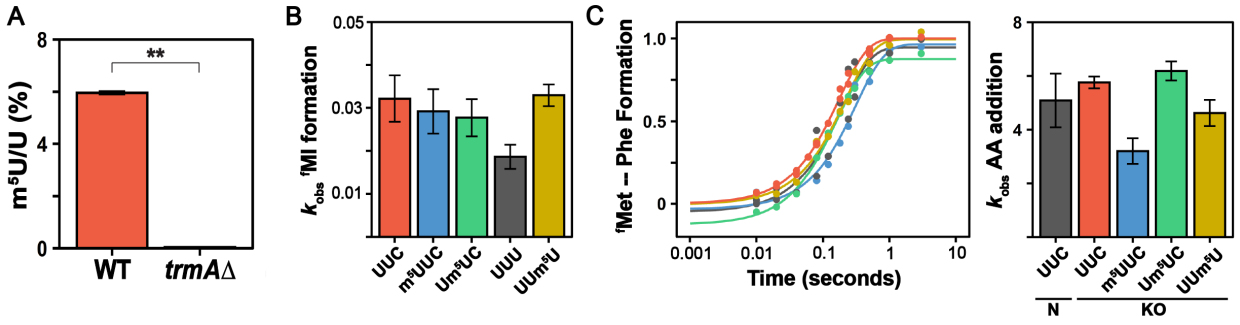

Figure 4.2: ***m^5U has a minor affect on translationin a position dependent manner in mRNA and no major observed affectt in tRNA****. **(A)** LC-MS/MS analysis showing that our $tRNA^{phe}$ purified from trmA KO cells does not contain m^5U modfications. **(B)** Bar graph showing the formation of misocded Met-Ile product. **(C)** K_{obs} Curves and bar plots showing observered rates constant for met-phe dipeptide formation using the KO $tRNA^{phe}$.*

4.2.5 Translational fidelity is impacted on m^5U-containing codons in a position dependent manner

After successfully purifying our KO phenylalanine tRNA, and analyzing its modification landscape, we were able to perform translation assays using our *in vitro* reconstituted system to test our proposed hypothesis of the effect of m^5U on translation. In previously published work we assessed the impact of m^5U containing codons on translation rates using the same *in vitro*

translation system. In our assays, 70S ribosome initiation complexes were formed on messages encoding Met-Phe peptides programmed with ^{35}S-^{f}Met-tRNA^{fmet} bound to AUG in the P site, and UUC or m5U in the 1st, 2nd, or 3rd position in the A site. Initiation complexes (140 nM) were reacted with Phe-tRNA^{Phe}•EF-Tu•GTP (ternary complex; 2uM) at 37^{o} C. These reactions were stopped at discrete time points with KOH, and the resulting products were visualized by electrophoretic TLC. We measured k_{obs} on UUU and UUC codons because the observed rate constants for Phe addition are well established. We observed that amino acid addition rates are impacted on m^{5}U-containing codons in a position dependent manner, with a 2-fold decrease in the k_{obs}. Following this observations, we were interested in whether or not this phenomenon would have an impact on translation fidelity when m^{5}U was present on a UUC codon. m^{5}U has a methyl group on the non-Watson face of the nucleotide and should not affect hydrogen bond base pairing. As previously described, we observed a modest 2-fold change in amino acid addition only at the 3rd position when m^{5}U is present, therefore we hypothesized fidelity would not be affect by the addition of m^{5}U on a codon. To investigate the difference between unmodified Phe codons and m^{5}U codons in regards to allow the addition of near-cognate amino acids, we chose Ile-tRNA^{Ile} which is a small aliphatic near cognate amino acids. To try and obtain a kinetic understanding on how near-cognate amino acid addition is changing when m^{5}U is present, we performed kinetic assays with the near-cognate Ile-tRNA^{Ile}. These assays utilized an established regenerative mix[30] and contain EfTs. We observed that translation fidelity is slightly affected when m^{5}U is present at the 3rd position. (Figure 2B) This result is unsurprising due to the fact that we saw a rate defect in amino acid addition when m^{5}U was present in the 3rd position.

4.2.6 trmAΔ Phe tRNA does not alter amino acid addition

m^5U is one of the most abundant eukaryotic and bacterial modifications and m^5U is speculated to have an impact in tRNA structure, maturation, and thermal stability[14], [31], [32]. However, its impact regarding translation has not been studied. Since *trm2*Δ yeast displayed a growth phenotype and produces more protein than wildtype yeast under translational inhibition, we sought to determine whether m^5U54 in $tRNA^{Phe}$ affects amino acid addition under native conditions. We investigated this using a well-established fully reconstituted *in vitro* translation system where we input $tRNA^{Phe}$ purified from either *trmA*Δ or wildtype *E. coli*. Despite the tRNA changes in modification landscape that we observed in the *trmA*Δ purified $tRNA^{Phe}$, the rate constant for Phe incorporation on an unmodified UUC codon was comparable to wildtype purified $tRNA^{Phe}$ at a k_{obs} of ~ $5s^{-1}$ (Fig 2C). Therefore, we found that *trmAΔ* Phe tRNA does not affect the rate of amino acid addition and cannot explain the increased reported production in *trm2*Δ cells displayed previously.

Recently, m^5U was detected at low abundances in eukaryotic mRNA and reasoned that there could be a cooperative affect between m^5U containing mRNA codons and tRNA [28], [33]–[35.]Thus, we sought to interrogate how amino acid addition on m^5U-containing codons (1^{st}, 2^{nd}, and 3^{rd} position modified UUU or UUC codons) is affected when decoded by a *trmA*Δ $tRNA^{Phe}$ using the our fully reconstituted *in vitro* translation system. While the rate constants for amino acid was not impacted when m^5U was incorporated at 2^{nd} and 3^{rd} position modified codons, there was a small defect (~2-fold decrease at ~3 s^{-1}) when m^5U-deplete $tRNA^{Phe}$ translated an m^5UUC codon. We previously detected a 2-fold rate defect at the 3^{rd} position modified codon with wildtype $tRNA^{Phe}$ (Figure 2C), which was not present with *trmA*Δ $tRNA^{Phe}$ [28]. This data collectively demonstrate that *trmA*Δ $tRNA^{Phe}$ does not significantly alter amino acid addition of both unmodified and modified codons under unstressed conditions.

4.2.7 trmAΔ tRNA^{Phe} increases tripeptide synthesis under hygromycin B translation inhibition

Hygromycin B prevents translocation to block translation by interacting with the RNA species in the A site within the ribosome, resulting in the cessation of translation. While we that *trmA*Δ tRNA^{Phe} does not alter amino acid addition, this does not interrogate whether this tRNA alters translocation. Thus, we utilized our *in vitro* translation system to synthesize a ^{f}MFK tripeptide without the presence of hygromycin B. Under these conditions, we found that tripeptide synthesis was not significantly altered when *trmA*Δ tRNA^{Phe} was used instead of wildtype tRNA^{Phe}. We found that the k_1 (^{f}M disappearance) was approximately 5.2 s^{-1} for both tRNA^{Phe} species while the k_2 (^{f}MFK formation) was 0.34 s^{-1} and 0.19 s^{-1} for wildtype and *trmA*Δ tRNA^{Phe}, respectively (Figure 3. We found that *trmA*Δ tRNA^{Phe} does not alter tripeptide synthesis and amino acid addition both unmodified and m^{5}U modified codons. This corroborates previous studies that did not detect a phenotype for cells lacking tRNA (uracil-5-)-methyltransferase.

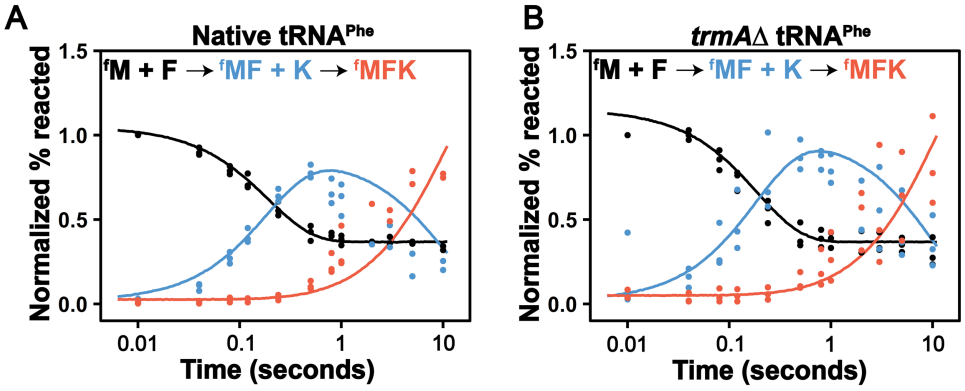

Figure 4.3: Time courses displaying the formation of fMet-Phe-lys tripeptide on unmodified phenylalanine codons reacting with 1uM Phe+lLys TC complex using either Native phe tRNA and Native Lysine ***(left)*** *or TrmA KO phe tRNA absent of m^{5}U and Native Lysine.* ***(right)*** All similuaiton aligned raw data with good fit, R^2 then .9.

In the presence of hygromycin B, *trm2*Δ yeast grow more efficiently and produced more protein (Figure 1). While we did not identify any significant differences in translation assays performed with wildtype and *trmA*Δ tRNA^{Phe} under unstressed conditions, we posited that the presence of hygromycin B would reveal if there are differences in translocation using both tRNA

species. We investigated this by synthesizing the same ^{f}MFK peptide described above, but hygromycin B was included in the reaction mix to inhibit protein synthesis. Since hygromycin B inhibits translation by preventing translocation, we theorized that any differences would be resultant from the ^{f}MFK peptide formation since ^{f}MF formation does not require translocation in the ribosome. While overall tripeptide synthesis was slower using both wildtype and *trmA*Δ tRNA^{Phe}, the formation of the ^{f}MF dipeptide was still rapid, as expected because hygromycin should exhibit an effect after the first peptide bond is formed (Figure 4). However, we find that tripeptide synthesis is greatly increased with *trmA*Δ tRNA^{Phe} compared to wildtype (Figure 4). This result is consistent with our observation that *trm2*Δ yeast cells produce more protein than wildtype cells in the presence of hygromycin B (Figure 1).

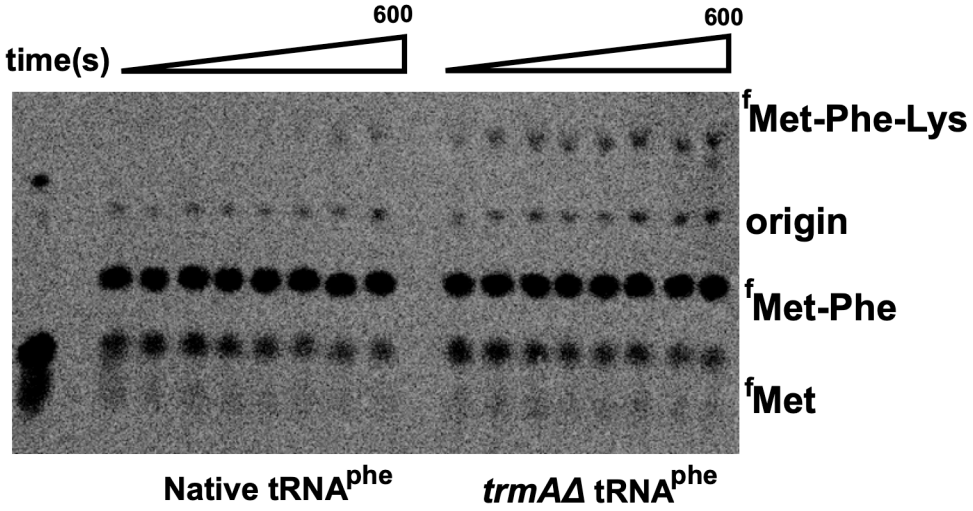

*Figure 4.4: eTLC displaying peptide products of fMet-Phe-lys tripeptide on unmodified phenylalanine codons reacting with 1uM Phe+lLys TC complex using either Native phe tRNA and Native Lysine **(left)** or TrmA KO phe tRNA absent of m^{5}U and Native Lysine **(right)** under hygromycin B (50ug/mL final) stress conditions.*

4.3 Discussion

In previously published literature, we discovered that Trm2 was the methyltransferase responsible for incorporating m^{5}U into yeast mRNA. With its installation understood, we decided to explore the potential role of m^{5}U in mRNA in translation events only to discover no-to-moderate

change. In fact, observable rates of amino acid addition had no changes when m^5U is installed in a UUC codon save a 2-fold rate defect detected only at the 3rd position of a phenylalanine codon[28]. In this work, we investigated the biological relevance/role of Trm2 and m^5U in RNA and discovered that *trm2*Δ yeast grow differently under antibiotic induced translation stress. In fact, we identified the first phenotype for tRNA (uracil-5-)-methyltransferase where yeast lacking the methyltransferase has altered cellular growth under translational inhibition by aminoglycosides – hygromycin B, cycloheximide, and paromomycin. In particular, we see that *trm2*Δ yeast grow more efficiently and produce more protein than wildtype yeast under hygromycin B stress (Figures 1 A and B). This phenotype suggests that m^5U in mRNA (UUC/UUU codon) may be spatially/stereochemically important in the hygromycin mechanism of action and that removal of m^5U disrupts this mechanism. Furthermore, the increase in m^5U abundance observed during our UHPLC-MS/MS analyses supported this idea. However, our *in vitro* reconstituted translation assays showed us that m^5U in mRNA has no major impact on amino acid addition, suggesting that the m^5U and *trm*2 may be important in other targets/aspects of translation. The next logical target was tRNA, since it carries m^5U modifications and is a key player in protein translation. Interestingly, we saw no apparent change in translation kinetics for both amino acid addition and translocation. Nevertheless, we consistently saw decrease in efficacy of hygromycin B in the absence of m^5U/*trm*2. Our *trmA*Δ $tRNA^{Phe}$ displayed a moderate change in its modifications landscape, and this increase resistance to hygromycin B could be due other modifications or lack thereof.

While *trmA*Δ $tRNA^{Phe}$ provides some resistance to hygromycin B translation inhibition, this effect could be caused by a few different factors– the deletion of m^5U54 in $tRNA^{Phe}$, the alteration in i^6A and acp^3U abundance in *trmA*Δ $tRNA^{Phe}$, or the remodeling of $tRNA^{Phe}$ structure

without tRNA (uracil-5-)-methyltransferase present. Previously, structural analysis revealed that hygromycin B binds to the RNA helix 44 (h44) in 30S rRNA small subunit, this position happens to be right next to the aminoacyl-tRNA binding site[23], [24]. It is currently hypothesized that hygromycin works by (1) causing nucleotide A 1493 to flip outwards into a position between the P and A site tRNAs, which could explain the tRNA affinity increase in the A site; (2) A1493 could be causing steric blockage stopping the tRNA from moving to from the p site to the a site; (3) the binding site of hygromycin B allows its second ring to make contact with backbone of the P site mRNA, therefore locking it in position [36]. We speculate that i^6A may the factor contributing to hygromycin B resistance, instead of m^5U. In the *trmA*Δ tRNA, we detected a significant upregulation of i^6A at position 37 tRNA. In the native *e. coli* and yeast $tRNA^{phe}$, this position is frequently modified to harbor a ms^2i^6A modification. The 37 position in tRNA is adjacent to the anticodon in the ASL, and are known to stabilize codon:anticodon interactions. We hypothesize that i^6A destabilizes the codon:anticodon interactions relative to the fully-modified ms^2i^6A.

Currently, we are working in collaboration with the Polikanov lab to crystlize our *trmA*Δ tRNA in the ribosome with, and without hygromycin B. The goal of this work is to get some structural insight into what exactly is perpetuating this resistance to hygromycin B. As previously stated above, we do believe it has something to do with the change in modification landscape, but this method would help us validate our hypothesis. Preliminary crystallographic data of a structure between native $tRNA^{phe}$ and the ribosome incubated with hygromycin B should that the ms^2i^6A modification at position 37, points directly at hygromycin B. Furthermore, this work may help to understand the mechanism of action for hygromycin B inhibition, by

showing which modifications or ribosome/tRNA interactions are crucial This would be an important discovery in the field.

Antibiotic resistance has become an increasingly prominent public health concern internationally. One mechanism to combat bacterial resistance mechanism is to create new drugs or modify the current antibiotics at our disposal. Therefore, it is important to understand how current translation-targeted drugs work at a molecular level Additionally, in the last few years, it has been discovered that RNA modifications could play a role in antibiotic resistance. This work contributes to the growing body of literature discussing the impact that tRNA modifications may have on antibiotics, in particular hygromycin induced translational stress control. Here we clearly see that a change in the modification landscape of $tRNA^{phe}$ allowed translocation to continue under hygromycin B induced stress. Furthermore, our data indicates there was no apparent change in translation of this tRNA itself, demonstrating a antibiotic specific response.

4.4 Methods

4.4.1 Spot plating and growth curves

For growth curves, wild-type and *trm2Δ* cells were inoculated into 5 mL YPD and grown overnight at 30˚C. Cultures were then diluted to a starting OD_{600} = 0.05 – 0.1 in 100 mL YPD media containing either 1 M NaCl, 0.1 µg/mL cycloheximide, 50 µg/mL hygromycin B, or 3 mg/mL paromomycin. Cultures were grown in duplicate at 30˚C with shaking unless indicated.

4.4.2 Reporter assay

Plasmid was transformed into wild-type and *Δtrm2 S. cerevisiae* using previously published protocol. The cells were streaked onto CSM-URA agar plates to isolate single colonies[37]. CSM-URA media (30 mL) was inoculated with a single colony and allowed to grow

overnight at 30°C and 250 RPM. The cells were diluted to an OD_{600} of 0.05 with 500 mL of CSM-URA medium and were grown to an OD_{600} of 0.5 at 30°C and 250 RPM. At this point, the cells were stressed with hygromycin B or cycloheximide and were allowed to continue to grow. At time points of 0 min, 20 min, 60 min, and 150 min after the translational stress, 10 mL of culture was pelleted at 8,000 x g for 10 min. The cell pellet was washed with 1 mL of water prior to storage at -80°C until the assay was performed.

4.4.3 Yeast Cell Growth and mRNA Purification

Wild-type and *Δtrm2* Saccharomyces cerevisiae were grown in YPD medium as previously described[38]. *Δtrm2* Saccharomyces cerevisiae were grown in the presence of 200 µg/mL Geneticin. Briefly, 10 mL of YPD medium was inoculated with a single colony selected from a plate and allowed to grow overnight at 30°C and 250 RPM. The cells were diluted to an OD_{600} of 0.1 with 200 mL of YPD medium and were grown to an OD_{600} between 0.6 and 0.8 at 30°C and 250 RPM. Translational stress *S. cerevisiae* were grown with 50 µg/mL hygromycin B or 100ng/mL cycloheximide. Hygromycin B *S. cerevisiae* were grown to an OD_{600} of 0.4 to ensure cells were in mid-log phase growth. This cell culture was pelleted at 15,000xg at 4°C and used for the RNA extraction.

Yeast cells were lysed as previously described with minor alterations[39]. The 200 mL cell pellet was resuspended in 8 mL of lysis buffer (60 mM sodium acetate pH 5.5, 8.4 mM EDTA) and 800 µL of 10% SDS. One volume (8.8 mL) of phenol was added and vigorously vortexed. The mixture was incubated at 65°C for five minutes and was again vigorously vortexed. The incubation at 65°C and vortexing was repeated once. Then, the mixture was rapidly chilled in an ethanol/dry ice bath and centrifuged for 15 minutes at 15,000xg. The total RNA was extracted from the upper aqueous phase using a standard acid phenol-chloroform extraction. The extracted total RNA was

treated with 140 U RNase-free DNase I (Roche, 10U/μL) at 37℃ for 30 min. The DNase I was removed through an acid phenol-chloroform extraction. The resulting total RNA was used for our UHPLC-MS/MS, bioanalyzer, and RNA-seq analyses.

mRNA was purified through a three-step purification pipeline[28]. First, small RNA (tRNA and small rRNA) was diminished using the MEGAclear Transcription Clean-Up Kit (Invitrogen) to purify RNA >200nt. Then, Dynabeads oligo-dT magnetic beads (Invitrogen, USA) were used to purify poly(A) RNAs twice from 140 μg of small RNA depleted RNA. The resulting RNA was ethanol precipitated and resuspended in 14 μL. Following, we used the commercial riboPOOL rRNA depletion kit (siTOOLs Biotech, Germany) to remove residual 5S, 5.8S, 18S, and 28S rRNA. The Bioanalyzer RNA 6000 Pico Kit (Agilent, USA) was used to evaluate the purity of the mRNA prior to UHPLC-MS/MS analysis.

4.4.4 qRT-PCR

The RevertAid First Strand cDNA Synthesis Kit (Thermo Scientific, USA) was used to reverse transcribe DNase I treated total RNA and three-stage purified mRNA (200 ng) using the random hexamer primer. The resulting cDNA was diluted 5000-fold and 1 μL of the resulting mixture was analyzed using the Luminaris Color HiGreen qPCR Master Mix (Thermo Scientific, USA) with gene-specific primers.

4.4.5 RNA -seq

The WT S. cerevisiae mRNA was analyzed by RNA-seq as previously described by paired-end sequencing using 2.5% of an Illumina NovaSeq (S4) 300 cycle sequencing platform flow cell (0.625% of flow cell for each sample)[28]. All sequence data are paired-end 150 bp reads.

4.4.6 RNA enzymatic digestion and UHPLC-MS/MS ribonucleoside analysis

Total RNA and mRNA (125 ng) was digested for each condition. The RNA was hydrolyzed to composite mononucleosides using a two-step enzymatic reaction and quantified using LC-MS/MS as previously described with no alterations[28].

4.4.7 E.coli Ribosomes, and translation factors tRNA and mRNA for in vitro assay

Ribosomes were purified from *E. coli* MRE600 as previously described[40]. All constructors for translation factors were provided by the Green lab unless specifically stated otherwise. Expression and purification of translation factors were carried out as previously described[40]. Unmodified transcripts were prepared using run-off transcription of a DNA template. Modified mRNA sequences containing 5-methyl uridine were purchased from Dharmacon. The mRNA was HPLC purified at Dharmacon. The mRNA sequenced used GGUGUCUUGCGAGGAUAAGUGCAUU AUG UUC UAA GCCCUUCUGUAGCCA, with the coding sequence underline. In these experiments, the modified position was always the first position in the UUC phenylalanine codon.

Method was previously published[41] . Bulk e. coli transfer RNA were either bought in bulk from Sigma, or purified in E. coli form an HB101 strain containing pUC57-tRNAphe that we obtained from Yury Polikanov. 2 liter cultures containing Terrific Broth (TB) media (TB, 4 mL glycerol/L, 50 mM NH_4Cl, 2 mM $MgSO_4$, 0.1 mM $FeCl_3$, 0.05% glucose and 0.2% lactose (if autoinduction media was used)) were inoculated with 1:400 dilution of a saturated overnight culture and incubated with shaking at 37°C overnight with 400mg/ml of ampicillin. Cells were harvested the next morning by 30 minute centrifugation at 5000 rpm and then stored at -80 C. Extraction of tRNA was done by first responding the cell pellet in 200ml of resuspension buffer (20mM Tris-Cl, 20 mM $Mg(OAc)_2$ pH 7.) The resuspended cells were then placed in Teflon centrifuge tubes with ETFE o-rings with an acid phenol/chloroform mixture. The cell to

phenol/chloroform ratio was approximately 1:1.25 respectively. The tubes were placed in a 4C incubator and left to shake for 1 hour. After incubation cells were spun down for 60 minutes at 4000 rpm at 4C. The supernatant was transferred to another container and the first organic phase was then back-extracted with resuspension buffer and centrifuged down for 60 minutes at 4000 rmp. Aqueous solutions were then combined and a 1/10 volume of 3M NaOAc ph5.2 was added and mixed well. Isopropanol was added to 20% and after proper mixing was centrifuged to remove DNA at 13,700g for 60 minutes at 4C. The supernatant was collected and isopropanol was added to 60% and was left to precipitate at -20C overnight. Precipitation was centrifuged at 13,700 g for 60 minutes at 4C. The pellet was then resuspended with approximately 10 mL 200 mM Tris-Acetate, pH 8.0, and incubate at 37 C for at least 30 minutes. After incubation $1/10^{th}$ volume of 3 M NaOAc and 2 volumes of ethanol was added and mixture was centrifuged at 16,000 g for 60 mins at 4 C. The pellet was washed with 70% ethanol and resuspended in water and desalted on amincon concentrator.

Next the tRNA was isolated on FPLC using buffer A (50 mM NH_4OAc, 300 mM NaCl, 10 mM $MgCl_2$) and buffer B (50 mM NH_4OAc, 800 mM NaCl, 10 mM $MgCl_2$). Resuspended pellet was filtered and loaded on the FPLC. It was eluted with a linear gradient from 0- 50% B over 18 column volumes on a Resource Q column. Fractions were pulled and precipitated overnight.

Pellet was resuspended in water and filtered before being put on the HPLC for further isolation and clean up. The column that was used was a Waters XBridge BEH C18 OBD Prep wide pore column (10x250, ~20 mL column volume, 5 μm). Column was stored in acetonitrile so before any buffers were added, the column was washed with 10 column volumes of water and then equilibrated with HPLC buffer A (20 mM NH_4OAc, 10 mM $MgCl_2$, 400 mM NaCl at pH 5). 400ul of volume was injected. A linear gradient of buffer B from 0-35% was done over 35 minutes. After

35 mins, the gradient was increased to 100% buffer B over 5 minutes and held at 100% for 10 mins, column was then equilibrated for 10 column volumes before next injection with Buffer A. TCA precipitations were performed on the fractions to determine tRNA of interested, in this case phenylalanine, as well as also determining the A260 and amino acid acceptor activity.

4.4.8 Formation of E. coli ribosome initiation complexes

Initiation complexes (IC's) were formed in 1X 219-Tris buffer (50 mM Tris pH 7.5, 70 mM NH_4Cl, 30 mM KCl, 7 mM $MgCl_2$, 5 mM ß-ME) with 1 mM GTP as previously described(X). 70s ribosomes were incubated with 1uM mRNA (with or without modification), initiation factors (1,2,3) all at 2uM final and 2uM of radiolabeled ^{F}met-tRNA for 30 mins at 37C. After incubation $MgCl_2$ was added to a final concentration of 12mM. The ribosome mixture was then layered onto 1 mL cold buffer D (20 mM Tris-Cl, 1.1 M sucrose, 500 mM NH_4Cl, 10 mM $MgCl_2$, 0.5 mM disodium EDTA, pH 7.5) and centrifuged at 69,000 rpm for 2 hours at 4C. After pelleting, the supernatant was discarded into radioactive waste, and the pellet was resuspended in 1X 219- tris buffer and stored at -80C.

4.4.9 In vitro amino acid addition assays: dipeptide formation

IC complexes were diluted to 140 nM with 1X 219-Tris buffer. Ternary complexes (TCs) were formed by first incubating the EF-Tu pre-loaded with GTP (1X 219-Tris buffer, 10 mM GTP, 60 μM EFTu, 1 μM EFTs) at 37°C for 10 min. The EF-Tu mixture was incubated with the tRNA mixture (1X 219-Tris buffer, Phe-$tRNA^{Phe}$ (1-10 μM), 1 mM GTP) for another 15 min at 37°C. After TC formation was complete, equal volumes of IC complexes (70 nM) and ternary complex (1 μM) were mixed either by hand or using a KinTek quench-flow apparatus. Discrete time-points (0-600 seconds) were taken as to obtain observed rate constants on m^5U-containing mRNAs. Each

time point was quenched with 500 mM KOH (final concentration). Time points were then separated by electrophoretic TLC and visualized using phosphorescence as previously described[40], [42]. Images were quantified with ImageQuant. The data were fit using Equation 1: $Fraction\ product\ = A \cdot (\ 1 - e^{k_{obs}t})$

4.4.10 In vitro assays amino acid misincorporation

In-vitro translation assays were performed by mixing IC complex (70nM final concertation) and ternary complex (1 μM total tRNA aminoacylated with S100 enzymes or specific synthetases, 40 μM EF-Tu, 10 mM GTP, 1X-219 tris buffer) mixed either by hand at room temperature for 10 minutes. Reactions were quenched with 500 mM KOH (final). Products were then separated on Electrophoretic TLC and visualized with phosphorescence as previously described[40].

4.4.11 In vitro amino acid addition assays: tripeptide formation

IC complexes were diluted to 140 nM with 1X 219-Tris buffer. Ternary complexes (TCs) were formed by first incubating the EF-Tu pre-loaded with GTP (1X 219-Tris buffer, 10 mM GTP, 60 μM EFTu, 1 μM EFTs) at 37°C for 10 min. The EF-Tu mixture was incubated with the tRNA mixture (2 μM aminoacyl-tRNA Phe/Lys(s), 24 μM EF-G, 60 μM EF-Tu) with ICs (140 nM) in 219-Tris buffer (50 mM Tris pH 7.5, 70 mM NH_4Cl, 30 mM KCl, 7 mM $MgCl_2$, 5 mM βME). for another 15 min at 37°C. These experiments are done with both native phenylalanine tRNA or our KO phenylalanine tRNA. After TC formation was complete, equal volumes of IC complexes (70 nM) and ternary complex (1 μM) were mixed using a KinTek quench-flow apparatus. Discrete time-points (0-600 seconds) were taken as to obtain observed rate constants on non-mortified mRNAs, containing a UUC phenylalanine codon. Each time point was quenched with 500 mM

KOH (final concentration). Time points were then separated by electrophoretic TLC and visualized using phosphorescence as previously described[40], [42]. Images were quantified with ImageQuant. The data were fit using Equation 1 as previously described.

4.4.12 In vitro amino acid addition assays: tripeptide formation with Hygromycin B

IC complexes were diluted to 140 nM with 1X 219-Tris buffer. Ternary complexes (TCs) were formed by first incubating the EF-Tu pre-loaded with GTP (1X 219-Tris buffer, 10 mM GTP, 120 μM EFTu, PEP, 12mM, PK .40μM, 40 μM EFTs) at 37°C for 10 min. The EF-Tu mixture was incubated with the tRNA mixture (20–60 μM aminoacyl-tRNA Phe/Lys(s), 24 μM EF-G, 60 μM EF-Tu) with ICs (140 nM) in 219-Tris buffer (50 mM Tris pH 7.5, 70 mM NH_4Cl, 30 mM KCl, 7 mM $MgCl_2$, 5 mM βME). for another 15 min at 37°C. These experiments are done with both native phenylalanine tRNA or our KO phenylalanine tRNA. After TC formation was complete, 50μg/ml of Hygromycin B was added to the IC complex. Then by haand equal volumes of IC complexes (70 nM) and ternary complex (1 μM) were mixed and discrete time-points (0-600 seconds) were taken as to obtain observed rate constants on non-mortified mRNAs, containing a UUC phenylalanine codon. Each time point was quenched with 500 mM KOH (final concentration). Time points were then separated by electrophoretic TLC and visualized using phosphorescence as previously described[40], [42]. Images were quantified with ImageQuant. The data were fit using Equation 1 as previously described.

4.4.13 Fitting observed rate constants and Global analysis simulations of amino acid addition

Fits for used to obtain observed rate constant k_1 was done using a single differential equation in Kaleidagrpah for products in di peptide formation. When multiple peptide products were formed, the disappearance of FMET product was fit sing a single differential equation in

Kaleidagrpah to get an observed rate constant k_1. This value was then used in KinTex Explorer to measure subsequent rate constant k_2 using simulations. Simulations were modeled against the equation:

$$^{f}M + F \rightarrow {}^{f}MF + K \rightarrow {}^{f}MFK$$

4.4.14 Spot plating assay and growth curve characterization under stress

Wild-type and *trm2*Δ cells were inoculated into 3 mL YPD and grown overnight. Then these cultures were diluted to OD_{600}=1 as a starting point, and 7 µl of 10-fold serial dilutions were spotted on fresh YPD agar plates including 0.75-1.0 M NaCl, 250 mM $MgSO_4$, 200 µM puromycin, 100 ng/mL cycloheximide, 25-50 µg/mL hygromycin B, 50 µM MG132 and 1.5-3 mg/mL paromomycin. Growth of the cells were also tested in the presence of different carbon sources including 2% glucose, 2% sucrose, 2% galactose and 3% glycerol in YEP agar media (1% yeast extract and 2% peptone). The plates were incubated for 2-5 days at 30 ^{o}C unless indicated. For growth curves, wild-type and *trm2Δ* cells were inoculated into 5 mL YPD and grown overnight. Cultures were then diluted to a starting OD_{600} = 0.05 – 0.1 in 100 mL YPD media containing either 1 M NaCl, 0.1 µg/mL cycloheximide, 50 µg/mL hygromycin B, or 3 mg/mL paromomycin. Cultures were grown in duplicate at 30˚C with shaking unless indicated, and growth was monitored by OD_{600}

4.5 References

[1] M. T. Angelova *et al.*, "The emerging field of epitranscriptomics in neurodevelopmental and neuronal disorders," *Frontiers in bioengineering and biotechnology*, vol. 6, p. 46, 2018.

[2] M. S. Ben-Haim, S. Moshitch-Moshkovitz, and G. Rechavi, "FTO: linking m 6 A demethylation to adipogenesis," *Cell research*, vol. 25, no. 1, pp. 3–4, 2015.

[3] Q. I. Cui *et al.*, "m6A RNA methylation regulates the self-renewal and tumorigenesis of glioblastoma stem cells," *Cell reports*, vol. 18, no. 11, pp. 2622–2634, 2017.

[4] T. Du *et al.*, “An association study of the m6A genes with major depressive disorder in Chinese Han population,” *Journal of affective disorders*, vol. 183, pp. 279–286, 2015.
[5] N. Jonkhout, J. Tran, M. A. Smith, N. Schonrock, J. S. Mattick, and E. M. Novoa, “The RNA modification landscape in human disease,” *Rna*, vol. 23, no. 12, pp. 1754–1769, 2017.
[6] Y. Bykhovskaya, K. Casas, E. Mengesha, A. Inbal, and N. Fischel-Ghodsian, “Missense mutation in pseudouridine synthase 1 (PUS1) causes mitochondrial myopathy and sideroblastic anemia (MLASA),” *Am J Hum Genet*, vol. 74, no. 6, pp. 1303–1308, Jun. 2004, doi: 10.1086/421530.
[7] P. Boccaletto *et al.*, “MODOMICS: a database of RNA modification pathways. 2017 update,” *Nucleic Acids Res*, vol. 46, no. D1, pp. D303–D307, Jan. 2018, doi: 10.1093/nar/gkx1030.
[8] T. D. Price, H. A. Hinds, and R. S. Brown, “Thymine ribonucleotides of soluble ribonucleic acid of rat liver,” *Journal of Biological Chemistry*, vol. 238, no. 1, pp. 311–317, 1963.
[9] V. Anantharaman, E. V. Koonin, and L. Aravind, “TRAM, a predicted RNA-binding domain, common to tRNA uracil methylation and adenine thiolation enzymes,” *FEMS microbiology letters*, vol. 197, no. 2, pp. 215–221, 2001.
[10] D. T. Dubin, “Methylated nucleotide content of mitochondrial ribosomal RNA from hamster cells,” *Journal of molecular biology*, vol. 84, no. 2, pp. 257–273, 1974.
[11] S. Auxilien *et al.*, “Specificity shifts in the rRNA and tRNA nucleotide targets of archaeal and bacterial m5U methyltransferases,” *RNA*, vol. 17, no. 1, pp. 45–53, Jan. 2011, doi: 10.1261/rna.2323411.
[12] C. W. Chan, B. Chetnani, and A. Mondragón, “Structure and function of the T-loop structural motif in noncoding RNAs,” *Wiley Interdisciplinary Reviews: RNA*, vol. 4, no. 5, pp. 507–522, 2013.
[13] S. Hur, R. M. Stroud, and J. Finer-Moore, “Substrate recognition by RNA 5-methyluridine methyltransferases and pseudouridine synthases: a structural perspective,” *Journal of Biological Chemistry*, vol. 281, no. 51, pp. 38969–38973, 2006.
[14] P. Davanloo, M. Sprinzl, K. Watanabe, M. Albani, and H. Kersten, “Role of ribothymidine in the thermal stability of transfer RNA as monitored by proton magnetic resonance,” *Nucleic Acids Res*, vol. 6, no. 4, pp. 1571–1581, Apr. 1979, doi: 10.1093/nar/6.4.1571.
[15] L. C. Keffer-Wilkes, E. F. Soon, and U. Kothe, “The methyltransferase TrmA facilitates tRNA folding through interaction with its RNA-binding domain,” *Nucleic acids research*, vol. 48, no. 14, pp. 7981–7990, 2020.
[16] G. R. Björk and F. C. Neidhardt, “Physiological and biochemical studies on the function of 5-methyluridine in the transfer ribonucleic acid of Escherichia coli,” *Journal of Bacteriology*, vol. 124, no. 1, pp. 99–111, 1975.
[17] G. R. Björk and F. C. Neidhardt, “Analysis of 5-methyluridine function in the transfer RNA of Escherichia coli,” *Cancer Research*, vol. 31, no. 5, pp. 706–709, 1971.
[18] A. Babosan, L. Fruchard, E. Krin, A. Carvalho, D. Mazel, and Z. Baharoglu, “Non-essential tRNA and rRNA modifications impact the bacterial response to sub-MIC antibiotic stress,” *bioRxiv*, 2022.
[19] I. Masuda *et al.*, “tRNA methylation is a global determinant of bacterial multi-drug resistance,” *Cell systems*, vol. 8, no. 4, pp. 302–314, 2019.

[20] Y.-M. Hou, I. Masuda, and L. J. Foster, “tRNA methylation: an unexpected link to bacterial resistance and persistence to antibiotics and beyond,” *Wiley Interdisciplinary Reviews: RNA*, vol. 11, no. 6, p. e1609, 2020.
[21] Y. Pan, T.-M. Yan, J.-R. Wang, and Z.-H. Jiang, “The nature of the modification at position 37 of tRNAPhe correlates with acquired taxol resistance,” *Nucleic acids research*, vol. 49, no. 1, pp. 38–52, 2021.
[22] G. Kapoor, S. Saigal, and A. Elongavan, “Action and resistance mechanisms of antibiotics: A guide for clinicians,” *Journal of anaesthesiology, clinical pharmacology*, vol. 33, no. 3, p. 300, 2017.
[23] D. E. Brodersen, W. M. Clemons Jr, A. P. Carter, R. J. Morgan-Warren, B. T. Wimberly, and V. Ramakrishnan, “The structural basis for the action of the antibiotics tetracycline, pactamycin, and hygromycin B on the 30S ribosomal subunit,” *Cell*, vol. 103, no. 7, pp. 1143–1154, 2000.
[24] D. Moazed and H. F. Noller, “Interaction of antibiotics with functional sites in 16S ribosomal RNA,” *Nature*, vol. 327, no. 6121, pp. 389–394, 1987.
[25] A. Gonzalez, A. Jimenez, D. Vazquez, J. E. Davies, and D. Schindler, “Studies on the mode of action of hygromycin B, an inhibitor of translocation in eukaryotes,” *Biochimica et Biophysica Acta (BBA)-Nucleic Acids and Protein Synthesis*, vol. 521, no. 2, pp. 459–469, 1978.
[26] M. J. Cabañas, D. Vázquez, and J. Modolell, “Inhibition of ribosomal translocation by aminoglycoside antibiotics,” *Biochemical and biophysical research communications*, vol. 83, no. 3, pp. 991–997, 1978.
[27] C. T. Y. Chan, M. Dyavaiah, M. S. DeMott, K. Taghizadeh, P. C. Dedon, and T. J. Begley, “A Quantitative Systems Approach Reveals Dynamic Control of tRNA Modifications during Cellular Stress,” *PLoS Genet*, vol. 6, no. 12, Art. no. 12, Dec. 2010, doi: 10.1371/journal.pgen.1001247.
[28] Joshua D. Jones *et al.*, “Methylated guanosine and uridine modifications in S. cerevisiae mRNAs modulate translation elongation,” *Rsc chem biol*.
[29] S. M. McGaha and W. S. Champney, “Hygromycin B inhibition of protein synthesis and ribosome biogenesis in Escherichia coli,” *Antimicrobial agents and chemotherapy*, vol. 51, no. 2, pp. 591–596, 2007.
[30] J. Choi *et al.*, “N(6)-methyladenosine in mRNA disrupts tRNA selection and translation-elongation dynamics,” *Nat Struct Mol Biol*, vol. 23, no. 2, Art. no. 2, Feb. 2016, doi: 10.1038/nsmb.3148.
[31] M. J. Johansson and A. S. Byström, “Dual function of the tRNA (m5U54) methyltransferase in tRNA maturation,” *Rna*, vol. 8, no. 3, pp. 324–335, 2002.
[32] C. A. Powell and M. Minczuk, “TRMT2B is responsible for both tRNA and rRNA m5U-methylation in human mitochondria,” *RNA Biol*, vol. 17, no. 4, pp. 451–462, Apr. 2020, doi: 10.1080/15476286.2020.1712544.
[33] W. Dai *et al.*, “Activity-based RNA-modifying enzyme probing reveals DUS3L-mediated dihydrouridylation,” *Nat Chem Biol*, vol. 17, no. 1178–1187, 2021, doi: https://doi.org/10.1038/s41589-021-00874-8.
[34] Q.-Y. Cheng *et al.*, “Chemical tagging for sensitive determination of uridine modifications in RNA,” *Chem. Sci.*, vol. 11, no. 7, Art. no. 7, 2020, doi: 10.1039/C9SC05094A.

[35] J.-M. Carter *et al.*, “FICC-Seq: a method for enzyme-specified profiling of methyl-5-uridine in cellular RNA,” *Nucleic Acids Research*, vol. 47, no. 19, Art. no. 19, Nov. 2019, doi: 10.1093/nar/gkz658.
[36] M. A. Borovinskaya, S. Shoji, K. Fredrick, and J. H. Cate, “Structural basis for hygromycin B inhibition of protein biosynthesis,” *Rna*, vol. 14, no. 8, pp. 1590–1599, 2008.
[37] R. D. Gietz and R. H. Schiestl, “High-efficiency yeast transformation using the LiAc/SS carrier DNA/PEG method,” *Nature protocols*, vol. 2, no. 1, pp. 31–34, 2007.
[38] M. Tardu, J. D. Jones, R. T. Kennedy, Q. Lin, and K. S. Koutmou, “Identification and quantification of modified nucleosides in Saccharomyces cerevisiae mRNAs,” *ACS chemical biology*, vol. 14, no. 7, pp. 1403–1409, 2019.
[39] M. E. Schmitt, T. A. Brown, and B. L. Trumpower, “A rapid and simple method for preparation of RNA from Saccharomyces cerevisiae.,” *Nucleic Acids Res*, vol. 18, no. 10, Art. no. 10, May 1990.
[40] D. E. Eyler *et al.*, “Pseudouridinylation of mRNA coding sequences alters translation,” *PNAS*, vol. 116, no. 46, pp. 23068–23074, Nov. 2019, doi: 10.1073/pnas.1821754116.
[41] J. G. Monroe, T. J. Smith, and K. S. Koutmou, “Investigating the consequences of mRNA modifications on protein synthesis using in vitro translation assays,” in *Methods in Enzymology*, vol. 658, Elsevier, 2021, pp. 379–406.
[42] J. G. Monroe, T. J. Smith, and K. S. Koutmou, “Chapter Sixteen - Investigating the consequences of mRNA modifications on protein synthesis using in vitro translation assays,” in *Methods in Enzymology*, vol. 658, J. E. Jackman, Ed. Academic Press, 2021, pp. 379–406. doi: 10.1016/bs.mie.2021.06.011.

Chapter 5 Conclusions And Future Directions

5.1 Overview

The goal of the work presented in this Dissertation is to elucidate the impact of uridine mRNA modifications on translation and protein synthesis. The altered structures of uridine modifications, pseudouridine and 5-methyluridine, within the coding region of mRNA were able to modulate the rate and accuracy of translation. These changes were at different extents depending on the modifications, and both were context dependent. Furthermore, this work highlights the importance of understanding the implications of modifications on the molecular level. The m^5U modification was cooperatively installed during periods of antibiotic (hygromycin B) stress. My work sought to understand the interplay between uridine modification translational impact and cellular stress conditions. Furthermore, the scope of this research not only furthers the understanding the mechanist impacts modifications have on translation, but open avenues of exploration into other prominent are such as drug resistance, therapeutics, protein evolution, and the overall understand of the cellular stress response.

5.2 Conclusions and Future Directions

5.2.1 Chemical modifications to mRNA nucleobases affect translation elongation and termination

With the advent of advances in analytical methodologies myriad of different post transcriptional modifications have been discovered in mRNA coding regions over the last decade. The presence of these modifications within the coding region befits an understanding of

if and how these modifications have the ability to modify translation regulation. In this work we discussed and compared the impact on translation of over 10 different mRNA modifications. What we see is that each modification had the ability to affect translation, but to different effects and extents despite similarities in modification chemical moiety. For example, largest impacts on amino acid addition rate constants are observed for methylations to the N1 positions on purine nucleobases, however modifications made to the adjacent O6 and N6 functional groups (m^6A, O^6G, inosine) still permit amino acid addition. Non-methylated additions to nucleic acids were also able to modulate the accuracy of the ribosome. Though we see numerous phenotypes including but not limited to changes to amino acid addition, aberration of translation termination, increased miscoding, an important observation to note is that simply changing the Watson-Crick base pairing is enough to cause these effects on translation. Though modifications that are on the non-Watson Crick face impact translation are not well-defined, work studying these modifications show that it is more than just codon:anticodon interactions that influence translation. Understanding how modifications impact translation elongation and termination is not only important for deciphering their role in the translation landscape but can have broader impacts. Modifications have always had a role in mRNA therapeutics research, but during the COIVD-19 pandemic that was streamlined with the COVID-19 mRNA vaccine released by both Moderna and Pfizer. Both vaccines contained the modification N1-methylpsueoduridine, that has been shown to increase stability, and help with the immune response. By elucidating the role that modifications play in translation, we can properly incorporate them into mRNA therapeutics, and create better and more efficient treatments.

5.2.2 Pseudouridinylation of mRNA coding sequences alters translation

Chemical modifications of non-coding RNA has long been understood to be modulators of both structure and function of the biomolecule. In the past decade or so, it has been discovered that a subset of modifications that affect messenger RNA, the biomolecule that serves as the blueprint for protein synthesis by the ribosome. Pseudouridine is one of the most common and well-studied internal mRNA modifications. In this work, we investigate the role of pseudouridine in mRNA using our in vitro reconstituted system. We discovered that when pseudouridine in present in a phenylalanine it has the ability to modestly impact amino acid addition, as well as, EF-Tu GTP activation. Furthermore, we discovered that pseudouridine promotes low levels of miscoding both in vitro and in cellular. To develop a structural understanding of why critical parts of translation were being altered by the pseudouridine modification we utilized a crystal structure of the Thermus thermophilus 70S ribosome with a $tRNA^{Phe}$ bound to a ΨUU codon in the A site shows more disordered regions around the CCA terminal of the tRNA, a site important for amino acylation. This supports why we could see the changes in amino acid addition and changes in EF-Tu GTP activation. Overall, this work gives more insight in to what role pseudouridine could play in translation or not.

There are two main paths this research could lead the community. 1: That these minor alterations that I observed do not mean anything at all. Maybe, these are just accepted errors made during the process. It could be that there would be more energy expended in the body to fix it than to just let it stay. We do see only minor changes, and protein production can still go on. However I feel more so strongly about the latter path, that pseudouridine has a purpose in mRNA translation that goes beyond translation mechanism itself. As previously discussed, it has been shown that not only is pseudouridine in the coding region but it is upregulated in times of stress[1]. This could mean that pseudouridine has a bigger role in the cellular stresses response

system. I was able to show that pseudouridine allows the addition of non-cognate amino acids into the protein product. This could be useful in a stress response because it could allow the body to make proteins necessary to combat the stress. In fact, this is a phenomena previously reported to happen under different stress conditions such as thermal change or oxidative stress [2]–[4]. I propose experiments to evaluate this in section 5.2.6. Alternately, this misincorporation phenomena could be a way that the body slowly but over time creates different proteins. So the incorporation of pseudouridine could be part of the evolutionary process.

References

[1] T. M. Carlile, M. F. Rojas-Duran, B. Zinshteyn, H. Shin, K. M. Bartoli, and W. V. Gilbert, "Pseudouridine profiling reveals regulated mRNA pseudouridylation in yeast and human cells," *Nature*, vol. 515, no. 7525, pp. 143–146, Nov. 2014, doi: 10.1038/nature13802.

[2] Y. Fan, J. Wu, M. H. Ung, N. De Lay, C. Cheng, and J. Ling, "Protein mistranslation protects bacteria against oxidative stress," *Nucleic Acids Research*, vol. 43, no. 3, Art. no. 3, Feb. 2015, doi: 10.1093/nar/gku1404.

[3] P. J. O'Brien and D. Herschlag, "Catalytic promiscuity and the evolution of new enzymatic activities," *Chemistry & biology*, vol. 6, no. 4, pp. R91–R105, 1999.

[4] M. H. Schwartz and T. Pan, "Temperature dependent mistranslation in a hyperthermophile adapts proteins to lower temperatures," *Nucleic Acids Research*, vol. 44, no. 1, Art. no. 1, Jan. 2016, doi: 10.1093/nar/gkv1379.

5.2.3 Pseudouridine modulates translation fidelity during codon recognition and accommodation

My previously published work showed that when pseudouridine was present in a phenylalanine codon, it had the ability to perturb amino acid addition and decrease translation fidelity by allowing the incorporation of near-cognate amino acids. (See chapter 2). In the future, the field should work to elucidate which step in amino-acyl tRNA accommodation that pseudouridine affects. The in-vitro systems allows us to obtain an observed rate constant for amino acid addition that covers all seven kinetically definable steps amino-acyl tRNA

accommodation. I propose to use this system in conjunction with kinetic stop-flow analysis to help determine the mechanism in which pseudouridine has the ability to perturb amino acid addition and fidelity. This work will focus on the use of fluorescently labeled phenylalanine tRNA to identify if incorporation of pseudouridine on a phenylalanine codon causes a change in one of the seven kinetically definable steps of amino acyl tRNA accommodation.

Previous studies detailing the kinetic mechanism for aminoacyl-tRNA selection on unmodified mRNAs revealed that there are 7 kinetically definable steps in translation aminoacyl-tRNA selection (Figure 1)[1]–[3]. The first step involves ternary complex (EF-Tu, GTP, aminoacyl-tRNA) binding to the ribosome.

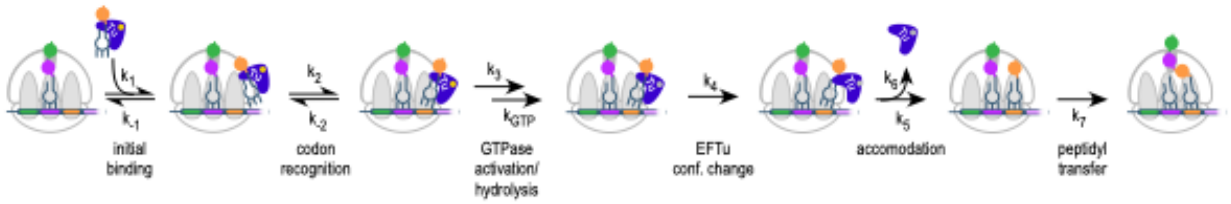

Figure 5.1: ***Aminoacyl-tRNA selection kinetic scheme.*** *1) EF-Tu, aminoacyl-tRNA, GTP (Ternary complex) bind to 70S ribosome. (2) The codon is recognized by the ternary complex. (3) GTPase activated and GTP is hydrolyzed. (4) EF-Tu undergoes conformation change due to GTP hydrolysis. (5) tRNA is accommodated to the A site, (6) EF-TU dissociates, (7) and peptidyl transfer may commence.*

In this initial step, the on/off (k_1/k_{-1}) rate constants of binding are indistinguishable between an aminoacylated-tRNA whose anticodon sequences directly matches the coding sequence for the mRNA (cognate) and an aminoacylated-tRNA whose anticodon sequence differs by one nucleoside (near-cognate), this means codon specificity is not necessary for initial binding. The second step is codon recognition, and in this step cognate and near cognate tRNAs share the same on rate constant (k_2), but the dissociation constant (k_{-2}) for near-cognate is 100 times faster making this the first check-point for proper amino acid addition. The subsequent activation/hydrolysis of GTP bound to EF-Tu is a second crucial step that is strongly dependent on cognate codon recognition; GTP hydrolysis (k_3) is very fast for correctly base-paired cognate aminoacylated-

tRNAs compared to their near-cognate counterparts. Once GTP is hydrolyzed to GDP, EF-Tu undergoes a conformational change with a rate constant (k_4) that is again indistinguishable for cognate/near cognate aminoacyl-tRNAs. The final step (k_5) for tRNA selection is accommodation. Accommodation serves as the last surveillance step for correct tRNA incorporation, and near-cognate aminoacyl-tRNAs exhibit a faster dissociation rate constant (k_{-5}) relative to cognate aminoacyl-tRNAs. EF-Tu then dissociates (k_6) and peptidyl transfer can commence (k_7). Based on our previous work, where we see effects on both fidelity and amino acid addition, as well as a change in GTP hydrolysis/activation (see chapter 2) I hypothesize that Ψ may also alter the binding or accommodation steps of aminoacyl-tRNA selection.

One should investigate the effect of Ψ on each step in the aminoacyl-tRNA selection kinetic scheme (Figure 1) using a fluorescent stopped-flow approach. Stopped flow is a rapid mixing technique used to study kinetic mechanisms. In this technique two solutions containing the molecules of interest (eg. ribosomes, ternary complex) are rapidly mixed and a change in fluorescent signal is observed. This is a standard approach in the ribosome field and has been widely used to study the individual kinetic steps of translation elongation [1]–[6]. Therefore, ample control data exists in the literature to compare results with[3]. To measure binding rate constants, limiting concentrations of ternary complex (EF-Tu bound Fluorescein-tRNA (Fl-tRNA) and GTP) will be titrated with excess 70S ribosome initiation complexes and the signal change will be measured using a KinTek SF2004 stopped flow instrument. The purified 70S ribosome initiation complexes will be programed with AUG in the P-site, and UUU in the A-site. tRNA will be labeled at the 16/17 position with proflavin, as previously described[7]. The first step is to label cognate Phe-tRNA^{Phe} and perform the experiments. This would be helpful to get baseline rate constants that can be compared to previous work. Then, one could move on and use

a series of near-cognate and non-cognate aminoacyl-tRNAs that react efficiently or inefficiently with Ψ-containing codons (e.g., Leu-tRNA^{Leu}, Ser-tRNA^{Ser}; see chapter 2). The proflavin will be excited at 436nm and measured with two photomultiplers after passing through KV 500 filters as previously described and the change in signal will report on the initial binding step in the mechanism (Fig 1)[8]. Additional kinetic assay will be designed in a similar manner, but I will add/remove particular reagents (e.g., GTP, unhydrolyzable GTP analogs such GMPNP) in order to observe particular kinetic steps in isolation. This experimental set up is well established and would be an easy project for a member of the Koutmou Lab to pick up. This is not only a project the lab is capable of put the most logical next step for studying psuedouridine in the field.

References

[1] M. V. Rodnina, T. Pape, R. Fricke, L. Kuhn, and W. Wintermeyer, "Initial Binding of the Elongation Factor Tu· GTP· Aminoacyl-tRNA Complex Preceding Codon Recognition on the Ribosome (∗)," *Journal of Biological Chemistry*, vol. 271, no. 2, pp. 646–652, 1996.

[2] T. Pape, W. Wintermeyer, and M. Rodnina, "Induced fit in initial selection and proofreading of aminoacyl-tRNA on the ribosome," *The EMBO journal*, vol. 18, no. 13, pp. 3800–3807, 1999.

[3] T. Pape, W. Wintermeyer, and M. V. Rodnina, "Complete kinetic mechanism of elongation factor Tu-dependent binding of aminoacyl-tRNA to the A site of the E. coli ribosome," *The EMBO journal*, vol. 17, no. 24, pp. 7490–7497, 1998.

[4] M. V. Rodnina and W. Wintermeyer, "GTP consumption of elongation factor Tu during translation of heteropolymeric mRNAs," *Proceedings of the National Academy of Sciences*, vol. 92, no. 6, pp. 1945–1949, 1995.

[5] M. V. Rodnina, R. Fricke, and W. Wintermeyer, "Transient conformational states of aminoacyl-tRNA during ribosome binding catalyzed by elongation factor Tu," *Biochemistry*, vol. 33, no. 40, pp. 12267–12275, 1994.

[6] B. Wilden, A. Savelsbergh, M. V. Rodnina, and W. Wintermeyer, "Role and timing of GTP binding and hydrolysis during EF-G-dependent tRNA translocation on the ribosome," *Proceedings of the National Academy of Sciences*, vol. 103, no. 37, pp. 13670–13675, 2006.

[7] W. WINTERMEYER and H. G. ZACHAU, "Fluorescent derivatives of yeast tRNAPhe," *European journal of biochemistry*, vol. 98, no. 2, pp. 465–475, 1979.

[8] K. B. Gromadski and M. V. Rodnina, "Kinetic determinants of high-fidelity tRNA discrimination on the ribosome," *Molecular cell*, vol. 13, no. 2, pp. 191–200, 2004.

5.2.4 Methylated guanosine and uridine modifications in S. cerevisiae mRNAs modulate translation elongation

Over 15 different types of mRNA modifications have been identified by sequencing and liquid chromatography coupled to tandem mass spectrometry (LC-MS/MS) technologies. In this work we are able to quantify 50 different mRNA specific modifications in *S. cerevisiae* at a time, by improving mRNA purity and the LC-MS/MS pipeline. Using this method, we were able to detect and quantify 13 different known modifications, as well as detect four new low level modifications e.g. 1-methyguanosine, N2-methylguanosine, N2, N2-dimethylguanosine, and 5-methyluridine. Furthermore, we were able to identify the enzymes responsible for incorporating these modifications into mRNA, Trm10, Trm11, Trm1, and Trm2. Using an in vitro reconstituted system we discovered that 1-methyguanosine, N2-methylguanosine and 5-methyluridine impede amino acid addition in a position dependent manner on a mRNA codon.

5.2.5 Modulation of tRNA modification landscape alters the efficacy of Hygromycin B translation inhibition

Chemical modifications of RNAs have long been recognized as key modulators of tRNA structure and function in cells. 5-methyluridine (m^5U) is among the most common modifications included in tRNAs. The conserved enzyme, Trm2, is responsible for incorporating m^5U into the T-loop of tRNAs as well as into some eukaryotic mRNA sequences. Here, we investigate the contributions of m^5U to translation. In line with previous studies, we find that yeast cells lacking Trm2 (*trm2Δ*) do not exhibit a growth defect. However, in the presence of translational inhibitors *trm2Δ* cell growth is modulated. Relative to wild-type, *trm2Δ* cells are more sensitive cycloheximide, while they were less sensitive to hygromycin B and paromomycin. Consistent with this, expression of luciferase reporter proteins is significantly increased in *trm2Δ* cells after hygromycin B treatment compared to wild-type cells. To establish the reason for the loss of hygromycin sensitivity we observe, we assessed the consequences of m^5U in tRNA and mRNA

on translation using a fully reconstituted E. coli translation system. We find that the inclusion of m^5U into an mRNA UUU/UUC phenylalanine codons can modestly impact the rate constants for amino acid addition by cognate and near-cognate tRNAs. Additionally, translation reactions performed with $tRNA^{Phe}$ purified from wild-type and *trm2Δ E. coli* cells, demonstrate that m^5U does not alter $tRNA^{Phe}$ aminoacylation or change the rate constants for phenylalanine addition by the ribosome. However, when we conducted our assays in the presence of the hygromycin, we find that the loss of m^5U in $tRNA^{Phe}$ reduces the sensitivity of the translation system to hygromycin, enabling the ribosome to translocate after phenylalanine addition. This work reveals how a single modification can impact translation when incorporated into different RNA species in the translational machinery.

5.2.6 How do Uridine Modifications impact cellular stress response?

The role of Ψ in mRNA in the cellular context is still unknown, but speculation suggests it may be important during the cellular stress response. One reason in general is that it has been shown that pseudouridine levels in mRNA fluctuate in response to cellular stress[1], [2]. Furthermore, in my in-vitro work we see that incorporation of pseudouridine in a codon decrease amino acid addition, increases miscoding errors and decreases GTP/Activation hydrolysis(Chapter 2). Coupled together, and with the knowledge that we know during stress that there are increase in miscoded protein products that have been found to be beneficial for the cell during stress, it seems very likely that the role of pseudouridine in mRNA is to produce miscoded proteins during times of stress. This idea is not too far-fetched either, seeing that our latest work investigating the role of m^5U in RNA(Chapter 4). Here we show that when you change the tRNA modification landscape that cells react to hygromycin B stress differently, and

in fact grow better. In this work, I propose we use human cells to explore the role of pseudouridine, and other uridine modifications, in the cellular stress response.

The cell line used in the experiments would be HEK 293 cells. Moreover, transfecting mRNA into HEK 293 is a well-established technique used by our by our collaborators at NEB, Dr. B Bijoyita Roy[3], [4]. This technique utilizes a luciferase reporter with both HA and flag tags at the ends of the reporter (used to facilitate the purification of protein products). During the transcription process the mRNA is either synthesized fully modified, meaning that every spot a uridine would be there is a modification such as pseudouridine, or they are fully unmodified. These mRNAs are 3' polyadenylated as well as capped at the 5' end. After the product is complete it would be transfected into cells using a lipofectamine reagent. The part the gets complicated is inducing stress conditions. It would be optimal to have a wide variety of stress conditions, thermal stress, oxygen deprivation, and starvation. Heath shock is more obvious, we would increase the temperature of the cells from 37C to 42C. For oxygen deprivation we could just add H_2O_2 also known as Hydrogen Peroxide. One could starve the cells by giving it custom made media that does not include amino acids. Lastly, we could put the cells under translational stress like Hygromycin B, cycloheximide, or even paramomycin. We would grow cells in these different conditions, and compare those lacking modifications to those that contain modifications. This experiment could be done with pseudouridine first, but could be easily adapted to include other modifications like m^5U or $m^1\Psi$.

After cells are lysed and protein is extracted, these protein products are isolated for liquid chromatography/tandem MS is then used to look for the miscoded products. Furthermore, we could look at the protein products and see if there is a change in the amount of full-length product left. Also, it would be interested to see if any change in expression is observed. Lastly,

we can also perform qRT-PCR on the samples by extracting the mRNA from them. This would give us an idea if half-life of mRNA increases in this time of stress. Overall, these experiments are not complicated to set up and would give the field a plethora of data to work with. Additionally, this data would help give us so much needed insight in the role pseudouridine plays in stress response.

References

[1] T. M. Carlile, M. F. Rojas-Duran, B. Zinshteyn, H. Shin, K. M. Bartoli, and W. V. Gilbert, "Pseudouridine profiling reveals regulated mRNA pseudouridylation in yeast and human cells," *Nature*, vol. 515, no. 7525, pp. 143–146, Nov. 2014, doi: 10.1038/nature13802.

[2] A. F. Lovejoy, D. P. Riordan, and P. O. Brown, "Transcriptome-wide mapping of pseudouridines: pseudouridine synthases modify specific mRNAs in S. cerevisiae," *PLoS One*, vol. 9, no. 10, p. e110799, 2014, doi: 10.1371/journal.pone.0110799.

[3] D. E. Eyler *et al.*, "Pseudouridinylation of mRNA coding sequences alters translation," *Proc Natl Acad Sci U S A*, vol. 116, no. 46, pp. 23068–23074, Nov. 2019, doi: 10.1073/pnas.1821754116.

[4] B. Roy, J. D. Leszyk, D. A. Mangus, and A. Jacobson, "Nonsense suppression by near-cognate tRNAs employs alternative base pairing at codon positions 1 and 3," *Proceedings of the National Academy of Sciences*, vol. 112, no. 10, pp. 3038–3043, 2015.

5.2.7 How do tRNA modifications impact translation?

It is well known that non-coding RNA is modified, and this has implications on both structure and function. However, the cooperativity of these modifications both intramolecularly in the tRNA or intermolecular with the surrounding rRNA and mRNA is not well studied. This is to do the fact that knocking out some of these modifying enzyme would cause cells die, therefore studying the effects are impossible. Our lab has a way to mitigate that. Since the Koutmou lab has the means to grow and harvest their own tRNA, they could create knockout cells lines with non-essential modifying enzymes to create tRNA with modulated tRNA landscapes. They can then use the tRNA coupled with their in-vitro system to study how the modification landscape affects tRNA translation. They could use all the experiments I have performed in my thesis work

and more! This would give us crucial insight into an aspect of modifications that we still have yet to be able to comprehend.

Appendix A: Chapter 2 Supplemental

This appendix contains all supplemental discussion, and data/supporting figures that were published in the paper titled “Pseudouridinylation of mRNA coding sequences alters translation." through the Proceedings of the National Academy of Sciences.

SUPPLEMENTAL DISCUSSION

Effects of modified bases on peptide release at stop codons

We investigated how Ψ impacts translation of nonsense codons. Ψ in stop-codons has been shown to promote translational read-through of stop-codons in both bacteria (18) and eukaryotes (19) and alter the conformation of the critical ribosomal RNA bases A1492 and A1493 in ribosomes crystallized with A site mismatches (18). Theoretical studies predicted that Ψ might perturb peptide release due to a difference in dipole moment, where pseudouridinylated stop codons have a ~30% smaller angular difference, leading to weaker helical interactions and weaker interactions with RF1 (20). However, the only *in vitro* study to date with ribosomes terminating on Ψ containing stop-codons found no difference between RF1-catalyzed release on modified and un-modified codons (21). We performed a similar set of studies under different buffer conditions and find that the action of RF1, but not RF2, is impacted by the presence of Ψ (Figure 4). Our RF2 results are not comparable to the previous study since the previous study used the A246T variant of RF2 with decreased activity (4, 22). Although the discrepancy between our RF1 result and the published report (21) is puzzling, we are encouraged by the structural, theoretical, and cell-based data that all support altered termination by RF1 on ΨAA and ΨAG codons, as well as by the fact that the rate constants ($k_{obs,release}$) we measure on the UAA stop codon are consistent with those

previously measured (6, 23-27). We find that ΨAA both modestly decreases the $k_{max,release}$ of RF1 and promotes miscoding, which could account for the nonsense suppression observed at ΨAA codons in yeast and at the RF1-specific stop codon ΨAG bacterial cells. More detailed structural and mechanistic investigation of tRNA selection and RF1-mediated peptide release on Ψ-containing codons will therefore be rewarding.

Our data suggest that the affinity of RF2 for UAm^{6}A codons may be reduced. An earlier study demonstrated that RF2, but not RF1, inefficiently terminates translation on a full-length ErmCL reporter when an O6 carbonyl group is substituted for an N6 amino group in an adenosine present at the third position of a stop-codon (28). While m^{6}A does not have an O6 group, the additional methyl group similarly removes the ability of the adenosine to form hydrogen-bonds at N6, and also increases the steric bulk nucleobase. Our findings support the idea that the presence of an N6 amino group at A3 is important for RF2 catalyzed peptide release on stop codons (28).

Important considerations in mass spectrometry analysis of peptides with alternative decoding

The detection of amino acid-substituted peptides by mass spectrometry is difficult due to the low frequency of the initial event and the fact that the signal is distributed amongst the several different possible substitutions. Careful design of the assay system was therefore required to permit detection of amino acid substituted peptides. For these studies, luciferase mRNA was transcribed *in vitro* with either uridine or Ψ and transfected into 293H cells and their expression was comparable (Fig. S4). We performed tandem purification of the luciferase protein with N-terminal HA and C-terminal FLAG tags to eliminate analyses of premature translation truncation products. Equal amounts of luciferase protein expressed from uridine- and Ψ-containing mRNAs were

subjected to mass spectrometric analyses (Fig. S5). To ensure detection of low frequency events the codons were first analyzed on a specific luciferase peptide (^{41}KGPAPFYPLEDGTAGEQLHK^{60}) that is highly represented in the spectra (16, 17). An error-tolerant search allowing for identification of any of the 20 possible amino acids substituted at a specific position in the peptide was performed. To analyze if Ψ promoted amino acid substitution in cells, we assessed if substitution events took place at several U-containing codons (Fig. 4C, Table S4). For the peptide of interest, no amino acid substitutions were detected on the samples generated from uridine-containing mRNAs, while the peptide generated from Ψ-containing mRNAs contained several low-frequency amino acid substitutions (totaling ~1%) (Fig. S6, Table S5). We also extended our analyses to the entire luciferase dataset. Luciferase protein translated from Ψ-containing mRNAs possessed a significantly higher rate of amino acid substitution (totaling ~1.5%, integrated over all U-containing codons) relative to protein synthesized from uridine-containing mRNAs (substitutions only on two < 0.05% Val codons were observed) (Table S6).

SUPPLEMENTARY TABLES

Supplemental Table A.1 ***Single turnover rate constants for amino acid addition and GTP hydrolysis.*** *This table reflects the values plotted in Figure 1C for the ribosome catalyzing the addition of a single phenylalanine on unmodified and modified codons, and the values shown in Figure 2B for GTP hydrolysis by the EF-Tu●phe-tRNA$_{phe}$●[^{32}P]-GTP ternary complex. The reported k_{obs} and standard error values are from the fit of a single curve to all replicate time courses. N.D., not determined.*

Codon	k_{obs} (s^{-1}) ± SE	Maximum % ^{f}Met in MF (endpoint)	k_{GTP} (s^{-1}) ± SE
UUU	5.1 ± 0.4	71 ± 6	78.5 ± 9.5
ΨUU	2.1 ± 0.3	68.7 ± 3.8	42.2 ± 6.1
UΨU	2.9 ± 0.2	63.5 ± 1	N.D.
UUΨ	2.3 ± 0.2	72 ± 3	N.D.

Supplemental Table A.2: ***X-ray data collection and refinement statistics.***

Crystals	**70S complex with ΨUU-mRNA and A-, P- and E-tRNAs**
Diffraction data	
Space Group	$P2_12_12_1$
Unit Cell Dimensions, Å (a x b x c)	208.73 x 445.1 x 613.63
Wavelength, Å	0.9795
Resolution range (outer shell), Å	360-2.95 (3.03-2.95)
I/σI (outer shell with I/σI=1)	4.95 (0.89)
Resolution at which I/σI=1, Å	2.95
Resolution at which I/σI=2, Å	3.20
CC(1/2) at which I/σI=1, %	17.2
CC(1/2) at which I/σI=2, %	44.1
Completeness (outer shell), %	99.7 (99.6)
R_{merge} (outer shell)%	20.6 (179.8)
No. of crystals used	1
No. of Reflections Used: Observed	5,954,867
No. of Reflections Used: Unique	1,181,400
Redundancy (outer shell)	5.04 (4.76)
Wilson B-factor, $Å^2$	104.3
Refinement	
R_{work}/R_{free}, %	23.5/29.7
No. of Non-Hydrogen Atoms	
RNA	200,225
Protein	90,976
Ions (Mg, K, Zn, Fe)	2,867
Waters	5,058
Ramachandran Plot	
Favored regions, %	88.45
Allowed regions, %	9.61
Outliers, %	1.93
Deviations from ideal values (RMSD)	
Bond, Å	0.010
Angle, degrees	1.426
Chirality	0.061
Planarity	0.008
Dihedral, degrees	16.059

Average B-factor (overall), Å^2	96.8

R_{merge} = Σ |I – <I>| / Σ I, where I is the observed intensity and <I> is the average intensity from multiple measurements.
R_{work} = Σ|F_{obs} – F_{calc}| / Σ F_{obs}. For calculation of R_{free}, 5% of the truncated dataset was excluded from the refinement.

Supplemental Table A.3: ***Summary of possible base pairing interactions of pseudouridine in decoding****. This table summarizes the possible base-pairing interactions between mRNAs and tRNAs that we observe in our reconstituted translation system. In E. coli, the tRNA^{Val} anticodons are 5'-GAC and 5'-cmo^{5}UAC (29), which require the formation of a Ψ:C basepair during decoding of the ΨUU codon, as well as either a Ψ:G or Ψ:cmo^{5}U depending on which tRNA^{Val} isoacceptor decodes the modified codon. The tRNA^{Leu} anticodon sequences are 5'-CAG, 5'-GAG, 5'-cmnm^{5}U$_m$AA, 5'-C$_m$AA, and 5'-cmo^{5}UAA. These anticodons require Ψ to base pair with G or A to decode the ΨUU codon, and pairing with C, G, cmnm^{5}U$_m$, C$_m$, or cmo^{5}U when Ψ is in the third position. Anticodons tRNA^{Ile} are 5'-GAU and 5'-k^{2}CAU, which both require a Ψ:U base pair in the first position. When present in tRNA anticodons, Ψ is known to base pair with A and G, and more broadly with A, G, and (in 16S rRNA).*

Codon	Observed aa	Possible anticodons	Ψ base pair	Mismatch at other position
5'-ΨUU (1st pos)	valine	5'-GAC 5'-cmo^{5}UAC	Ψ:C	U:G (3rd pos) –
	leucine	5'-CAG 5'-GAG	Ψ:G	U:C (3rd pos) U:G (3rd pos)
		5'-cmnm^{5}U$_m$AA 5'-C$_m$AA 5'-cmo^{5}UAA	Ψ:A	– – –
	isoleucine	5'-GAU 5'-k^{2}CAU	Ψ:U	U:G (3rd pos) U:k^{2}C (3rd pos)
5'-UUΨ (3rd pos)	valine	5'-GAC 5'-cmo^{5}UAC	Ψ:G Ψ:cmo^{5}U	C:U (1st pos) C:U (1st pos)
	leucine	5'-CAG 5'-GAG 5'-cmnm^{5}U$_m$AA 5'-C$_m$AA 5'-cmo^{5}UAA	Ψ:C Ψ:G Ψ: cmnm^{5}U$_m$ Ψ:C$_m$ Ψ:cmo^{5}U	G:U (1st pos) G:U (1st pos) – – –

Supplemental Table A.4: ***Uridine-containing codons analyzed for elongation miscoding***

Amino acids evaluated for miscoding in 293H cells	**Codons evaluated for miscoding in 293H cells**
Phe	UUU, UUC
Leu	UUA, UUG, CUU, CUC, CUA, CUG
Ile	AUU, AUC, AUA
Val	GUU, GUC, GUA, GUG
Trp	UGG
Tyr	UAU, UAC

Supplemental Table A.5: This table summarizes the amino acid substitutions detected from U-containing Phe, Tyr, Leu codons in the KGPAPFYPLEDGTAGEQLHK peptide when mRNAs were synthesized with Ψ. The frequencies of the substitutions are also denoted. For calculating the frequencies, an extracted ion chromatogram was generated at <5ppm for each of the peptides of interest from the total ion current, and the area under the curve for each EIC was

calculated. This was then used to calculate the percentage of substitution (area under the curve for peptides with a specific substitution/[area under the curve for all wild-type peptides with no substitution + area under the curve for all peptides with substitutions]).

	Substitutions observed	**Frequency of substitution (%)**
Phe	Ser, Ile/Leu	0.42
Tyr	Cys, His	0.19
Leu	Pro, Gln	0.52

Supplemental Table A.6: This table summarizes the amino acid substitutions detected in the U-containing codons in the entire luciferase dataset for multiple peptides when mRNAs were synthesized with Ψ. For calculating the frequencies, an extracted ion chromatogram was generated at <5ppm for each of the peptides of interest from the total ion current, and the area under the curve for each EIC was calculated. This was then used to calculate the percentage of substitution (area under the curve for peptides with a specific substitution/[area under the curve for all wild-type peptides with no substitution + area under the curve for all peptides with substitutions]).

	Substitutions observed	**Frequency of substitution (%)**
Phe	Ser, Ile, Glu	0.38
Tyr	His, Cys, Asp	0.11
Leu	Pro, Ser, Gln	0.47
Ile	Thr, Phe, Trp, Cys, Val	0.19
Val	Glu, Ala, Arg, Phe	0.2
Trp	Asp	0.142

Supplemental Table A.7: ***Observed rate constants for peptide release****. †Reported k_{max} values are the fitted maximum observed rate constants from the fits in Figure S3, along with the 95% confidence interval in the fitted value of k_{max}. *Reported k_{max} values are the observed rate constants for reactions with 10 μM release factor. Error values are the standard error.*

RF	codon	k_{max} (s^{-1})	95% CI
RF1	UAA	0.24†	(0.15 – 0.34)
	ΨAA	0.085†	(0.044 – 0.14)
	Um^6AA	0.23 ± 0.02*	–
	UAm^6A	0.19 ± 0.01*	–
RF2	UAA	0.061†	(0.029 – 0.11)
	ΨAA	0.077†	(0.050 – 0.11)
	Um^6AA	0.13 ± 0.02*	–
	UAm^6A	0.068 ± 0.003*	–

SUPPLEMENTARY FIGURES

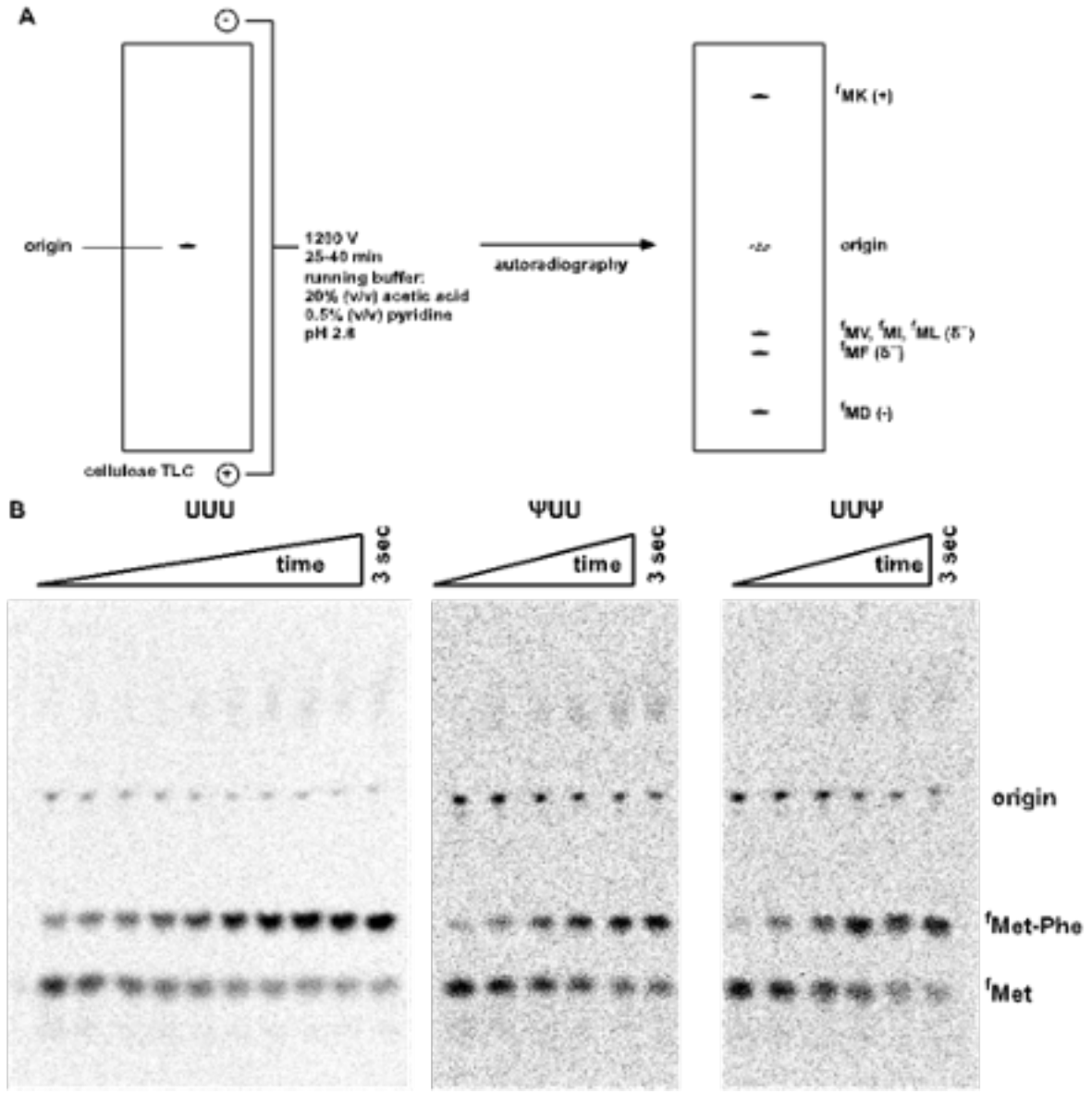

Supplemental Figure A.1: ***Electrophoretic TLC system used for separation and detection of peptide products.(A)****Scheme showing how short, N-formyl-[^{35}S]- methionine-labeled peptides are separated by electrophoresis on a cellulose TLC in a volatile, acidic buffer, and detected by phosphorimaging. Peptide migration is determined primarily by the net charge and secondarily by the identity of the amino acid R groups.* ***(B)*** *Representative images of time courses for the data in Figure 2 are shown. The brightness and contrast of these images have been adjusted to clearly show all bands and the background, and as a consequence pixel intensity is no longer linear with signal.*

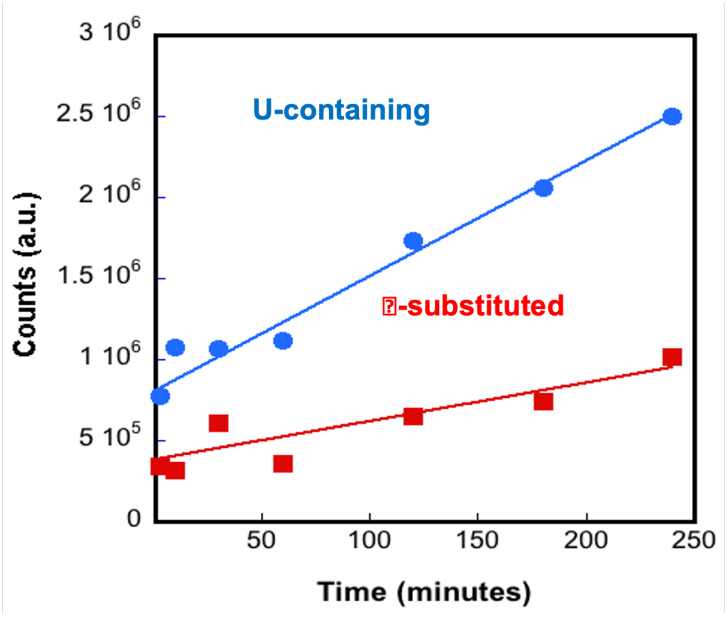

Supplemental Figure A.2: ***Constitutively pseudouridinylated mRNA produces less full-length protein in a bacterial in vitro translation system.*** *Luciferase mRNA was in vitro transcribed in the presence of either uridine triphosphate or pseudouridine triphosphate, and in vitro translated using the NEB PURExpress® system in the presence of L-[^{35}S]-methionine. Protein products were separated by SDS-PAGE and the full-length luciferase protein was quantified by phosphorimaging. The y-axis is the integrated photostimulated luminescence units in the full-length luciferase band and the x-axis is the reaction time. The experiment was performed twice; a representative plot is shown.*

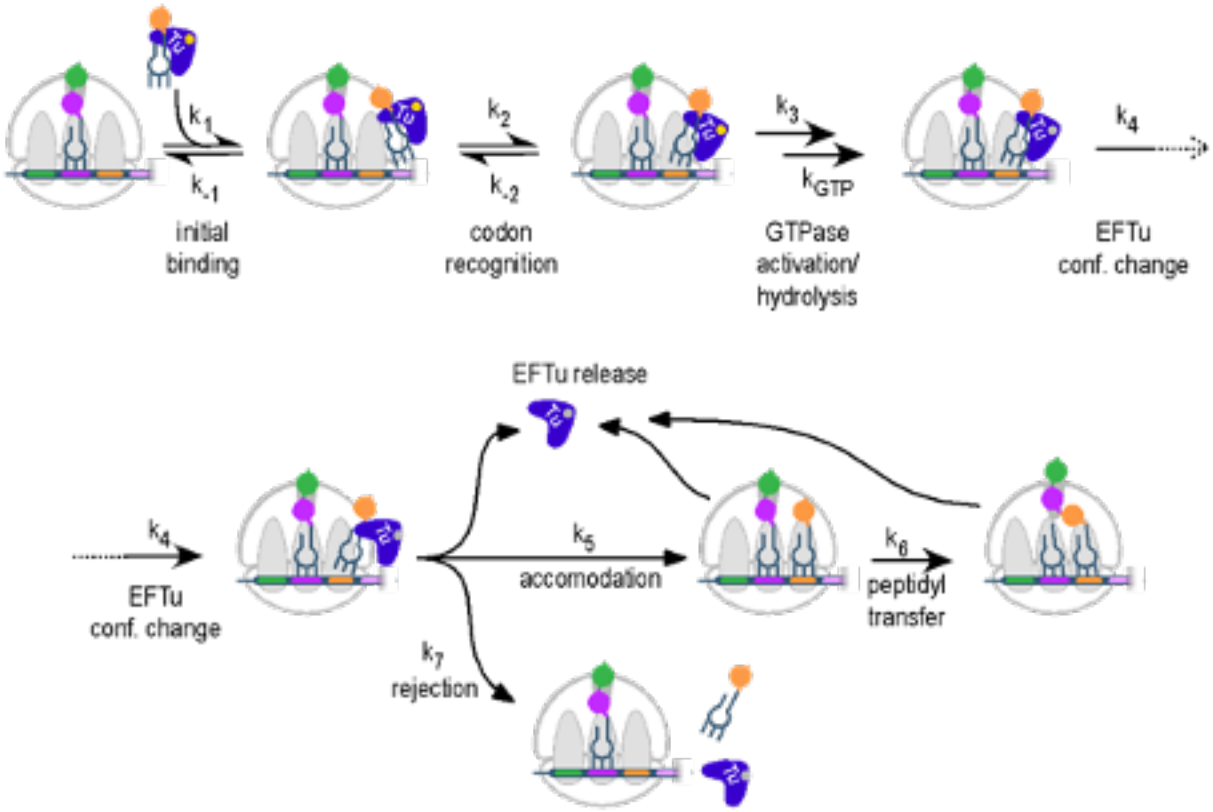

Supplemental Figure A.3: ***Mechanistic model for tRNA selection and amino acid addition****. The observed rate constants from experiments in Figure 1 are a function of all shown rate constants. The observed rate constants for GTP hydrolysis in Figure 2 reflect the rate constants for initial binding through GTPase activation and hydrolysis. The model shown is based on published models from Rodnina and coworkers (30, 31).*

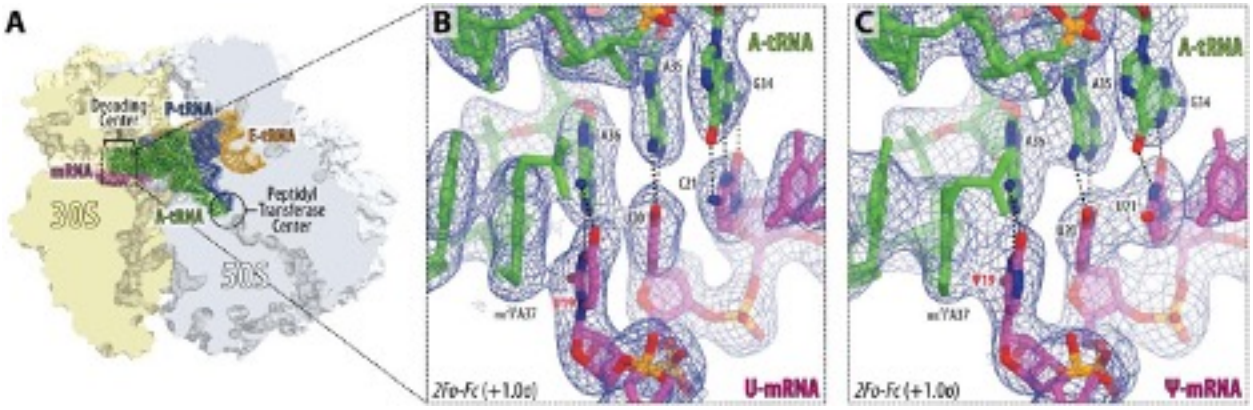

Supplemental Figure A.4: ***The electron density maps showing codon-anticodon interactions of tRNAPhe with regular vs. Ψ-containing mRNA. (A)*** *Overview of the 70S ribosome from T. thermophilus showing locations of main ribosomal functional centers: the decoding center and the peptidyl transferase center. The view is from the cytoplasm onto the A site. 30S subunit is shown in light yellow, 50S subunit is in light blue. mRNA is shown in magenta and tRNAs are displayed in green for the A site, in dark blue for the P site, and in orange for the E site.* ***(B, C)*** *Close-up views of the 2Fo-Fc electron difference Fourier maps (blue mesh) around the decoding center showing codon-anticodon interactions of tRNA^{Phe} with either unmodified mRNA* ***(C)*** *or Ψ-containing mRNA* ***(D)****. In* ***(C)****, both the map and the model are from PDB entry 4Y4P (8). H-bond interactions of the mRNA codon (nucleotides 19-21) with the tRNA anticodon (nucleotides 34-35) are indicated with the dashed black lines. The refined models of mRNA (magenta) and tRNA (green) are displayed in their respective electron densities contoured at 1.0σ. Nitrogen atoms*

of codon and anticodon nucleotides are colored blue; oxygens are red. Note that no major differences could be observed between the 70S complexes bound to regular mRNA vs. Ψ-containing mRNA.

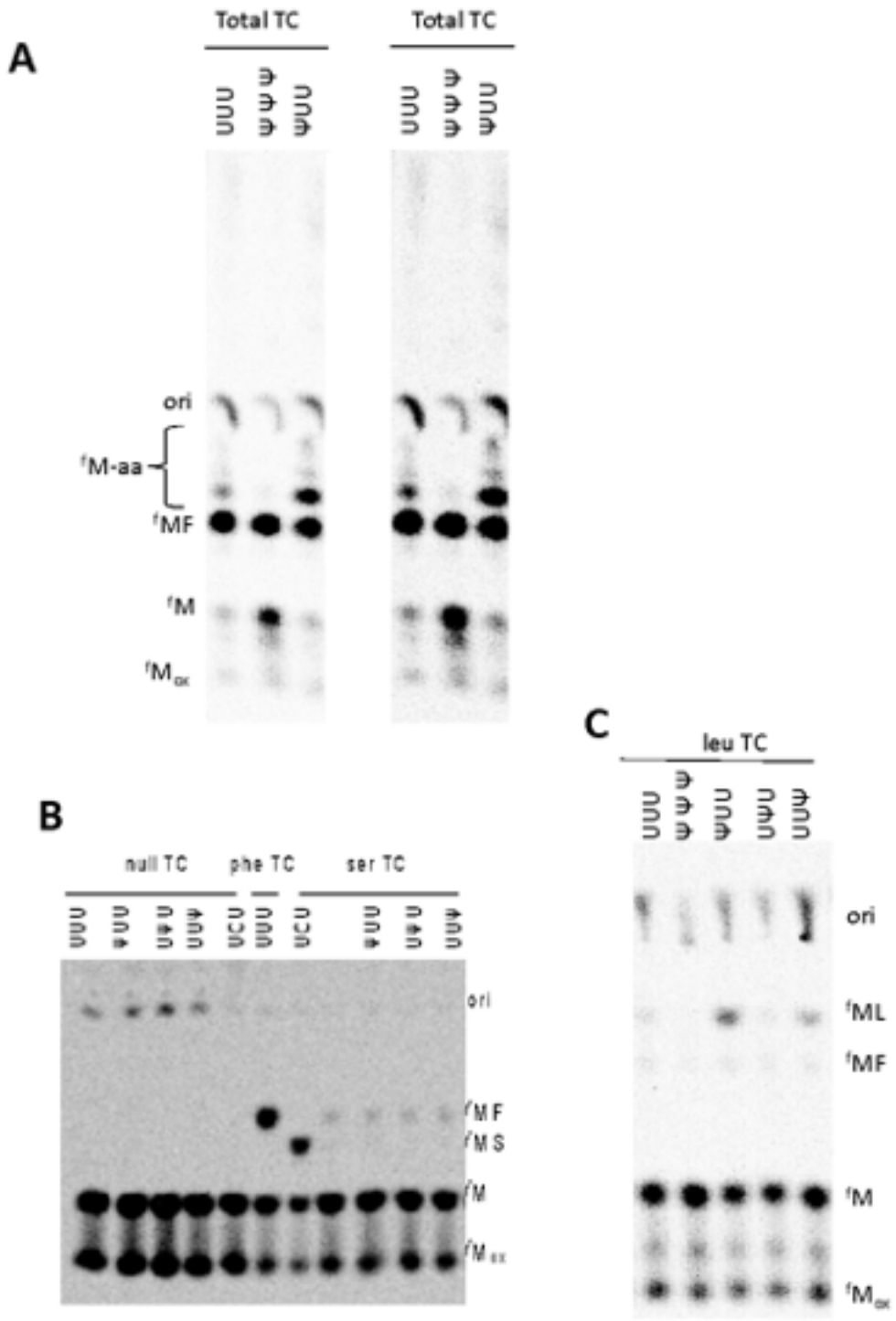

Supplemental Figure A.5: ***Increased amino acid substitution on Ψ-containing UUU codons, relative to un-modified UUU codons in vitro. (A)*** *Electrophoretic TLC displayed at low (left) and high (right) contrast showing the translation products of UUU, ΨΨΨ, and ΨUU-containing messages in the reacted with the same TC containing*

total aa-tRNA. Total tRNA was aminoacylated with a mixture of all possible 20 amino acids using S100 extract, as described in our methods. A higher level of amino acid substitution is observed on the modified ΨUU codon relative to the UUU codon. ***(B)*** *Serine does not incorporate on Ψ-containing phenylalaine codons in vitro. Electrophoretic TLC displaying the translation products of UCU (serine codon), unmodified and Ψ-containing messages in the presence of no tRNA (null), Phe-tRNA^{Phe} tRNA (phe TC), total tRNA aminoacylated with serine (ser TC).* ***(C)*** *Leucine substitution of enhanced on Ψ-containing phenylalaine codons in vitro. Electrophoretic TLC displaying the translation products of UUU and Ψ-substituted codons (ΨΨΨ, ΨUU, UΨU, UUΨ) the presence of TCs formed with total tRNA aminoacylated with leucine (leu TC). More leucine is incorporated on ΨUU and UUΨ codons relative to UUU.*

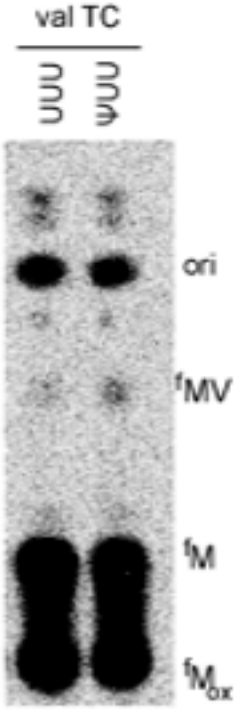

Supplemental Figure A.6: ***Alternative decoding by pseudouridine-containing codons depends on the sequence context of the modified codon.*** *Initiation complexes were formed on mRNAs containing a UUU or ΨUU codon as the second codon in an mRNA coding for MFKKX and reacted with Val-tRNAVal ternary complex. Electrophoretic TLC displaying the translation products of unmodified and 1st position Ψ-containing messages in the presence of total tRNA aminoacylated with valine (val TC).*

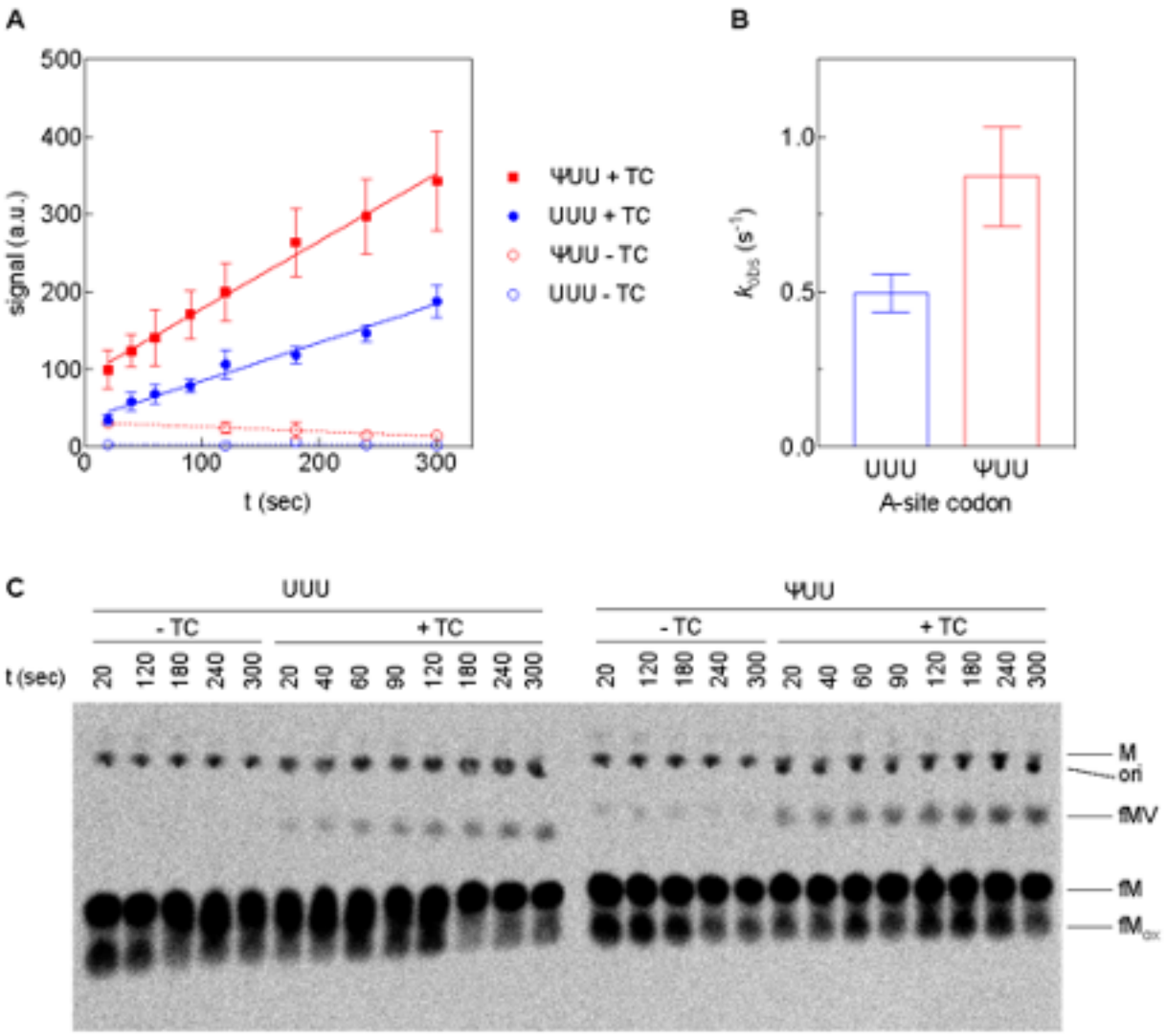

Supplemental Figure A.7: ***Valine is incorporated more rapidly on a ΨUU codon than on a UUU codon.*** *Excess Val-tRNA^{Val} (10 μM) was reacted with 100 nM initiation complexes in the presence of 40 μM EFTu, 10 mM free Mg^{2+}, GTP, and an energy regeneration system.* ***(A)*** *Signal (integrated photostimulated luminescence units) in the ^{f}Met-Valine band is plotted as a function of time for initiation complexes reacted with the ternary complex (+), or buffer only (-). Each point is the mean from three independent experiments and the error bars are the standard error of the mean.* ***(B)*** *Observed rate constants for the linear fits of + ternary complex reactions in A. Error bars are the 95% confidence intervals on the fitted value of k_{obs}.* ***(C)*** *One of the three electrophoretic TLCs used to generate the data in* ***(A)*** *and* ***(B).***

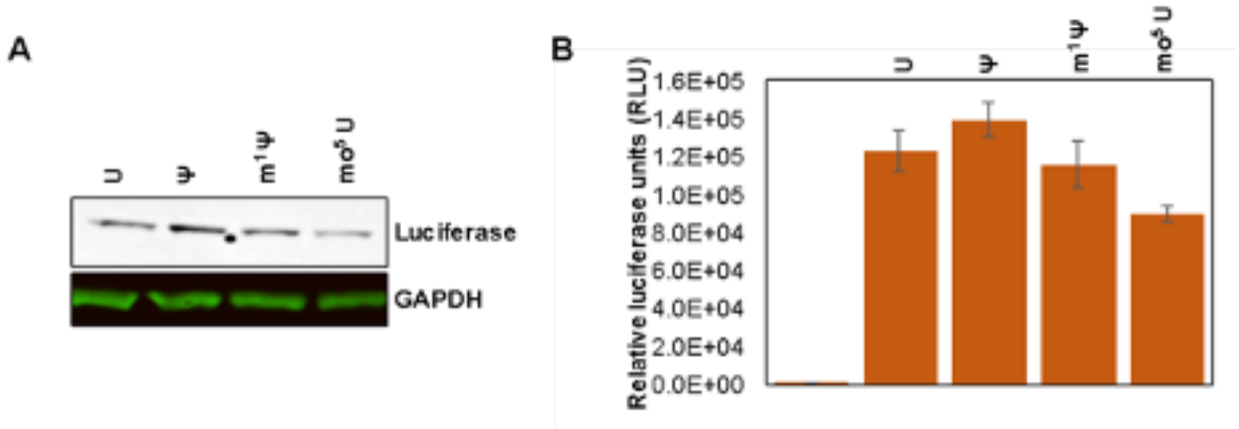

Supplemental Figure A.8: ***Expression of luciferase mRNA in vivo. (A)*** *Western blot analysis of the full-length luciferase products purified from 293H cells after expression of luciferase mRNA synthesized with either standard (U) or modified (Ψ, $m^1Ψ$, mo^5U) nucleotides. $m^1Ψ$ and mo^5U were used as a control to check the effect of other uridine analogs on the expression of the luciferase mRNA.* ***(B)*** *Luciferase activity assay demonstrating functionality of unmodified and modified luciferase mRNAs.*

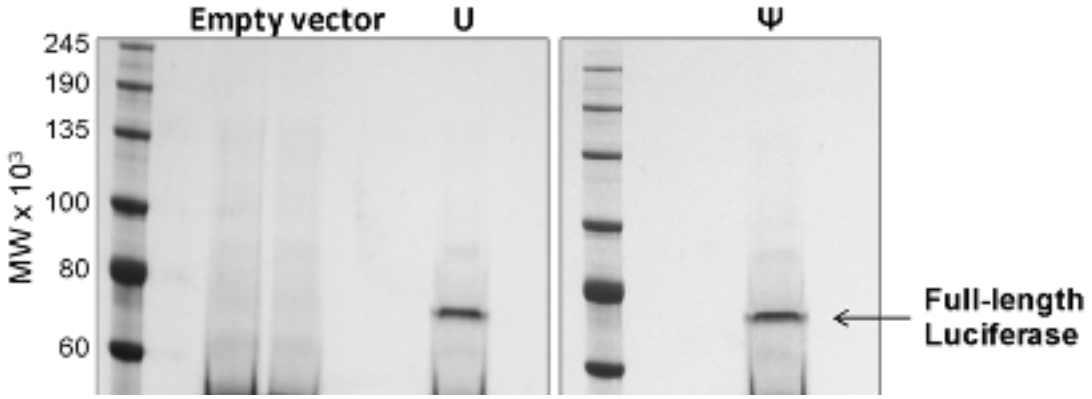

Supplemental Figure A.9: Silver-stained SDS/PAGE gel showing the purification of luciferase protein from 293H cells when transfected with either U-containing or Ψ-containing luciferase mRNAs.

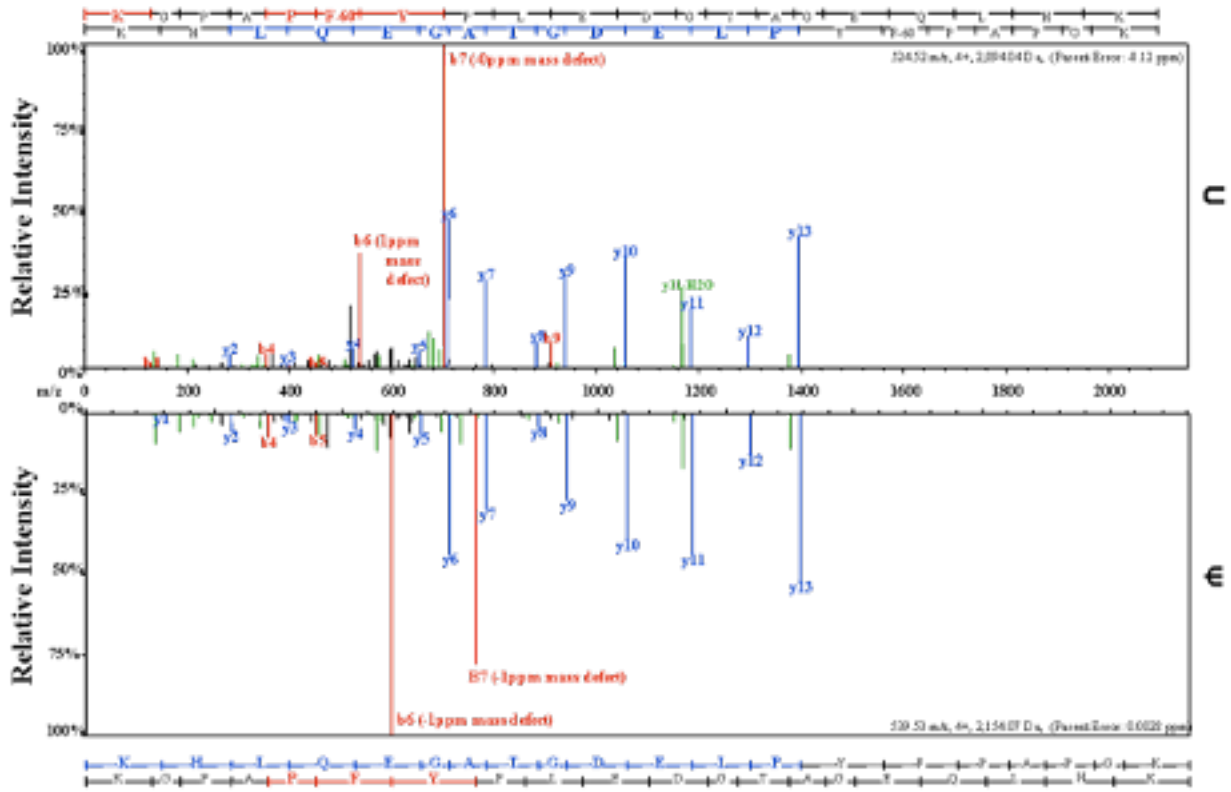

Supplemental Figure A.10: ***Fragmentation spectra showing Phe to Ser substitution in peptides from Ψ-containing mRNA.*** *Results from the error-tolerant search were loaded onto Scaffold (Proteome Software, version 4.8.7) and DDA fragmentation spectra from a proteotypic peptide were compared. The site of modification (Phe46) was covered by two adjacent fragment ions in both peptides, b6 and b7, with all relevant precursor and fragment ions identified with < 2ppm mass accuracy. The peptide generated from the unmodified U-containing mRNA has an m/z for phenylalanine at position 46 (bottom panel). In contrast, the peptide generated from Ψ-containing mRNA demonstrates an m/z for serine, not phenylalanine at position 46 (top panel). The nominal mass difference between serine and phenylalanine is 60 Da, and the serine is denoted as F-60 in the top panel.*

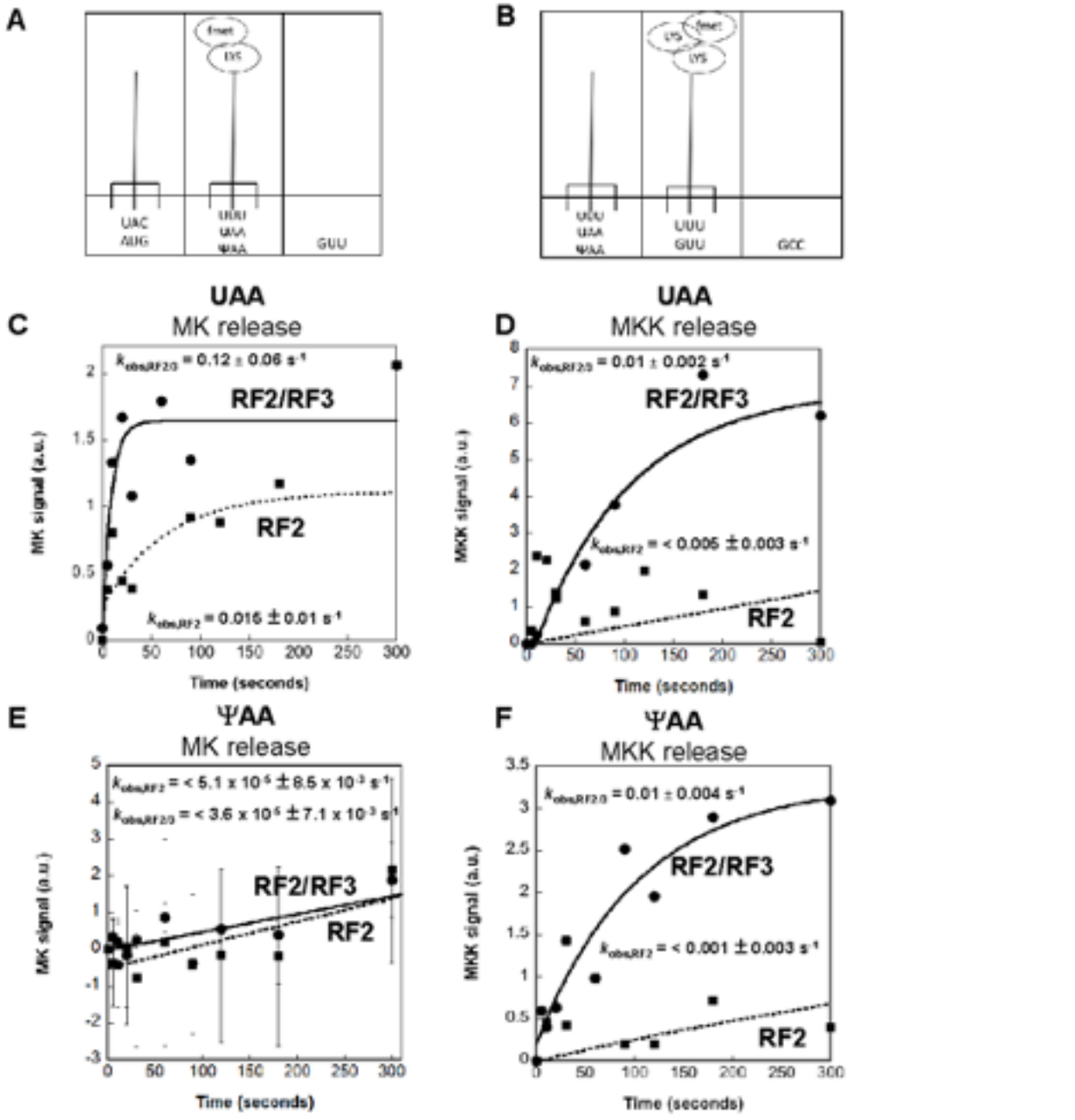

Supplemental Figure A.11: ***P site mismatch surveillance mechanism is not triggered by amino acid substitution on Ψ-containing codon.*** *Panels A and B summarize the position of the codons and peptidyl-tRNA and codons in the purified ribosome elongation complexes prior to addition of RF2 and RF2/RF3.* ***(A)*** *Codons in the E-, P- and A site (left to right) when the MK peptide is attached to the mismatched tRNA in the P site.* ***(B)*** *Codons in the E-, P- and A site (left to right) when the MKK peptide is attached to the mismatched tRNA in the P site. While a de-acylated tRNA is displayed for clarity in the E site of A and B, in all likelihood, has dissociated from the ribosome in our complexes. Panels C and D are example experiments in which MK* ***(C)*** *and MKK* ***(D)*** *peptide release is catalyzed by RF2 and RF2/RF3 from an unmodified mRNA. As expected, because there is a mismatch between the tRNA anticodon and mRNA codon in the P site, MK and MKK are released in an RF2-dependent manner from the ribosome. In both cases, the rate constant for peptide release is enhanced by at least 10-fold when RF3 is present. Panels C and D are example experiments on a Ψ-modified mRNA. In these assays, RF2 or RF2/RF3 are added to complexes with either MK-tRNA^{Lys}* ***(C)*** *or MKK-tRNA^{Lys}* ***(D)*** *bound to a mis-matched codon in the P site (as shown in panels A and B). Notably, MK release was not catalyzed in five separate experiments when ΨAA is in the P site;*

*each of the time courses we collected generated scatter plots. The points displayed on the plot in panel E are the average of points from three identical time-courses, and the error bars reflect the range in values measured. In contrast to MK release on the UAA message, these plots could not be meaningfully fit (see errors on fits) and RF3 did not enhance the rate constant for MK release, as happens when the P site surveillance mechanism is triggered. This suggests that the ribosome does not read the $tRNA^{Lys}$:mRNA pairing as a mismatch on the ΨAA codon in the P site. However, as shown in panel **F**, when a mismatch occurs on the same message between $tRNA^{Lys}$ and a GUU codon (see Fig. S11B), the P site surveillance mechanism is activated and MKK is released in an RF2/RF3 dependent manner. As on the unmodified message, the rate constant for MKK release is significantly enhanced by the presence of RF3. These experiments were repeated on at least 4 different days, and all experimental repeats consistently demonstrated the RF2/RF3 dependent release of both MK and MKK from the unmodified message, and only MKK from the modified message.*

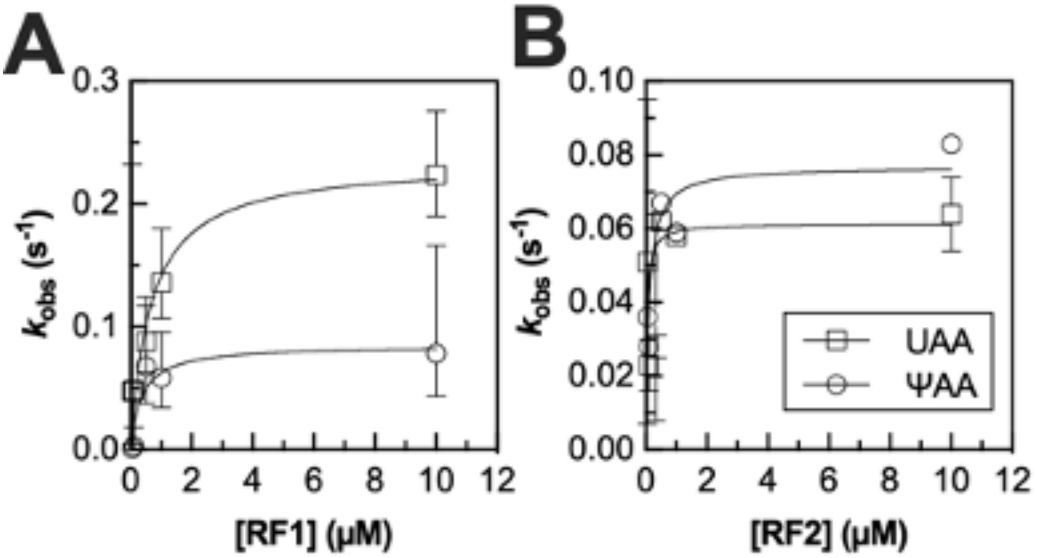

Supplemental Figure A.12: ***Peptide release on the ΨAA codon is slightly perturbed****. kobs values were measured at range of RF1* ***(A)*** *and RF2* ***(B)*** *concentrations. Each time course was repeated at least twice and error bars are the standard error of the fitted value of kobs.*

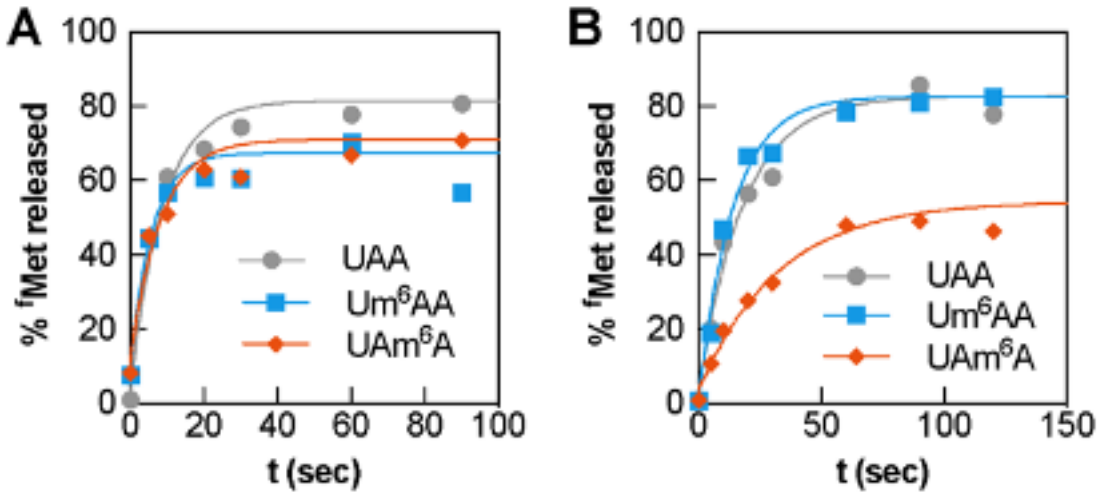

Supplemental Figure A.13: ***Endpoint defects on m6A-containing stop codons are rescued by additional RF2.*** *Several chemical modifications in stop codons alter the activity of release factors (28), but m^6A has not been investigated. We measured the rate constants for ^{f}Met release on mRNAs containing m^6A modifications to the universal stop codon (Um^6AA/UAm^6A). We found that m^6A did not change the rate constants for peptide release by either RF1* ***(A)*** *or RF2* ***(B)*** *(Table S7), but did reduce the yield for release catalyzed by 1 μM RF2 on a UAm^6A modified codon (82% for UAA, and 55% for UAm^6A). This end-point defect was rescued by the addition of 10 μM RF2 (92% for UAA, 90% for Um^6AA) (Fig. S14).*

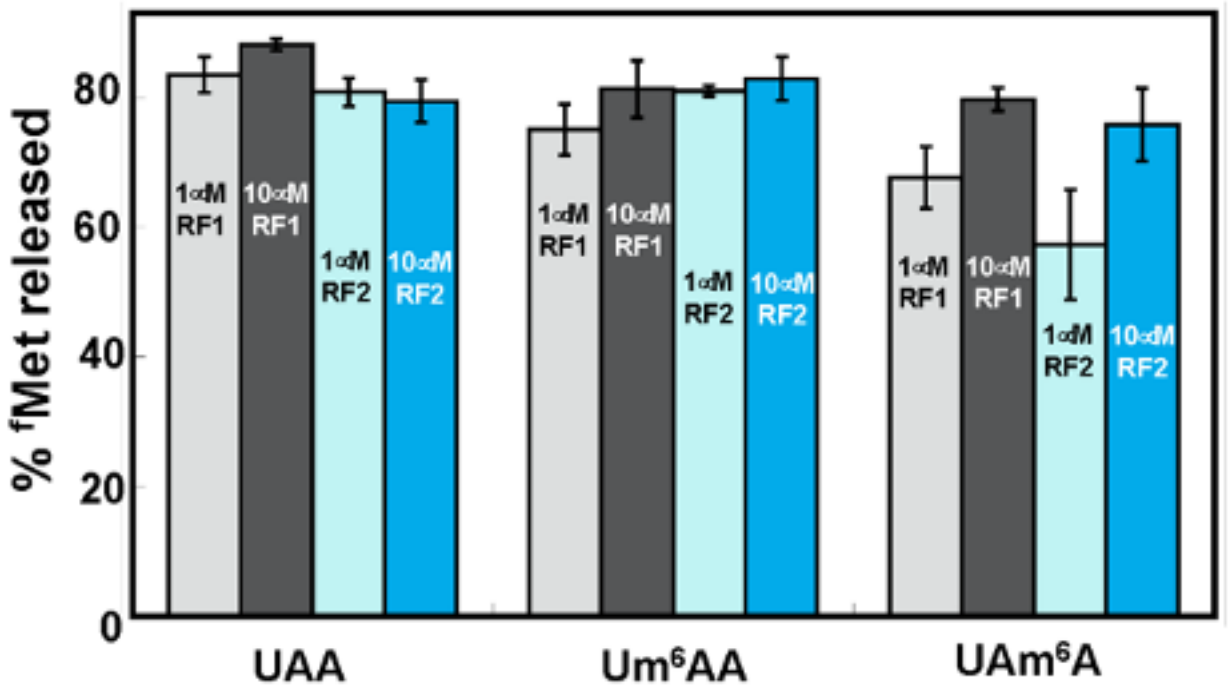

Supplemental Figure A.14: ***Endpoint defects on m6A-containing stop codons are rescued by additional RF2.***

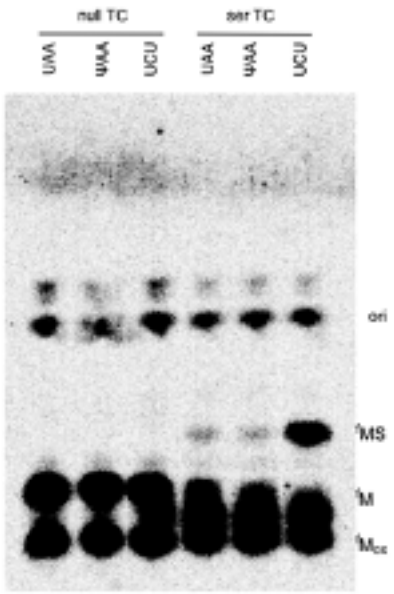

Supplemental Figure A.15: ***A ΨAA-modified stop codon does not direct serine incorporation in vitro.*** *Electrophoretic TLC displaying the translation products of unmodified and Ψ-containing stop codon messages in the presence of no tRNA (null), total tRNA aminoacylated with serine (ser TC).*

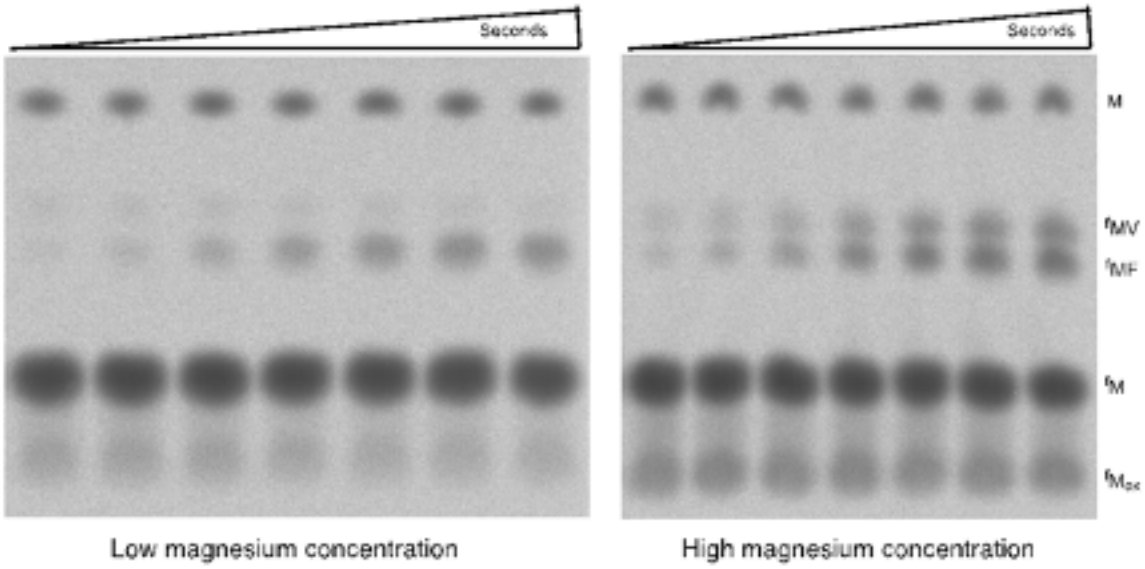

Supplemental Figure A.16: ***Magnesium dependence of competition between Val-tRNAVal ternary complex Phe-tRNAPhe ternary complex on a ΨUU codon.*** *ΨUU initiation complexes (100 nM) were reacted with 50 nM Phe-tRNA^{Phe} and 20 μM Val-tRNA^{Val} in the presence of 10 nM EFTu, EFTs, energy regeneration mix, and low (sub-mM) or high (~ 10 mM) free Mg(II). Almost no fMet-Val dipeptide is formed at low magnesium concentrations, while at high magnesium concentrations fMet-Val formation is almost stoichiometric with fMet-Phe.*

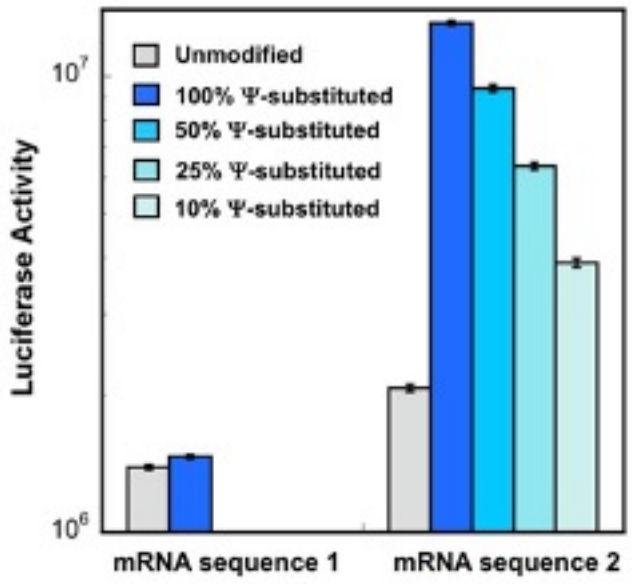

Supplemental Figure A.17: ***The yield of active protein from pseudouridinylated mRNAs depends on the level of pseudouridinylation and sequence context.*** *Two mRNAs coding for luciferase but with silent coding region changes were in vitro transcribed in the presence of varying ratios of uridine and pseudouridine triphosphate. Purified mRNAs were transfected into cultured mammalian cells and luciferase activity was assayed at a single time point.*

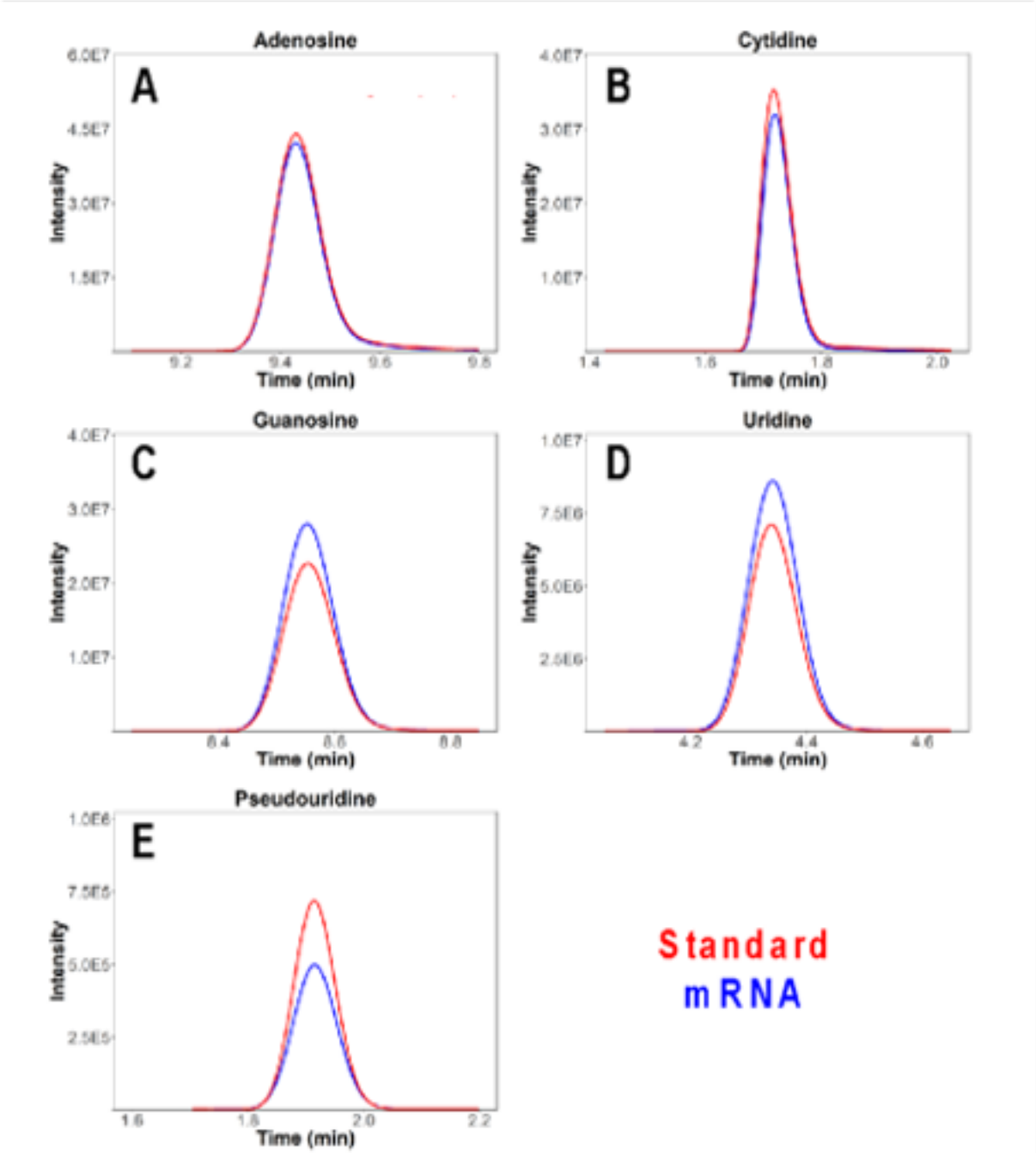

Supplemental Figure A.18: ***Verification of pseudouridine in synthetic mRNAs.*** *Overlaid extracted ion chromatograms of the four main bases* ***(A-D)*** *and pseudouridine* ***(E)*** *in a nucleoside standard (red line) and synthetic mRNA oligonucleotide (blue line). Note that the ranges on the x-axes vary from panel to panel.*

References for SI Appendix

1. Milligan JF, Groebe DR, Witherell GW, & Uhlenbeck OC (1987) Oligoribonucleotide synthesis using T7 RNA polymerase and synthetic DNA templates. *Nucleic Acids Res* 15(21):8783-8798.
2. Walker SE & Fredrick K (2008) Preparation and evaluation of acylated tRNAs. *Methods* 44(2):81-86.

3. Basanta-Sanchez M, Temple S, Ansari SA, D'Amico A, & Agris PF (2016) Attomole quantification and global profile of RNA modifications: Epitranscriptome of human neural stem cells. *Nucleic Acids Res* 44(3):e26.
4. Pavlov MY*, et al.* (1998) A direct estimation of the context effect on the efficiency of termination. *J Mol Biol* 284(3):579-590.
5. Maracci C, Peske F, Dannies E, Pohl C, & Rodnina MV (2014) Ribosome-induced tuning of GTP hydrolysis by a translational GTPase. *Proc Natl Acad Sci U S A* 111(40):14418-14423.
6. Zaher HS & Green R (2009) Quality control by the ribosome following peptide bond formation. *Nature* 457(7226):161-166.
7. Koutmou KS*, et al.* (2015) Ribosomes slide on lysine-encoding homopolymeric A stretches. *Elife* 4.
8. Polikanov YS, Melnikov SV, Soll D, & Steitz TA (2015) Structural insights into the role of rRNA modifications in protein synthesis and ribosome assembly. *Nat. Struct. Mol. Biol.* 22(4):342-344.
9. Selmer M*, et al.* (2006) Structure of the 70S ribosome complexed with mRNA and tRNA. *Science* 313(5795):1935-1942.
10. Korostelev A, Trakhanov S, Laurberg M, & Noller HF (2006) Crystal structure of a 70S ribosome-tRNA complex reveals functional interactions and rearrangements. *Cell* 126(6):1065-1077.
11. Polikanov YS, Blaha GM, & Steitz TA (2012) How hibernation factors RMF, HPF, and YfiA turn off protein synthesis. *Science* 336(6083):915-918.
12. Kabsch W (2010) Xds. *Acta Crystallogr. D. Biol. Crystallogr.* 66(Pt 2):125-132.
13. McCoy AJ*, et al.* (2007) Phaser crystallographic software. *J. Appl. Crystallogr.* 40(Pt 4):658-674.
14. Adams PD*, et al.* (2010) PHENIX: a comprehensive Python-based system for macromolecular structure solution. *Acta Crystallogr. D Biol. Crystallogr.* 66(Pt 2):213-221.
15. Emsley P & Cowtan K (2004) Coot: model-building tools for molecular graphics. *Acta Crystallogr. D Biol. Crystallogr.* 60:2126-2132.
16. Roy B, Leszyk JD, Mangus DA, & Jacobson A (2015) Nonsense suppression by near-cognate tRNAs employs alternative base pairing at codon positions 1 and 3. *Proc Natl Acad Sci U S A* 112(10):3038-3043.
17. Roy B*, et al.* (2016) Ataluren stimulates ribosomal selection of near-cognate tRNAs to promote nonsense suppression. *Proc Natl Acad Sci U S A* 113(44):12508-12513.
18. Fernandez IS*, et al.* (2013) Unusual base pairing during the decoding of a stop codon by the ribosome. *Nature* 500(7460):107-110.
19. Karijolich J & Yu YT (2011) Converting nonsense codons into sense codons by targeted pseudouridylation. *Nature* 474(7351):395-398.
20. Parisien M, Yi C, & Pan T (2012) Rationalization and prediction of selective decoding of pseudouridine-modified nonsense and sense codons. *RNA* 18(3):355-367.
21. Svidritskiy E, Madireddy R, & Korostelev AA (2016) Structural Basis for Translation Termination on a Pseudouridylated Stop Codon. *J Mol Biol* 428(10 Pt B):2228-2236.
22. Mora L, Heurgue-Hamard V, de Zamaroczy M, Kervestin S, & Buckingham RH (2007) Methylation of bacterial release factors RF1 and RF2 is required for normal translation termination in vivo. *J Biol Chem* 282(49):35638-35645.

23. Youngman EM, Brunelle JL, Kochaniak AB, & Green R (2004) The active site of the ribosome is composed of two layers of conserved nucleotides with distinct roles in peptide bond formation and peptide release. *Cell* 117(5):589-599.
24. Zavialov AV, Mora L, Buckingham RH, & Ehrenberg M (2002) Release of peptide promoted by the GGQ motif of class 1 release factors regulates the GTPase activity of RF3. *Mol Cell* 10(4):789-798.
25. Hetrick B, Lee K, & Joseph S (2009) Kinetics of stop codon recognition by release factor 1. *Biochemistry* 48(47):11178-11184.
26. Kuhlenkoetter S, Wintermeyer W, & Rodnina MV (2011) Different substrate-dependent transition states in the active site of the ribosome. *Nature* 476(7360):351-354.
27. Burakovsky DE*, et al.* (2010) Mutations at the accommodation gate of the ribosome impair RF2-dependent translation termination. *RNA* 16(9):1848-1853.
28. Hoernes TP*, et al.* (2018) Atomic mutagenesis of stop codon nucleotides reveals the chemical prerequisites for release factor-mediated peptide release. *Proc Natl Acad Sci U S A* 115(3):E382-E389.
29. Boccaletto P*, et al.* (2018) MODOMICS: a database of RNA modification pathways. 2017 update. *Nucleic Acids Res* 46(D1):D303-D307.
30. Pape T, Wintermeyer W, & Rodnina MV (1998) Complete kinetic mechanism of elongation factor Tu-dependent binding of aminoacyl-tRNA to the A site of the E. coli ribosome. *EMBO J* 17(24):7490-7497.
31. Ranjan N & Rodnina MV (2017) Thio-Modification of tRNA at the Wobble Position as Regulator of the Kinetics of Decoding and Translocation on the Ribosome. *J Am Chem Soc* 139(16):5857-5864.

Appendix B: Chapter 3 Supplemental

This Appendix contains supplemental figures and tables information for Chapter 3.

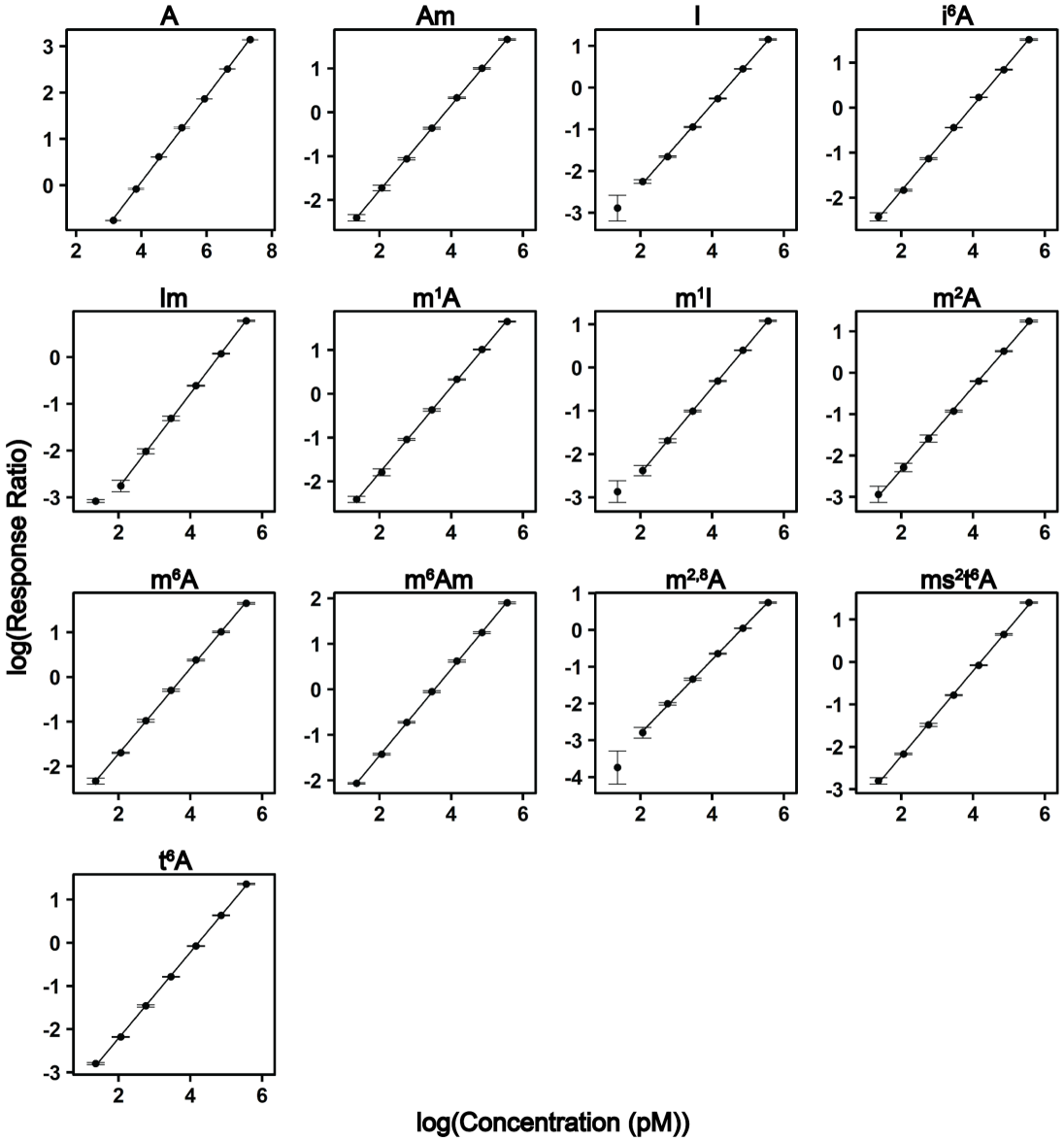

Supplemental Figure B.1: ***Calibration curves used to quantify adenosine modification concentrations.*** *Calibration curves of adenosine ribonucleoside modifications plotted in log(response ratio) vs. log(concentration (pM)). The linear regression, limit of detection, and R^2 are displayed in* ***Supplemental Table S1.***

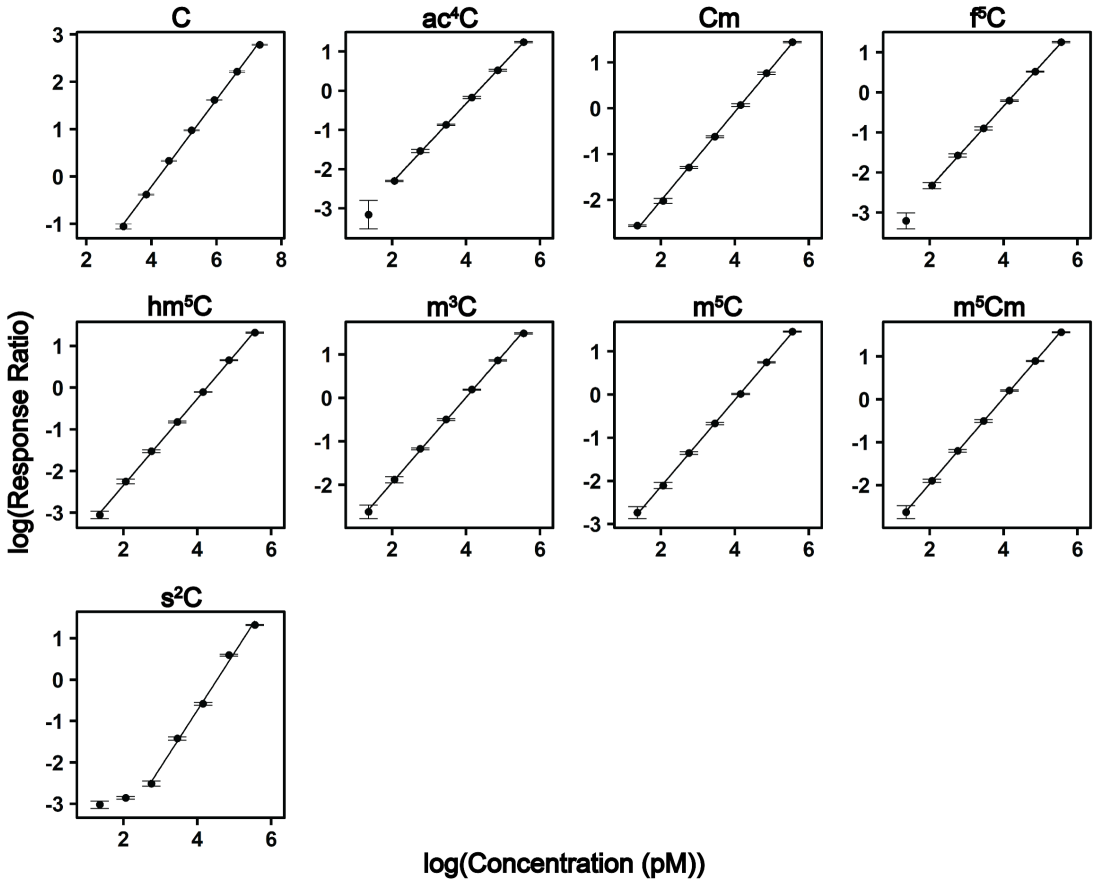

Supplemental Figure B.2: ***Calibration curves used to quantify cytidine modification concentrations.*** *Calibration curves of cytidine ribonucleoside modifications plotted in log(response ratio) vs. log(concentration (pM)). The linear regression, limit of detection, and R^2 are displayed in* ***Supplemental Table S1.***

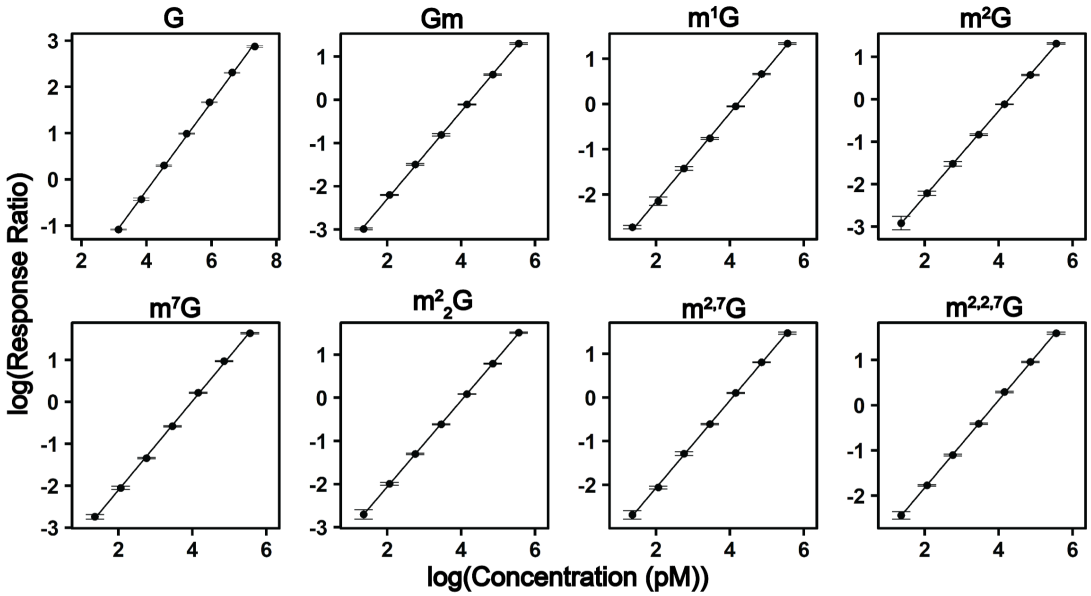

Supplemental Figure B.3: ***Calibration curves used to quantify guanosine modification concentrations.*** *Calibration curves of guanosine ribonucleoside modifications plotted in log(response ratio) vs. log(concentration (pM)). The linear regression, limit of detection, and R^2 are displayed in* ***Supplemental Table S1.***

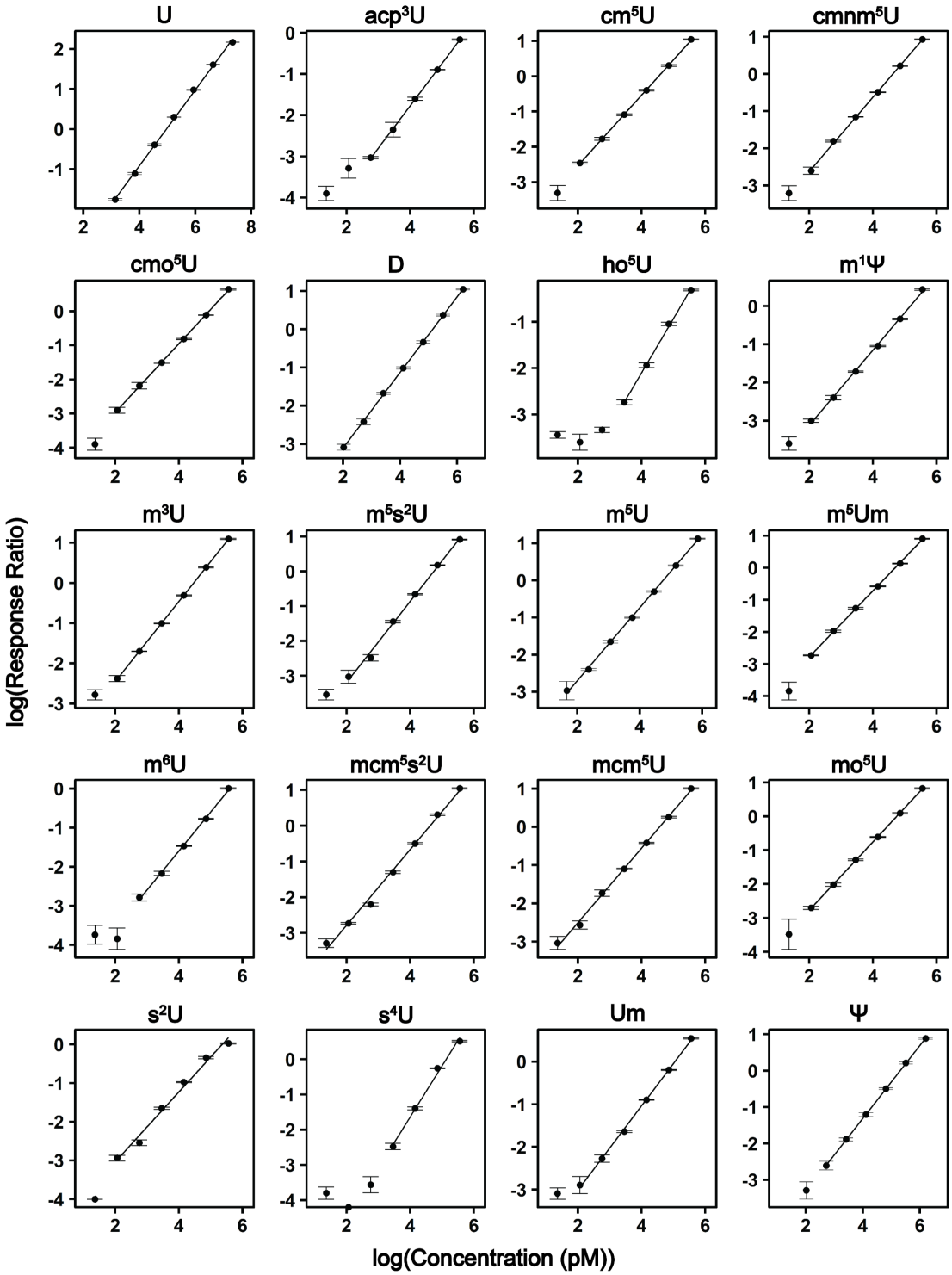

Supplemental Figure B.4: ***Calibration curves used to quantify uridine modification concentrations.*** *Calibration curves of uridine ribonucleoside modifications plotted in log(response ratio) vs. log(concentration (pM)). The linear regression, limit of detection, and R^2 are displayed in* ***Supplemental Table S1.***

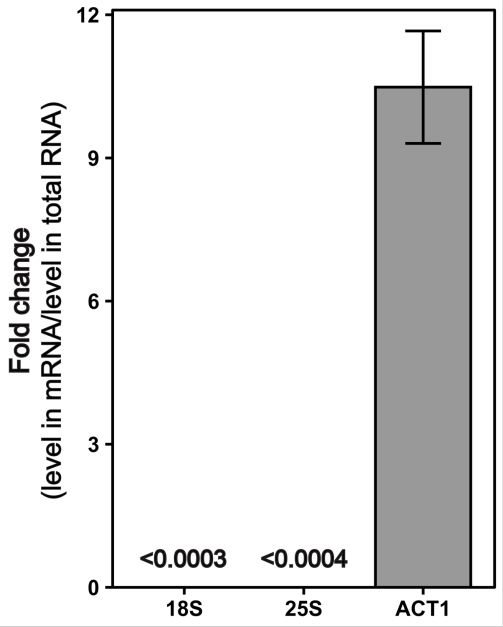

Supplemental Figure B.5: ***Ribosomal RNAs are depleted in three-stage purified mRNA.*** *qRT-PCR demonstrates that the 18S and 25S rRNAs are depleted by greater than 3000-fold in the purified mRNA. Contrarily, ACT1 is enriched by greater than 10-fold. This data in addition to the Bioanalyzer electropherograms, RNA-seq, and LC-MS/MS proves that our three-stage purified mRNA is highly pure.*

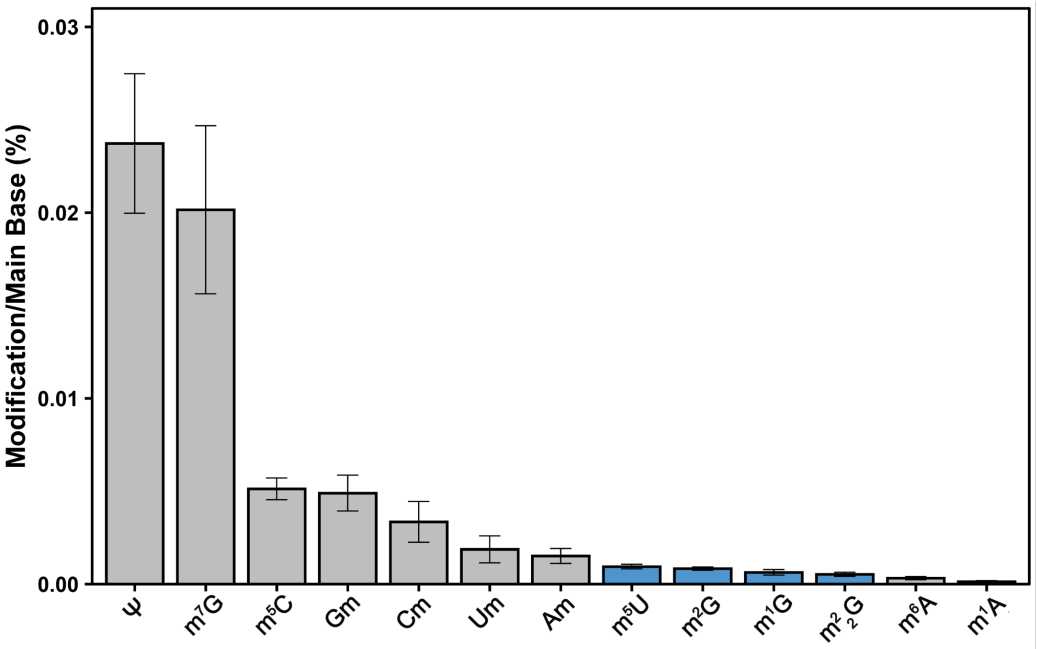

Supplemental Figure B.6: ***Ribonucleoside modification abundance in the three-stage purified mRNA****. The ribonucleoside abundance is represented as modification/main base% (i.e., $m^7G/G\%$) where pseudouridine was the most abundant modification detected. All modifications detected were previously detected in purified mRNA besides for the three methylated guanosine modifications displayed in blue (m^1G, m^2G, and $m^2{}_2G$). Our improvements regarding LC-MS/MS sensitivity and mRNA purity enables us to confidently claim these modifications exist with S. cerevisiae mRNA.*

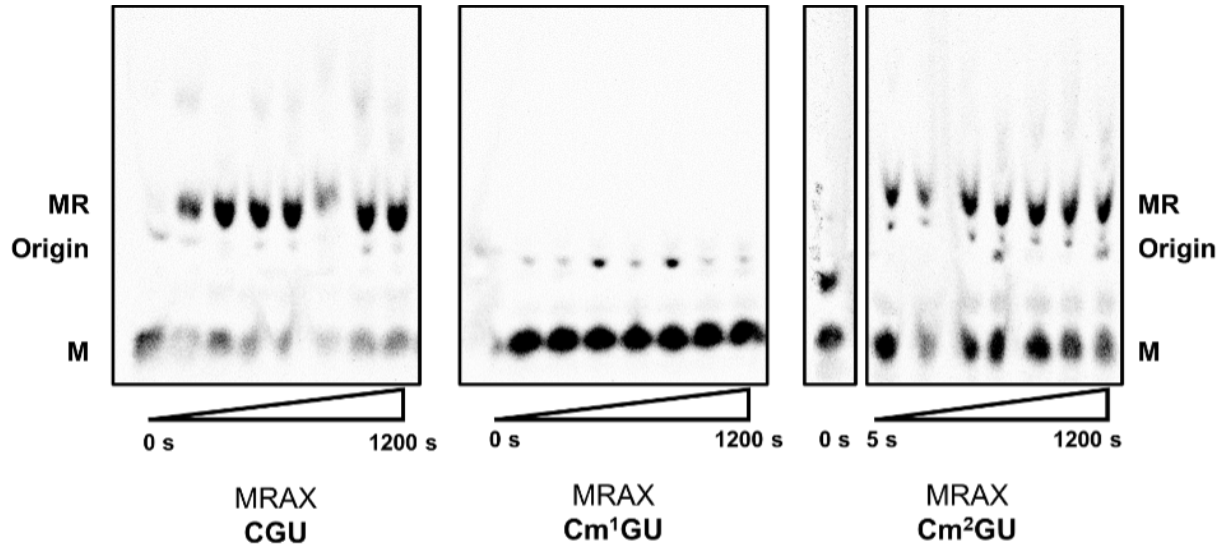

Supplemental Figure B.7: Electrophoretic TLC displaying the translation products of CGU, Cm1GU, and Cm2GU codons in the presence of arginine tRNA (ArgTC), forming MR dipeptide over the span of 1200 seconds.

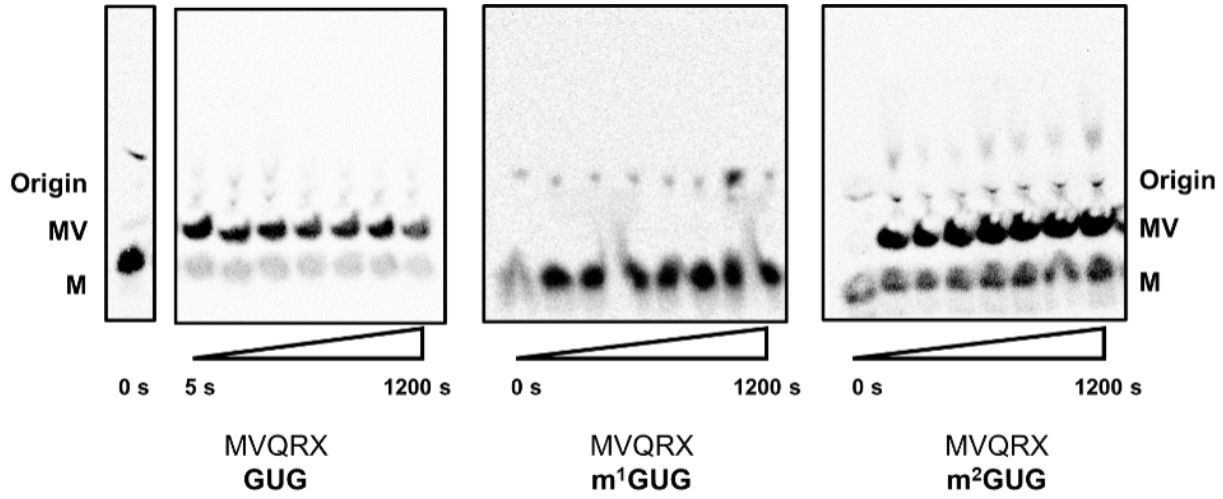

Supplemental Figure B.8: Electrophoretic TLC displaying the translation products of GUG, m1GUG, and m2GUG codons in the presence of valine tRNA (ValTC), forming MV dipeptide over the span of 1200 seconds.

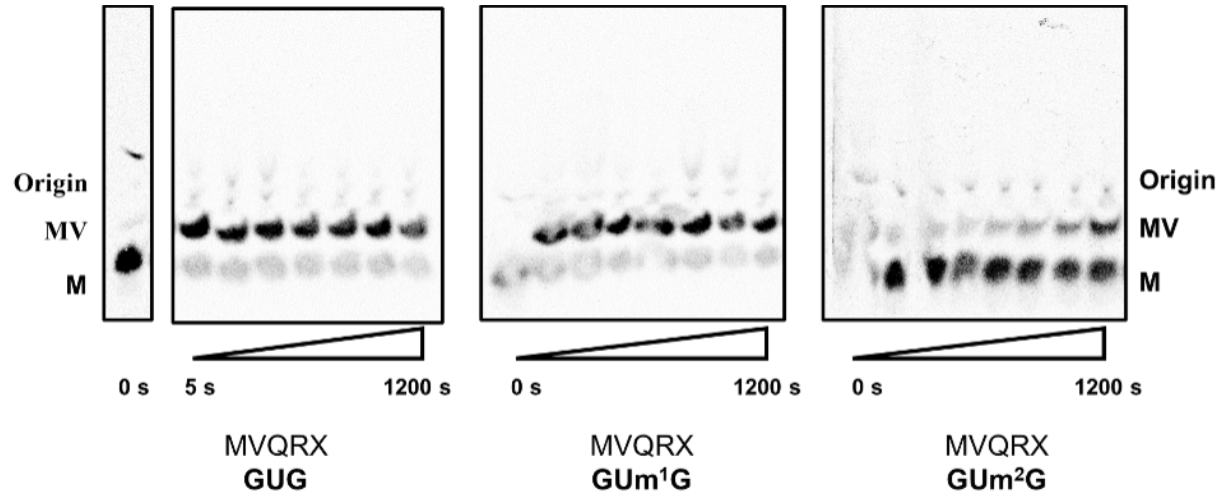

Supplemental Figure B.9: Electrophoretic TLC displaying the translation products of GUG, GUm1G, and GUm2G codons in the presence of valine tRNA (ValTC), forming MV dipeptide over the span of 1200 seconds.

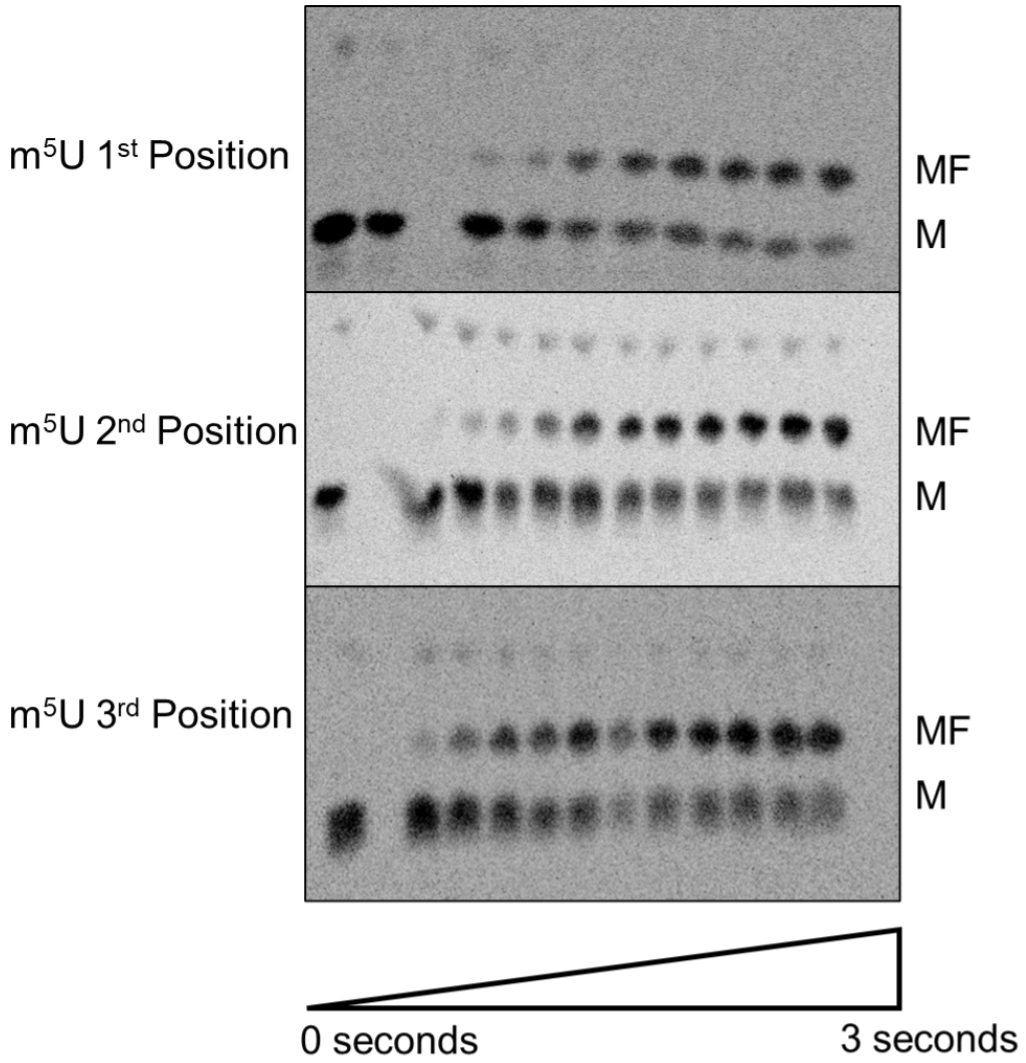

Supplemental Figure B.10: Electrophoretic TLC displaying the translation products of m5U messages in the presence of phenylalanine tRNA (PheTC), forming MF dipeptide over the span of 3 seconds.

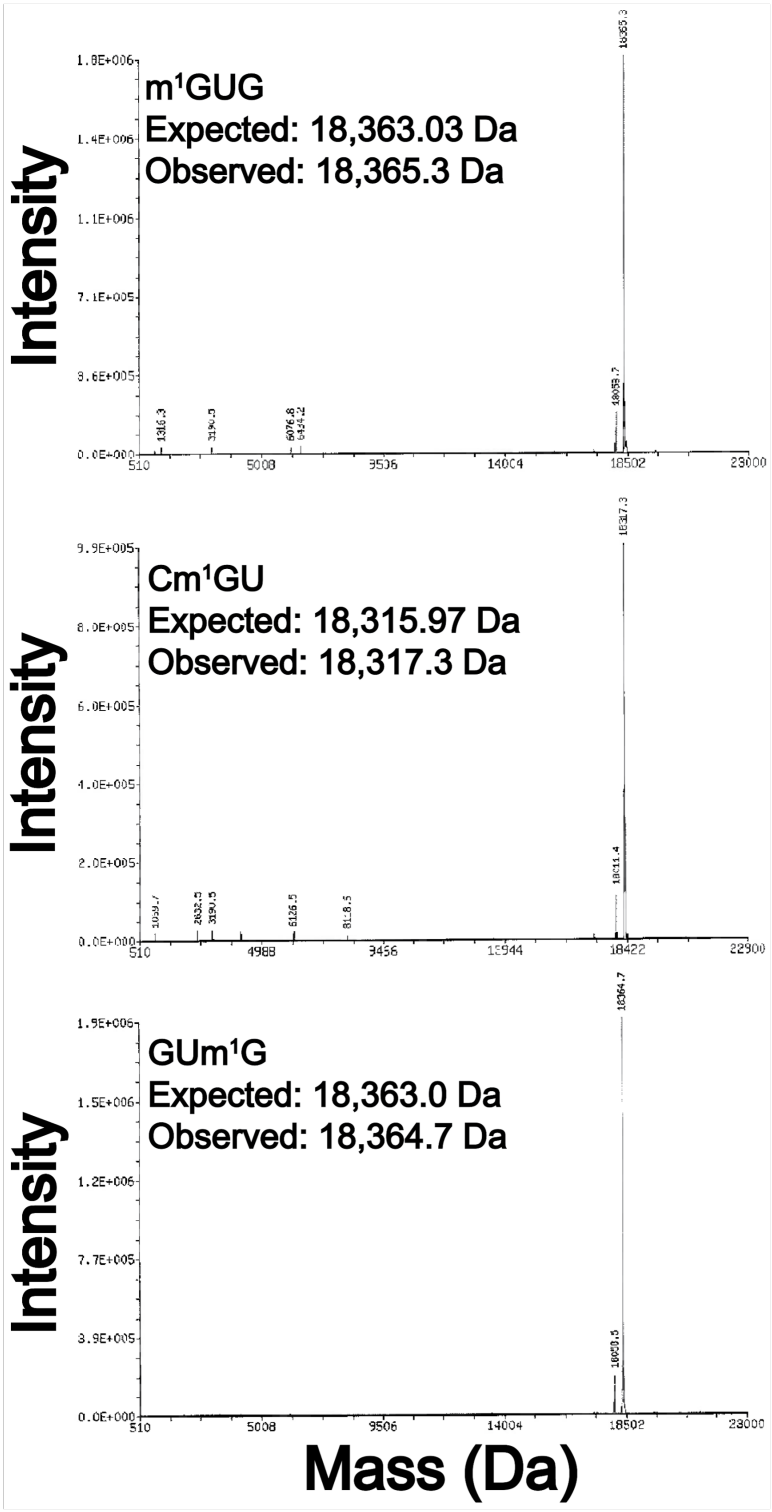

Supplemental Figure B.11: Deconvoluted ESI-MS spectra of modified oligonucleotides provided by Dharmacon to confirm purity. The expected and observed masses of the m[1]GUG, Cm[1]GU, and GUm[1]G modified codon oligonucleotides are found in the top, middle, and bottom panels, respectively. Minor n-1 oligonucleotides products were detected, but they would not affect the in vitro translation assays because the nucleotide loss occurs in the non-coded region of the purchased mRNA transcript.

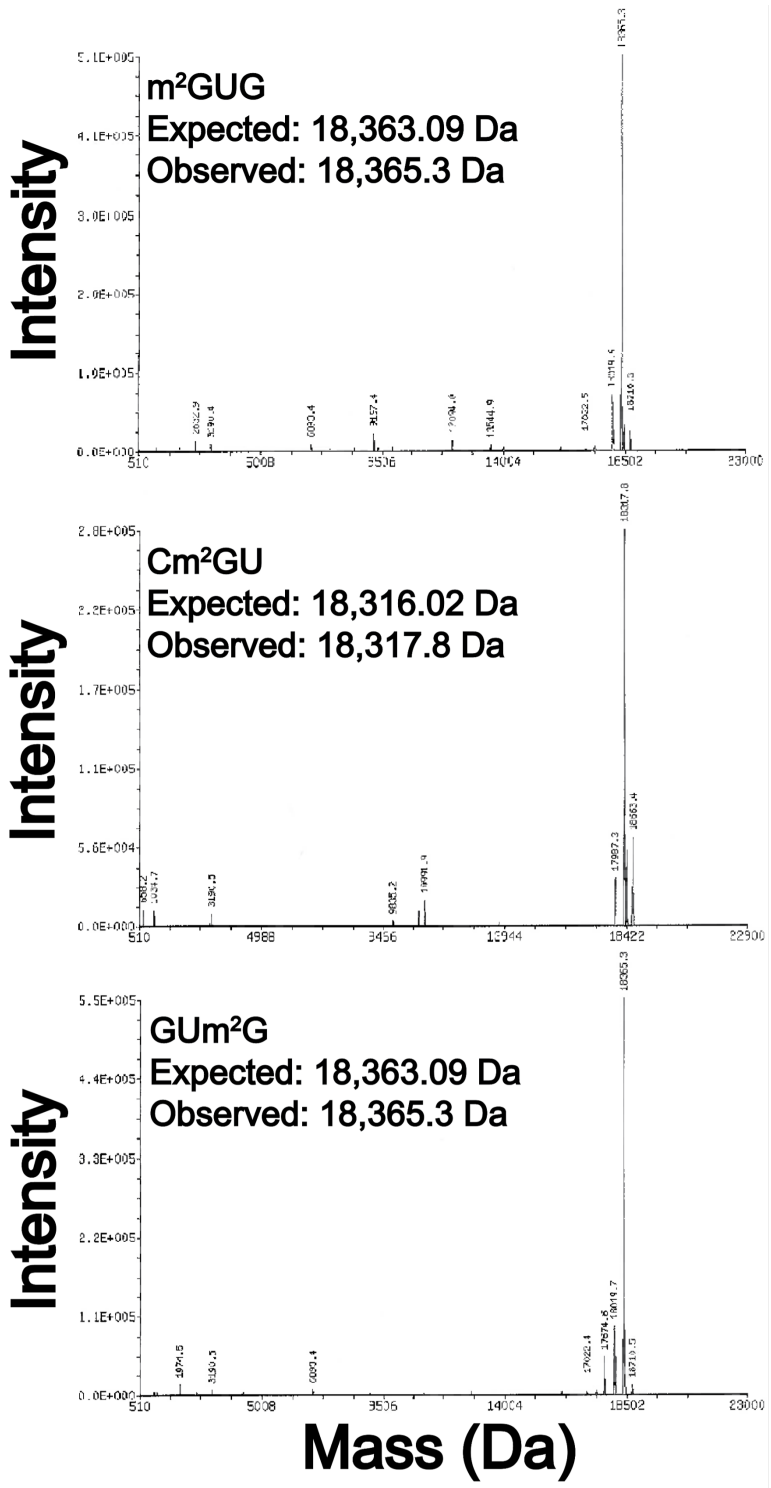

Supplemental Figure B.12: Deconvoluted ESI-MS spectra of modified oligonucleotides provided by Dharmacon to confirm purity. The expected and observed masses of the m²GUG, Cm²GU, and GUm²G modified codon oligonucleotides are found in the top, middle, and bottom panels, respectively. Minor n-1 oligonucleotides products were detected, but they would not affect the in vitro translation assays because the nucleotide loss occurs in the non-coded region of the purchased mRNA transcript.

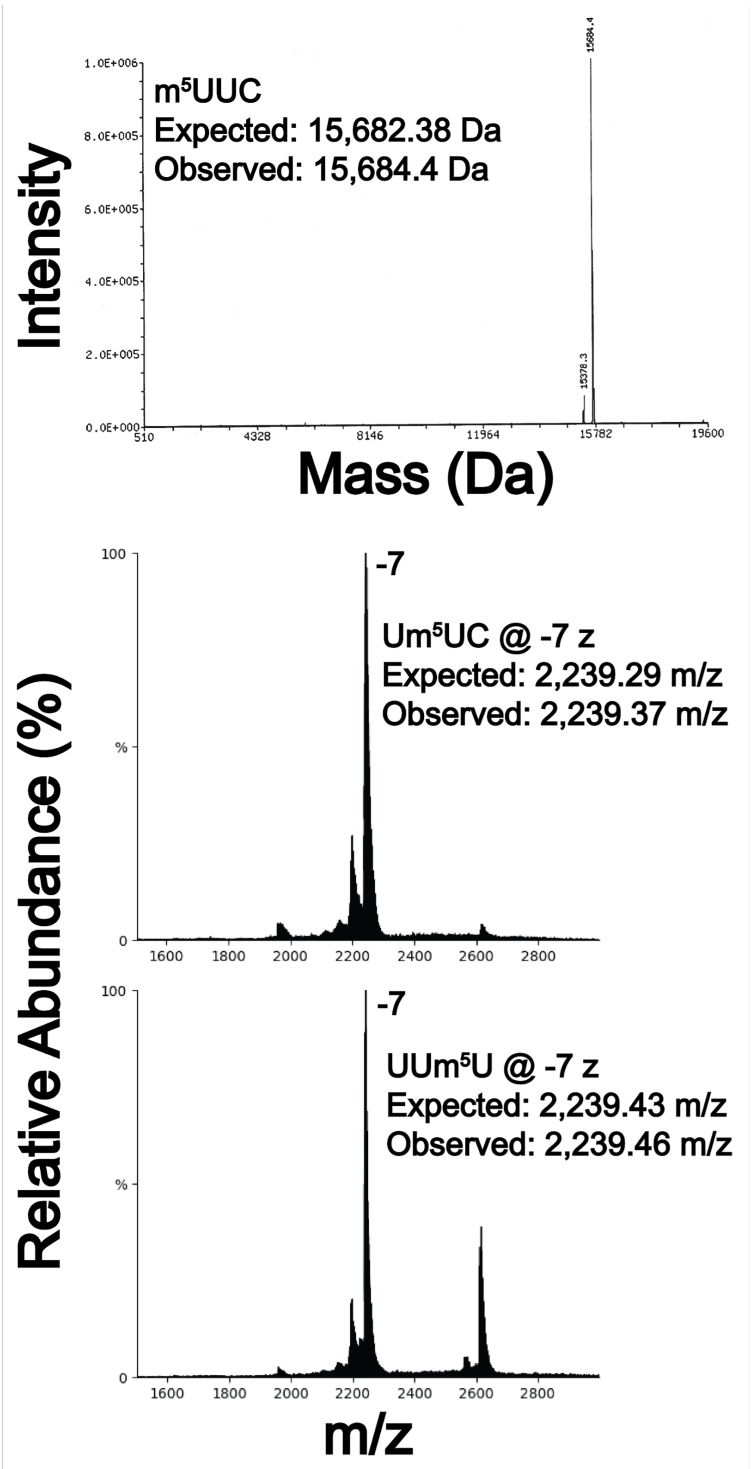

Supplemental Figure B.13: Deconvoluted ESI-MS spectra of m5UUC modified codon oligonucleotides provided by Dharmacon to confirm purity (top panel). Full scan spectra of Um^{5}UC (middle) and UUm^{5}U (bottom) modified codon oligonucleotide. The corresponding expected and observed mass (Da) or mass-to-charge (m/z) is displayed for each spectrum. Minor n-1 oligonucleotides products were detected, but they would not affect the in vitro translation assays because the nucleotide loss occurs in the non-coded region of the purchased mRNA transcript.

Supplemental Table B.1: Linear regression, limit of detection, and R2 calculated from calibration curves made from nucleoside standards. Y corresponds to log(response ratio) and X corresponds to log(concentration(pM)).

Nucleoside	Linear Regression	Limit of Detection (amol)	R^2
A	**Y** = 0.9264**X** - 3.632	Not Determined	>0.999
ac^{4}C	**Y** = 1.005**X** - 4.344	43	>0.999
acp^{3}U	**Y** = 1.027**X** - 5.882	1000	0.995
Am	**Y** = 0.972**X** - 3.727	7	>0.999
C	**Y** = 0.9185**X** - 3.884	Not Determined	0.998
Cm	**Y** = 0.9685**X** - 3.953	41	0.998
cm^{5}U	**Y** = 0.998**X** - 4.53	21	>0.999
cmnm^{5}U	**Y** = 0.9981**X** - 4.62	160	0.998
cmo^{5}U	**Y** = 1.007**X** - 4.982	67	0.998
D	**Y** = 0.9866**X** - 5.073	530	>0.999
f^{5}C	**Y** = 1.017**X** - 4.412	21	>0.999
G	**Y** = 0.956**X** - 4.061	Not Determined	0.998
Gm	**Y** = 1.012**X** - 4.319	18	>0.999
hm^{5}C	**Y** = 1.04**X** - 4.424	18	>0.999
ho^{5}U	**Y** = 1.168**X** - 6.776	3300	0.997
I	**Y** = 0.9827**X** - 4.325	170	>0.999
i^{6}A	**Y** = 0.946**X** - 3.735	44	>0.999
Im	**Y** = 1.007**X** - 4.808	150	0.998
m^{1}A	**Y** = 0.9792**X** - 3.76	4	0.999
m^{1}G	**Y** = 0.9791**X** - 4.117	9	0.999
m^{1}I	**Y** = 0.9922**X** - 4.429	50	0.999
m$^1\Psi$	**Y** = 0.9835**X** - 5.088	250	0.998
m$_3$G	**Y** = 0.9686**X** - 3.761	4	>0.999
m$^2{}_2$G	**Y** = 1.001**X** - 4.064	10	>0.999
m^{2,7}G	**Y** = 1.002**X** - 4.073	8	>0.999
m^{2,8}A	**Y** = 1.004**X** - 4.822	79	0.998
m^{2}A	**Y** = 0.9996**X** - 4.341	24	0.997
m^{2}G	**Y** = 1.004**X** - 4.29	26	0.998
m^{3}C	**Y** = 0.9792**X** - 3.906	8	0.998
m^{3}U	**Y** = 0.9944**X** - 4.439	45	>0.999
m^{5}C	**Y** = 1.005**X** - 4.139	21	0.998
m^{5}Cm	**Y** = 1.00**X** - 3.97	14	0.999
m^{5}s^{2}U	**Y** = 1.164**X** - 5.52	250	0.993
m^{5}U	**Y** = 0.9825**X** - 4.665	72	0.996
m^{5}Um	**Y** = 1.029**X** - 4.836	40	>0.999
m^{6}A	**Y** = 0.9558**X** - 3.629	3	>0.999
m^{6}Am	**Y** = 0.9503**X** - 3.356	4	>0.999
m^{6}U	**Y** = 0.9981**X** - 5.588	640	0.997

m^7G	**Y** = 1.06**X** - 4.22	11	>0.999
mcm^5s^2U	**Y** = 1.061**X** - 4.909	83	0.993
mcm^5U	**Y** = 0.9751**X** - 4.457	29	0.995
mo^5U	**Y** = 1.007**X** - 4.786	67	>0.999
ms^2t^6A	**Y** = 1.004**X** - 4.223	21	>0.999
Ψ	**Y** = 1.00**X** - 5.313	930	0.998
s^2C	**Y** = 1.386**X** - 6.284	1100	0.995
s^2U	**Y** = 0.9031**X** - 4.843	120	0.986
s^4U	**Y** = 1.448**X** - 7.433	2000	0.992
t^6A	**Y** = 0.9956**X** - 4.201	21	>0.999
U	**Y** = 0.9492**X** - 4.714	Not Determined	0.999
Um	**Y** = 0.9891**X** - 4.993	170	0.995

Supplemental Table B.2: Ribonucleoside standard concentrations displayed in Figure 1A extracted ion chromatogram

Nucleoside	Peak Label	Concentration (nM)
A	26	6.9
ac^4C	39	14.4
acp^3U	10	72
Am	40	2.9
C	1	6.9
Cm	15	14.4
cm^5U	16	14.4
$cmnm^5U$	5	14.4
cmo^5U	18	72
D	2	64.8
f^5C	23	14.4
G	20	6.9
Gm	34	14.4
hm^5C	3	14.4
ho^5U	9	360
I	19	14.4
i^6A	50	2.9
Im	32	14.4
m^1A	7	2.9
m^1G	33	14.4
m^1I	35	14.4
$m^1Ψ$	14	72
m_3G	36	2.9
$m^2{}_2G$	45	2.9

$m^{2,7}G$	25	2.9
$m^{2,8}A$	43	14.4
m^2A	30	14.4
m^2G	38	14.4
m^3C	6	2.9
m^3U	31	14.4
m^5C	8	2.9
m^5Cm	21	2.9
m^5s^2U	41	14.4
m^5U	22	32
m^5Um	42	14.4
m^6A	44	2.9
m^6Am	47	0.58
m^6U	17	72
m^7G	12	2.9
mcm^5s^2U	46	14.4
mcm^5U	37	14.4
mo^5U	24	14.4
ms^2t^6A	49	2.9
Ψ	4	64.8
s^2C	13	14.4
s^2U	27	72
s^4U	29	72
t^6A	48	2.9
U	11	34.6
Um	28	72

Supplemental Table B.3: Number of mapped RNA-seq reads for each transcript detected in total RNA and purified mRNA samples

Place holder

Supplemental Table B.4: Raw data of UHLPC-MS/MS analysis WT and KO cell types. Measurements were done in triplicates (technical replicate) for each sample and each measurement represents picomolar concentration (pmol/L) of each nucleoside.placeholder

Place holder

Supplemental Table B.5: : Modification Percentage of UHLPC-MS/MS analysis WT and KO cell types. Measurements were done in triplicates (technical replicate) for each sample and each measurement represents modification percentage (modification/canonical base %).

Placeholder

Supplemental Table B.6: Average Modification Percentage of UHLPC-MS/MS analysis WT and KO cell types. Measurements were averaged between the two biological replicates and three technical replicates of each biological replicate. Each measurement represents modification percentage (modification/canonical base %).

Nucleoside	Abbreviation	Found in S. cerevisiae	PTM Class	WT total RNA	Δtrm1 total RNA	Δtrm2 total RNA	Δtrm10 total RNA	Δtrm11 total RNA	WT mRNA	Δtrm1 mRNA	Δtrm2 mRNA	Δtrm10 mRNA	Δtrm11 mRNA
Dihydrouridine	D	Yes	r, t	1.88617182 3	2.00469037 3	1.99118947 8	2.05319471	2.04294476	N.D.	N.D.	N.D.	N.D.	N.D.
5-hydroxymethylcytidine	hm5C	No	m, r	N.D.	N.D.	N.D.	N.D.	N.D.	N.D.	N.D.	N.D.	N.D.	N.D.
Pseudouridine	Ψ	Yes	m, r, sn, snno, t	4.79816861 8	5.00988432 6	4.65682032 8	4.95165033 6	5.05488164 4	0.02372314 7	0.01944457 9	0.02475 26	0.02191125 6	0.02041 4
3-methylcytidine	m^3C	Yes	m, t	0.04248235 4	0.04256740 3	0.06554411 9	0.04911339 6	0.04483600 8	N.D.	N.D.	0.00045098 8	N.D.	N.D.
1-methyladenosine	m^1A	Yes	m, r, t	0.22235762 6	0.23325342 8	0.35110335	0.23494119 5	0.22448584	0.00013545 5	0.00017155 5	0.00013927	0.00015797 9	0.00013 9
5-hydroxyuridine	ho^5U	No	t	N.D.	N.D.	N.D.	N.D.	N.D.	N.D.	N.D.	N.D.	N.D.	N.D.
5-methylcytidine	m^5C	Yes	m, r, t	0.79748402 5	0.81129611 6	0.68296682 1	0.85577728 9	0.82305980 6	0.00512690 4	0.00475011 6	0.00449423 1	0.00388942 1	0.00362 4
1-methylpseudouridine	$m^1\Psi$	Yes	r, t	0.00357	0.00402	0.00430904	0.00371	0.00433	N.D.	N.D.	N.D.	N.D.	N.D.

				6844	3192		8911	3463					
7-methylguanosine	m^7G	Yes	m, r, t	0.14193920 6	0.15467844 2	0.17502152 6	0.15205227 2	0.14558261 4	0.02015543 6	0.02459492 8	0.01632834 7	0.02004338 5	0.0200007
2′-O-methylcytidine	Cm	Yes	m, r, sn, t	1.37481105	1.39694531 1	1.22414202 4	1.38974958 9	1.37895703 4	0.00335076 5	0.00287794 1	0.00245616 2	0.00292403 2	0.0023353
Inosine	I	Yes	m, t	0.13114099 1	0.11026253 5	0.11571857 4	0.10882521 5	0.10933440 6	N.D.	N.D.	0.00813029 8	N.D.	N.D.
5-methyluridine	m^5U	Yes	m, r, t	0.46416817 9	0.49341869 5	0.03267948 5	0.52310229 3	0.50613699 2	0.00094245 1	0.00082182 6	0.00036695 6	0.00078190 1	0.0008003
5-formylcytidine	f^5C	Yes	m, t	N.D.	N.D.	N.D.	N.D.	N.D.	N.D.	N.D.	N.D.	N.D.	N.D.
2′-O-methyluridine	Um	Yes	m, r, sn, sno, t	0.63934344	0.65275162 9	0.59783841	0.64708832 9	0.65350272 6	0.00187048 7	0.00103638 3	0.00188174 2	0.00138293 4	0.0014003
2-methyladenosine	m^2A	No	r, t	N.D.	N.D.	N.D.	N.D.	N.D.	N.D.	N.D.	N.D.	N.D.	N.D.
1-methylguanosine	m^1G	Yes	m, r, t	0.38074368	0.43596958 8	0.39662782	0.15137225 5	0.40785217 1	0.00063379	0.00061411 4	0.00072848 3	0.00036004 2	0.000046
2′-O-methylguanosine	Gm	Yes	m, r, sn, t	1.15401153 1	1.16267441 9	1.00039686 4	1.18684482 4	1.15348592 8	0.00489 9	0.00437984 9	0.00526379	0.00392379 3	0.0038779

1-methylinosine	m^1I	Yes	t	0.02876658 3	0.02965615 8	0.02602036 3	0.03090472 1	0.02898468	N.D.	N.D.	N.D.	N.D.	N.D.
N2-methylguanosine	m^2G	Yes	r, sn, t	0.34426496 1	0.34800389	0.37324236 3	0.36284867 7	0.00464219 4	0.00083352 1	0.00071819 7	0.00125783 5	0.00067256 8	0.0003387
N4-acetylcytidine	ac^4C	Yes	m,r, t	0.22272901 3	0.23242025 8	0.26948754	0.23151416 2	0.23009017 8	N.D.	N.D.	N.D.	N.D.	N.D.
2′-O-methyladenosine	Am	Yes	m, r, sn, sno, t	1.22688889 9	1.22220413 8	1.23146153 6	1.21806362 8	1.21079377 6	0.00151562 9	0.00114517 1	0.00154674 9	0.00139292 5	0.0011132
N6-methyladenosine	m^6A	Yes	m, r, sn, t	0.12300485 9	0.12120245	0.10537066 5	0.12365633 6	0.12089648 7	0.00032066 3	0.00027325 8	0.00033981 8	0.00025273 8	0.0002213
N2,N2-dimethylguanosine	m^2_2G	Yes	r, t	0.30345824 4	0.00047411 5	0.34377020 2	0.32371564 7	0.31570524 1	0.00052743 1	0.00014785 1	0.00066943 6	0.00046607 2	0.0005113
N6,2′-O-dimethyladenosine	m^6Am	No	m, sn	N.D.	N.D.	N.D.	N.D.	N.D.	N.D.	N.D.	N.D.	N.D.	N.D.
N6-isopentenyladenosine	i^6A	Yes	t	0.07871547 8	0.08217717 4	0.06778839 4	0.08516653 4	0.08355658 6	N.D.	N.D.	N.D.	N.D.	N.D.
N2,N7-dimethylguanosine	$m^{2,7}G$	Yes	sn, sno	N.D.	N.D.	N.D.	N.D.	N.D.	N.D.	N.D.	N.D.	N.D.	N.D.

6-methyluridine	m^6U	No	NF	N.D.	N.D.	N.D.	N.D.	N.D.	N.D.	N.D.	N.D.	N.D.	N.D.
5,2'-O-dimethylcytidine	m^5Cm	No	NF	N.D.	N.D.	N.D.	N.D.	N.D.	N.D.	N.D.	N.D.	N.D.	N.D.
5-carboxymethyluridine	cm^5U	Yes	t	0.000179788 2	0.000202788 7	0.000182129 5	0.000219957 8	0.000200830 6	N.D.	N.D.	N.D.	N.D.	N.D.
2-thiocytidine	s^2C	No	t	N.D.	N.D.	N.D.	N.D.	N.D.	N.D.	N.D.	N.D.	N.D.	N.D.
2′-O-methylinosine	Im	No	r	N.D.	N.D.	N.D.	N.D.	N.D.	N.D.	N.D.	N.D.	N.D.	N.D.
5-methoxycarbonylmethyluridine	mcm^5U	Yes	t	0.02143793 4	0.02384683 5	0.02672345 2	0.02673782	0.02455736 6	N.D.	N.D.	N.D.	N.D.	N.D.
5-carboxymethylaminomethyluridine	$cmnm^5U$	Yes	t	0.000027672	0.000032096 8	0.000060468 5	0.000017227 7	0.000025361 1	N.D.	N.D.	N.D.	N.D.	N.D.
5-methoxyuridine	mo^5U	No	t	N.D.	N.D.	N.D.	N.D.	N.D.	N.D.	N.D.	N.D.	N.D.	N.D.
3-(3-amino-3-carboxypropyl)uridine	acp^3U	No	r, t	N.D.	N.D.	N.D.	N.D.	N.D.	N.D.	N.D.	N.D.	N.D.	N.D.
uridine 5-oxyacetic acid	cmo^5U	No	t	N.D.	N.D.	N.D.	N.D.	N.D.	N.D.	N.D.	N.D.	N.D.	N.D.
2,8-dimethyladenosine	$m^{2,8}A$	No	r	N.D.	N.D.	N.D.	N.D.	N.D.	N.D.	N.D.	N.D.	N.D.	N.D.
5-methoxycarbonylmethyl-2-thiouridine	mcm^5s^2U	Yes	t	0.02889898 4	0.02839637 7	0.04372151 8	0.02570161 5	0.02887603	N.D.	N.D.	N.D.	N.D.	N.D.
N2,N2,N7-trimethylguanosine	m_3G	Yes	sn, s	N.D.	N.D.	N.D.	N.D.	N.D.	N.D.	N.D.	N.D.	N.D.	N.D.

			no										
5,2′-O-dimethyluridine	m^5Um	No	t	N.D.	N.D.	N.D.	N.D.	N.D.	N.D.	N.D.	N.D.	N.D.	N.D.
2-methylthio-N6-threonylcarbamoyladenosine	ms^2t^6A	No	t	N.D.	N.D.	N.D.	N.D.	N.D.	N.D.	N.D.	N.D.	N.D.	N.D.
4-thiouridine	s^4U	No	t	N.D.	N.D.	N.D.	N.D.	N.D.	N.D.	N.D.	N.D.	N.D.	N.D.
N6-threonylcarbamoyladenosine	t^6A	Yes	t	0.08298883	0.089210315	#DIV/0!	0.091570552	0.087321215	N.D.	N.D.	N.D.	N.D.	N.D.
2-thiouridine	s^2U	Yes	t	N.D.	N.D.	N.D.	N.D.	N.D.	N.D.	N.D.	N.D.	N.D.	N.D.
5-methyl-2-thiouridine	m^5s^2U	No	t	N.D.	N.D.	N.D.	N.D.	N.D.	N.D.	N.D.	N.D.	N.D.	N.D.
3-methyluridine	m^3U	Yes	r	0.00432787 3	0.00250571 4	0.07966519 3	0.00152024 7	0.00172727 4	N.D.	N.D.	N.D.	N.D.	N.D.

*Supplemental Table B.7: Percent retention of modification in purified mRNA. Values were calculated by comparing the mod/main% of the mRNA and the total RNA ((mRNA mod/main%)/total RNA mod/main% *100)*

Nucleoside	Abbreviation	% Retention in WT mRNA
Pseudouridine	Ψ	0.49
1-methyladenosine	m^1A	0.06
5-methylcytidine	m^5C	0.64
7-methylguanosine	m^7G	14.2
2′-O-methylcytidine	Cm	0.24
5-methyluridine	m^5U	0.20
2′-O-methyluridine	Um	0.29
1-methylguanosine	m^1G	0.17
2′-O-methylguanosine	Gm	0.42
N2-methylguanosine	m^2G	0.24
2′-O-methyladenosine	Am	0.12
N6-methyladenosine	m^6A	0.26
N2,N2-dimethylguanosine	m^2_2G	0.17

Supplemental Table B.8: qRT-PCR primer sequences

Gene ID	Gene Name	Forward sequence (5'-3')	Reverse sequence (5'-3')
YFL039C	ACT1	GCCTTCTACGTTTCCATCCA	GGCCAAATCGATTCTCAAAA
RDN18-2	18S rRNA	GAGTCCTTGTGGCTCTTGGC	AATACTGATGCCCCCGACC
RDN25-1	25S rRNA	ATGTGATTTCTGCCCAGTGC	AATCCATTCATGCGCGTCAC

Supplemental Table B.9: UPLC gradients for analytical separation and wash methods. %B corresponds to the percentage of B mobile phase (acetonitrile + 0.01% formic acid)

Analytical Separation	
Time (min)	**B (%)**
0	0
0.3	0.1
0.6	0.4
0.9	0.9
1.3	1.6
4.2	2.5
7.7	4
12.2	15
13.2	50
15.2	100
17	100
17.5	0
27	0

Wash Method	
Time (min)	**B (%)**
0	0
1	60
2	0
2.5	0
3.5	60
4.5	0
5	0
6	60
7	0
7.5	0
8.5	60
9.5	0
10	0
11	60

12	0
12.5	0
13.5	60
14.5	0
15	0
16	100
17.8	100
18.3	0
27.8	0

Supplemental Table B.10: Multiple reaction monitoring parameters of nucleosides

Nucleoside	**Precursor Ion (m/z)**	**MS1 Resolution**	**Product Ion (m/z)**	**MS2 Resolution**	**Fragmentor (V)**	**Collision Energy (V)**	**Cell Accelerator Voltage (V)**	**Retention Time (min)**	**Delta Retention Time (min)**	**Polarity**
$^{15}N_4$-I	273.2	Wide	141	Unit	90	5	2	6.64	2.5	Positive
A	268.2	Wide	136	Unit	80	15	2	7.66	2.5	Positive
ac^{4}C	286.2	Wide	154	Unit	70	5	2	9.98	2.5	Positive
acp^{3}U	346.1	Wide	214.1	Unit	60	13	4	2.75	2.5	Positive
Am	282.2	Wide	136	Unit	80	15	2	10.07	2.5	Positive
C	244.2	Wide	112	Unit	70	12	3	1.62	2.5	Positive
Cm	258.1	Wide	112	Unit	70	10	3	4.45	2.5	Positive
cm^{5}U	303	Wide	171.1	Unit	80	5	1	5.56	2.5	Positive
cmnm^{5}U	332.1	Wide	125	Unit	70	13	3	1.97	2.5	Positive
cmo^{5}U	319	Wide	187.1	Unit	60	7	1	5.75	2.5	Positive
D	247.2	Wide	115.1	Unit	70	5	3	1.76	2.5	Positive
f^{5}C	272.2	Wide	140	Unit	70	10	2	7.31	2.5	Positive
G	284.1	Wide	152	Unit	70	10	2	6.86	2.5	Positive
Gm	298.1	Wide	152	Unit	80	5	2	9.18	2.5	Positive

hm^{5}C	274.2	Wide	142	Unit	60	5	2	1.83	2.5	Positive
ho^{5}U	261.2	Wide	129	Unit	80	5	3	2.44	2.5	Positive
I	269.2	Wide	137	Unit	80	10	2	6.64	2.5	Positive
i^{6}A	336	Wide	204.1	Unit	90	17	4	15.14	2.5	Positive
Im	283.1	Wide	136.9	Unit	90	1	2	9.14	2.5	Positive
m^{1}A	282.2	Wide	150	Unit	100	15	2	2.41	2.5	Positive
m^{1}G	298.2	Wide	166.1	Unit	80	5	2	9.15	2.5	Positive
m^{1}I	283	Wide	151	Unit	100	5	2	9.19	2.5	Positive
m^{1}Ψ	259.1	Wide	139	Unit	80	15	2	3.69	2.5	Positive
m$_3$G	326.1	Wide	194	Unit	60	15	1	9.89	2.5	Positive
m$^2{}_2$G	312.3	Wide	180.1	Unit	80	10	2	11.44	2.5	Positive
m^{2,7}G	312.1	Wide	180.1	Unit	60	10	1	7.82	2.5	Positive
m^{2,8}A	296.1	Wide	164.1	Unit	80	15	1	11.25	2.5	Positive
m^{2}A	282.1	Wide	150	Unit	100	20	2	8.6	2.5	Positive
m^{2}G	298.1	Wide	166.1	Unit	70	10	2	9.77	2.5	Positive
m^{3}C	258.1	Wide	126.1	Unit	60	5	3	2.09	2.5	Positive
m^{3}U	259	Wide	127	Unit	70	5	3	8.47	2.5	Positive
m^{5}C	258.2	Wide	126	Unit	60	5	3	2.61	2.5	Positive
m^{5}Cm	272.1	Wide	126.1	Unit	80	8	3	7.19	2.5	Positive
m^{5}s^{2}U	275	Wide	143	Unit	70	5	2	10.85	2.5	Positive
m^{5}U	259.1	Wide	127	Unit	70	5	3	7.1	2.5	Positive
m^{5}Um	273.1	Wide	127	Unit	60	5	3	11.06	2.5	Positive
m^{6}A	282.2	Wide	150	Unit	80	15	2	11.3	2.5	Positive

m^6Am	296.1	Wide	150	Unit	90	15	2	12.5	2.5	Positive
m^6U	259	Wide	127.1	Unit	50	5	2	5.74	2.5	Positive
m^7G	298.2	Wide	166	Unit	80	5	2	3.8	2.5	Positive
mcm^5s^2U	333	Wide	201.1	Unit	60	6	4	12.26	2.5	Positive
mcm^5U	317.1	Wide	185.1	Unit	80	6	1	9.64	2.5	Positive
mo^5U	275	Wide	143.1	Unit	90	1	6	7.38	2.5	Positive
ms^2t^6A	459.2	Wide	327.1	Unit	80	12	2	14.56	2.5	Positive
Ψ	245.1	Wide	209	Unit	70	5	4	1.81	2.5	Positive
s^2C	260	Wide	128	Unit	90	6	3	3.67	2.5	Positive
s^2U	261	Wide	129	Unit	40	3	3	7.61	2.5	Positive
s^4U	261.1	Wide	129	Unit	60	11	3	8.21	2.5	Positive
t^6A	413.1	Wide	281.1	Unit	70	5	5	13.24	2.5	Positive
U	245.2	Wide	113	Unit	50	5	3	3.36	2.5	Positive
Um	259.2	Wide	113	Unit	70	5	3	8.13	2.5	Positive

Supplemental Table B.11: Concentrations of ribonculeosides in calibration curves standards after the addition of internal standard

Standard Level	Canonical Nucleosides (nM)	Ψ and DHU (pM)	m5U (pM)	All other modifcations (pM)
1 (highest)	21600	1620000	800000	360000
2	4320	324000	160000	72000
3	864	64800	32000	14400
4	172.8	12960	6400	2880
5	34.56	2592	1280	576
6	6.912	518.4	256	115.2
7	1.3824	103.68	51.2	23.04
8 (lowest)	0	0	0	0

Supplemental Table B.12: Suppliers of ribonucleoside standards used in LC-MS/MS analyses

Nucleoside	Supplier
$^{15}N_4$-I	Cambridge Isotope Laboratories
A	ACROS Organics
ac^{4}C	Santa Cruz Biotechnology
acp^{3}U	Biosynth Carbosynth
Am	Santa Cruz Biotechnology
C	ACROS Organics
Cm	Alfa Aesar
cm^{5}U	Biosynth Carbosynth
cmnm^{5}U	Biosynth Carbosynth
cmo^{5}U	Biosynth Carbosynth
D	MedChemExpress
f^{5}C	Berry & Associates, Inc.
G	ACROS Organics
Gm	Alfa Aesar
hm^{5}C	Berry & Associates, Inc.
ho^{5}U	Aurum Pharmatech
I	Santa Cruz Biotechnology
i^{6}A	Cayman Chemical
Im	Biosynth Carbosynth
m^{1}A	Cayman Chemical
m^{1}G	Aurum Pharmatech
m^{1}I	Toronto Research Chemicals
m$^1\Psi$	Abcam
m$_3$G	Biosynth Carbosynth
m$^2{}_2$G	Santa Cruz Biotechnology
m^{2,7}G	Biosynth Carbosynth
m^{2,8}A	Biosynth Carbosynth
m^{2}A	Santa Cruz Biotechnology
m^{2}G	MedChemExpress
m^{3}C	Santa Cruz Biotechnology
m^{3}U	Toronto Research Chemicals
m^{5}C	Santa Cruz Biotechnology
m^{5}Cm	Biosynth Carbosynth
m^{5}s^{2}U	Santa Cruz Biotechnology
m^{5}U	Santa Cruz Biotechnology
m^{5}Um	Biosynth Carbosynth
m^{6}A	Berry & Associates, Inc.
m^{6}Am	Toronto Research Chemicals
m^{6}U	Biosynth Carbosynth

m^7G	Santa Cruz Biotechnology
mcm^5s^2U	Biosynth Carbosynth
mcm^5U	Toronto Research Chemicals
mo^5U	Biosynth Carbosynth
ms^2t^6A	Santa Cruz Biotechnology
Ψ	Berry & Associates, Inc.
s^2C	Biosynth Carbosynth
s^2U	Cayman Chemical
s^4U	Cayman Chemical
t^6A	Toronto Research Chemicals
U	ACROS Organics
Um	Alfa Aesar

Supplemental Table B.13: Suppliers of ribonucleoside standards used in LC-MS/MS analyses

Nucleoside	**Supplier**
$^{15}N_4$-I	Cambridge Isotope Laboratories
A	ACROS Organics
ac^4C	Santa Cruz Biotechnology
acp^3U	Biosynth Carbosynth
Am	Santa Cruz Biotechnology
C	ACROS Organics
Cm	Alfa Aesar
cm^5U	Biosynth Carbosynth
$cmnm^5U$	Biosynth Carbosynth
cmo^5U	Biosynth Carbosynth
D	MedChemExpress
f^5C	Berry & Associates, Inc.
G	ACROS Organics
Gm	Alfa Aesar
hm^5C	Berry & Associates, Inc.
ho^5U	Aurum Pharmatech
I	Santa Cruz Biotechnology
i^6A	Cayman Chemical
Im	Biosynth Carbosynth
m^1A	Cayman Chemical
m^1G	Aurum Pharmatech
m^1I	Toronto Research Chemicals
$m^1Ψ$	Abcam
m_3G	Biosynth Carbosynth
$m^2{}_2G$	Santa Cruz Biotechnology
$m^{2,7}G$	Biosynth Carbosynth

$m^{2,8}A$	Biosynth Carbosynth
m^2A	Santa Cruz Biotechnology
m^2G	MedChemExpress
m^3C	Santa Cruz Biotechnology
m^3U	Toronto Research Chemicals
m^5C	Santa Cruz Biotechnology
m^5Cm	Biosynth Carbosynth
m^5s^2U	Santa Cruz Biotechnology
m^5U	Santa Cruz Biotechnology
m^5Um	Biosynth Carbosynth
m^6A	Berry & Associates, Inc.
m^6Am	Toronto Research Chemicals
m^6U	Biosynth Carbosynth
m^7G	Santa Cruz Biotechnology
mcm^5s^2U	Biosynth Carbosynth
mcm^5U	Toronto Research Chemicals
mo^5U	Biosynth Carbosynth
ms^2t^6A	Santa Cruz Biotechnology
Ψ	Berry & Associates, Inc.
s^2C	Biosynth Carbosynth
s^2U	Cayman Chemical
s^4U	Cayman Chemical
t^6A	Toronto Research Chemicals
U	ACROS Organics
Um	Alfa Aesar

Supplemental Table B.14: The DNA template and the resulting RNA sequence following run-off T7 transcription

Amino Acid	**Codon**	**DNA template for transcription**	**RNA Sequence**
Phe	**UUU**	TGGCTACAGAAGGGCTTAGAACATAATGCACTTATCCTCGCAAGACACCCTATAGTGAGTCGTATTA	GGGUGUCUUGCGAGGAUAAGUGCAUUAUGUUUUAAGCCCUUCUGUAGCCA
Phe	**UUC**	TGGCTACAGAAGGGCTTAGAACATAATGCACTTATCCTCGCAAGACACCCTATAGTGAGTCGTATTA	GGGUGUCUUGCGAGGAUAAGUGCAUUAUGUUCUAAGCCCUUCUGUAGCCA
Val	**GUG**	TGGCTACAGAAGGGCTTTTATCGTTGCACCATAATGCACTTATCCTCGCAAGACACCCTATAGTGAGTCGTATT	GGUGUCUUGCGAGGAUAAGUGCAUUAUGGUGCAACGAUAAAAGCCCUUCUGUAGCCA
Arg	**CGU**	TGGCTACAGAAGGGGTCACTTTATGCACGCATAATGCACTTATCCTCGCAAGACACCCTATAGTGAGTCGTATT	GGUGUCUUGCGAGGAUAAGUGCAUUAUGCGUGCAUAAAGUGACCCCUUCUGUAGCCA

Supplemental Table B.15: Modified RNA transcriptions purchased from Dharmacon

Amino Acid	Codon	Modified codon	RNA Sequence
Phe	UUU	**UUm^{5}U**	GGGUGUCUUGCGAGGAUAAGUGCAUUAUGUUm^{5}UUAAGCCCUUCUGUAGCCA
Phe	UUC	**m^{5}UUC**	GGGUGUCUUGCGAGGAUAAGUGCAUUAUGm^{5}UUCUAAGCCCUUCUGUAGCCA
Phe	UUC	**Um^{5}UC**	GGGUGUCUUGCGAGGAUAAGUGCAUUAUGUm^{5}UUCUAAGCCCUUCUGUAGCCA
Val	GUG	**m^{1}GUG**	GGUGUCUUGCGAGGAUAAGUGCAUUAUGm^{1}GUGCAACGAUAAAAGCCCUUCUGUAGCCA
Val	GUG	**m^{2}GUG**	GGUGUCUUGCGAGGAUAAGUGCAUUAUGm^{2}GUGCAACGAUAAAAGCCCUUCUGUAGCCA
Val	GUG	**GUm^{1}G**	GGUGUCUUGCGAGGAUAAGUGCAUUAUGGUm^{1}GCAACGAUAAAAGCCCUUCUGUAGCCA
Val	GUG	**GUm^{2}G**	GGUGUCUUGCGAGGAUAAGUGCAUUAUGGUm^{2}GCAACGAUAAAAGCCCUUCUGUAGCCA
Arg	CGU	**Cm^{1}GU**	GGUGUCUUGCGAGGAUAAGUGCAUUAUGCm^{1}GUGCAUAAAGUGACCCCUUCUGUAGCCA
Arg	CGU	**Cm^{2}GU**	GGUGUCUUGCGAGGAUAAGUGCAUUAUGCm^{2}GUGCAUAAAGUGACCCCUUCUGUAGCCA

Appendix C: Chapter 4 Supplemental

This appendix contains all supplemental discussion, and data/supporting figures for the paper titled “Modulation of tRNA modification landscape alters the efficacy of Hygromycin B translation inhibition." This work has yet to be published.

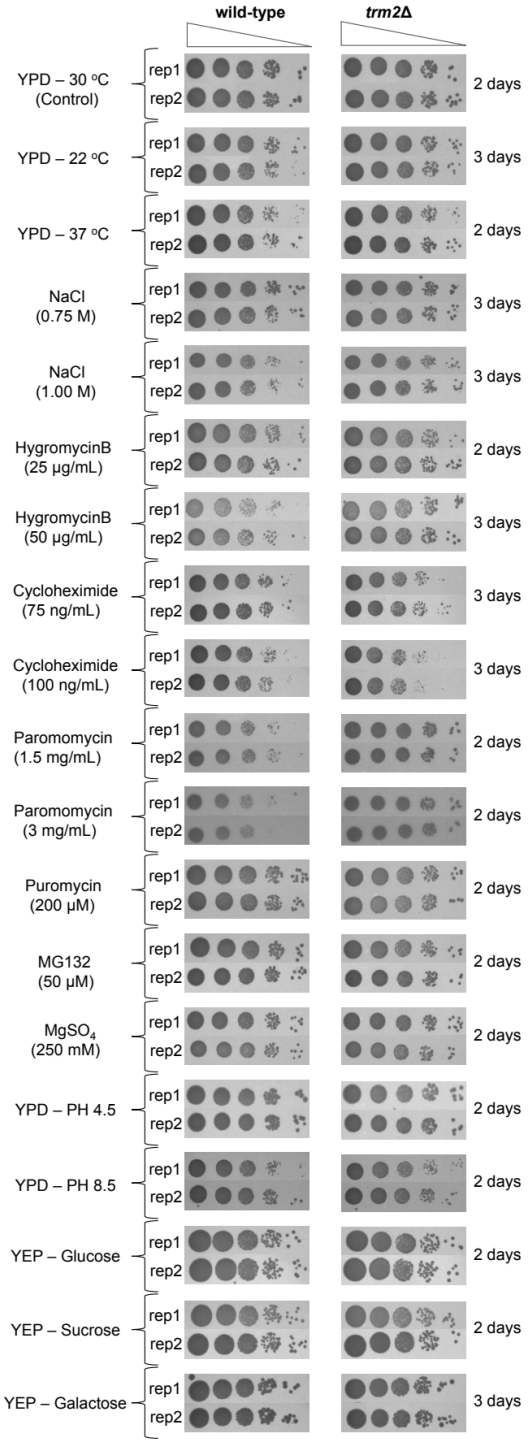

Supplemental Figure C.1: Spot platting for both native cells and cells with trm2 KO under different growth conditions.

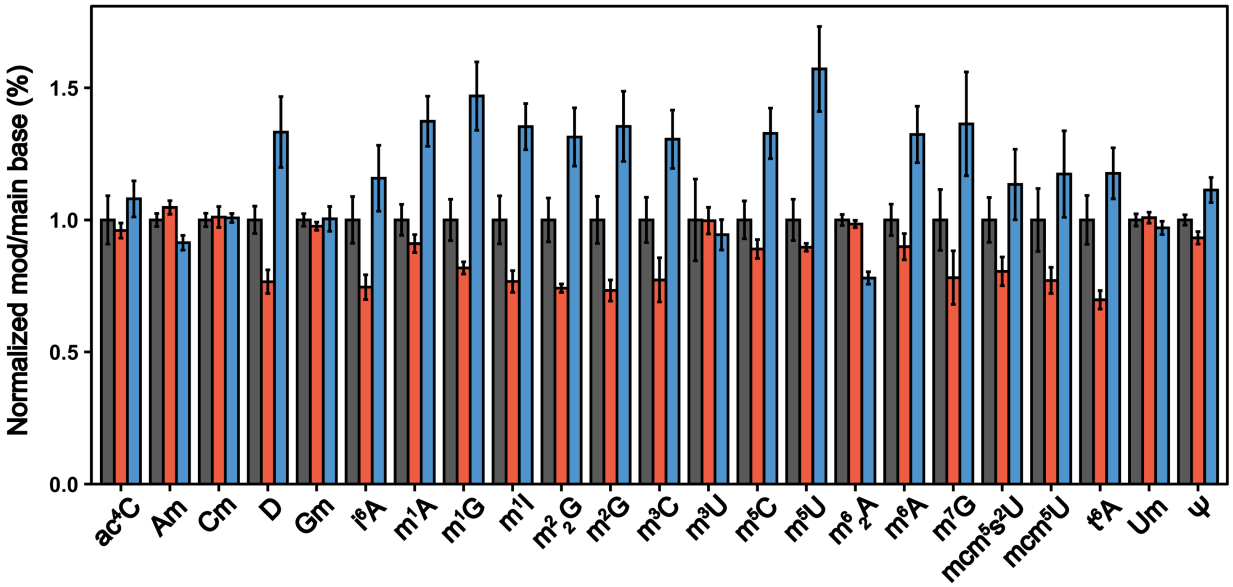

Supplemental Figure C.2: ***Bar plot displaying modification levels under different stress conditions*** *Wild type-black, Cycloheximide-red, Hygromycin-blue.*

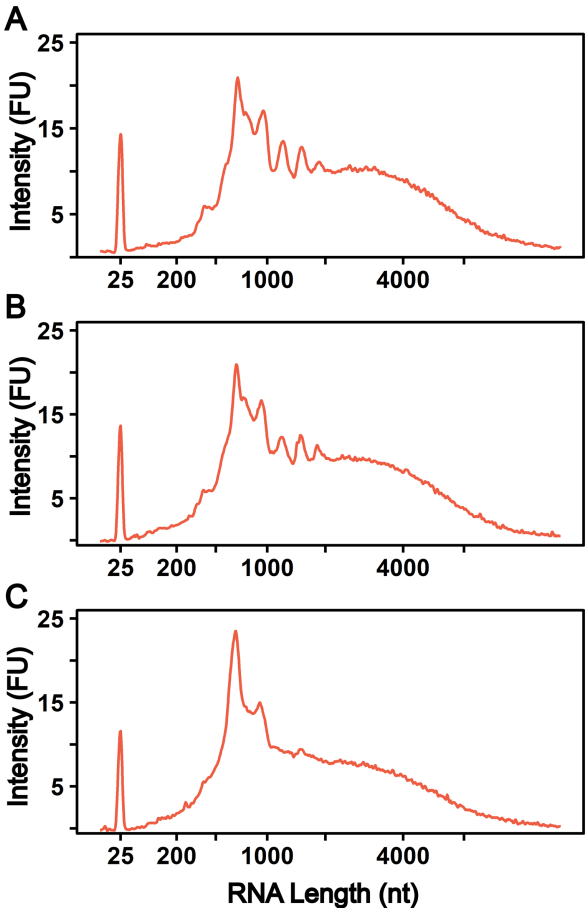

Supplemental Figure C.3:Bioanalyzer for total tRNA A – wild type, B-cyclohexamide, C-hygromycin B

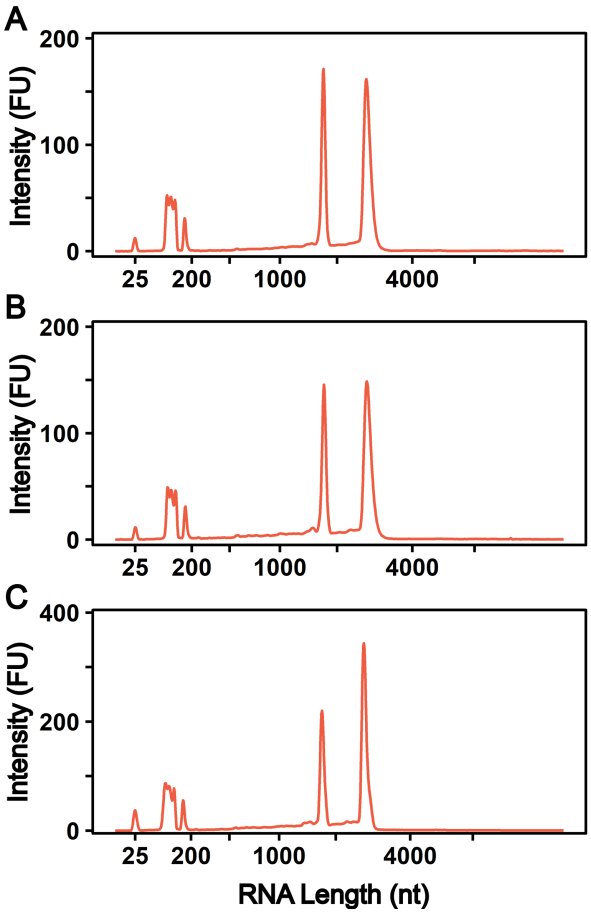

Supplemental Figure C.4: Bioanalyzer for rRNA A – wild type, B-cyclohexamide, C-hygromycin B

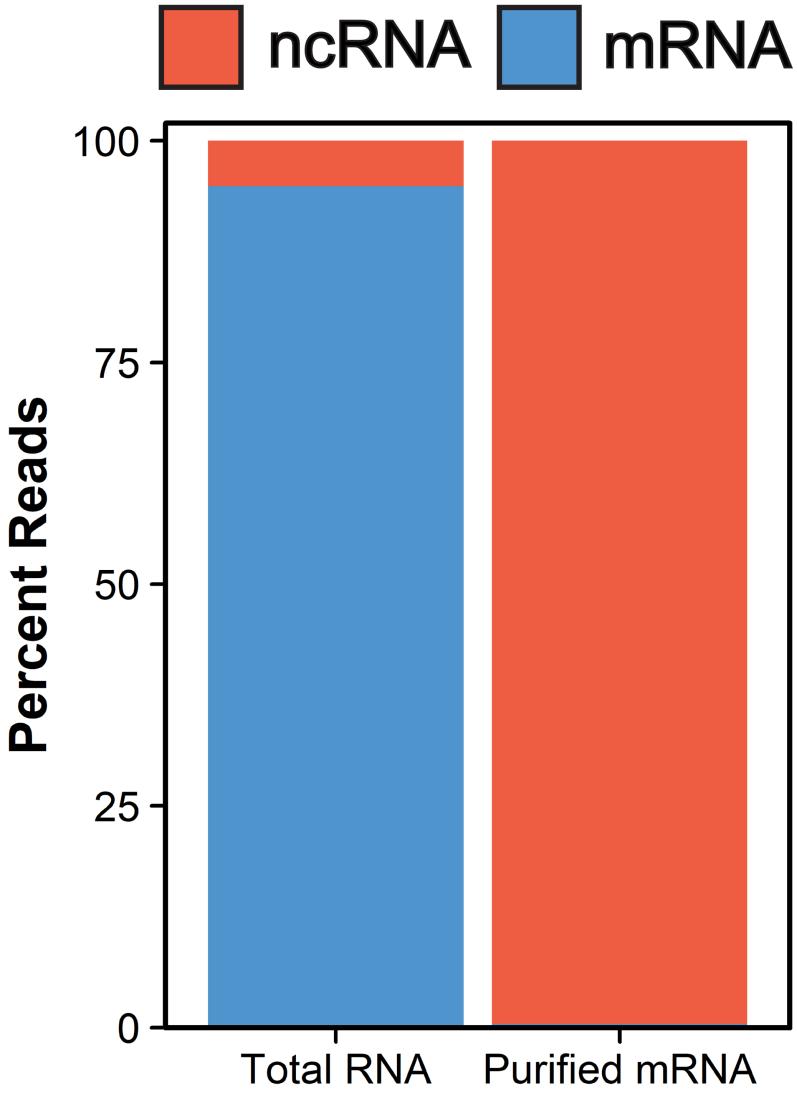

Supplemental Figure C.5: RNA-sequencing results showing depletion of non-coding RNA's.

Appendix D: Pseudouridine Synthase 7 Is An Opportunistic Enzyme That Binds And Modifies Substrates With Diverse Sequences And Structures[4]

This appendix contains work done by myself for the publication: *Pseudouridine synthase 7 is an opportunistic enzyme that binds and modifies substrates with diverse sequences and structures.* **M. Purchal**, D.E. Eyler, M. Tardu, M.K. Franco, M. Korn, T. Khan, R. McNassor, R. Giles, K. Lev, H. Sharma, J. Monroe, L. Mallik, M. Koutmos and K.S. Koutmou (**2021**) *PNAS.* 119, 4 e2109708119. PMID: 35058356. This paper applies structural biology and enzymology to interrogate how pseudouridine synthase 7 (Pus7) identifies and selects its mRNA targets. In this work, Purchal et al found that Pus7 is remarkably promiscuous, binding and modifying a myriad of diverse RNA substrates and Pus7 exhibited both specific and non-specific binding to RNA. We proposed a model to describe the distribution of Pus7-dependent mRNA pseudouridylation that is based on substrate accessibility. I performed stopped-flow experiments/kinetics to interrogate the non-specific binding of multiple Pus7 enzyme to a single RNA substrate.

Introduction:

Cells use chemical modifications to regulate the production, function and degradation of biomolecules. In the last decade, a small subset of RNA modifications have been discovered that affect mRNA at every stage of the mRNA lifecycle. This is important because other it is long been known that modification of non-coding RNA's (tRNA and rRNA) affects both structure,

[4] Appendix D was published in PNAS. The authors on this paper are Mededith Purchal, Dan E. Eyler, Mehme Tardu, Monika K. Franco, Megan Korn, Taslima Khan, Ryan McNassor, Rachel Giles, Katherine Lev, Hari. Sharma, Jeremy. Monroe, Leena Mallik, Markos Koutmos and Kristin S Koutmou. Monika Franco collected data using Kinetic Stop Flow to analyse Pus7 binding.

stability, and function. These modifications are modulated by three different classes of proteins: readers, writers, and erasers. The names indicate the function of these proteins, but reader enzyme read/identify the modification, writer enzymes incorporate the modification into the RNA biomolecule, and erasers remove said modification. The study of how these enzymes function is foundational to understanding the how RNA modifications contribute to cellular function and gene regulation.

Pseudouridine is one of the most common RNA modifications, found in both tRNA and rRNA, where it plays an important role in both structure and function. It is installed into RNAs by a family of enzymes called pseudouridine synthases (PUS). Disruptions in the pseudouridylation of non-coding RNA substrates have been linked to multiples diseases including both dyskeratosis congenital (DC) and mitochondrial myopathy with lactic acidosis and sideroblasic anemia (MLASA)[1]–[5]. In the last decade discovery of abundant levels of pseudouridine in mRNA has peaked question of whether it's done purposefully or not[6]–[10]. Pus7 was chosen due to is diverse substrate scope, high activity towards mRNA, interesting behavior under heat shock, and it often installs pseudouridine in important functional regions of non-coding RNA.

Purchal et al. investigated binding patterns of the Pus 7 enzyme to try an identify if there was a structural or sequence dependent basis for binding. They first wanted to evaluate how the active site and the inserted domain unique to Pus 7 affected binding. This was done by performing electrophoretic mobility shift assays (EMSAs) with fluorescently labeled CDC8 (a known substrate) with a series of catalytically inactive mutants of Pus 7. They found that at low enzyme concentrations of less than 50nM there was only a single band shift. This dictates that there was a singular binding event (Figure 1). However, when the concertation of Pus7 was

increased multiple binding events were observed (Figure 1). My work was used to further analyze the potential mechanism of binding through the use of stop-flow kinetics.

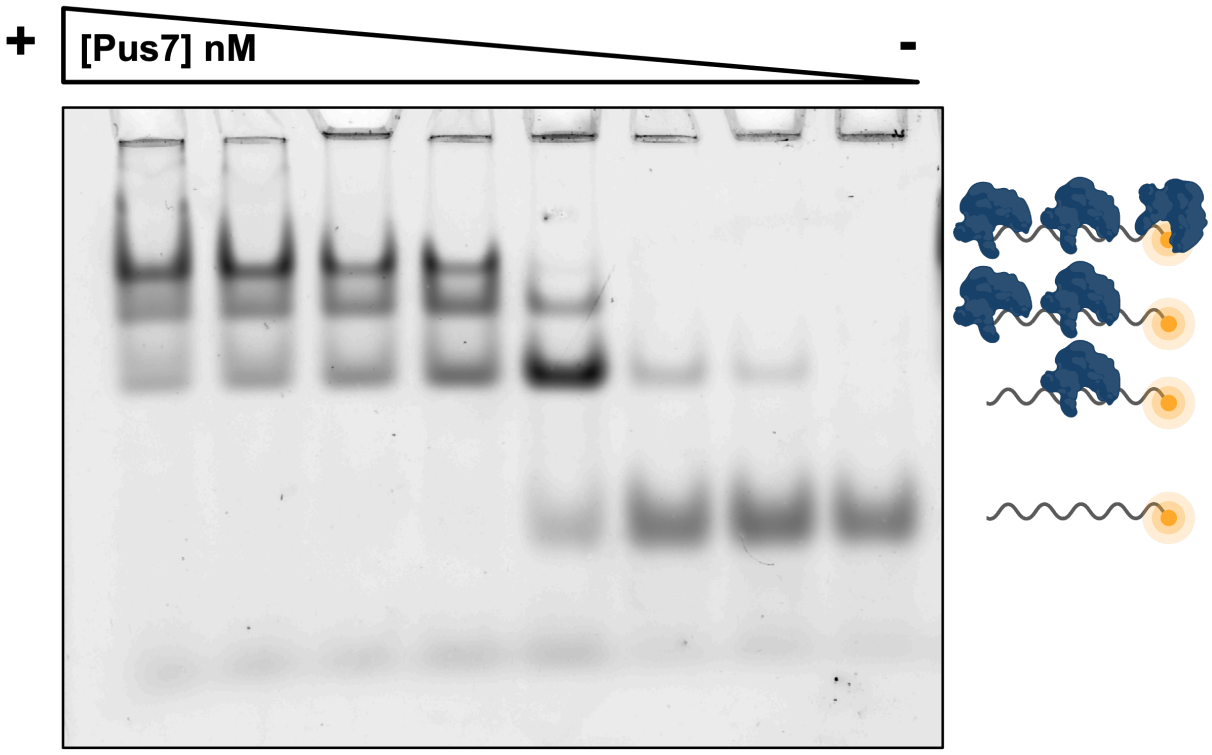

Supplemental Figure D.1: Multiple Pus7 proteins bind to CDC8 RNA. The association of increasing concentrations of catalytically inactive D256A Pus7 with limiting amounts of 50 -fluorescein-labeled CDC8 visualized on a nondenaturing agarose gel. Increased concentrations of D256A resulted in multiple binding events.

Results

Using a Kintek SF-300x stop flow apparatus, I was able to show support that Pus7 performs multiple binding events, exhibiting both specific binding to the consensus sequence and non-specific binding elsewhere on the substrate. We observed multiple super-shifted bands in the EMSA which suggested multiple binding events of Pus7 enzymes. To further interrogate this behavior we extrapolated observed rate constants with fluorescent stop flow. The experiment was set up with wt or d256a? Pus7(20 nM – 750 nM final) in syringe 1 and the fluorescently labeled CDC8 (5nM final) in the other (Figure 2). They were then rapidly mixed and the change

of fluorescent single with observed.

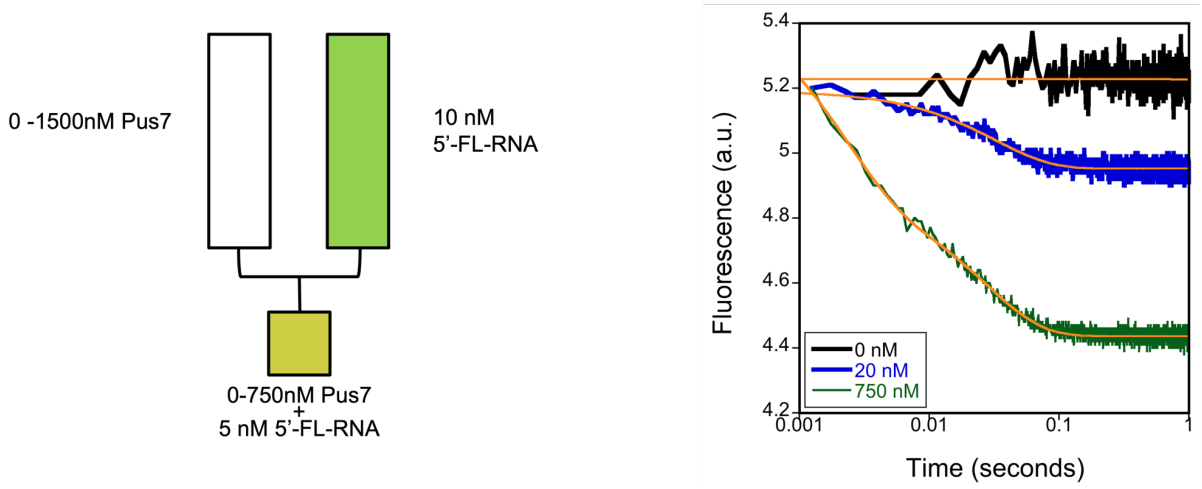

Supplemental Figure D.2: (left)Experimental set-up, as described in the corresponding Methods. (right)Stopped-flow traces of Fl-CDC8 rapidly mixed with 0, 20 and 750 nM of D256A Pus7 protein.

At low enzyme concentrations we observe a single exponential phase, whose rate constant (k_{obs1}) is linearly dependent on enzyme concentration (Figure 3). As I increased enzyme concentration, a second phase emerges (k_{obs2}) consistent with the EMSAs data indicating that multiple proteins bind to Pus7 RNA targets. Using this information the EMSA data was fit with the proposed binding model to give a K_D . that indicates tight binidg of D256A with CDC8, $K_{D,app1} = 60 \pm 15$ nM. This is comparable with the K_D estimated for D256A from my stopped flow assays ($k_{on,app} = 4.3 \times 10^8$ $M^{-1}s^{-1}$, $k_{off,app} = 35$ $^{-1}$, $k_{off,app}/k_{on,app} = K_D \sim 85$ nM). Ultimately this data was used to help to understand the EMSA data and propose a binding model.

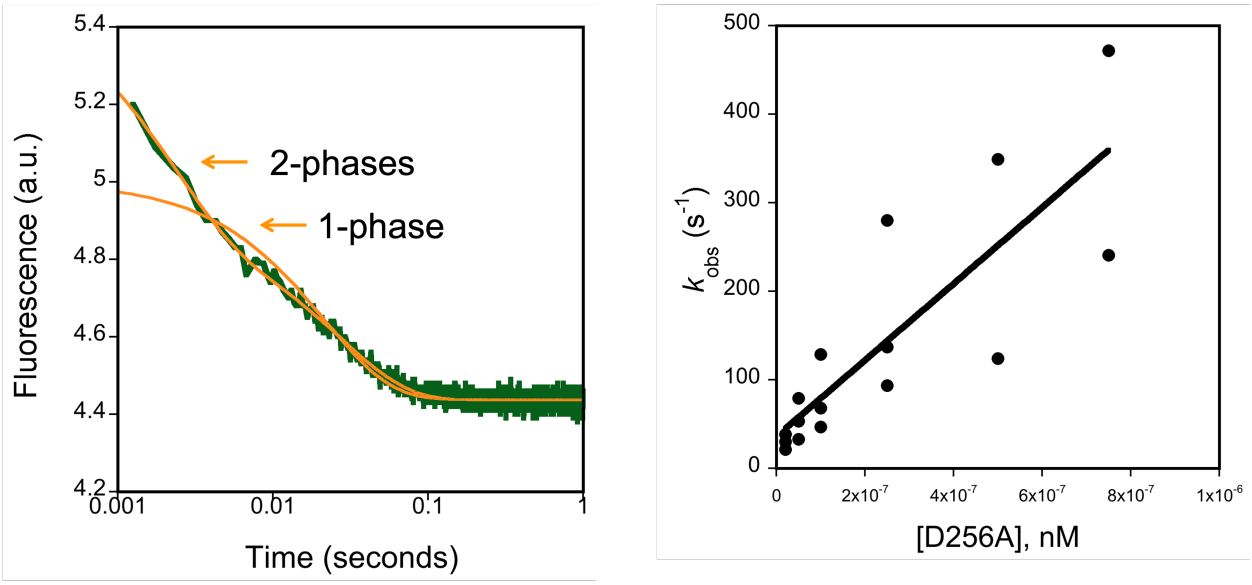

Supplemental Figure D.3: (Left) Traces at higher D256A concentrations were biphasic. This shows a 750 nM trace fit with one or two phases. (Right) All of the $k_{obs,}1$ values measured are plotted as a function of D256A Pus7 concentration.

Methods

D256A Pus7 and 5'-fluorescein labeled CDC8 were generated and purified as described as above. Kinetic binding experiments were performed using the Kintek SF-300x stop-flow apparatus. Fluorescently labeled mRNA (5 nM final concentration) was mixed with D256A at varied concentrations (20 nM – 750 nM final). Binding experiments were performed at room temperature in same buffer used in the EMSA experiments over the span of 1-1.5 seconds. Lower concentrations of Pus7/D256A (0-100nM) displayed monophasic behavior and were fit with a single exponential equation: $A_1e^{-k1t} + c$ to obtain a k_{obs1}. Higher concentrations displayed biphasic behavior and therefore were fit with a double exponential equation: $A_1e^{-k1t} + A_2e^{-k2t} + c$ to obtain k_{obs1} and k_{obs2}. The k_{obs1} values from both fits were then plotted against the concertation of D256A PUS7 mutant, displaying a linear relationship. The y-intercept gave a k_{off} of approximately 35 s^{-1} and the slope gave a k_{on} of ~4.3 x 10 8 $M^{-1}s^{-1}$. The K D For D256A binding CDC8 was obtained using Equation 5: $K_D = k_{off}/k_{on}$.

References

1] J. E. Mangum *et al.*, “Pseudouridine synthase 1 deficient mice, a model for Mitochondrial Myopathy with Sideroblastic Anemia, exhibit muscle morphology and physiology alterations,” *Sci Rep*, vol. 6, p. 26202, May 2016, doi: 10.1038/srep26202.
[2] D. Ruggero *et al.*, “Dyskeratosis congenita and cancer in mice deficient in ribosomal RNA modification,” *Science*, vol. 299, no. 5604, pp. 259–262, Jan. 2003, doi: 10.1126/science.1079447.
[3] J. R. Patton, Y. Bykhovskaya, E. Mengesha, C. Bertolotto, and N. Fischel-Ghodsian, “Mitochondrial myopathy and sideroblastic anemia (MLASA): missense mutation in the pseudouridine synthase 1 (PUS1) gene is associated with the loss of tRNA pseudouridylation,” *J Biol Chem*, vol. 280, no. 20, pp. 19823–19828, May 2005, doi: 10.1074/jbc.M500216200.
[4] Y. Bykhovskaya, K. Casas, E. Mengesha, A. Inbal, and N. Fischel-Ghodsian, “Missense mutation in pseudouridine synthase 1 (PUS1) causes mitochondrial myopathy and sideroblastic anemia (MLASA),” *Am J Hum Genet*, vol. 74, no. 6, pp. 1303–1308, Jun. 2004, doi: 10.1086/421530.
[5] S. W. Knight *et al.*, “1.4 Mb candidate gene region for X linked dyskeratosis congenita defined by combined haplotype and X chromosome inactivation analysis,” *J Med Genet*, vol. 35, no. 12, pp. 993–996, Dec. 1998, doi: 10.1136/jmg.35.12.993.
[6] T. M. Carlile, M. F. Rojas-Duran, B. Zinshteyn, H. Shin, K. M. Bartoli, and W. V. Gilbert, “Pseudouridine profiling reveals regulated mRNA pseudouridylation in yeast and human cells,” *Nature*, vol. 515, no. 7525, pp. 143–146, Nov. 2014, doi: 10.1038/nature13802.
[7] A. F. Lovejoy, D. P. Riordan, and P. O. Brown, “Transcriptome-wide mapping of pseudouridines: pseudouridine synthases modify specific mRNAs in S. cerevisiae,” *PLoS One*, vol. 9, no. 10, p. e110799, 2014, doi: 10.1371/journal.pone.0110799.
[8] S. Schwartz *et al.*, “Transcriptome-wide mapping reveals widespread dynamic-regulated pseudouridylation of ncRNA and mRNA,” *Cell*, vol. 159, no. 1, pp. 148–162, Sep. 2014, doi: 10.1016/j.cell.2014.08.028.
[9] N. M. Martinez *et al.*, “Pseudouridine synthases modify human pre-mRNA co-transcriptionally and affect pre-mRNA processing,” *Molecular Cell*, 2022.
[10] X. Li *et al.*, “Chemical pulldown reveals dynamic pseudouridylation of the mammalian transcriptome,” *Nat Chem Biol*, vol. 11, no. 8, pp. 592–597, Aug. 2015, doi: 10.1038/nchembio.1836